Practical indoor localization system using GSM fingerprints and embedded sensors

Ye Tian

THÈSE DE DOCTORAT DE
l'UNIVERSITÉ PIERRE ET MARIE CURIE

Spécialité

Électronique

École doctorale Informatique, Télécommunications et Électronique (Paris)

Présentée par

Ye Tian

Pour obtenir le grade de

DOCTEUR de l'UNIVERSITÉ PIERRE ET MARIE CURIE

Sujet de la thèse :

Développement d'une méthode de géolocalisation à l'intérieur de bâtiments par classification des fingerprints GSM et fusion de données de capteurs embarqués

soutenue le 13 février 2015

devant le jury composé de :

M. Bruce Denby	Directeur de thèse
M. Emmanuel Viennet	Rapporteur
M. Henk Wymeersch	Rapporteur
Mme. Geneviève Baudoin	Examinateur
M. Aziz Benlarbi-Delaï	Examinateur
Mme. Valérie Ciarletti	Examinateur
M. Pierre Roussel	Encadrant

Acknowledgments

During my PhD thesis, I received a lot of attention, support and help in both the research and life in Paris. I would like to express my sincere gratitude here.

First and foremost I wish to thank my supervisor, Professor Bruce Denby. He has been supportive since the first day I came to the lab. I appreciate all his contributions of time and effort to make my PhD thesis possible. Apart from the direction on my research work, his responsibility, time management, striving for perfection has deeply impressed me and set an example for me to follow.

I would also like to thank the current and former members of the SIGMA laboratory who have contributed immensely to my professional and personal time in the ESPCI-ParisTech. Special thanks goes to Professor Gérard Dreyfus, director of the SIGMA laboratory, for his great leadership and rigorous scholarship; and Pierre Roussel, Iness Ahriz and Ngo Quoc Tuong, the team members of our projects, for their friendships as well as good advice and collaboration.

I would like to thank the China Scholarship Council (CSS) and the ESPCI-ParisTech for their financial support to my thesis.

For this dissertation I would like to thank my reading committee members, Henk Wymeersch and Emmanuel Viennet, and the members of my oral defense committee, Geneviève Baudoin, Valérie Ciarletti and Aziz Benlarbi-Delaï, for their time, interest, and helpful comments.

Lastly, I would like to thank my parents, my sister and my companion for all their love, support and sacrifices.

Abstract

GPS has long been used for accurate and reliable location determination, navigation and time synchronization in outdoor environments. However, since GPS signals are too weak to penetrate building roofs, walls and other objects, it cannot operate in indoor environments, which suggests developing indoor localization methods that can provide seamless and ubiquitous services for mobile users.

In this thesis, indoor localization is realized making use of received signal strength fingerprinting technique based on the existing GSM networks, which can be adopted by standard mobile phones and eliminates the time and labor consuming deployment and maintenance of network infrastructures. A room is defined as the minimum location unit, and support vector machine are used as a mean to discriminate the rooms by classifying received signal strengths from very large number of GSM carriers. At the same time, multiple sensors, such as accelerometer, gyroscope and magnetic field, are widely available for modern mobile devices, which provide additional information that helps location determination. The hybrid indoor localization that combines the GSM fingerprinting results with mobile sensor information and building layout constraint using a particle filter provides a more accurate and fine-grained localization result.

The approaches were tested on datasets acquired under realistic conditions in both a laboratory building and a railway station. Experimental results demonstrate that correct room number can be obtained 94% of the time provided the derived model is used before significant received signal strength drift sets in. Furthermore, if the training data is sampled over a few days, the performance of the indoor room-level localization system can remain stable exceeding 80% over a period of months, and can be further improved with various post-processing techniques. Moreover, including the mobile sensors allows the system to localize the mobile trajectory coordinates with high accuracy and reliability.

Indoor localization approaches in this thesis rely only on GSM received signal strength fingerprint and multiple mobile sensors that are easy to obtain with the growing popularity of mobile phones, and in this sense can be considered ready for a practical implementation.

Résumé

L'objet de cette thèse est l'étude de la localisation et de la navigation à l'intérieur de bâtiments à l'aide des signaux disponibles dans les systèmes mobiles cellulaires et, en particulier, les signaux radio-fréquences GSM.

Le système GPS est aujourd'hui couramment utilisé en extérieur pour déterminer la position d'un objet mobile, fournir une aide à la navigation et permettre la synchronisation temporelle. Mais les signaux GPS ont une puissance trop faible pour traverser les toits et les murs des bâtiments et ils ne sont pas adaptés à la localisation en intérieur. Il est donc nécessaire d'envisager d'autres méthodes pour pouvoir fournir aux utilisateurs de systèmes mobiles ces services de manière uniforme dans le temps et dans l'espace.

Dans cette thèse, la localisation en intérieur est obtenue à partir de la technique des «empreintes» de puissance des signaux reçus sur les canaux utilisés par les réseaux GSM. Ces signaux sont bien évidemment reçus par tous les téléphones cellulaires ainsi qu'un certain nombre de tablettes, et ils présentent l'avantage d'être disponibles sans qu'il soit nécessaire d'installer ou d'entretenir une infrastructure spécifique. La localisation est réalisée à l'échelle de la pièce. La classification est effectuée à partir de machines à vecteurs supports et les descripteurs utilisés sont les puissances de toutes les porteuses GSM. De nombreux autres capteurs, tels qu'accéléromètre, gyromètre, magnétomètre, disponibles dans les téléphones portables, fournissent également des informations qui peuvent être utilisées pour déterminer la position ou le déplacement de l'utilisateur. Ces informations, ainsi que la cartographie de l'environnement, sont associées aux résultats obtenus à partir des «empreintes» GSM au sein de filtres particulaires. Il est ainsi possible d'obtenir une localisation plus précise, sous forme de coordonnées continues, et non plus seulement au niveau de la pièce.

Les méthodes proposées ont été testées en conditions réelles sur des données recueillies d'une part dans les sept pièces du laboratoire où s'est déroulée cette thèse et d'autre part, dans une gare. Les résultats obtenus montrent que la technique de localisation basée sur les empreintes

GSM seules permet de déterminer la pièce correcte dans 94% des cas lorsque les données sont collectées sur une durée courte. Il est également montré que les performances restent stables pendant plusieurs mois, de l'ordre de 80%, si les données d'apprentissage sont enregistrées sur quelques jours. De plus, si l'on associe la cartographie du lieu aux données de classification au sein d'un filtre bayésien, dans le cadre d'un suivi de déplacement, les résultats sont encore améliorés. Enfin les informations issues des autres capteurs permettent d'obtenir les coordonnées de la trajectoire du système mobile avec une bonne précision et une bonne fiabilité.

L'approche de localisation en intérieur adoptée dans cette thèse repose uniquement sur l'utilisation des empreintes de puissance des signaux GSM et des informations fournies par les capteurs embarqués dans la plupart des téléphones portables. Elle peut donc permettre d'en envisager la réalisation pratique et l'utilisation courante.

Table of Contents

List of Figures

Chapter 1

Introduction

1.1 Location based applications and services

Localization is the determination of the location of a mobile target, which is a basic need for a lot of scenarios and supports a variety of services and applications based on location information. Location Based Services (LBS) can be defined as services that integrate a mobile device's location or position with other information in order to provide added value to a user [1]. Figure 1.1 illustrates the categories of diverse LBS.

Among these services and applications, the digital map is the most fundamental yet most important service, which has become a native application in most smart phones. In addition to the basic map-related services like localization, navigation, routing and tracking, more importantly, it provides an interface upon which a great majority of LBS are based. Another important application of localization is information services, which allow mobile users to easily obtain the local information of interest such as weather, traffic, catering and location-based to-do list and reminders. Furthermore, content providers, public agencies and advertisers can deliver content, information and advertisements in a more targeted way to audiences based on their locations. Location based map services and information services are often linked to each other, supporting a further variety of LBS.

Public safety, such as emergency services of police, fire and ambulance, have turned out to be a very important application field. Localization techniques facilitate such services in locating the site of the incident and people waiting for rescue, tracking and navigating security agents and trapped people, which can save a lot of time and resources.

Every year, an estimated 240 million emergency "911" calls are made in the United States [2]. According to the Federal Communications Commission (FCC) of the United States, it is

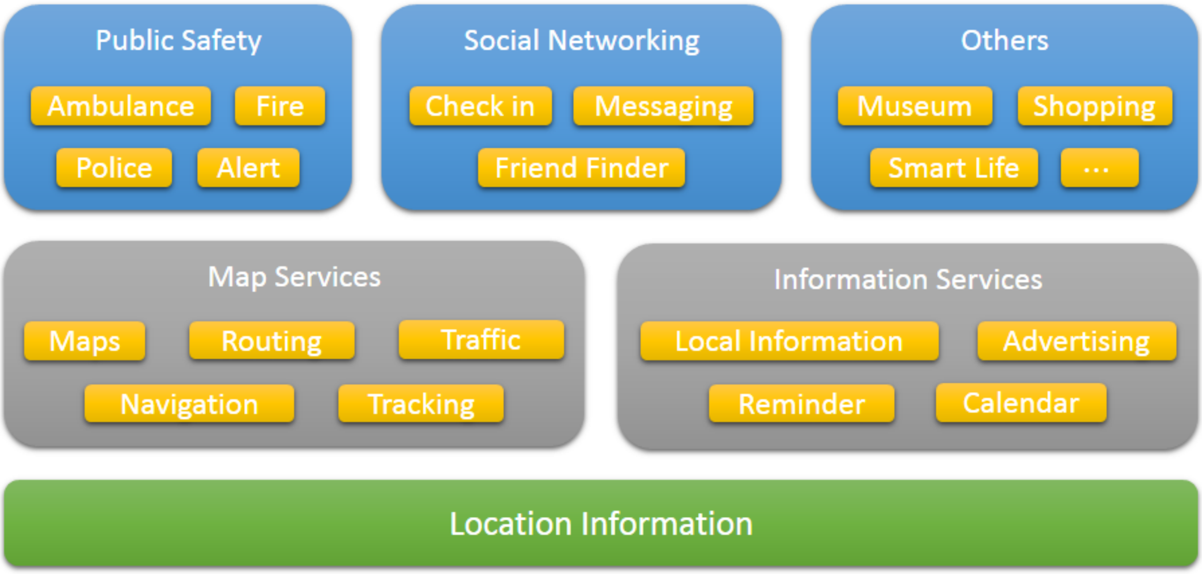

Figure 1.1 – Categories of location based services

estimated that about 70% of "911" calls are placed from wireless phones, and that percentage is growing [3]. The same case in Europe, statistics reveal that 65% of the approximate 320 million emergency calls made in European Union each year originate from mobile phones [4]. In most cases users will not know their position precisely enough to guide emergency personnel to the correct locations, and as a result wireless service providers are usually required to report the location information of the emergency callers via other means. At present, the supplied localization accuracy in outdoor scenarios is far from sufficient, and the situation in indoor environments is even more problematical. Consequently, more efficient and timely public security services must be developed including localization techniques that can provide more accurate information and which operate well in indoor environments.

Social networking has been another big market and LBS are booming in this application field. With the development of mobile Internet, smart devices and localization techniques, social activities become more and more location based. Existing location based social networking applications like check in, friend finder and messaging services are already very popular, and such services are continuously growing.

In addition to the typical applications in the areas of public safety and social networking, more diverse LBS can be found in both public and private settings. Berg Insight estimates that about 50% of all mobile subscribers in Europe were frequent users of at least one LBS at the end of 2013. In North America, an estimated 60% of all handset users now access LBS regularly [5]. The increase in usage of LBS and the number of active users has resulted in significant revenue growth, mainly from collecting, managing and distributing spatial information and imagery. If manufacturing and developing of devices and software for creating, visualizing, sharing and analyzing geographic information are included, it is an even larger industry. Despite rapid growth and widespread impact, however, LBS remain an emerging industry.

The main barrier that hinders the development and application of LBS is the inability to achieve sufficiently accurate indoor localization. According to Strategy Analytics, people spend 80-90% of their time indoors and 70% of cellular calls and 80% of data connections originate from indoors [6]. Along with an improvement of performance, future generations of indoor positioning systems will find even more applications which are at the present time not feasible. Satellites based localization techniques like GPS have played an important role in LBS, but will not be able to meet the requirements of higher accuracy and seamless localization of both indoor and outdoor.

1.2 The indoor localization problem

Efforts have been made over decades to obtain accurate, reliable and pervasive localization in different environments. For outdoor environments, satisfactory localization has been achieved by the Global Navigation Satellite Systems (GNSS), which utilize a fleet of satellites around the Earth providing global coverage with high accuracy and high availability. The most well-known GNSS is the Global Positioning System (GPS) developed by the United States, serving worldwide users with high accuracy localization and navigation in all weather conditions [7]. Localization based on the GPS necessitates no less than four satellites to accurately locate a receiver, while in some conditions signals from some of the satellites are too weak or obstructed.

Functioning in indoor environments is a critical challenge for localization, where GPS is infeasible because there is no Line Of Sight (LOS) between mobile receivers and satellites. Moreover, due to the smaller scale and more complicated geometries of indoor environments, better accuracy will be required as compared to outdoor localization. The inability of GPS receivers to function adequately in indoor environments has launched a search for new techniques of indoor localization that can provide seamless and ubiquitous service for mobile users. These approaches can be divided into:

- Beacon based solutions, which determine a mobile's location by measuring some physical quantities of wireless signals that changes with the position; and
- Beacon free solutions, which use mobile sensors to detect position changes using a so-called

dead-reckoning technique.

The complexity of indoor environments, with a large number of walls and obstacles, causes problems for beacon based solutions, where shadowing and multipath propagation effects of radio signals are common. The received signal, in most situations, will not be from the direct LOS signal, but will contain many Non Line Of Sight (NLOS) components. Thus, time synchronization and propagation time measurement will be less inaccurate, which handicaps systems relying on time measurement to operate in indoor environments. Received Signal Strength (RSS) is another common measured quantity for indoor localization because of its ease of access. However, RSS in indoor environments, as the superimposition of multipath signals of varying phases, are also unstable. Furthermore, it is extremely difficult to model the indoor signal propagation, since indoor environments are much less regular than outdoor environments. Such models, usually based on a propagation path and known obstacles, are scenario specific, while a genuine indoor environment can vary dramatically, from the open halls of factory to narrow corridors in office buildings, for example. In addition, minor indoor changes in the organization of furniture, or the presence of persons can render a signal propagation model invalid in short order.

At the same time, beacon free localization techniques, which rely only on mobile sensors such as accelerometers, gyroscopes, magnetometers, and barometer, can track users by continuously estimating their displacement from a known starting point. Sensor dead-reckoning, however, is not likely to be a standalone solution for indoor localization, as it is always necessary to know the starting position, and furthermore, the inherent low precision of mobile sensors, and the necessity to integrate sensor readings in order to measure a position will result in an unacceptable accumulation of error. However, as multiple sensors sensitive to position changes are increasingly popular in mobile devices, it is possible to include them in *hybrid* localization solutions combining the advantages of a variety of location estimation techniques sources, which has now become the general trend for indoor localization solutions.

1.3 The thesis work

The objective of this thesis is to develop a practical indoor localization system that can be used with standard mobile devices. Unlike many of the indoor localization systems that are implemented using such technologies as infrared, Bluetooth, Radio-Frequency Identification (RFID), Wireless Local Area Networks (WLAN), Ultra-Wide Band (UWB), acoustic signals, etc., the thesis investigates indoor localization based on the RSS from GSM networks, which eliminates time and labor consuming infrastructure deployment. A vector containing a set of RSS values at different positions is referred to as an RSS fingerprint, as will be discussed in more detail later. The widespread coverage, near-ubiquity and relative stability of GSM networks are attractive for practical indoor localization.

In the thesis, the characteristics of GSM RSS are first examined, showing the location specific nature and relative time robustness of GSM RSS, followed by an exploration of the functional relationship between RSS and position using regression techniques., No smooth functional relationship between RSS and position is found, however, for the indoor environment, indicating from the start that interpolation and extrapolation schemes based on RSS measurements at a small number of reference points are not going be viable for indoor localization.

Room-level indoor localization, i.e., estimation of the room in a building in which a mobile node is located, is then studied using Support Vector Machines (SVM) to classify RSS from all the available GSM carrier frequencies. Previous results using GSM for indoor localization suggested that accurate and efficient indoor localization can be achievable using RSS fingerprints containing *very large numbers* of GSM channels [8, 9]. However, those studies did not yet present a genuinely practical solution, since RSS values were only explored over a limited set of points within each room. The thesis applies a more general scanning strategy, in which RSS examples are acquired during a "random walk" throughout the inside each room of interest, enabling a user can be localized at room level regardless of his or her exact position within a room.

A further advancement provided by this thesis, as compared to earlier work on GSM, is a study of the evolution of localization performance over a rather significant time period. Due to variations in shadowing, multipath, and environmental effects such as building geometry changes, variable network traffic, presence or not of individuals in the vicinity under study, and atmospheric conditions, even mean RSS values can vary over time, leading to unacceptable performance degradation. In this thesis, several prescriptions are made to counteract these effects and maintain performance levels, including re-training of the localization model and semi-supervised learning using transductive inference. The ultimate solution is found by going back to the basics of RSS characteristics, which are known to fluctuate on a variety of time scales. By recording RSS examples dispersed over a long time window, rather than in short spurts, it reduces substantially the rate at which performance degradation occurs.

In addition to the studies on indoor localization based on GSM, this thesis also studies mobile sensor dead-reckoning and particle filter hybrid scheme that combine multiple sensors with GSM indoor localization. Using step detection and an orientation estimate based on mobile sensors applied to an adaptive stride length model, a hybrid localization system can accurately respond to small displacement of a mobile user over small time steps. A building layout map is furthermore employed to forbid solutions in which a mobile user moves to an inaccessible region, or crosses a wall, for example. In this way, room-level GSM fingerprinting results provide an absolute, but error-prone, position estimation, which can be combined with relative movements detected by mobile sensors, in order to obtain a more precise estimation of user location along a trajectory.

1.4 Structure of the thesis

In this chapter, after an initial introduction to the rich variety of location based applications and services, the indoor localization problem is discussed, wherein challenges for both beacon-based and beacon-free indoor localization techniques are explained. Then the thesis work is summarized, highlighting the contributions and improvements as compared with the previous solutions.

Chapter 2 discusses the fundamentals of indoor localization, including the measurement techniques upon which localization relies, as well as the location calculation and estimation algorithms to be explored. As there are a variety of technologies that can be used for indoor localization, there are as well different types of location estimation techniques. Common performance metrics are also presented in this chapter, which constitute a criterion for evaluating localization systems for use indoors.

Chapter 3 presents the characteristics of GSM signals, which are the basis of the indoor localization method developed in this thesis. This chapter first gives an overview of the GSM network concerning architecture, radio air interface, channel functions, and signal propagation. Then the two types of RSS measurement devices used in this thesis are introduced, followed by an evaluation of the location-specific nature and temporal properties of RSS measurements. As indoor localization in this thesis is based on using RSS fingerprints, in the last part of this chapter, RSS "fingerprint distance" is compared to standard geometric distance.

In chapter 4, the main indoor localization algorithms based on GSM fingerprints are investigated, wherein an exploration of the functional relationship between GSM fingerprints and location is first presented. Room-level indoor localization is then studied, in which different rooms within a building are distinguished by using SVM to classify measured GSM fingerprints.

The degradation of system performance over time is also evaluated here, and solutions to preserve the performance are proposed. Finally, a post-processing technique using Bayesian filtering is proposed, to employ a priori information about indoor layout and mobile's trajectory to improve the performance of the raw SVM classification.

In chapter 5, the dead-reckoning approach using mobile sensors is investigated and particle filtering is introduced, in order to combine in a unique solution information from GSM classification, sensor dead-reckoning, and map layout information.

Chapter 6 presents some complementary work that has been done within this thesis, including experiments at additional sites, GSM carrier selection, and post-processing techniques for the SVM classification. RSS from WiFi networks, as another widely available wireless signals, are also studied in the context of indoor localization.

The last chapter concludes the thesis, outlining the lessons drawn from our study, its limitations, and proposing directions for future research.

Chapter 2

Indoor localization fundamentals

2.1 Introduction

Prior to the development of modern positioning technology, various physical "signs" were used to obtain position information. An animal in a forest might leave an odor marking, for example, for use in recognizing an approximate location later on. It has long been common for man to use the positions of stars and the earth's magnetic field in order to establish directions and thereby estimate their locations.

The evolution of such "signs" is an important driving force in the development of positioning technology. GPS using Radio Frequency (RF) technology have achieved great success for outdoor localization. Precise inertial measurement devices, such as accelerometers and gyroscopes, allow missile and airplanes to localize themselves and navigate accurately. Indoors, wireless information access is now widely available, including RF signals, light and sound waves, etc., which can be explored to make location estimates in indoor environments. Micro-Electro-Mechanical System (MEMS) inertial sensors are today incorporated into tiny chips that can be integrated into the smart devices that are so popular nowadays. The main driving force behind these developments is the advancement in technologies such as wireless communication and miniature electronics allowing a panoply of exciting developments within the last decade.

Location estimation techniques differ enormously depending on the kind of technologies used and measurements made. The major location estimation algorithm types are: triangulation, proximity, fingerprinting, and dead reckoning; while possible measured quantities include time of flight (TOF), angle of arrival (AOA), RSS, link quality, sensor readings, and the like. Many challenges are still to be faced in the adaptation of these technologies for particular situations. Different algorithms have their unique advantages and disadvantages for particular application scenarios. This leads to suppose that combining more than one type of complementary positioning technique could provide better performance, which is, of course, what is actually observed in most modern localization systems.

Better performance is the constant pursuit of the researcher, and is also an urgent need for many location based applications and services, particularly for indoor applications. Accuracy might be the most important performance indicator of such a system, while meanwhile other parameters, such as coverage, complexity, robustness and cost also need to be taken into account. Indoor and outdoor environments are of course fundamentally different, which influences in a crucial way the adoption of particular localization solutions for indoor environments.

In this chapter, the common location estimation algorithms are first discussed, followed by a review of the underlying technologies of localization. Gradually, by comparing the performance metrics of localization systems based on different technologies, the field can be whittled down, allowing the methods adopted in this thesis to be selected – bearing in mind, of course, that our targeted approach is that of an RF-based system, potentially coupled with additional, complementary techniques.

2.2 Location estimation algorithms

The location of an object in space is determined by measuring some physical quantities that change accordingly to changes in position of the object. Based on the measured physical quantity that the localization approaches use, there are a variety of location estimation algorithms adapted to different localization technologies. The main categories of algorithms include proximity, triangulation, fingerprinting and dead-reckoning, each of which has its own advantages and disadvantages.

2.2.1 Proximity

Proximity, also known as connectivity or cell based localization, refers to a class of methods that provide symbolic relative location information if an object is present within the vicinity of a sensor. The proximity of the subject can be detected through physical contact, the presentation of a device such as a magnetic band to an appropriate reader, or by monitoring of a physical quantity in the vicinity of the sensor, for instance, a magnetic field.

In proximity based systems, when a mobile target is detected by a single reference point, the mobile position is associated to it. When a target is detected by more than one reference point, the mobile target's position might be referred to the reference point having the strongest signal. Centroid determination can improve results by calculating the centroid of a set of reference point positions, or alternatively a weighted centroid location can be computed, using RSS values or connectivity values as weights.

To achieve a good localization accuracy, proximity approaches rely on a dense deployment of reference points. Therefore, proximity approaches are typically implemented in systems that can detect the presence of a target but cannot obtain RSS or time measurements. In particular, the systems using Wireless Sensor Networks (WSN) [10], Bluetooth Low Energy (Bluetooth LE or simply BTLE) [11, 12, 13], RFID [14] and Near Field Communication (NFC) [15] are often based on this method. Another example is cell-identification or Cell ID, which is widely used in long range cellular networks. Cell ID uses a unique code to identify the Base Transceiver Station (BTS) in use, and the known BTS position, stored in a database, adopted as an approximate mobile node location. The advantages of Cell ID approach are that it is simple and ubiquitous and can be used without additional requirements by any device supporting cellular network technology.

2.2.2 Triangulation

Triangulation is a technique to estimate the target's location based on the geometric properties of triangles, which has two implementations: lateration and angulation. The lateration technique estimates the location of a mobile target by measuring the distances from multiple reference points. The distances can be obtained from measuring quantities like RSS and time-of-flight, which are known to be distance dependent. Quite a number of time-based estimators can be used, including Time Of Arrival (TOA), Time Difference Of Arrival (TDOA) and Round-Trip Time Of Flight (RTOF), also known as two way ranging. The angulation technique locates an object by computing angles relative to multiple reference points, which is commonly referred to as AOA.

2.2.2.1 TOA

The TOA technique computes the distance between two devices by measuring the one way propagation time between them, knowing a priori the signal propagation speed. To perform 2D localization of a mobile device, at least three TOA measurements from different reference points are required. The location estimate can be obtained using a geometric method to compute the intersection point of circles with centers at the reference points and radii corresponding to the

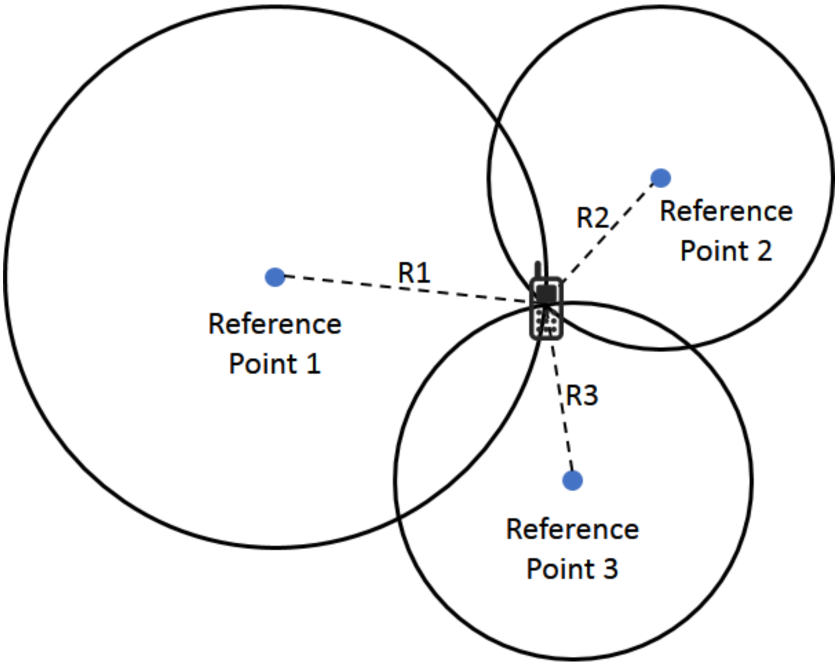

Figure 2.1 – Localization based on TOA measurements

estimated distances to the mobile device, as illustrated in Figure 2.1.

In real conditions, however, where multipath and shadowing effects occur, inaccurate distance estimation results in an area of uncertainty rather than a single intersection point. Least Squares (LS) and Maximum Likelihood (ML) estimation are the two common solutions to minimize these errors and get the best estimate of the mobile location.

Let (x_m,y_m) denote the unknown mobile target's location coordinates in a 2D Cartesian coordinate system. Also, denote the three known reference coordinates as (x_1,y_1), (x_2,y_2) and (x_3,y_3). Since the wireless signal travels at the speed of light, the distance between the mobile target and the reference point i is given by

$$r_i = (t_i - t_0)c \tag{2.1}$$

where t_0 and t_i are the time instant of signal transmission and signal reception respectively, and $c = 3 \times 10^8 m/s$ is the speed of light. According to the geometric relationship, the following set of equations is obtained:

$$d_1^2 = (x_1 - x_m)^2 + (y_1 - y_m)^2 \tag{2.2}$$

$$d_2^2 = (x_2 - x_m)^2 + (y_2 - y_m)^2 \tag{2.3}$$

$$d_3^2 = (x_3 - x_m)^2 + (y_3 - y_m)^2 \tag{2.4}$$

LS is an approach to solve this over-determined nonlinear system of equations. Let $d_i = r_i$ and subtract (2.2) from (2.3) and (2.4), whence it gives:

$$r_2^2 - r_1^2 = x_2^2 - 2x_2x_m + y_2^2 - 2y_2y_m - x_1^2 + 2x_1x_m - y_1^2 + 2y_1y_m \tag{2.5}$$

$$r_3^2 - r_1^2 = x_3^2 - 2x_3x_m + y_3^2 - 2y_3y_m - x_1^2 + 2x_1x_m - y_1^2 + 2y_1y_m \tag{2.6}$$

The above equations can be rewritten in matrix form as

$$\begin{bmatrix} x_2 - x_1 & y_2 - y_1 \\ x_3 - x_1 & y_3 - y_1 \end{bmatrix} \begin{bmatrix} x_m \\ y_m \end{bmatrix} = \frac{1}{2} \begin{bmatrix} K_2^2 - K_1^2 - r_2^2 + r_1^2 \\ K_3^2 - K_1^2 - r_3^2 + r_1^2 \end{bmatrix} \tag{2.7}$$

where

$$K_i^2 = x_i^2 + y_i^2 \tag{2.8}$$

Then, (2.7) can be written as

$$\mathbf{Hx} = \mathbf{b} \tag{2.9}$$

where

$$\mathbf{H} = \begin{bmatrix} x_2 - x_1 & y_2 - y_1 \\ x_3 - x_1 & y_3 - y_1 \end{bmatrix}$$

$$\mathbf{x} = \begin{bmatrix} x_m \\ y_m \end{bmatrix}$$

$$\mathbf{b} = \frac{1}{2} \begin{bmatrix} K_2^2 - K_1^2 - r_2^2 + r_1^2 \\ K_3^2 - K_1^2 - r_3^2 + r_1^2 \end{bmatrix}$$

If more than three TOA measurements are available, it can be verified that (2.9) still holds with

$$\mathbf{H} = \begin{bmatrix} x_2 - x_1 & y_2 - y_1 \\ x_3 - x_1 & y_3 - y_1 \\ \vdots & \vdots \end{bmatrix}$$

$$\mathbf{b} = \frac{1}{2} \begin{bmatrix} K_2^2 - K_1^2 - r_2^2 + r_1^2 \\ K_3^2 - K_1^2 - r_3^2 + r_1^2 \\ \vdots \end{bmatrix}$$

Applying the LS solution, the final estimation has the following form:

$$\hat{\mathbf{x}} = (\mathbf{H^T H})^{-1} \mathbf{H^T b} \tag{2.10}$$

Alternatively, the location of a mobile target can be estimated via maximum likelihood based on TOA measurements. The ML estimator maximizes the probability of observing the distances r_1, r_2 and r_3 giving the target location in $\mathbf{x}$ as:

$$\hat{\mathbf{x}} = \text{argmax}\{P(r_1, r_2, r_3|\mathbf{x})\} \tag{2.11}$$

With the assumption that r_1, r_2 and r_3 are independent of each other, the joint conditional probability $P(r_1, r_2, r_3|\mathbf{x})$ has the form:

$$P(r_1, r_2, r_3|\mathbf{x}) = P(r_1|\mathbf{x})P(r_2|\mathbf{x})P(r_3|\mathbf{x})$$

The distance estimations between the mobile target and the reference point i are commonly considered to have a Gaussian error distribution $N(r_i, \sigma_i)$. Consequently, the ML estimator (2.11) can be written:

$$\begin{aligned}\hat{\mathbf{x}} &= \text{argmax}\left(\frac{1}{\sqrt{2\pi}\sigma_1}e^{-\frac{(d_1-r_1)^2}{2\sigma_1^2}}\frac{1}{\sqrt{2\pi}\sigma_2}e^{-\frac{(d_2-r_2)^2}{2\sigma_2^2}}\frac{1}{\sqrt{2\pi}\sigma_3}e^{-\frac{(d_3-r_3)^2}{2\sigma_3^2}}\right)\\ &= \text{argmin}\sum_{i=1}^{3}\frac{(d_i-r_i)^2}{\sigma_i^2}\end{aligned}$$

where r_i and d_i are defined as in equations (2.1), (2.2), (2.3) and (2.4) above. The ML estimator thus turns out to be the well-known Non-linear Least Squares (NLS) estimator, which can be obtained by gradient descent algorithms, or via linearization techniques such as the Taylor series expansion [16, 17].

TOA techniques can provide high localization accuracy, but they require precise time synchronization for system transmitters and receivers. Also, the NLOS propagation of radio signals affects the time measurement accuracy, thus compromising the accuracy of TOA based localization systems. TOA techniques are commonly used in UWB systems [18, 19, 20, 21, 22], which have the inherent advantage of good penetration and insensitivity to multipath effects.

2.2.2.2 TDOA

TDOA techniques determine the relative position of a mobile target by comparing the difference of arrival time from multiple reference points. Unlike TOA systems measuring directly the time of arrival from all the reference points and calculating the distances, TDOA systems calculate the distance differences between mobile target and reference points based on time difference measurements, as shown in Figure 2.2. From the geometric point of view, given a TDOA measurement the mobile target must lie on a hyperboloid with a constant range

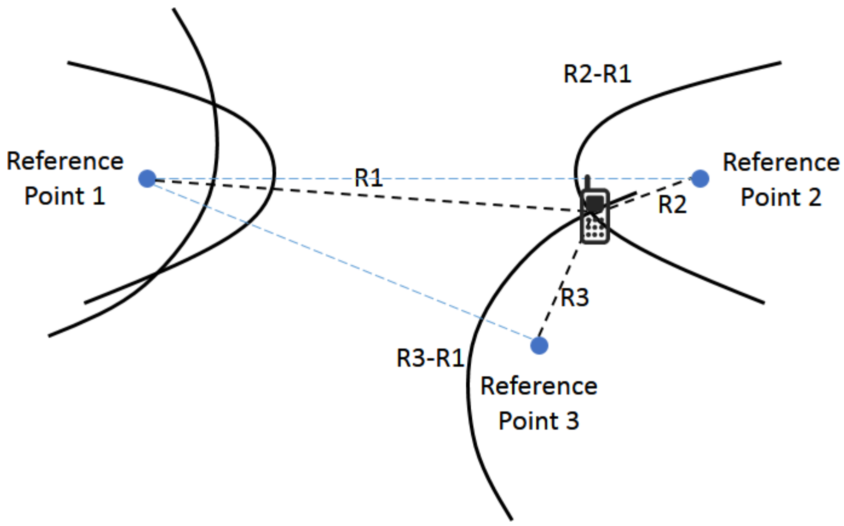

Figure 2.2 – Localization based on TDOA measurements

difference between the two reference points.

Following the symbol definitions of the mobile target and reference points above in TOA systems, the difference of distance to reference points and to the reference point where the signal first arrives is

$$\begin{aligned} d_{ij} &= r_i - r_j = (t_i - t_j)\, c \\ &= \sqrt{(x_i - x_m)^2 + (y_i - y_m)^2} - \sqrt{(x_j - x_m)^2 + (y_j - y_m)^2} \end{aligned} \tag{2.12}$$

where t_i and t_j are the time instant of signal reception from reference point i and j respectively. Similar to the solutions for the TOA, location estimation based on TDOA measurements can be obtained by solving non-linear LS problems or ML estimation.

The advantage of TDOA systems, compared with TOA systems, is that only the reference points needs to be time synchronized. The TDOA scheme is widely used in indoor localization systems based on GPS [23, 24], television (TV) [25], WSN [26] and UWB [27, 28]. It is also widely applied in 3G and 4G cellular network based indoor localization, since the base stations are time-synchronized in these networks [29, 30, 31].

2.2.2.3 RTOF

The RTOF technique, which is also known as two-way ranging, determines the distance between the mobile target and the reference point by measuring the complete round-trip TOF of signal between the transmitter and the receiver. RTOF processing is algorithmically identical to that used in radar systems, although in RTOF systems the receiver unit performs some signal processing instead of simply reflecting a radar pulse.

The RTOF technique is widely used in UWB systems [32]. Similarly to TOA, RTOF uses the absolute signal propagation time to calculate the distance. Location estimation algorithms for TOA can be directly applicable to RTOF; however, precise clock synchronization is not required for RTOF systems, as it is for TOA based systems.

2.2.2.4 RSS-based lateration

The RSS-based approach estimates the distance between the mobile target and multiple reference points using the attenuation of the emitted signal strength. Time synchronization is difficult to obtain for a wide variety of devices that are not dedicated exclusively to localization; however the received signal power measurement function is relatively standard, since mobile devices need to regularly assess the quality of signals they receive in order to establish effective wireless communication links. As a result, RSS-based lateration is very popular in WiFi [33, 34, 35], Bluetooth [36], RFID [37] and UWB [38].

RSS-based methods attempt to estimate the signal path loss due to propagation. For outdoor environments, the relation between signal strength and distance can be approximated by the Log Distance Path Loss (LDPL, see section 3.2.4) model [39]. However, for indoor environments, the shadowing and multipath environment becomes very complex. Consequently, long range signals are not well-suited to RSS-based lateration, since pathloss attenuation is difficult to determine. For short range signals, propagation path modeling can be modified to take into account obstacles in order to improve the performance by better estimating distances.

Once the distances are estimated based on RSS, the rest of the location estimation procedure is the same as in TOA based systems.

2.2.2.5 AOA

AOA is an angulation technique used for localization that estimates the location of a mobile target as the intersection point of pairs of hypothetical signal paths along particular angles, as shown in Figure 2.3. To localize a target in a 2D plane, the AOA approach requires only two reference points, while for for 3D localization, three are needed. To improve accuracy, three or more reference points can also be used, in a technique referred to as multi-angulation. To obtain angle measurements, a directional antenna or antenna array is required [40, 41].

The advantage of AOA systems is that they require fewer reference points, as compared with lateration techniques, to determine the location of a mobile target. In addition, time synchronization between transmitters and receivers is not needed. However, AOA systems

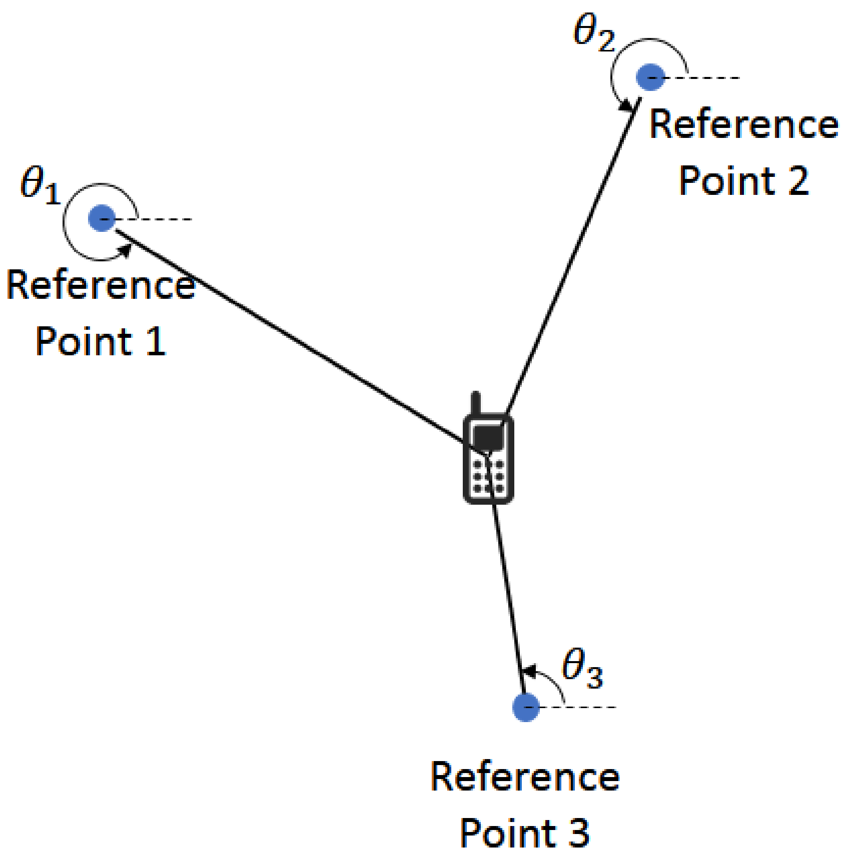

Figure 2.3 – Localization based on AOA measurements

necessitate relatively complex hardware to obtain angle measurements, which makes it applicable only for localization-dedicated devices. Moreover, the precise angle measurements that AOA systems rely on are difficult to obtain in multipath indoor environments.

2.2.3 Fingerprinting

The above-mentioned localization techniques rely heavily on the estimation of distances between mobile target and the references. Obtaining time and angle measurements is a function that is absent from most mobile devices in everyday use. Moreover, the complex indoor environments make it difficult to accurately derive distances from measurements made on narrow band signals. Nevertheless, in many indoor environments, some location dependent signal characteristics tend to remain relatively stable over time. The fingerprinting technique is based on this observation, attempting to match real time characteristics of an RF signal to a previously constructed map of RF environment in a particular area. RSS is the measured quantity most often associated with fingerprint based systems, although propagation time, channel impulse response, or inquiry response rate measurements, and the like, can also be used.

The fingerprinting approach is performed in two phases. The first is offline and is known as the training or calibration phase. In this phase, position-tagged RSS values over a wide range of positions are recorded, and used to construct a model relating RSS to position. The locations at which measurements are performed can correspond to grid points, specific reference points, or regions, depending on the targeted application and desired accuracy. The second phase is the online localization phase, in which measurements are recorded online and sent to the localization model previously developed in the offline phase, which provides a location estimation. Fingerprinting techniques commonly make use of classification algorithms such as Bayesian inference, k-Nearest Neighbors (k-NN), neural networks, or support vector machines, in order to supply a location estimate for a fingerprint example.

Fingerprinting is widely used in the localization systems based on WiFi, Bluetooth, RFID and cellular networks, since RSS measurements are easier to access than precise time measurements like TOA, TDOA and RTOF. An important drawback of fingerprinting techniques is the necessity of creating and maintaining a localization model. The entire site of interest needs to be surveyed in advance for this purpose, recording the RSS and labeling the location, which is of course a time and labor consuming task. And since the signal measurements acquired are quite variable and noisy, it is necessary to record as many measurements as possible in each location area, so that the training set takes into account as much as possible the large diversity of possible fingerprints and adequately models their distributions. Moreover, due to changes in environmental effects, such as building geometry, network traffic, presence of people, atmospheric conditions, etc., RSS is expected drift over time, which can degrade localization performance.

2.2.4 Dead-reckoning

Dead reckoning is the process of estimating an unknown current position based on the last determined position modified by a displacement calculated from velocity and heading information over an elapsed time step, as shown in Figure 2.4. Dead-reckoning has drawn increasing attention for indoor localization, since it relies only on sensors which are widely available in standard modern mobile devices.

Inertial navigation is based on the dead-reckoning principle, whereby speed is computed based on accelerometer readings, and orientation is determined by gyroscopes and magnetic field measurements. The time integral of acceleration yields a continuous estimate of the instantaneous speed of the target, if the initial speed is known. With a second integration the

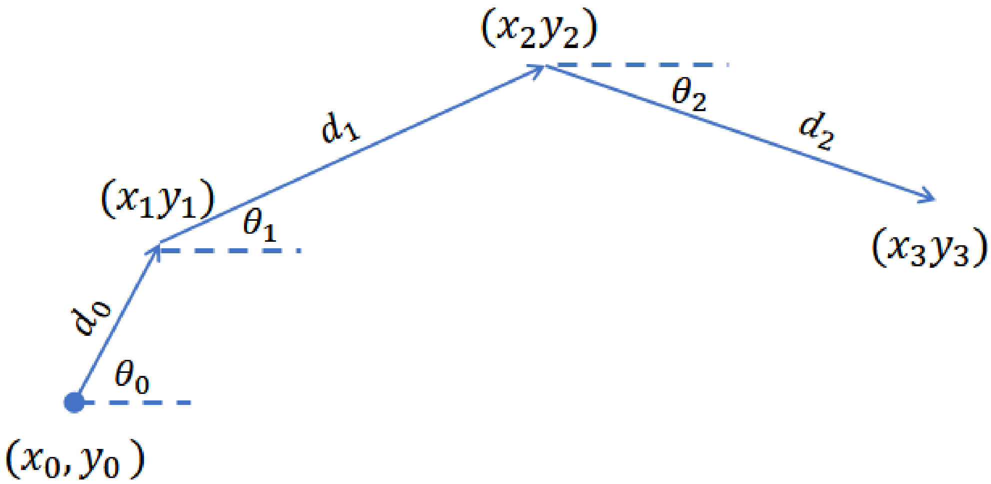

Figure 2.4 – Location estimation based on sensor dead-reckoning

displacement with respect to a starting point can be obtained as:

$$\vec{p}(t) = \int_0^t \vec{v}(\tau)d\tau = \int_0^t \int_0^\tau \vec{a}(x)dxd\tau \tag{2.13}$$

where $\vec{p}(t)$ is the displacement vector, $\vec{v}(\tau)$ is the instantaneous speed and $\vec{a}(x)$ is the acceleration from the sensor reading. The heading can be obtained in the same way by integrating the gyroscope sensor readings as:

$$\theta(t) = \int_0^t \omega(\tau)d\tau \tag{2.14}$$

where $\theta(t)$ is the angle of rotation with respect to the previous azimuth angle and $\omega(\tau)$ is the angular velocity obtained from the sensor reading.

At the same time, magnetic field provides an absolute angle value between target heading and the geomagnetic North Pole. Usually the magnetic field orientation is robust over time, but susceptible to interference, while gyroscope readings, although very sensitive, suffer from severe error accumulation due to integrating angular velocity over long time periods. In practice these two sensors are combined using complementary filters to generate a more accurate azimuth angle estimation.

Unlike the conventional inertial navigation systems used in aircraft, indoor dead-reckoning is quite different in both speed and orientation estimation. While walking in indoor environments, the mobile device moves about following the rhythm of a walking pace, and, consequently, the accelerometer will record periodic up-an-down accelerations, rather than a gradual change as might be expected for a jet or rocket engine. This fact allows displacements to be estimated via step detection and stride length estimation. In addition to displacement estimation, orientation is also needed to determine the mobile location, which, for mobile sensors, is the same as that of the conventional inertial navigation systems. Nevertheless, the orientation obtained by the embedded sensors corresponds to the mobile device itself, and is not necessarily the same as the orientation of the user, who may carry in a pocket, or in the hand in various configurations, which adds another challenge to the localization problem.

2.3 The technologies for localization

The technologies for localization can be categorized into RF, light wave, acoustic wave and MEMS sensor based, which are categorized in Figure 2.5. Since the thesis aims to study indoor localization approaches based on the RF and MEMS sensors, an overview of the localization solutions based on these technologies is emphasized.

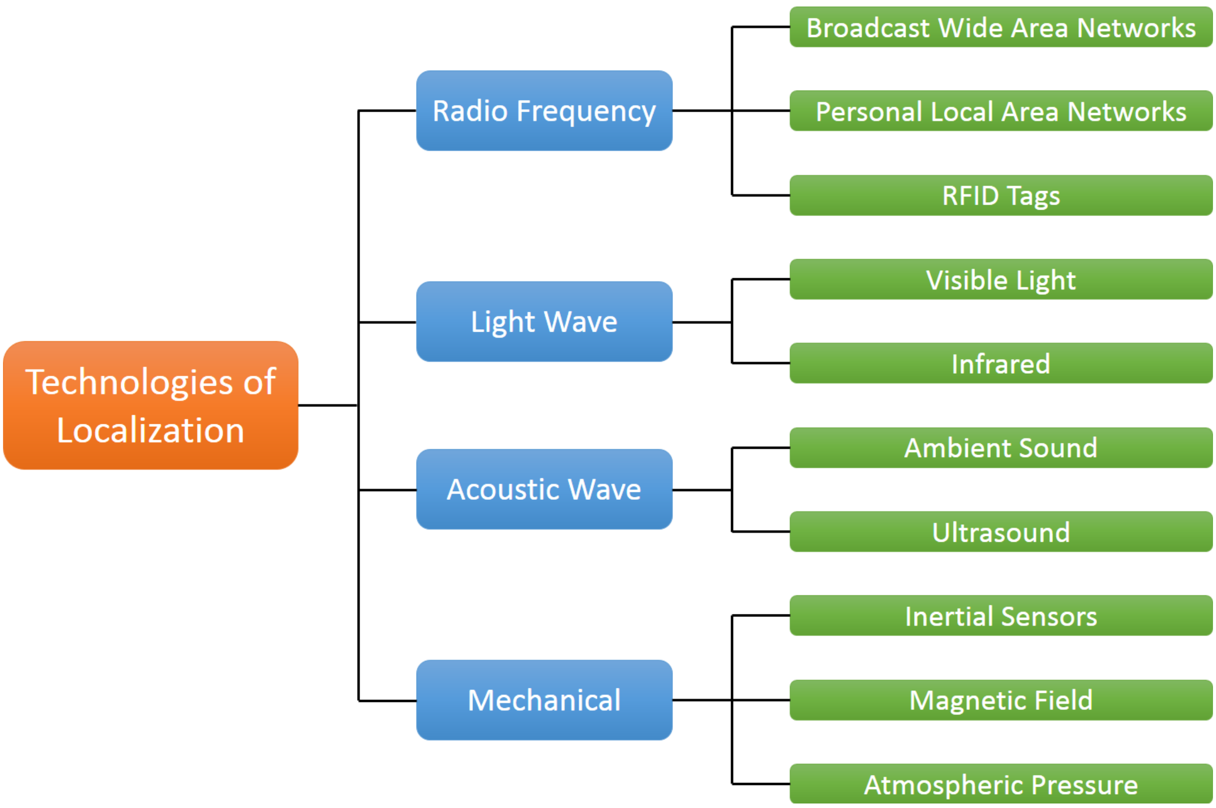

Figure 2.5 – Categories of the main technologies for indoor localization

2.3.1 RF technologies

RF is the most widely used technologies for indoor localization, including broadcast Wide Area Networks (WAN), Wireless Personal Area Networks (WPAN), RFID tags, NFC etc. WAN include GPS, cellular networks, TV and FM radio signals, while WiFi, Bluetooth, WSN and UWB belong to the WPAN family.

2.3.1.1 GPS

GPS is thus far the most successful dedicated localization system, which provides world-wide users with accurate and reliable positioning and navigation services in outdoor spaces [7]. However, the poor coverage of GPS signal in indoor environments makes it unusable in indoor environments. As a result, different approaches were proposed to overcome the shortcoming of GPS indoors, and render it feasible for indoor localization.

Early efforts focused on improvement of the sensitivity of GPS receivers to help track weak signals, including new hardware designs and assisted GPS techniques [42, 43, 44, 45]. These efforts improved the localization accuracy of the GPS, allowing, in one test, to obtain an accuracy of 6 to 16 meters inside a residential building consisting mostly of wood and concrete stucco [46]. Such approaches, however, are far from adequate in more complex indoor environments where GPS signals are totally blocked. Another type of solution is to deploy local stations and antennas that repeat GPS-like, signals, known as GPS pseudolites and repeaters [47]. GPS pseudolites transmit signals with code-phase, carrier-phase, and data components in the same timing and format as the GPS signals. An indoor GPS receiver can then acquire this signal and derive code-phase, pseudo-ranges or carrier-phase measurements for localization exactly as it would outdoors. Sub-centimeter indoor localization accuracy was reported in [23] indicating such approach is promising for accurate indoor localization. As the name implies, GPS repeater solutions broadcast ranging signals in indoor environments by replicating the GPS constellation's functions. In [24], using sequential switching GPS repeaters and a modified open delay-lock loop GPS receiver architecture, sub-metrical accuracy was achieved.

Though GPS pseudolites and repeaters are accurate for indoor localization, they are somewhat specialized as of today; furthermore they require precise time synchronization, and suffer from the multipath signal propagation problem common to narrow band signals.

2.3.1.2 Cellular networks

A cellular network is a long range wireless network distributed over regions known as cells, each served by at least one fixed-location transceiver, called the base station. Cellular communication technology has many technical standards, which are classified and named according to their generation, such as 2G, 3G and 4G. Localization systems based on cellular networks benefit from good indoor signal penetration, wide coverage, existing infrastructure, long term operational stability, and multiple frequency bands. Furthermore, cellular networks have relatively uniform standards across the world and are supported by a large number of mobile communication devices.

Among the cellular networks, GSM is thus far the most widely deployed cellular telephony standard in the world. GSM systems employ the Frequency Division Multiple Access (FDMA) scheme to divide the frequency band into a number of GSM channels. RSS is a simply measurable quantity for GSM signals, featuring strong spatial variability and relative consistency over time [8]. Zimmermann et al. [48] proposed a database correlation method for positioning mobile terminals in urban outdoor environments based on GSM networks, which compares the measured RSS from the current serving cell and six neighbor cells with a RSS-position look-up-table defined a priori, during the network planning process. The location accuracy of [48] tested in the urban scenario is in the range of 80 meters in 67% of the measurements and 192 meters for the 95% percentile. In [8], indoor localization was achieved using the k-NN technique to match online GSM fingerprints to a fingerprint database recorded offline prior to the experiment, where each fingerprint was made up of the RSS values from 35 GSM channels. A median localization accuracy ranging from 1.94 to 4.07 meters was achieved in large buildings, within a single floor, and the approach was able to identify the floor correctly 60% of the time, and be correct within 2 floors fully 98% of the time. A study in [9] went further, incorporating RSS from carriers of the entire 900 MHz and 1800 MHz GSM bands into the fingerprint, using SVM classifiers to handle the high dimensionality while classifying fingerprints with room labels. In this case, the correct room could be determined, in two separate indoor environments, 98% to 100% of the time, but only with a limited number of fixed positions within the rooms.

In CDMA-based networks, such as the 3G network UMTS, transmit power is controlled in order to accommodate network load, which affects RSS consistency and therefore limits the practicality of traditional fingerprinting approaches based on RSS measurements for such networks. Rehman et al. [49] nonetheless proposed a CDMA indoor localization system, named CILoS, which applies fingerprinting technique based on signal delay rather than the RSS. Since CDMA base stations must remain tightly synchronized with each other, fingerprints in CILoS consist of the relative time difference at which signals emanating from different base stations are received at a given location. With the k-NN technique, the location estimation had a median accuracy of 5 meters. However, the fingerprint in [49] is rather sparse, containing only 6 pseudo random noise delays, which is potentially inadequate to distinguish large amount of locations. Furthermore, the poor indoor penetration is another challenge for the 3G network UMTS.

Though in 3G and 4G networks timing based localization approaches and even dedicated positioning reference signals are introduced, the localization accuracy is influenced by radio environment such as signal attenuation and multipath propagation, network topography (density of base stations) and geography, resulting in localization accuracy in some instances varying from tens to hundreds of meters [29, 30, 31]. Gentner et al. [50] however proposed an indoor localization solution with 3GPP-LTE femtocells, using a particle filter to correct TDOA measurement errors, and obtaining a median accuracy of 5.35 meters. The result is not appropriate for a generally practical scenario, since the four femtocells in the experiment are hardware-customized and manually placed. A significant problem for indoor localization using 3G and 4G networks, though, lies in the fact that 3G and 4G networks operate in relatively high frequency bands, and thus they have poor indoor penetration. While this thesis was in progress, however, 4G adopted the 800 MHz frequency band for the first time, on 29 August 2013, which could once again become interesting for indoor localization. It is predicted in [51] that precise localization can be harnessed in the coming 5G networks, achieving an accuracy on the order of one meter.

2.3.1.3 TV and FM radio

TV and FM radio networks were obviously not originally designed for localization, but they can nevertheless be adapted to provide indoor localization services. They are in some ways similar to cellular networks, as the signal properties and geometrical arrangement of the TV and FM broadcast network have been designed to penetrate well indoors, and they clearly offer greater indoor coverage than GPS-based solutions. Implementation of a localization solution would also require no modification of the existing broadcast signal.

As the TV transmission is becoming digital, synchronization signals are commonly included in TV networks, which can be used for accurate indoor and outdoor localization. Rabinowitz and Spilker [25] made use of considerable Digital TV infrastructure to achieve reliable and accurate positioning. In order to obtain the precise timing of the TV synchronization signals for accurate location computation, monitor units at known positions are used to independently monitor the TV station clock offsets, in the cases when the TV transmitters do not broadcast the clock offset information. In the outdoor tests, 3.2 and 12.3 meters median accuracy was obtained in two sites with standard deviation of 2.6 and 8 meters respectively, and in two indoor environments, the median accuracies are 10.3 to 23.3 meters with standard deviation of 4.4 and 19.6 meters.

Despite its considerable age, FM radio is still very popular. FM radio networks operate in the 100 MHz frequency band, with exact range varying from different regions. Like GSM systems, FM radio uses the FDMA approach, which splits the band into a number of separate frequency channels that are used by different radio stations. As a result, RSS fingerprinting technique is a common practice for FM radio based indoor localization [52, 53, 54], with the mean distance error found to be 3 to 4 meters.

The major drawback for TV and FM radio based indoor localization solutions, of course, is that special antenna and devices are required, which severely limits the application of this technique for mobile devices. In addition, with the emergence of Digital Audio Broadcasting as its next generation, FM radio could be replaced worldwide someday, as it has already in some countries.

2.3.1.4 WiFi

WiFi is technically an industry term that represents a type of WPAN protocol based on the 802.11 IEEE network standard, operating in the 2.4 and 5 GHz Industrial, Scientific and Medical (ISM) radio bands. It is the most popular means of communicating data wirelessly and is widely used for home, enterprise and public hot spots. It currently operates at a data rates of up to 1300 Mbit/s and has a range of approximately 70 meters. With the increasingly deployment of WiFi hot spots in both home and public indoor environments, indoor localization using WiFi infrastructures is being intensively studied.

The vast majority of indoor localization based on WiFi networks involves using the two-stage fingerprinting technique, i.e., an offline "training" step followed by "online" testing [55, 56, 57, 58, 59, 60, 61]. The offline WiFi fingerprint database is typically made up of RSS values from a number of WiFi Access Points (AP). In [58], the fingerprints were recorded in four orientations to help differentiate locations and roughly estimate user orientation, since the human body affects the propagation of WiFi signals, and the RSS recorded facing different orientations will be different. Location estimation is usually based on finding the best match between an online recorded RSS fingerprint and a fingerprint stored in the training database [55, 59, 60, 58, 61]; however, more complex classification techniques such as neural networks [57] and SVM [56] can also be used.

The main drawback of any fingerprinting approach is that it requires the time and labor consuming site survey training stage; however, crowd-sourcing and "calibration-free" solutions have been proposed to help circumvent this difficulty. Rai et al., for example, [62] proposed an inertial sensor based crowd-sourcing approach, which uses a particle filter to track mobile devices as they traverse an indoor environment, while simultaneously performing WiFi scans. Wu et al. [61] designed a wireless indoor localization system without site survey, which uses the room map and a accelerometer to help recognize different rooms.

There are also WiFi indoor localization approaches based on signal propagation modeling instead of fingerprinting calibration [33, 34, 35]. These commonly adopt the LDPL model to estimate distances from RSS values, finally using triangulation to estimate the location of a mobile node. The parameters of the LDPL model were hard-coded in [33], linearly fitted in [34], and calculated when the GPS is available, for example, when near a window [35].

WiFi indoor localization accuracy presented in the literatures is commonly of the order of a few meters in some 90% of the time (4 meters in 95% of the time [56], 3.3 meters in 98% of the time [57], and 2 meters in 90% of the time [58]). The biggest challenge for such approaches, however, is the non-stationarity of WiFi RSS [63, 8]. This is reflected in the RSS-distance relationship, in that while the mean RSS versus distance over a large number of examples may fit the LDPL model well, the distance obtained from a single RSS measurement could in fact have a very large error. Thus, as in the case of WiFi fingerprinting, the instability of WiFi signals results in the failure of the RSS-to-distance function, requiring time and labor consuming re-calibration.

2.3.1.5 Bluetooth

Bluetooth is another wireless standard for WPAN and also operates in the 2.4 GHz ISM band. It has a wide variety of applications, and has boosted the convenience and functionality of portable devices by providing a simple way for them to interact with each other. Bluetooth employs frequency hopping technique with 1 MHz wide channels, which is less sensitive to strong narrow band interference [64]. However, Bluetooth suffers severe interference from other devices operating in the same radio bands.

Many of the localization techniques used on WiFi networks are also applied to Bluetooth, with RSS based fingerprinting and triangulation the two principal techniques adopted for Bluetooth indoor localization [65, 66, 36]. In [65], RSS and the mobile's orientation were measured as a mobile device connects to each Bluetooth node; multiple neural networks were then used to build a localization model. Subhan et al. [36] proposed a hybrid approach that combines RSS fingerprinting and RSS-based lateration. In [36], RSS fingerprinting results are used to estimate the parameters of the LDPL propagation model, and coordinate positions are obtained by RSS-based lateration using the obtained LDPL model. Compared with WiFi, Bluetooth uses a lower transmit power (below 10 dBm), has a shorter nominal range (around 10 meters) and is lower in price, which allows for dense deployment of Bluetooth tags for indoor localization. For example, Chawathe [11] used a large number of inexpensive Bluetooth beacons to make a cell-based indoor localization system that determines the intersection area of visible beacon ranges. Nonetheless the localization accuracy of Bluetooth rivals that of WiFi [65, 66, 36]. The clearest challenge for Bluetooth systems is latency, as standard Bluetooth requires more than 10 seconds to carry out an inquiry process [12]. Too, supplying power supply to a set of densely deployed Bluetooth tags can be problematical.

Perhaps more promising for indoor localization is the recently introduced BTLE [67]. As the name implies BTLE features ultra-low peak, average and idle mode power consumption, thereby extending the use of Bluetooth wireless technology to devices that are powered by small, coin-cell batteries such as those used in smart watches and wearable sports and health care devices. In indoor localization, BTLE technology makes it possible to operate localization tags for more than a year on such batteries. Another improvement is that BTLE greatly reduces the inquiry time, using only three channels for advertising, messages, and establishing a connection in only a few milliseconds. In addition, BTLE provides an enhanced range, which can be optimized for different application scenarios.

Apple iBeacon [13] is a typical application that extends location services in Apple mobile devices based on the BTLE technology. It uses a proximity technique, which, instead of giving longitude and latitude coordinates, determines if a mobile device is in or out of the range of an iBeacon and monitors the distance as their proximity changes over time. The iBeacon technology is not unique to Apple, however, as all recent Android devices also support such solutions. For instance, the TI SensorTag [68] is a generic BTLE product supporting both Apple iBeacon and Android mobile devices. In addition to the solutions based on standard BTLE tags, NOKIA research center [40] developed a High Accuracy Indoor Positioning (HAIP) technology based on AOA of Bluetooth signals. It uses a modified version of BTLE with custom antennas to enable cost efficient and highly accurate indoor positioning, achieving 0.5 meter positioning accuracy.

2.3.1.6 WSN

WSN consist of small nodes, which are low-power devices equipped with processor, storage, a power supply, a transceiver, and one or more sensors and, in some cases, with an actuator. Each node is able to sense the environment, perform simple computations and communicate with other nodes or to a centralized serving unit. Typically the deployment of a WSN is obtained by "scattering" the nodes throughout some space of interest, thus making the network topology random. Ad hoc networking techniques are often employed, thus obviating the need for a central router or wireless base station. WSN can use a number of off the shelf wireless technologies, such as Bluetooth, ZigBee, WiFi, UWB, although most applications make use of IEEE 802.15.4 and ZigBee [69].

Localization is an important application aspect and also a basic need for WSN. In WSN, some sensor nodes, known as anchors, are aware of their own positions, while the localization problem is to determine the location of other nodes based on the location references obtained from the anchors [70]. Quite a number of studies using WSN for localization have appeared in the literature [71, 26, 72, 73, 74, 75, 10]. Localization in WSN commonly consists of estimating distances or angles between nodes and combining these in a location estimation algorithm. Measured quantities include connectivity, RSS, timing, and angle, while the most popular location combination algorithms are trilateration and ML estimation [76].

2.3.1.7 RFID and NFC

An RFID system is commonly composed of a reading device that can wirelessly obtain the electronically stored information of tags present in the environment in the recognizable region. The reader contains a transceiver to transmit RF signals and read the data emitted from the tags. The tags present in the environment reflect the signal, modulating it by adding a unique identification code. The tags can be passive, drawing energy from the incoming radio signal, or it can be powered by a battery. RFID systems operate in four frequency bands: Low Frequency (LF) (125 kHz), High Frequency (HF) (13.56 MHz), Ultra-High Frequency (UHF) (433, 868–915 MHz), and microwave frequency (2.45 GHz, 5.8 GHz). As RFID can detect and recognize nearby tagged objects, it can be used for localization and tracking.

RFID systems share most of the deployment schemes and positioning algorithms cited for short range Bluetooth and WSN introduced above, and have comparable localization accuracy [77, 78]. In [14], Montaser and Moselhi adopted a weighted proximity approach to localize a moving RFID reader, where RSS from passive RFID tags are used as weights to calculate a barycenter. Ni et al. [79] presented the LANDMARC localization system based on the RSS fingerprinting approach using k-NN algorithm. Ko et al. [37] developed a 3D location sensing algorithm using RFID technology based on RSS. The distances between a target tag and multiple RFID readers are first estimated based on the RSS, and then tag location is calculated based on the gradient descent method. In [41], a passive UHF RFID system was proposed based on AOA, where, instead of using RSS, the more robust phase characteristics were used to estimate the angles.

NFC, as a specialized branch within the family of RFID technologies, specifically the HF RFID, has drawn attention recently since it is now available in the majority of mobile phones. NFC is designed to be a secure form of data exchange over very short distance (5 centimeters or less). Localization can be accomplished with NFC by putting a number of tags at places of interest, where location is reported simply by touching the tag with an NFC equipped device [15]. NFC also supports two-way communication and can be used for peer-to- peer content sharing. It is thus attractive for application scenarios such as in museums, which, in addition to letting the visitors localize themselves, can provide the information about exhibitions as well.

2.3.1.8 UWB

UWB transmits very low power radio signals using extremely short electrical pulses, typically in the picosecond range, which have a very broad spectral profile, of 500 MHz or more. An emitted radio wave is considered to be UWB if its bandwidth exceeds 500 MHz or 20% of the carrier frequency. The high bandwidth allows UWB to support high wireless data rates of 480 Mbps up to 1.6 Gbps, over distances of several meters.

UWB has inherent advantages for indoor localization. First of all, UWB typically consumes very little power. Also, unlike narrow band signals, UWB systems can also penetrate effectively through dense materials, and the very short duration of UWB pulses renders them less sensitive to the multipath effect as well [80]. Location estimation based on UWB waves can be very accurate due to the possibility of precise time measurements of the propagation times of UWB pulses. Bocquet et al. [81] proposed an Enhanced TDOA (E-TDOA) measurement technique for indoor localization, considering a Differential Impulse Response (DIR) in the TDOA domain, which mitigates the multipath to only measure the LOS TDOA contribution. Localization precision less than 1 meter has been reported [18, 19, 20, 21, 22, 27, 28]. In addition, RSS-based lateration approach based on UWB infrastructure is reported to have the equivalent accuracy, between 0.1

and 0.2 meters [38]. In [82], a passive person-detection and localization approach is proposed using off-the-shelf UWB devices. UWB appears to have a bright future for accurate indoor localization, but for the present is not in widespread use on standard mobile devices.

2.3.2 MEMS

MEMS is a technology that combines computers with tiny mechanical devices such as sensors, valves, gears, mirrors, and actuators embedded in semiconductor chips. Traditional inertial navigation devices such as the accelerometers and gyroscopes used in navigation for decades are too bulky to use in indoor localization. MEMS enables localization applications by integrating multiple sensors into a small chip embedded in mobile devices such as smart phones and wearable devices.

Indoor localization based on inertial sensors is referred to as sensor dead-reckoning, which makes use of the same techniques as those developed for airplanes and ballistic missiles. The current position of a target is calculated based on a previously determined position plus a displacement estimated over elapsed time and path step. The relevant timescales of inertial events in embedded applications, of course, are entirely different from those encountered in navigation. When users walk in an indoor environment, their speed is comparatively slow, and there are alternative intervals of walking and rest. As a result, vertical acceleration changes are usually greater than horizontal ones, with the result that accelerometers are commonly used for step detection rather than speed estimation. Acceleration-based step detection typically relies on the peak detection [83] or zero-crossing [84] approaches, which can be improved through the use of time and amplitude thresholds [85, 86]. There are also gyroscope based step detection approaches [87], in which a foot-mounted gyroscope detects the swing of leg. The displacement of a mobile user is estimated based on step detection, step length estimation, and the detected direction of movement. Since step lengths may vary from person to person, and any given person may adopt different walking modes, a constant step length value can result in the accumulation of very large errors over time. In [85] step length estimation is based on a model constructed with the amplitude of acceleration, and in [84, 86] on the walking speed. Orientation can be obtained from the magnetic field value or by integrating gyroscope readings for foot-mounted sensors; however it remains a challenge for sensor dead-reckoning using standard mobile devices. In [85] the accuracy of orientation estimation was improved by using two or more set of sensors carried by one person and performing sensor fusion. Li et al. [86]

considered a special case when the mobile phone is in a trouser pocket, using the acceleration zero-crossing as a ground truth to compute the heading orientation while walking.

In short time period, the location estimation based on sensor dead-reckoning can be very accurate, but with increasingly severe error accumulation caused by drift of sensors and misdetection of steps. As a consequence, MEMS sensors are unlikely to be a standalone solution for indoor localization, but it is interesting to combine it with other localization approaches being a hybrid approach to produce a more accurate location estimation. Alternatively, map information is usually used as a constraint to exclude impossible locations estimated based on sensor dead-reckoning. In [88] and [89], particle filters are introduced for map matching, which combines sensor dead-reckoning results and the map layout information.

2.4 The performance metrics

As introduced above, there are a variety of technologies and techniques that can be adopted to build an indoor localization system. Localization performance is the crucial element for both localization service providers and users. Accuracy of location estimates, although very important, is not the only performance indicator. Indeed, robustness, complexity, scalability and cost in the adopted solutions are also crucial metrics to be considered.

2.4.1 Accuracy and precision

The accuracy of a localization system relates to the difference, defined in some metric, between a location estimate and the true target location. The precision relates to reproducibility and repeatability, and indicates the degree to which repeated location estimates, under unchanged conditions, will produce identical results.

Mean distance error or Root Mean Squared Error (RMSE) is usually used as the accuracy indicator, revealing the potential bias or systematic offset of a localization system. The accuracy of a localization system is desired to be high, but to attain high accuracy is usually costly. For example, in fingerprinting scenarios, the higher the accuracy, the more finely the location units need to be subdivided and surveyed in order to make a radio map. Consequently, there is often a trade off between accuracy and other practical considerations.

Precision provides the knowledge of how consistently a system works. It indicates how convergent the localization results can be over many trials. Theoretically, location precision is the performance indicator of the location estimation itself, which has no relationship to the true location. However, usually location estimates are assumed to follow a Gaussian distribution, with the mean centered at the true location. Under this assumption, higher precision means a larger fraction of location estimates are will be located near the true location. Indeed, a preferable approach to indicate the degree to which location estimates accumulate near the true value of the position, is the Cumulative Distribution function (CDF). The CDF describes the distribution of the distance error between the estimated location and the true location. Thus when two positioning techniques are compared, if their accuracies are the same, we shall prefer to exploit the CDF of them.

2.4.2 Robustness

Robustness of a localization system is very important, as it allows the system to function normally without human intervention when the operating environment changes. For example, some signal transmitters could be out of service occasionally; or, room layout changes could cause some signals to no longer propagate in an LOS fashion. RSS is time varying due to environmental effects. In such a case, localization systems are obliged to deal with incomplete or noisy information in order to estimate location. Creating and maintaining a localization system is expensive in terms of time, labor and monetary cost. Thus, when such a localization system is built, the hope is that it will continue to operate properly for a long time. Robustness can be achieved, for example, by introducing redundant information into a location estimation. Thus for triangulation, rather than using the minimum required number of reference points, including many supplementary points can help make the system more robust. Fingerprinting approaches, in turn, can adopt a larger set of RSS values in order to increase robustness.

2.4.3 Complexity

The complexity of a localization system concerns both hardware and software. As for hardware, it will depend on the adopted technology and chosen measured quantity. If a certain technology is already to a great extent present, with an existing infrastructure and a panoply of available mobile devices, it becomes simple to deploy and use. Cellular networks, WiFi and Bluetooth, for example, are generic wireless technologies, and most mobile devices support at least one of them. In contrast, such technologies as UWB and ultrasound are not supported in standard mobile devices. If a localization system is to use UWB or ultrasound, most likely it is a dedicated system requiring proprietary equipment. Regarding the chosen measured quantity, it is relatively easy to obtain RSS with standard mobile devices, since this ability is typically needed for the routine functioning of such devices. Conversely, accurate time and angle measurements are not easy to obtain, which increases the complexity of a localization system. As for software, complexity is in part reflected in the computation load represented by the calculations required to perform localization. If the execution of the positioning algorithm is carried out on a centralized server, the positioning could be calculated quickly due to its powerful processing capability and abundant power supply. If it is instead carried out on the mobile unit itself, the effects of complexity could be more evident, as most mobile units employ less powerful processors powered by batteries. Sometimes, complexity must be compromised in favor of other desirable characteristics, such as high accuracy, for example.

2.4.4 Scalability

A localization system with good scalability is supposed to function normally when the scale of required positioning capability increases. When an indoor localization system is constructed, it of course provides services in a limited area. Or, in some cases, its user capacity could be limited by bandwidth and processing time considerations. At some future time, though, an upgrade might be needed, to extend coverage or increase user capacity, let us say. Scalability means that the system does not need to be taken down and totally rebuilt in such a scenario. Typically, the coverage areas of localization systems based on proximity and triangulation are easy to expand by simply adding additional, identical hardware, or increasing transmit power. Fingerprint based systems, however, which necessitate an offline site survey stage, have relatively low scalability. Adding new signals into fingerprints, for example, would necessitate a re-calibration of the entire system.

2.4.5 Cost

The cost of a localization system refers not only to monetary outlay, but also to questions of time, effort, space and energy. It depends on many factors, including how the system is built, the required accuracy, and the size of desired coverage area. Some signals such as GSM and WiFi have already been extensively deployed for other purposes, but can still be used for localization. If a localization system is based on existing infrastructure, substantial savings in infrastructure costs can be realized. The time and effort factor relates to system installation and maintenance procedures. Consequently, if a localization system is robust and scalable, a saving in time and labor may be possible. Space is another consideration in that many indoor localization systems require a dense deployment of dedicated beacons, which may be difficult to realize in certain indoor environments. Power consumption is also a critical issue, for both fixed reference nodes and mobile nodes. Due to the space constraints, the reference nodes may not always be plugged into mains, and battery life is always a concern for mobile users. There are many factors involved in power consumption considerations. For example, Bluetooth is less power hungry than WiFi. Also, if the location estimation is carried out on the server side, the power consumption of the mobile devices can be reduced. Finally, the desired system accuracy and location update rates will also influence battery life.

2.5 Summary

This chapter reviews the technologies that indoor localization can be based on, the fundamental methods for location estimation and some key metrics to evaluate a localization system.

Indoor localization is a challenging task and various technologies are considered to deal with this challenge in complex indoor environments. Current indoor localization systems are mainly based on the radio frequency technologies such as GPS, cellular networks, WiFi, Bluetooth, RFID and UWB, but there are also solutions based on light waves and acoustic waves. In addition, mobile sensors are becoming more and more popular in mobile devices, and can provide an additional complementary source of information for beacon based systems. The adoption of location calculation and estimation algorithms depends predominantly on the selection of a localization technology and a set of physical quantities to measure (time, RSS, etc.). There are four categories of location estimation approaches: proximity; triangulation; fingerprinting; and sensor dead-reckoning. Performance metrics are used to evaluate a localization system in different aspects, determined by the chosen localization technology, the measured quantities selected, and the location estimation algorithm adopted. As some performance metrics are conflicting, it is reasonable to make some compromises in a practical deployment of an indoor localization system.

Of course, not all technologies and measuring quantities are easily available on standard mobile devices, even though these may achieve very good localization performance in many respects using their inherent capabilities. Among the variety of possible RF technologies that common mobile devices support, this thesis adopts the use of the GSM system, to explore its feasibility and performance as a practical indoor localization system. Indeed, compared with other solutions, indoor localization based on GSM has the following advantages:

- GSM signals are near pervasive, much more so than the typical 3G and 4G signals. The 4G networks operating in the 800 MHz could also be viable, but deployment of these networks is very recent.
- Indoor localization based on GSM networks can leverage existing hardware and the network infrastructures. Most cellular mobile devices continue to support GSM, which enables GSM based indoor localization to serve large number of users without requiring additional hardware. The cellular networks are well deployed and maintained by network operators.
- GSM networks are operated in licensed frequency bands, which are not likely to have interference from nearby devices operating in the same band, as is the case with wireless signals like WiFi and Bluetooth operating in the very crowded ISM bands.
- GSM networks are robust in two important ways. First, cellular mobile stations are unlikely to evolve, change, or be frequently reconfigured, which leads to a stable signal environment that can be the basis for indoor localization system to function over a long period without additional calibration. Secondly, cellular systems are designed to continue functioning even in the case of a power supply failure, which allows a GSM based indoor localization system to work even in the event of an electrical system failure in a building.

These advantages indicate that according to the performance metrics introduced above, indoor localization based on the GSM networks would be with low cost, low complexity and high robustness, which benefits from the near-ubiquity and stable operating of GSM networks. Though 4G LTE has arrived, GSM is slated to continue operating at least through 2021. In addition to the existing large amount of cellular mobile devices supporting GSM, MEMS sensors are increasingly popular in these devices, which allows for the potential hybrid approaches that combine GSM and inertial sensors. In regard to the low scalability which is a common shortcomings of fingerprinting based localization techniques, it is a compromise but not painful if necessary, since the calibration process is done offline. Finally, earlier studies have shown that accurate indoor localization based on GSM is viable and promising [90, 8, 9], which lay the groundwork for what will be studied in this thesis.

Chapter 3

Characteristics of GSM signals

3.1 Introduction

As mentioned in the previous chapter, this PhD work focuses on indoor localization based on the GSM networks, which distinguishes different indoor locations using RSS fingerprints, i.e. sets of RSS from a number of GSM channels.

In this chapter, an overview of GSM networks, the basis of the indoor localization approaches investigated in this thesis, is first presented, including the system architecture and radio air interface. An interesting aspect of the GSM norm, the fact that GSM mobiles must be able to rapidly measure RSS values of large sets of GSM channels, is stressed. An analysis of GSM signal properties is then presented, which aims to explain the causes of RSS variations over space and time. Indeed, to reliably differentiate spatial locations, measured RSS values must be correlated with position, but relatively robust over time. The RSS of GSM signals are further explored using real measurements on two different types of data acquisition devices. It is demonstrated that RSS from a single GSM channel does not provide adequate location distinction, while fingerprints containing RSS from all available GSM channels do indeed show strong location-related properties, assuring us that accurate indoor localization based on RSS fingerprints will be viable.

3.2 An overview of GSM system

During the early 1980s, analog modulation telephone systems experienced rapid growth, including AMPS in the United States, TACS in the United Kindom, C-Netz in Germany, Radiocom 2000 in France, and NMT in Scandinavia [91]. These networks were planned to achieve maximum coverage with as few antennas as possible, but unfortunately insufficient regard for the amount of voice traffic they would ultimately need to carry. As the subscriber base grew, these networks could no longer cope with the increasing traffic. The analog systems furthermore lacked reliability and adequate security measures. Moreover, each country developed its own system, in most cases incompatible with the equipment and operational methods used in other countries.

To address these issues, the European Conference of Posts and Telecommunications Administrations (CEPT) established the *Groupe Special Mobile* to study and develop a digital public land mobile system for Europe. The system was expected to be compatible with Integrated Services Digital Network (ISDN), have good subjective speech quality, low terminal and service cost, efficient use of radio spectrum, and support international roaming. The new digital standards were completed in the late 1980s, and deployment of GSM networks in Europe began in the early 1990s. Although initially standardized in Europe, GSM today has been is adopted and deployed worldwide. Now known as Global System for Mobile Communications, GSM is at present the most widely deployed cellular telephony standard in the world, with networks deployed in more than 220 countries by nearly 800 mobile operators [92].

3.2.1 Architecture of GSM network

The GSM network architecture can be divided into three sub-systems: the Radio Subsystem (RSS); the Network and Switching Subsystem (NSS); and the Operation and Support Subsystem (OSS), as illustrated in Figure 3.1. Each subsystem is an entity composed of one or more pieces of physical equipment to carry out a specific task. The connection between the BSS and the NSS is through the A interface (solid lines) and the connection to the OSS through the O interface (dashed lines).

The RSS controls the radio part of GSM network, including the radio specific elements including the Mobile Stations (MS), the BTS and the Base Station Controller (BSC). A MS is comprised of the mobile device or terminal and its Subscriber Identity Module (SIM). A BTS, which contains the signal processing modules, antennas, amplifiers, etc., necessary for radio transmissions, serves users within its radio *cell*, the basic subunit of a cellular network. The cellular structure allows for frequency reuse in non-overlapped cells, which increases considerably the capacity of the cellular system. Normally several BTSs are controlled by a single BSC. The size of GSM cells can vary considerably in radius, from 100 m to 35 km.

The NSS is responsible for all functions required to handle the signaling protocols through

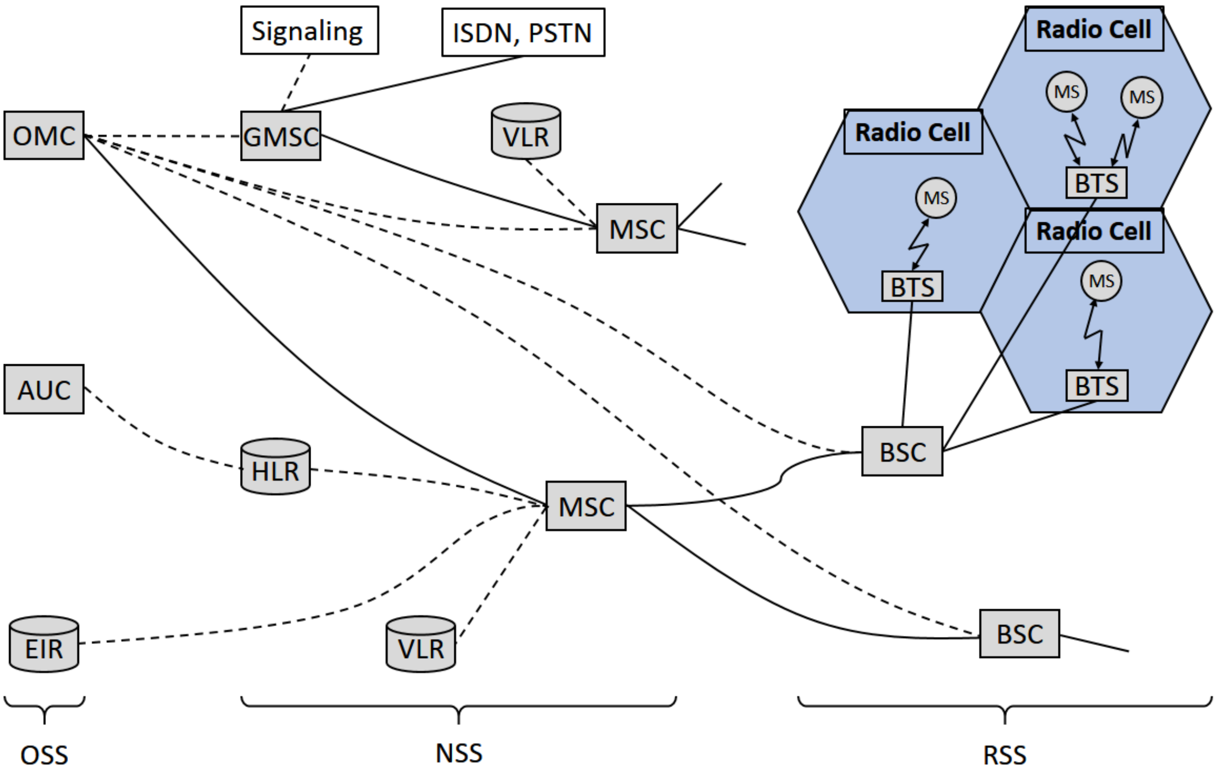

Figure 3.1 – Architecture of a GSM system

which calls are established, maintained and cleared. It is also responsible for handling short messages and packet data, maintaining a database of its own users (the Home Location Register or HLR) as well as visitors (Visitor Location register, VLR), and carrying out authentication and encryption procedures. The Mobile Switching Center (MSC) is the main component of the NSS, as the BSCs coordinate with it. This subsystem is a gateway (the Gateway MSC, GMSC) to the Public Switched Telephone Network (PSTN), ISDN, and other mobile networks. The 2.5G GPRS/EDGE (General Packet Radio Services/Enhanced Data for GSM Evolution) is a packet switched version of GSM with a similar radio and network infrastructure, which adds a Serving GPRS Support Node (SGSN) and a Gateway GPRS Support Node (GGSN) to support packet switching traffic in GSM network.

The OSS is in charge of remote operations and maintenance of the GSM network. The Authentication Center (AUC) is a strongly protected database that handles the authentication and encryption keys for all subscribers in the HLR and VLR. The Equipment Identity Register (EIR) is a database containing the identification of all devices registered on the GSM network. In case a MS is reported stolen, the EIR can block the device based on its International Mobile Equipment Identity (IMEI).

3.2.2 GSM radio air interface

The radio air interface is the primordial interface of any mobile communication system, and is important for the quality and success of a mobile standard. It must make efficient use of available frequencies as the available spectrum is quite limited. Although there are a total of fourteen different recognized GSM frequency bands, GSM networks are mostly operated in the 900 MHz and 1800 MHz bands, details of which are shown in Table 3.1. As Frequency Division Duplex (FDD) is used in GSM system, the frequency are separated into the downlink and uplink with a duplex split of 45 MHz (GSM 900 band) or 95 MHz (GSM 1800 band).

Table 3.1 – Frequency Division in 900 MHz and 1800 MHz GSM bands

Band	**ARFCN (n)**	**Uplink ($\mathbf{f_{UL}}$)**	**Downlink ($\mathbf{f_{DL}}$)**
GSM 900	0-124 975-1023	890+0.2n 890+0.2(n−1024)	f_{UL}(n)+45
GSM 1800	512-885	1710.2+0.2(n−512)	f_{UL}(n)+95

GSM uses a combination of Frequency Division Multiple Access (FDMA) and Time Division Multiple Access (TDMA) on the air interface, resulting in a two dimensional channel structure as shown in Figure 3.2. The FDMA scheme involves the division by frequency of the bandwidth into 200 kHz wide carrier frequencies, which are specified by their Absolute Radio Frequency Channel Number (ARFCN). There are 174 and 374 carriers in GSM 900 and GSM 1800 respectively. Each carrier is then additionally divided into time slots using a TDMA scheme, which accommodates different users on a single carrier frequency in different time slots, without mutual interference. The smallest data subunit is the "burst", transmitted within a time slot. Each GSM time slot lasts for 0.577 ms, and eight time slots, numbered from 0 to 7, are grouped into a TDMA frame lasting approximately 4.615ms. In order to avoid frequency selective fading, and to mitigate adjacent-channel interference, GSM specifies an optional slow frequency hopping mechanism, in which MS and BTS change carrier frequency from frame to frame based on a known hopping sequence.

TDMA frames repeating indefinitely, with the recurrence of one of the eight time slots on a particular carrier frequency making up one *physical channel*. A physical channel is thus determined by the carrier frequency, or a number of carrier frequencies with a defined hopping sequence, and the time slot number. There are thus 8 physical channels per carrier frequency in GSM. Logical channels are defined according to the type of information they contain, for example, data or signaling information. *Logical channels* are mapped onto physical channels in specific ways as

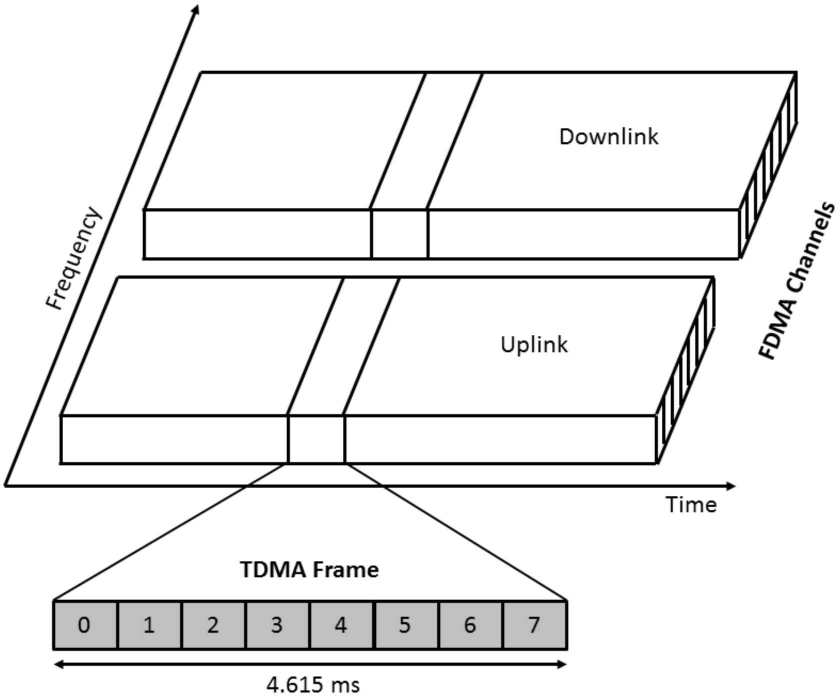

Figure 3.2 – GSM FDMA channels, TDMA frame and time slots

a function of the required data rate, repetition cycle, etc. We may identify two main types of logical channel, namely Control Channels (CCH) for signaling, and Traffic Channels (TCH) for data (voice data in GSM, packet data in GPRS being carried in Packet Data Traffic Channels PDTCH).

The CCH carry signaling and synchronization commands between the base station and the mobile station. Specific types of control channels are defined only for the downlink or only for the uplink. There are three main categories of signaling channels in GSM: Broadcast Channels (BCH); Common Control Channels (CCCH); and Dedicated Control Channels (DCCH). The BCH broadcasts cell-wide information necessary for correct operation, such as lists of ARFCN that will be used, handover parameters, location area code or LAC, etc. In addition, the BCCH provides beacon signals for time and frequency synchronization, at fixed power, in the first time slot of the first ARFCN in the frequency list, without slow frequency hopping.

3.2.3 GSM sign on procedures

When a mobile station is switched on, after performing the initial boot up procedure of hardware initialization and software setup, its first task is to find a suitable BTS to access to the GSM network. As mentioned above, all BTS broadcast their beacon carriers via the BCCH channel. The mobile station must obtain a list of beacon carriers to find a suitable cell to camp on. This process is called cell selection. The mobile station may have stored a BCCH frequency list in its memory or SIM card when last switched off. In this case, the mobile station scans the BCCH frequency in the list, which reduces the time of cell selection. In some cases, though, where the list was not successfully stored or no BCCH frequency can be found in the list, the mobile station must to cover the entire frequency band and measure the Received Signal Strength Indication (RSSI) of all carrier frequencies. Once the scan completed, the carrier frequencies are arranged in a list with descending order of signal strength. Then the mobile station will tune to the strongest carrier frequency, checking if this is a BCCH carrier by looking for a frequency correction burst send by the Frequency Correction Channel (FCCH), a part of the BCCH suite, which is a burst of pure sine wave. The strongest carrier frequency, however, could be a TCH instead of a beacon. In this case, if an FCCH burst, which occurs every 10 frame intervals in the time slot 0 of a BCCH carrier, is not detected, the mobile station will go to the next strongest carrier in the list and repeat the procedure. Once an FCCH burst is found, the MS will try to decode the Synchronization Channel (SCH) information in order to read the Base Station Identity Code, BSIC.

Subsequently the MS will read the BCCH to recover system information such as Cell Global Identity (CGI), Location Area Identity (LAI), BCCH carriers of the neighboring cells, maximum output power allowed in the cell, and other broadcast messages. Then the mobile station can camp on this cell and go to idle mode, from which it wakes up periodically to listen to the CCCH and BCCH.

3.2.4 GSM signal strength

A measured RSS value will of course depend on the transmit power level of the BTS, which is defined in GSM 05.05 but may also be specified by the network operator according to needs. The transmission power depends on the output power of the power amplifier and the losses from power amplifier to the antenna connector. Output power is a fundamental transmitter characteristic and is linked directly to range. Adaptive control of the RF transmit power of the BSS is also implemented in order to optimize link performance and minimize power consumption in the mobile station and co-channel interference. However, as mentioned earlier, the BCCH carrier is continuously transmitted on all TDMA frames without variation of RF power level. Intuitively, RSS measurements on the fixed-power beacon channels would seem the best adapted for positioning applications. We shall return to this point later.

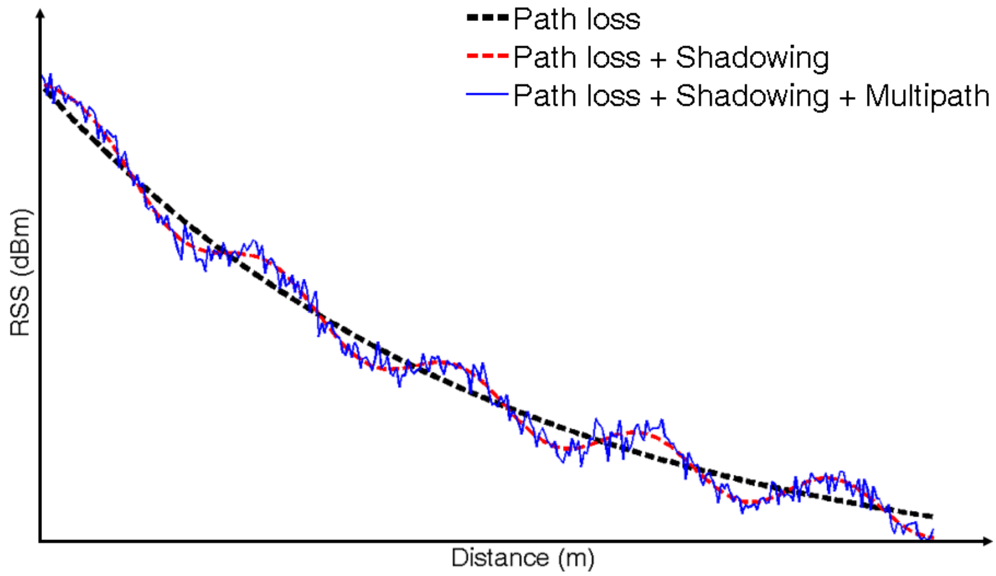

Figure 3.3 – Path loss, shadowing and multipath versus distance

The RSS is also influenced by path loss, shadowing and multipath effects, as illustrated in Figure 3.3.

The transmitted signal attenuates with distance since the energy is spread in the space around the transmitting antenna. This effect is named the path loss, which can be represented by the common LDPL model:

$$PL(d)[dB] = \overline{PL}(d_0) + 10nlog\left(\frac{d}{d_0}\right) \tag{3.1}$$

where $PL(d)$ denotes the measured path loss at distance d, $\overline{PL}(d_0)$ is the average path loss at reference point d_0, and n is the path loss exponent.

If there are objects along the path of the emitted EM wave, some part of the transmitted power may be lost through absorption, reflection, scattering, or diffraction. Such losses, termed shadowing losses, follow a zero-mean normal distribution χ_σ with standard deviation σ. As a result of shadowing, power received at the points that are at the same distance d from the transmitter may be different, and will follow a log normal (in dB) distribution. Then the path loss equation now becomes:

$$PL(d)[dB] = \overline{PL}(d_0) + 10nlog\left(\frac{d}{d_0}\right) + \chi_\sigma \tag{3.2}$$

Objects located in the vicinity of the path of the wireless signal can also reflect the signal back to the receiver. Since these reflected signals take different paths, each will have a different amplitude and phase, and depending upon these phases, the sum of the multiple signals may result in increased or decreased received power at the receiver. Even a slight change in position or in measuring time may result in a significant difference in phases of the signals and so in the total received power. This effect is called multipath effect, which is modeled by the environment-dependent path loss exponent n of the LDPL model.

3.3 RSS measurement of GSM signals

Measuring RSS of GSM networks is the starting point for the fingerprinting based indoor localization studied in the thesis. As already mentioned, according to the GSM standard, any GSM mobile device must have the ability to measure the RSS on all carrier frequencies. In addition, in normal operation an MS will often move from one BTS to another during a handover if the quality of the link to the current base station becomes unacceptable. The handover protocol requires the handset to regularly provide measurements of the received power, not only of its current serving cell, but also of several neighboring cells, so that a list of possible handover targets may be assembled. Finally, the slow frequency hopping mechanism requires GSM phones must be able to jump from frequency to frequency quickly. It follows that any standard cell phone has the ability to measure the power level on any of the frequency carriers present in a typical GSM system (174 for GSM 900 and 374 for GSM 1800). It also must be able to synchronize with base stations at any of these frequencies, in order to recover network parameters such as the BSIC. To ensure the sufficient accuracy for the correct functioning of the system, GSM standard requires the RSS be measured by the mobile stations over the full range of -110 dBm to -48 dBm.

3.3.1 RSS measurement devices

Although GSM mobile devices must have the ability to measure the RSS on all carrier frequencies, normally they are not able to save the RSS scan result to local storage for later analysis. Consequently, in this thesis, two types of data acquisition devices were used to record the GSM RSS, namely the Telit GM862 GSM/GPRS modules [93] and the ASCOM TEMS Pocket [94].

The Telit GM862 GSM/GPRS module is a Machine to Machine (M2M) module, which is shown in Figure 3.4. It is made up of several components including a GSM chip with an antenna, a GPS chip, an ARM microcontroller, power supply unit and some accessories. The GSM chip is controlled by the ARM microcontroller to initiate scans of GSM RSS on multiple carriers using AT commands. It can perform a full scan recording the ARFCN and RSS level RxLev at all GSM carrier frequencies and decode the BSIC for all carriers in about three minutes. The scan results are recorded in a memory card installed on the board for later analysis.

a) b)

Figure 3.4 – RSS measurement devices: a) Telit module and b) TEMS pocket connected to a laptop

In fact three minutes scanning time is too long to make this module exploitable for practical indoor localization. In this thesis, the Telit module was used in initial tests to investigate the characteristics of GSM signals in indoor environments. Although they can be mobile devices, the Telit modules were here connected to mains power and the GPS module disabled. They were programmed in an endless loop to make full scans on a periodic basis, with the cycle time set at ten minutes to avoid filling the storage space of the memory card.

The ASCOM TEMS Pocket is part of a network test suite for management, maintenance and troubleshooting of wireless networks. TEMS is an acronym of Test Mobile System. The TEMS Pocket phones are in fact standard mobile phones with network investigation software embedded, see Figure 3.4. When not scanning, the TEMS Pocket works no differently from the commercial version of the same phone. Indeed TEMS Pocket simply exploits the RSS scanning ability required by the GSM norm, using the phone itself as a scanner. The hardware model of TEMS Pocket use in this thesis is Sony Ericsson W995.

This TEMS Pocket as a standalone can scan a list of specified carrier frequencies or all the carrier frequencies of either GSM 900 or GSM 1800 band. When connected to a computer, it can work with TEMS Investigation software to scan both bands GSM bands simultaneously. A particular feature of TEMS Pocket is that when BSIC decoding is unnecessary, RSS scanning becomes extremely fast, capturing a full scan of all the carrier frequencies of both bands in about 300 milliseconds. Such scanning speed makes TEMS Pocket practical for real time indoor localization, with location updating theoretically reaching 3 per second. Scans with BSIC decoding enabled require about an order of magnitude more time to complete. In this study, the BSIC decoding function of the TEMS Pocket was switched off as, in practice, it was not found to be a useful parameter in obtaining RSS fingerprints. The TEMS Pocket is also of course interesting in another aspect, which is that any standard mobile phone supporting GSM is potentially capable to get full carrier RSS scans, employing only a software modifications.

3.3.2 Analysis of RSS measurements

The location fingerprinting technique discriminates locations based on location-dependent measured RSS values. Consequently, we would like RSS to be distinctive over different locations while remaining relatively consistent over time, thus ensuring a time-robust localization system. In this section, the GSM signal strength characteristics, particularly its behavior over location and over time, are investigated, via measured data. All data here is acquired using the Telit GSM/GPRS module.

An experiment was performed in a room of a 4th floor laboratory building (steel frame, concrete and plaster walls) in central Paris, France. In the experiments, eight identical Telit modules with nominally identical specifications and technical parameters were used. During data collection, the Telit modules were placed at fixed positions, in a line, spaced at an interval of 0.6 meter, as illustrated in Figure 3.5. Around 700 GSM scans for each module were recorded over 5 working days. Each scan contains the RSS of all 548 carriers in the GSM 900 and GSM 1800 bands, and consists of RSS values ranging in value from -108 dBm to -40 dBm. Since there are gaps of ARFCN between GSM 900 and GSM 1800 bands, in this thesis the carriers are numbered from 0 to 548, which we call carrier index, in which 1–125 corresponds to the ARFCN 0–124 of GSM 900, 126–500 corresponds to ARFCN 512–885 of GSM 1800 and 501–548 corresponds to ARFCN 975–1023 of GSM 900.

Figure 3.6 shows one scan of RSS over all carrier frequencies recorded by the first Telit module, with the red star indicating the beacon carriers, where we recall that the Telit modules automatically decode BSIC information. It should be noted that the absence of a valid BSIC does not necessarily mean that a given carrier is a traffic channel rather than a beacon. The BSIC decoding of a genuine beacon can in some cases fail. A common example is when a beacon resides in the channel *adjacent* in frequency to the carrier currently being scanned. It is seen in

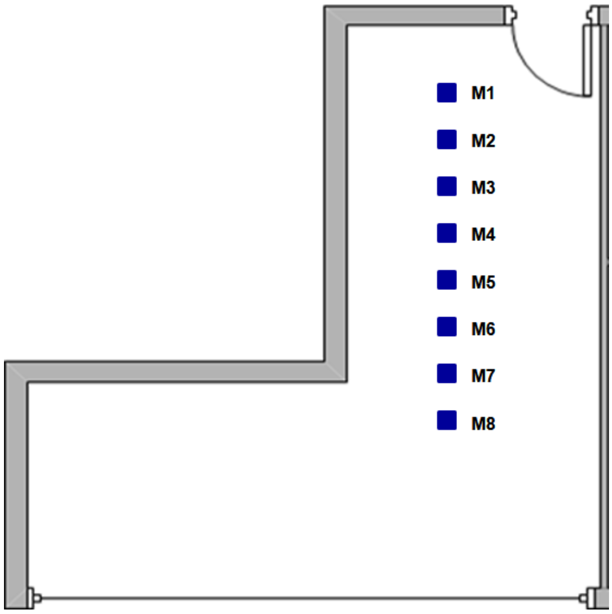

Figure 3.5 – Experimental setup for RSS measurements

the figure that RSS vary significantly from channel to channel.

Figure 3.7 shows the evolution of RSS recorded by the same Telit module as in Figure 3.6 over five days. As is shown in the figure, the fluctuation of RSS is not severe over a duration of five days, in both beacon and non-beacon channels. The Coefficient of Variation (CV) of RSS is illustrated in Figure 3.8, which, analogously to Signal-to-Noise Ratio (SNR), presents the ratio between standard deviation of RSS and the mean value of RSS over time. It is seen that the largest value of CV is 0.16, but values of CV in most of the carriers are below 0.05. Thus for an RSS in one channel of -80 dBm, the standard deviation remains below 4 dB, which is relatively stable.

In the experiment, the day-night effects of RSS is also observed, as shown in Figure 3.9. It is seen the mean RSS have obvious fluctuation between day and night, higher in the night, and lower by day.

RSS changes with different locations are described in Figure 3.10, where the X axis are the locations from 1 to 8 (Figure 3.5) and Y axis are the RSS. In this figure, a beacon carrier (carrier index 537) and a non-beacon carrier (carrier index 46) are compared, which are drawn in blue line with squares and red line with circles respectively. In each location, the lower bound, upper bound and mean value are presented. Generally, the a carrier labeled “beacon” has higher RSS and less fluctuation compared with one labeled “non-beacon”, although, again, we must interpret BSIC decoding with care. The figure shows that there is no clear distinction in RSS values among the eight different locations, neither for beacon nor for non-beacon carriers. We conclude that

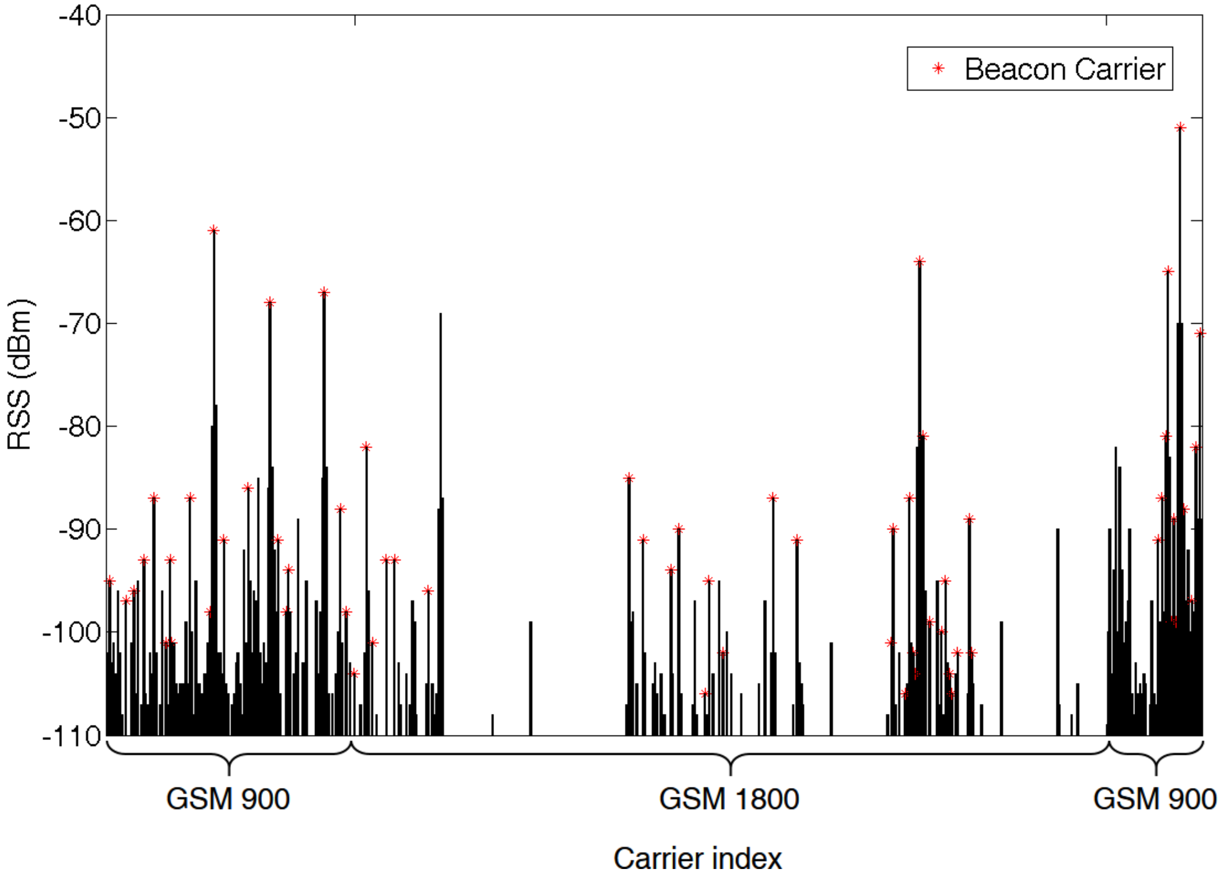

Figure 3.6 – RSS in all the carrier frequencies of GSM 900 and GSM 1800

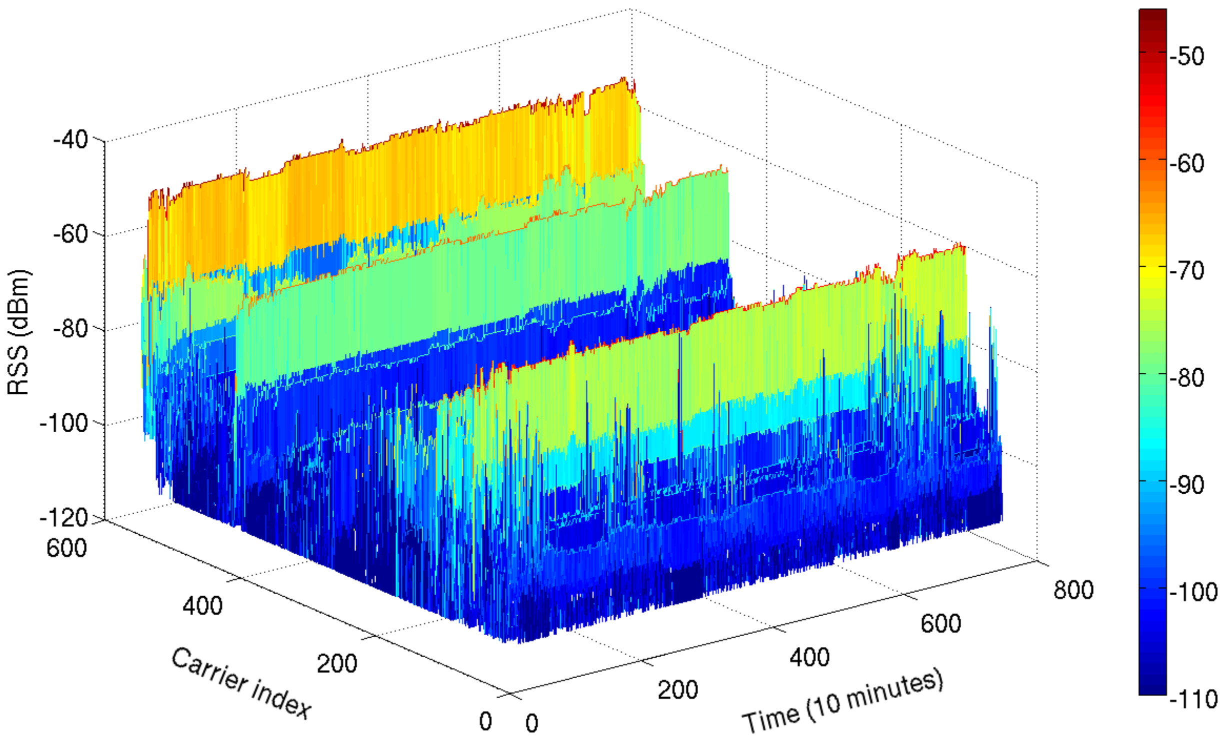

Figure 3.7 – Received signal strength over time

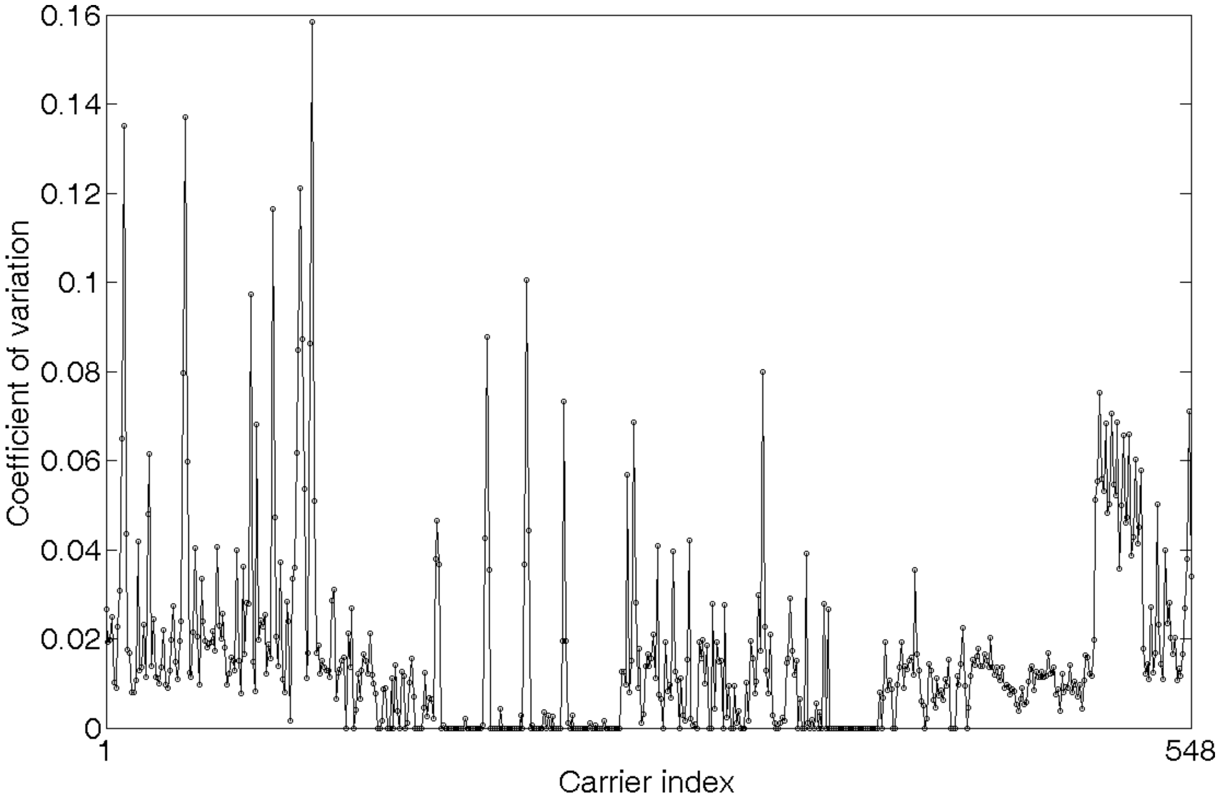

Figure 3.8 – The coefficient of variation of RSS over time

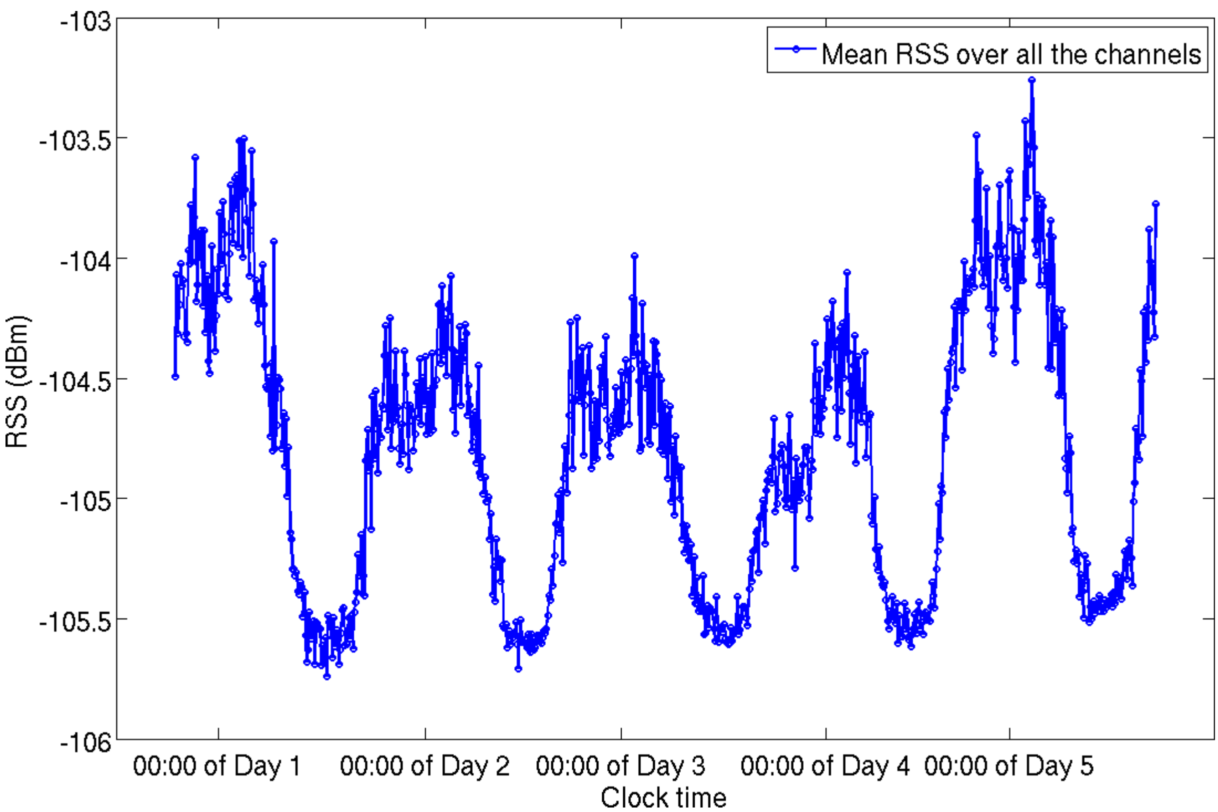

Figure 3.9 – RSS changes over day and night

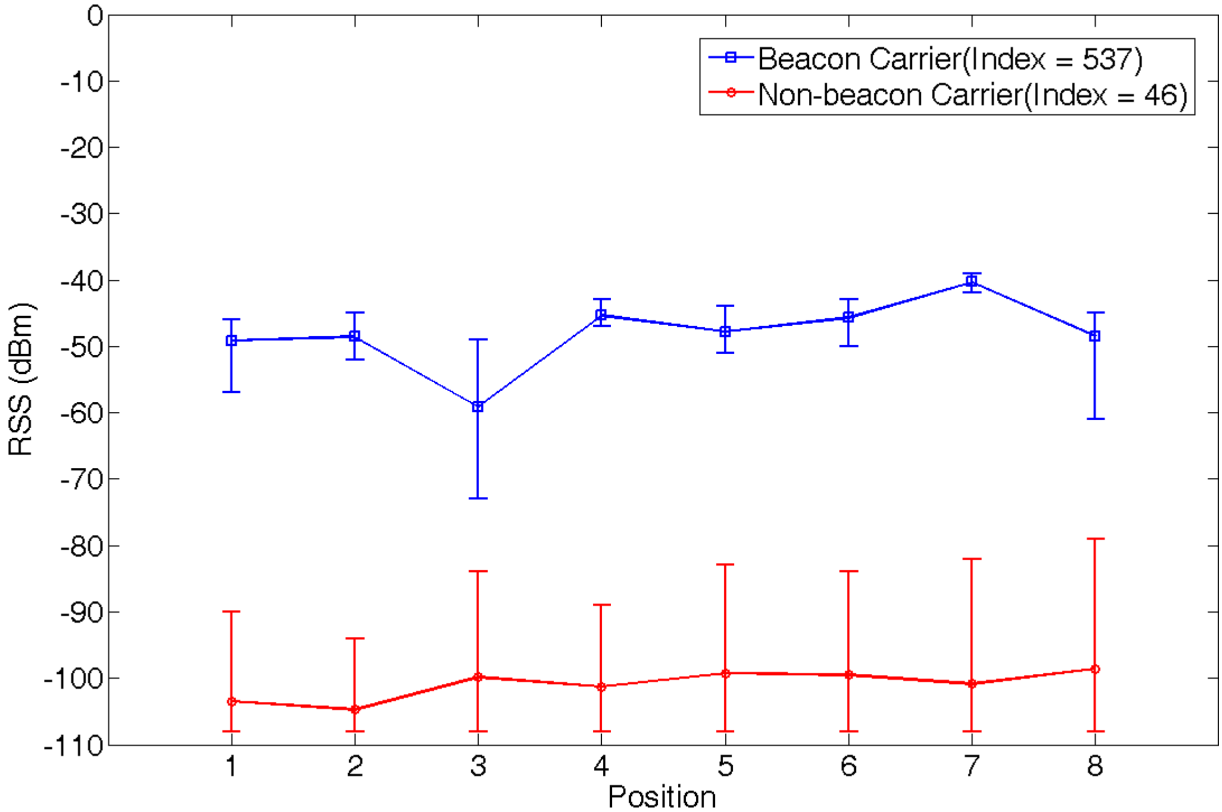

Figure 3.10 – RSS of beacon and non-beacon channels in different positions

RSS of a single carrier is unlikely to provide us with an exploitable estimation of the position of a mobile device in an indoor environment.

3.3.3 Location dependent properties of GSM fingerprints

As indicated above, a single carrier does not display any obvious correlation between RSS and locations. This chapter examines fingerprints incorporating RSS measurements at all carrier frequencies, which therefore contain much richer information about the local radio environment and may therefore provide superior location discrimination capability. The following describes an experiment done to explore the location-dependent properties of GSM fingerprints.

In the experiment, four Telit modules were placed in a group, at the four vertices of a square with the side length of one meter. This Telit module group was then put at four different locations successively as shown in Figure 3.11. In each location, data was collected consecutively over five days, and about 600 scans were obtained by each Telit module. The dataset recorded in group i was called C_i, and accordingly the dataset recorded by Telit module j of group i was called as C_{ij}.

Fingerprint distance, defined as the Euclidean distance in the signal strength space, is

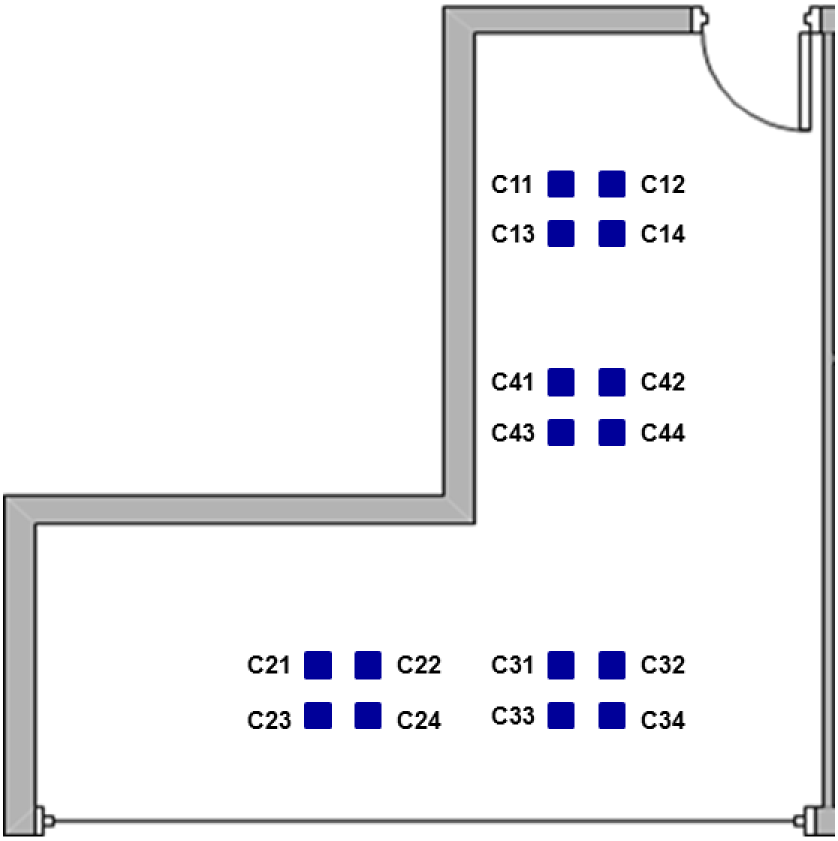

Figure 3.11 – Experimental setup of testing the fingerprint distance

compared to the geometric distance of the Telit modules. The fingerprint distance between two fingerprints RSS_1 and RSS_2 can be calculated according to the following equation (values in dBm):

$$d_{i,j} = \sqrt{\sum_{n=1}^{N} \left(RSS_i^n - RSS_j^n\right)^2} \tag{3.3}$$

where RSS_i^n is the nth entry of fingerprint RSS_i and N is the size of the fingerprint, which in this thesis is 548. Accordingly, the average intra group fingerprint distance is defined as:

$$\overline{d}_{C_{ij},C_{ik}} = \sqrt{\sum_{n=1}^{N} \left(\overline{RSS}_{C_{ij}}^n - \overline{RSS}_{C_{ik}}^n\right)^2} \tag{3.4}$$

where $\overline{RSS}_{C_{ij}}$ is is defined as the average fingerprint of dataset C_{ij}. And the average inter group fingerprint distance:

$$\overline{d}_{C_i,C_j} = \sqrt{\sum_{n=1}^{N} \left(\overline{RSS}_{C_i}^n - \overline{RSS}_{C_j}^n\right)^2} \tag{3.5}$$

where $\overline{RSS}_{C_i}$ is is defined as the average fingerprint of dataset C_i.

Average fingerprint distances both intra group and inter group are shown in Figure 3.12. As can be seen in the figure, though the fingerprint distance is not proportional to the geometric

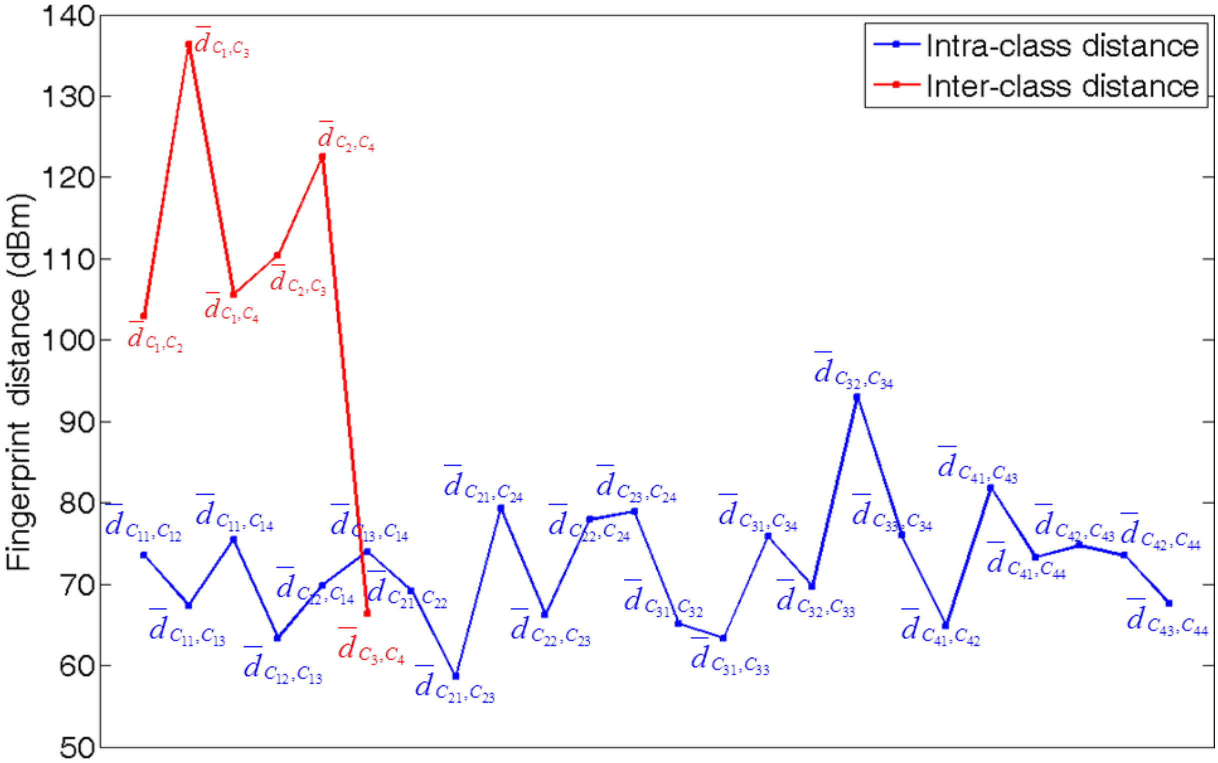

Figure 3.12 – Comparison of fingerprint distance and geometric distance. The intra-class distances (blue line) are the average fingerprint distances of each two datasets in the same group; the inter-class distances (red line) are the average fingerprint distances of all datasets in each two groups

distance, the intra group fingerprint distances are smaller than the inter group fingerprint distance in most cases. This indicates that the GSM fingerprints in nearby locations have a certain level of similarity, which is the basis of indoor localization using GSM fingerprints. However, there is still one exception in which the intra group fingerprint distance is about the same as the inter group fingerprint distance. One might expect, however, that better discrimination could be obtained with a more sophisticated analysis, a point to which we will return in the upcoming chapters.

3.4 Summary

This chapter first introduces the GSM network, including the architecture, radio air interface, sign on procedures and signal strength and propagation, which are the basis of the indoor localization techniques investigated in this thesis.

Then, two types of data acquisition devices are introduced and the characteristics of RSS measurements are examined. RSS are stable over time in a certain location, but with some fluctuations. In addition, the day and night effect is observed, which indicates that in the same position RSS are higher in the night and lower in the day. Considering the location related properties, RSS from a single GSM carrier, either beacon channel or non-beacon channel, does not provide much location distinction. However, RSS fingerprint, as a set of RSS from all the GSM carriers, has shown to be location dependent, which indicates indoor localization could be viable based on exploring the high dimensional RSS fingerprints.

Chapter 4

Indoor localization using GSM fingerprints

4.1 Introduction

This thesis investigates indoor localization using very high dimensional GSM fingerprints containing RSS from all the GSM carriers. According to the performance metrics of a localization system introduced in section 2.4, the indoor localization system based on GSM networks will have the advantages of low cost, wide coverage, and simplicity. Nevertheless, accuracy and robustness are key parameters to a localization system: they determine how small an area the system can distinguish and how long the system can function properly. In this chapter, the focus is on the accuracy and robustness problem of indoor localization using GSM fingerprints.

Coordinate location from RSS is first studied, which tries to find a functional relationship between locations and the GSM fingerprints obtained in these locations. SVM regression is used to map the high dimensional GSM fingerprints to locations. The experimental results, however, show that no such relationship exists for the tested indoor environment, indicating that interpolation and extrapolation schemes based on RSS measurements at a small number of points will not be viable for localization. Then, indoor localization based on fingerprint classification is presented, in which the mobile's position is estimated by classifying sets of fingerprints, obtained from distinct spatial regions, making use of a model constructed in a previous training phase.

Figure 4.1 depicts the complete location estimation algorithm, which consists of an offline training phase, an online localization phase and a post-processing phase. As the fingerprinting approach introduced in section 2.2.3, an offline training is first performed, involving region labeling of the site, RSS data acquisition, and training and validation to develop a localization model. The

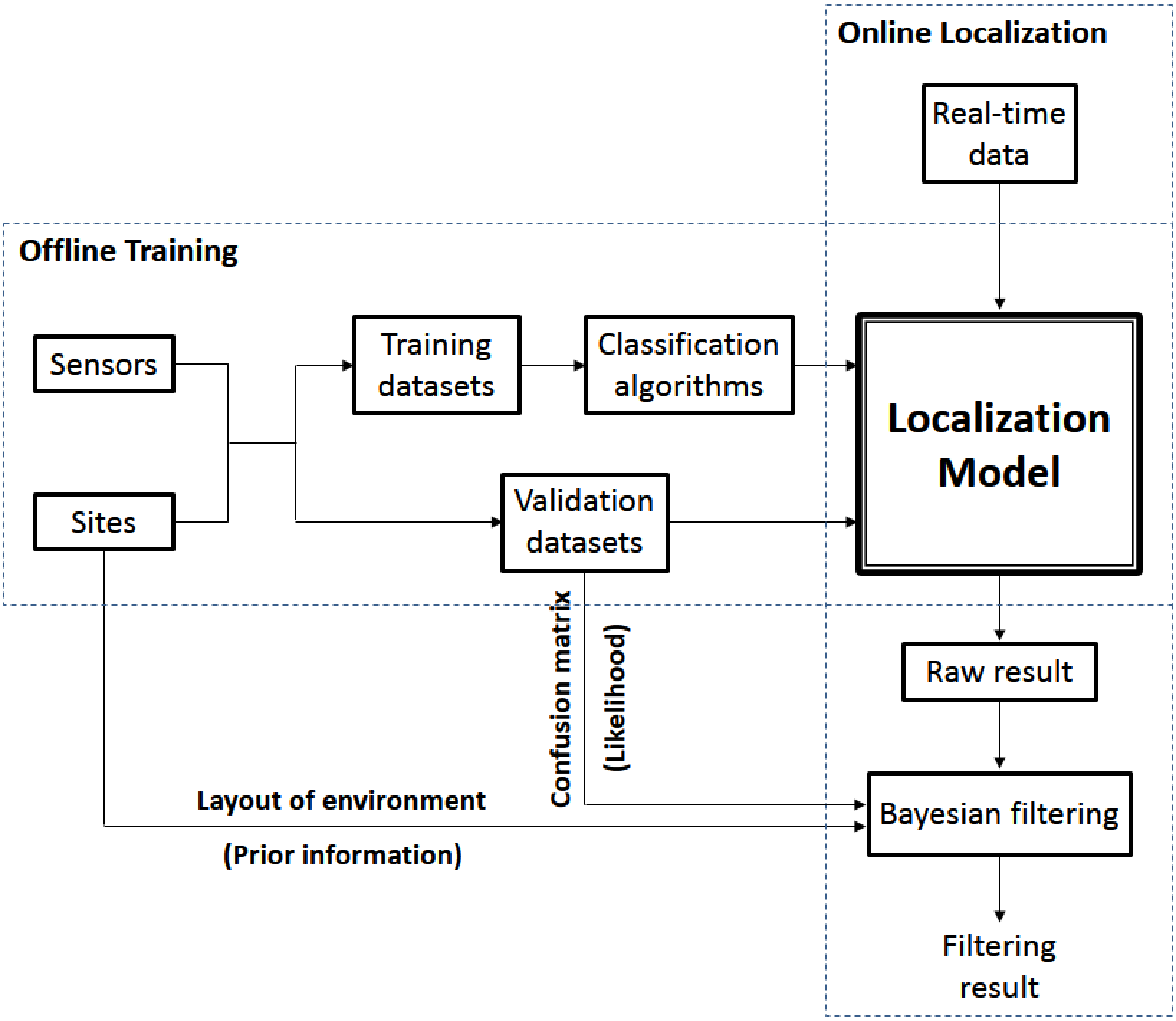

Figure 4.1 – The overall localization algorithm

model is then used in the online localization phase: real-time RSS data is input to produce an estimation of the location. Finally, a more accurate and reliable location estimate can be obtained after post-processing.

As the RSS vary within different positions even in the same region and interpolation and extrapolation schemes do not work, a "space sampling" scheme is proposed to randomly acquire data at points throughout the interiors of the spatial regions of interest, rather than at only a few representative points. This is achieved using the TEMS Pocket data acquisition device, which enables the collection of large amounts of data on a reasonable timescale. Experimental results show that GSM fingerprints acquired in this way can be used to differentiate rooms of about 10 square meters size in some 94% of cases, indicating that the classification method is promising.

Meanwhile, the RSS fluctuate over time, making the localization performance decrease significantly after a period of time, which is observed by experiments spanning several months.

In section 4.3.3, transductive inference is studied, which uses new, incoming unlabeled data to update SVM classifiers as a means of reducing performance degradation caused by RSS drift. In addition, a “time sampling” scheme is proposed in section 4.3.4: fingerprint examples are taken in different time slices over several days or even longer periods of time. Such a sampling scheme incorporates different types of RSS fluctuations and better represents the statistical properties of fingerprints. Long term experiments demonstrate that with the “time sampling” scheme the performance of the proposed localization system remains stable over months.

The post-processing of indoor localization is presented in the last section: it involves using Bayesian filtering to employ a priori information about the indoor layout and mobile’s trajectory for the correction of possible errors in the raw classification results.

4.2 Attempt to obtain position coordinates from RSS fingerprints

The idea of obtaining coordinate location from RSS fingerprint comes from the relationship between fingerprint distance and geometric distance studied in section 3.3.3 where it is shown that the nearby locations have similar RSS fingerprints. If locations can be abstracted, using fingerprint examples taken at a small number of representative points, as a function of RSS fingerprints, coordinate locations can be determined according to such a function by mapping RSS fingerprints to locations. This is interesting in that not only coordinate locations can be obtained, but time and labor consuming site survey work can be significantly mitigated. In the thesis, the relationship between locations and RSS fingerprints is explored by a regression method using fingerprint examples taken at locations in a line. Since the number of variables in a fingerprint is very large (548 carriers) and the size of the training set is relatively limited, SVM regression is deemed appropriate because of its built-in regularization mechanism [95, 96].

4.2.1 SVM regression algorithms

Consider a given dataset of n RSS scans $\{(\mathbf{x}_1, y_1), (\mathbf{x}_2, y_2), \cdots, (\mathbf{x}_n, y_n)\}$, where x_i is the fingerprint vector at location i and y_i is the coordinate of the location (assuming that 1-D localization is performed). There exists a variety of Support Vector Regression (SVR) techniques, serving different purposes. $\varepsilon - SVR$, which is used here, aims to find a parameterized function $f(\mathbf{x}, \theta)$ such that prediction errors $||y_i - f(\mathbf{x}, \theta)||$ do not exceed a given value ε for all elements of the training set, and, at the same time, is as regular as possible, i.e. does not oscillate unnecessarily. Assume that we are looking for a linear relationship between the RSS fingerprint and the location. The function has the form:

$$f(\mathbf{x}, \theta) = \mathbf{w} \cdot \mathbf{x} + b \tag{4.1}$$

where $\theta = [\mathbf{w} \;\; b]^T$. The parameters are sought as solutions to the constrained optimization problem:

$$\begin{aligned} &\text{minimize} && \frac{1}{2}||\mathbf{w}^2|| \\ &\text{subject to} && ||y_i - \mathbf{w} \cdot \mathbf{x}_i - b|| \leq \varepsilon \end{aligned} \tag{4.2}$$

The optimal solution, if it exists, can be shown to be of the form

$$f(\mathbf{x}) = \sum_{i=1}^{n} \alpha_i y_i (\mathbf{x}_i \cdot \mathbf{x}) + \alpha_0 \tag{4.3}$$

where the $\alpha_i (i = 0 \cdots n)$ are solutions of a constrained quadratic optimization problem.

If such a solution does not exist, slack variables ζ_i and ζ_i^* can be introduced to relax the constraints for positive and negative training examples respectively, allowing some examples of the training set to be predicted with an error larger than ε. The problem becomes:

$$\begin{aligned} &\text{minimize} && \frac{1}{2}||\mathbf{w}^2|| + C\sum_{i-1}^{n}(\zeta_i + \zeta_i^*) \\ &\text{subject to} && \begin{cases} y_i - \mathbf{w} \cdot \mathbf{x}_i - b \leq \varepsilon + \zeta_i \\ \mathbf{w} \cdot \mathbf{x}_i + b - y_i \leq \varepsilon + \zeta_i^* & \forall i \\ \zeta_i, \zeta_i^* \geq 0 \end{cases} \end{aligned} \tag{4.4}$$

where C is a hyperparameter called "regularization constant".

If we want to look for a non-linear relationship between the RSS fingerprint and the location, non-linear regression can be realized by first performing a nonlinear transformation of the variables that defines a more suitable feature space, in which linear regression is performed. The final solution is in the form

$$f(\mathbf{x}) = \sum_{i=1}^{n} \alpha_i y_i K(\mathbf{x}_i \cdot \mathbf{x}) + \alpha_0 \tag{4.5}$$

where $K(\mathbf{x}, \mathbf{y})$ is called the kernel function. In experiments of this thesis, linear and nonlinear regressions (using Gaussian and polynomial kernels) were performed, using the Spider toolbox [97].

4.2.2 Evaluation of SVM regression for indoor localization

4.2.2.1 Data acquisition and datasets

Data was recorded in the same setting as introduced in 3.3.2. In the experiment, eight identical Telit modules were placed at fixed positions, in a line, spaced at an interval of 0.6 meter. A total of 600 GSM scans per module were recorded over 5 working days. Each scan includes the RSS of all 548 carriers in the GSM 900 and GSM 1800 bands, containing RSS values ranging from -108 dBm to -40 dBm. All the scans were labeled manually with locations from 0 to 4.2 meters indicating where the scan was made.

4.2.2.2 SVM regression results

The results of SVRs are estimated through the mean squared localization error as

$$\frac{1}{8}\sum_{k=1}^{8}\sqrt{\frac{1}{600}\sum_{i=1}^{600}\left[y_k - f\left(\mathbf{x}_{ik}, \theta^{-k}\right)\right]^2} \tag{4.6}$$

where y_k is the position of measuring device k, x_{ik} is the RSS vector measured during scan i taken at location k, and θ^{-k} is the parameter vector found by training from the data pertaining to all locations except location k.

The results for linear and non-linear regressions are shown in Table 4.1. The soft margin parameter C, polynomial degree d and the Gaussian kernel parameter were selected through cross-validation. The result from linear LS regression is also given for comparison.

Table 4.1 – SVM Regression Results

Regression Method	Mean Squared Localization Error
Linear LS-Regression	2.3m
Linear SVM Regression	1.8m
Polynomial SVM Regression (d = 5)	1.3m
Gaussian SVM Regression	2.4m

As shown in the table, the mean positioning error of all the regression methods is so large as to be unexploitable. The regression error is approximately equal to the average distance between the 8 locations, meaning that no linear or non-linear relationship between RSS fingerprint and the position in a small indoor environment can be found. This appears to rule out using full-band RSS GSM vectors obtained in this way to interpolate between fixed positions in an indoor localization method.

4.3 Room-level indoor localization

As an alternative scheme, the fingerprinting technique is used and the indoor localization problem is considered as a multiclass classification problem. As such, an indoor environment is divided into different locations, which are distinguished by separating surfaces in the fingerprint space. The main task of building a localization system is to determine the separating surfaces, based on fingerprint examples taken offline. In the thesis, SVM classification technique is used to find the equations of the optimal separating surfaces between locations.

The locations at which measurements are performed can be grid points, specific reference points, or regions, depending on the targeted application and desired accuracy. For most indoor location based services, such as indoor navigation, advertising, rescue, etc., room-level is perfectly adequate. Furthermore, the fingerprinting classification method requires more detailed training data sets as region sizes are reduced, which is time and labor consuming, and results in increased computation time in both the training phase and localization phases. As a trade off between accuracy and ease of implementation, room-level localization was therefore chosen in the thesis.

4.3.1 SVM classification algorithms

There are plenty of statistical learning techniques, which aim to solve classification tasks like location fingerprinting: k-NN classifiers, Bayes classifiers, linear discriminant analysis classifiers, neural network classifiers, classification trees, SVM classifiers, etc. SVM classification techniques have proved very powerful [98]. Reference [9] describes the first application of SVM classifiers to localization with a large number of GSM carriers. SVM classification techniques provide a good out-of-sample generalization, if the regularization parameters are chosen appropriately. Since the optimization problem solved for training SVM is convex, as explained in the next subsection, it delivers a unique solution. Moreover, it uses the “kernel trick” [95], which allows for transforming the linearly inseparable training data to some other spaces where the problem can be solved. Regarding the specific localization problem, SVM is effective for classifying high dimensional RSS fingerprints, and the computational complexity of SVM in the online localization phase is very low, as most of the computation is done in the offline training phase.

4.3.1.1 Pairwise classifier

As a starting point for multi-class classification, a pairwise (also termed “two-class” or “binary”) classifier is first introduced.

Consider a set of M examples of items belonging to either class A or class B, each example being described by a p-dimensional vector $\mathbf{x}_i$. Further assume that the examples are linearly separable, i.e. that there exists, in the descriptor space, linear surfaces of equation $f(\mathbf{x}) = 0$ that separate all examples without error: $f(\mathbf{x}_i) > 0$ for all examples belonging to class A and $f(\mathbf{x}_i) < 0$ otherwise. It can be proved that $f(\mathbf{x})$ can be written under the form

$$f(\mathbf{x}) = \sum_{i=1}^{M} \alpha_i y_i (\mathbf{x}_i \cdot \mathbf{x}) + \alpha_0 \tag{4.7}$$

where the $\alpha_i (i = 0 \cdots M)$ are parameters whose values are estimated from the examples; $y_i = +1$ if example $\mathbf{x}_i$ belongs to class A and $y_i = -1$ otherwise.

A linear SVM is a linear classifier such that the minimum distance between the separation surface $f(\mathbf{x}) = 0$ and the examples that are closest to it (called support vectors) is maximum, thereby guaranteeing the best generalization given the available data. The values of the parameters α_i of such a classifier are obtained by solving a quadratic optimization problem under linear inequality constraints. The support vectors are the only examples whose α_i are nonzero.

Figure 4.2 is an example of an SVM classifier with two classes in a two-dimensional descriptor space, where the squares are examples of class A, and circles are examples of class B. Squares and circles in red outline indicate the support vectors.

If the examples are not linearly separable, one resorts to nonlinear SVM, whereby the separation surface is of the form

$$f(\mathbf{x}) = \sum_{i=1}^{M} \alpha_i y_i K(\mathbf{x}_i \cdot \mathbf{x}) + \alpha_0 \tag{4.8}$$

where $K(\mathbf{x}, \mathbf{y})$ is a *kernel* function that must be positive semi-definite.

As for linear SVM, the α_i are obtained by solving a quadratic optimization problem under constraints. If the constraints can be satisfied only if a large proportion of examples are support vectors, *i.e.* if the classifier has a large number of nonzero parameters, the constraint that all examples are classified without error and lie outside the margin can be relaxed; that “soft-margin” approach reduces the complexity of the classifier by performing a trade off between accuracy of classification of the training examples and ability to generalize; the price to pay is the introduction of a “regularization” constant whose value must be chosen appropriately.

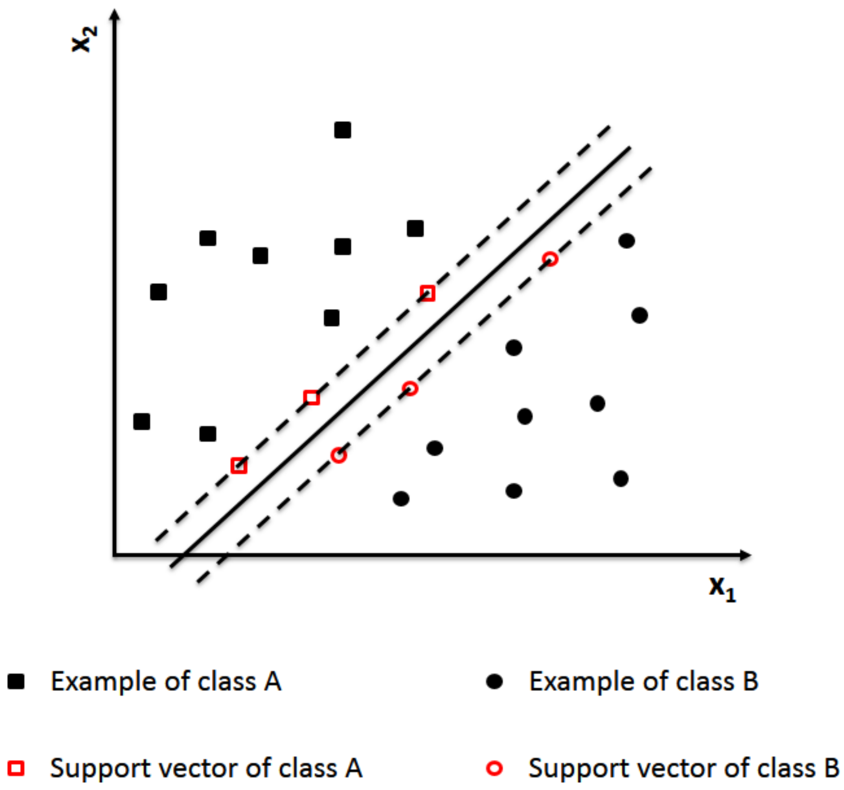

Figure 4.2 – An example of SVM classification

There exists a repertoire of valid kernel functions, among which the RBF kernel

$$K(\mathbf{x},\mathbf{y}) = \exp\left(-\frac{||\mathbf{x}-\mathbf{y}||^2}{2\sigma^2}\right) \tag{4.9}$$

with appropriate width σ, as used in the present study. The values of σ and the regularization constant are chosen by cross-validation.

To summarize, a GSM environment described by the fingerprint $\mathbf{x}$ is assigned to room A or room B according to the sign of $f(\mathbf{x})$, defined by (4.7) or (4.8) for linear or nonlinear SVM classification respectively. $\mathbf{x}_i$ is the ith fingerprint in a given dataset.

In the indoor localization problem, a number of locations need to be distinguished, which is a typically multiclass classification problem.

4.3.1.2 Decision rules for multiclass discrimination

For the indoor localization problem which obviously needs to distinguish not only two, but multiple locations, it is necessary for pairwise classifiers such as SVM, to define a method that allows combining multiple pairwise classifiers into a single multiclass classifier. This can be done in two ways: one-vs-one and one-vs-all.

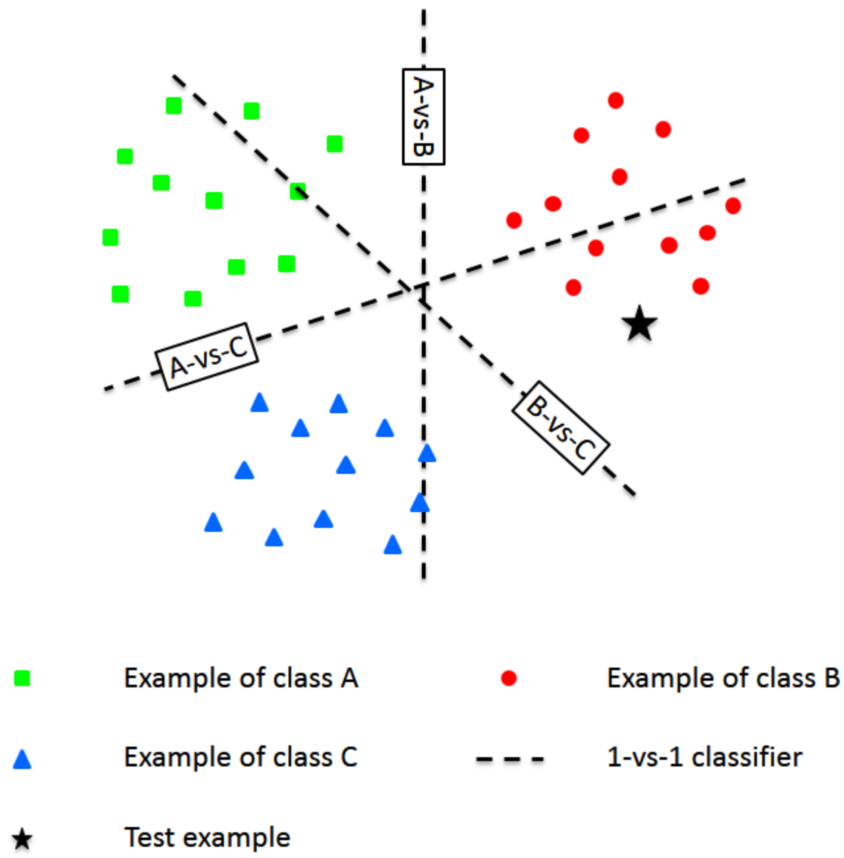

Figure 4.3 – One-vs-one classification

1) One-vs-one This approach decomposes the multiclass problem into the set of all possible one-vs-one problems. Thus, for an n-class problem, $n(n-1)/2$ classifiers must be designed. Figure 4.3 illustrates the architecture associated with this method.

The decision rule in this case is based on a vote. First, the outputs of all classifiers are calculated. Now let C_{ij} be the output of the classifier specializing in separating class i from class j. If C_{ij} is 1, the tally for class i is increased by 1; if it is -1, the class tally of class j is increased by 1. Finally, the class assigned to the example is that having the highest vote tally.

A disadvantage of the one-vs-one technique is of course the increase in the number of classifiers required as compared to one-vs-all discussed below.

2) One-vs-all The one-vs-all approach consists of dividing the n-class problem into an ensemble of n pairwise classification problems, each of which is specialized in separating one class from all the others. Figure 4.4 illustrates the procedure. Once the n classifiers are trained, the following decision rule is applied: the outputs of all n classifiers are first computed and, following the conventional procedure, the predicted class is taken to be that of the classifier with the largest magnitude of $f(x)$ (relation (4.7) or (4.8)). The one-vs-all technique is advantageous

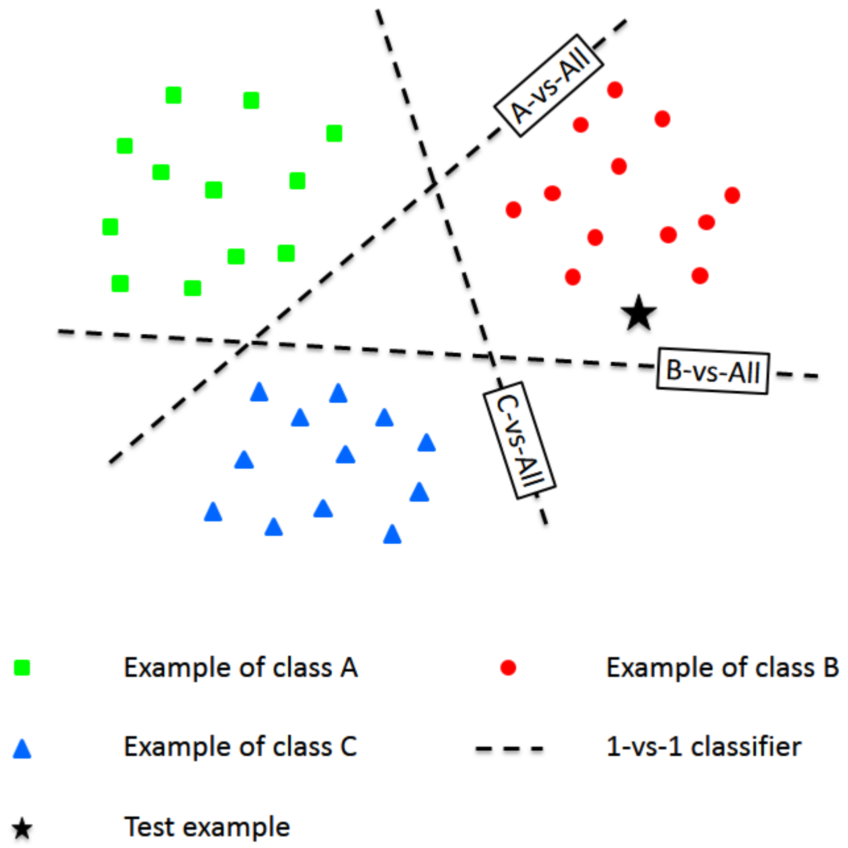

Figure 4.4 – One-vs-all classification

from a computational standpoint, in that it only requires a number of classifiers equal to the number of classes.

4.3.2 Evaluation of SVM classification for room-level localization

4.3.2.1 Data acquisition and datasets

For the room-level indoor localization, a user should be localized at the room level regardless of his exact position in a room. As the interpolation and extrapolation of locations using some reference points do not work, a space sampling scheme is proposed. To construct a "radio map" of the indoor environment, one needs to know the distribution of signal strengths in each location area, given that RSS values vary in space over the area. Since the room is used as the smallest location unit, space sampling is performed by collecting a large number of signal strengths in each room. This was done by recording the RSS with the TEMS Pocket held in hand during a "random walk" throughout the accessible space of each room, rather than, for example, using a grid or a set of special representative points. The fast scanning characteristic of TEMS Pocket

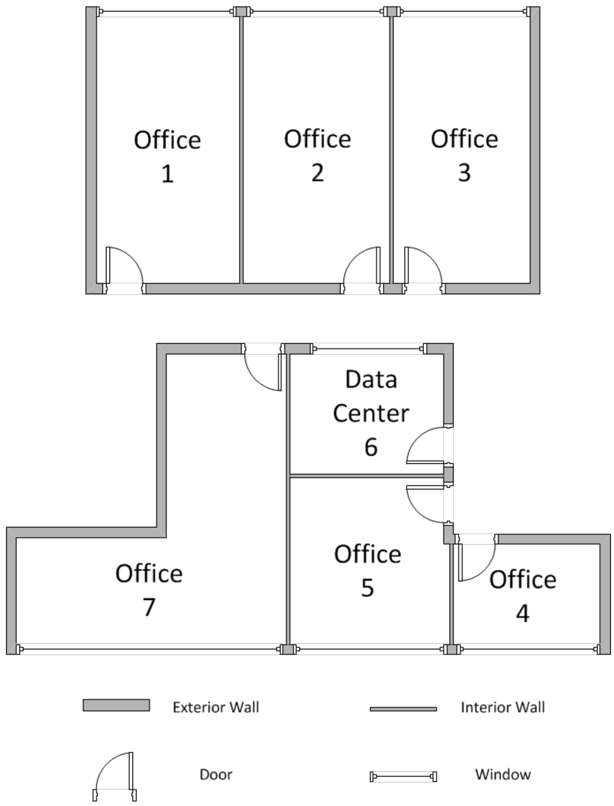

Figure 4.5 – Layout of the laboratory where the classification datasets were recorded

enables the collection of large amounts of data on a reasonable timescale.

The data used in the experiments was obtained by scanning the entire GSM band in 7 rooms of the laboratory building, hereby named "laboratory site". In April of 2012, on a Saturday afternoon from 2 pm to 6 pm, 5500 scans (representing about one half hour of recording per room) were recorded in each of the 7 unoccupied rooms and manually labeled with the corresponding room numbers, as illustrated in Figure 4.5. Each scan contains the RSS of all 548 carriers in the GSM 900 and GSM 1800 bands, with values ranging from -117 to -38 dBm. All scans were made during "random walks" in the 7 rooms with the TEMS Pocket handheld by the user. The exact positions of the individual scans within a room were not recorded; indeed all points in a given room are treated as belonging to that room, consistent with the room-level indoor localization approach adopted.

4.3.2.2 SVM classification results

The performance of each classifier is presented as the percentage of correctly classified test examples. In the dataset, in each room, the first 3000 examples are used offline for training the classifiers and finding the appropriate values of the hyper parameters by cross-validation. The final 2500 of the 5500 scans make up the test set. Testing involves the computation of the sign of

$f(x)$ from relations (4.7) or (4.8), which is very fast.

Experimental results are shown in Table 4.2. The soft margin parameter C and RBF kernel parameter σ are selected through cross-validation, giving $C = 10^{-4}$ in linear one-vs-one and linear one-vs-all classifiers, $C = 10^{-4}$ and $\sigma = 100$ in RBF one-vs-one and one-vs-all classifiers. Results for k-NN and 1-NN ($k = 1$ for k-NN) classifiers are also given for comparison.

Table 4.2 – Percentage of Correct Classification on Test Set

Classifier	**Fingerprint Type**		
	GSM 900	**GSM 1800**	**Both Bands**
1-NN	56.2%	54.4%	62.7%
k-NN	62.4%(k=77)	61.2%(k=21)	67.9%(k=14)
Linear 1-vs-1	86.3%	83.2%	93.9%
Linear 1-vs-All	87.1%	85.0%	94.2%
RBF 1-vs-1	85.5%	84.6%	93.0%
RBF 1-vs-All	87.2%	85.7%	94.1%

As can be seen in the table, the SVM room classifiers give correct results about 94% of the time with no significant difference between linear and nonlinear kernels. As expected, results from k-NN classifiers are significantly poorer. We also note that the GSM 900 (174 carriers) and GSM 1800 (374 carriers) bands are complementary in that better localization accuracy is obtained when both bands are present in the fingerprint. In Figure 4.6 we show how the accuracy improves with fingerprint size, for the linear one-vs-all algorithm, by increasing the number of carriers in steps of 50, according to the ordered sequence numbers of the GSM carriers.

In figure 4.7 we examine the effect of increasing the number of training examples for each of the 7 rooms, again using the linear one-vs-one algorithm. The figure plots the percentage of correct room classifications as a function of the training set size. We see that a rather substantial reduction in training set size gives only a very moderate degradation in performance. For example, 93% of the test examples were correctly classified using only 1000 training examples. This is a very interesting result as far as acquisition time is concerned, as the TEMS Pocket requires less than 10 minutes to record 1000 training examples.

Table 4.3 presents the confusion matrix for the case of the linear one-vs-one algorithm, showing how the mis-classified examples are distributed. It can be seen that most confusions occur between adjacent rooms, as could be expected. Rooms located on opposite sides of the corridor are easily discriminated.

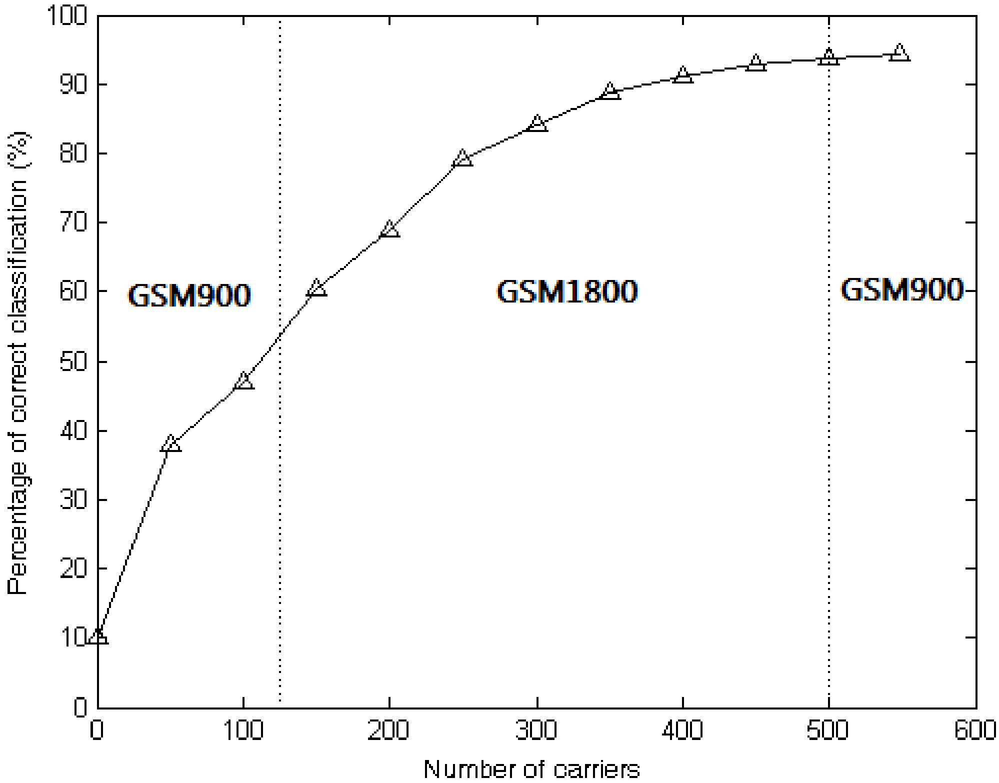

Figure 4.6 – Classification results as a function of fingerprint size

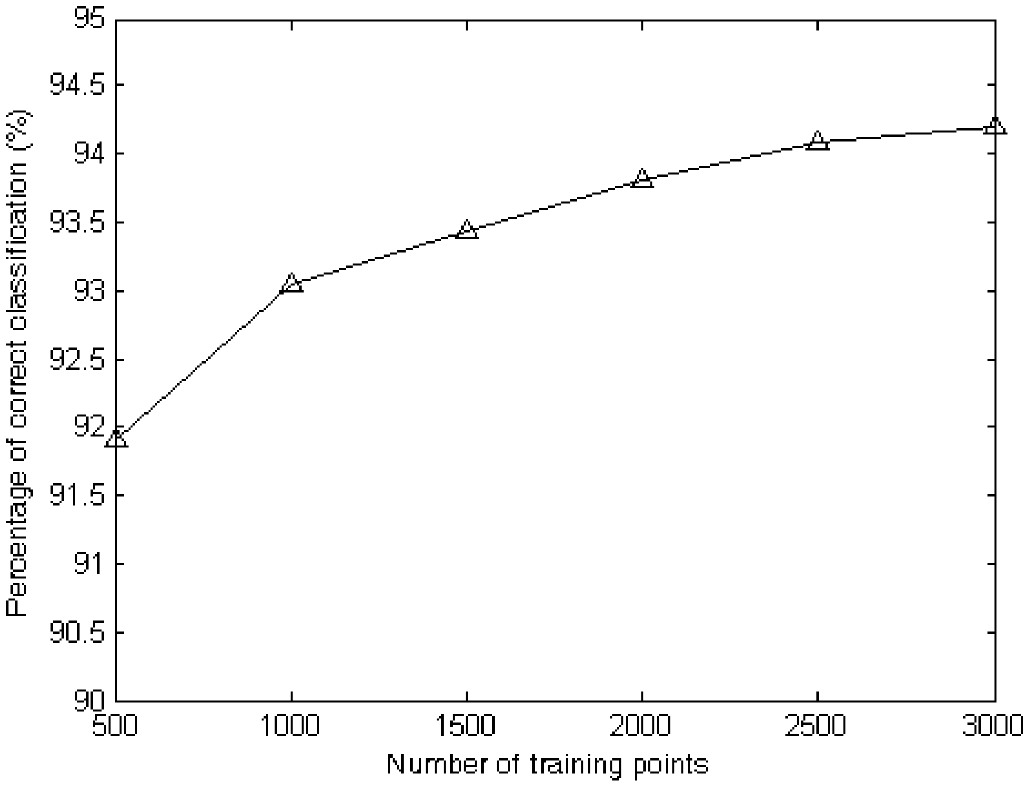

Figure 4.7 – Classification results as a function of training set size

Table 4.3 – Confusion Matrix for 7 Rooms Classification

Predicted Class	**True Class**						
	1	**2**	**3**	**4**	**5**	**6**	**7**
1	91.1%	4.7%	4.2%	0%	0%	0%	0%
2	3.9%	94.9%	1.2%	0%	0%	0%	0%
3	2.6%	1.7%	95.7%	0%	0%	0%	0%
4	0%	0%	0%	96%	1.1%	0%	2.9%
5	0%	0%	0%	0.8%	97.1%	0.5%	1.6%
6	0%	0%	0%	0%	0%	99.9%	0.1%
7	0%	0.6%	0%	4.1%	4.3%	3%	88%

4.3.2.3 The evolution of classification performance

These SVM classifiers work well on the data recorded in the same day, but a significant performance decrease was also observed after a period of time. After the model was constructed, subsequent experiments and verifications were performed for more than 6 months. Three datasets were recorded in the same setting as introduced in section 4.3.2.1, 22, 56, and 148 days respectively after that dataset. These three datasets, together with the dataset introduced in 4.3.2.1 are hereafter named $S1$ (5500 scans in each room), $S2$ (2000 scans in each room), $S3$ (1000 scans in each room) and $S4$ (1000 scans in each room). The evolution of performance was examined using these four datasets, which are shown in Figure 4.8. It can be seen in the figure, the performance has a sharp decline after the localization model is built. Compared with testing the "fresh" data that more than 94% of the test examples can be correctly labeled, after 22 days, the performance decrease to 60%. Only 40% of the test examples recorded after about two months can be correctly classified. This is the biggest challenge for fingerprinting based GSM indoor localization, since the localization model decays quite fast. In addition, such performance degradation problem were not taken into consideration by previous work on GSM indoor localization.

Indeed, due to shadowing, multipath and environmental effects such as building geometry, network traffic, presence of people, and atmospheric conditions, RSS is expected to be nonlinear with distance, non-Gaussian, and time varying, which can lead to performance degradation over time. In addition to the short-term fluctuation and day-night variations presented in section 3.3.2, sudden shifts of RSS in some GSM channels were also observed in a long-term experiment over two months. Figure 4.9 shows the sudden shifts of RSS of two GSM channels (carrier index 135 and 278), which were probably caused by an update or upgrade of local base stations.

This unpredictable performance decrease is a common problem of all fingerprinting techniques. However, it largely influences the prospects of fingerprinting based localization

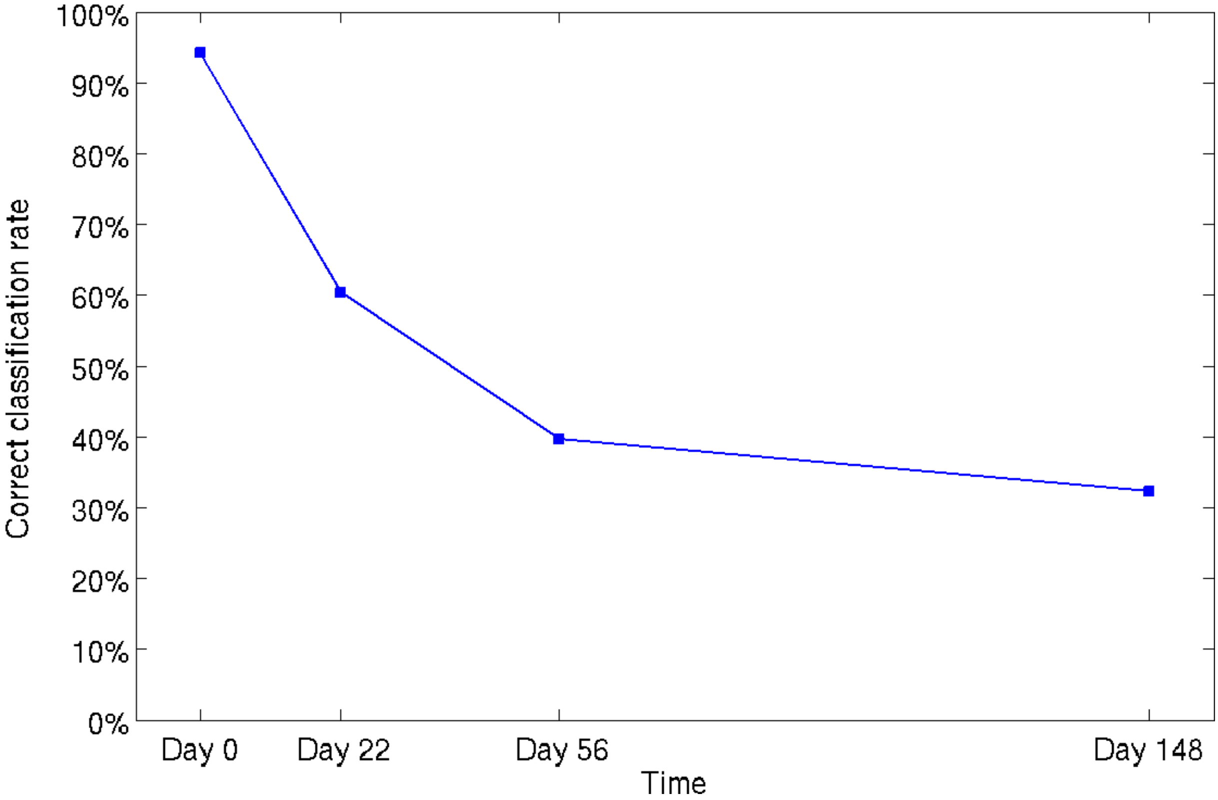

Figure 4.8 – Performance evolution of SVM classification

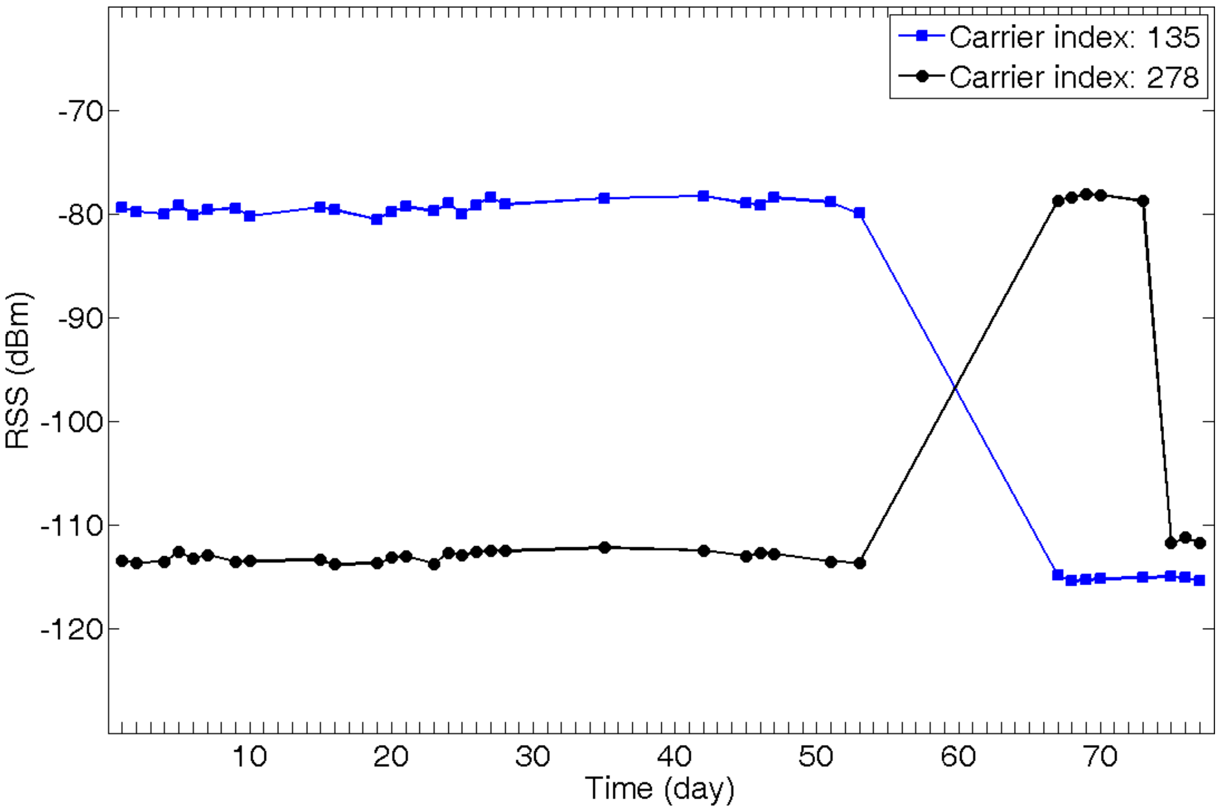

Figure 4.9 – RSS in channel 135 and 278 in room 1.

approaches, since calibration has already been time and labor consuming. In this thesis, maintaining the localization performance over time is studied, by introducing 1) transductive inference to update the localization classifiers with new unlabeled data and 2) a more general sampling method, "time sampling".

4.3.3 Evaluation of transductive SVM

Transductive inference is introduced to overcome the problem of performance decrease over time. As time goes on, the localization model may be outdated, because RSS in the same channels may have drifted. Transductive SVM (TSVM) can adjust the discriminant functions by taking some newly collected unlabeled data to update the classifiers.

4.3.3.1 Transductive SVM classifier

TSVM take unlabeled new examples into account and adjust the separating surface to separate both training examples and the new unlabeled examples with maximum margin. For a linearly separable data case, the separating surface is obtained by solving the following optimization problem:

$$\begin{aligned} &\text{minimize} && \frac{1}{2}||\mathbf{w}^2|| \\ &\text{subject to} && \begin{cases} y_i\left(\mathbf{w}\cdot\mathbf{x}_i + b\right) \geq 1 \\ y_j^*\left(\mathbf{w}\cdot\mathbf{x}_j^* + b\right) \geq 1 \end{cases} \quad \forall i, j \end{aligned} \tag{4.10}$$

where $\mathbf{x}_j^*$ is the unlabeled data and y_j^* is the label corresponding to $\mathbf{x}_j^*$ given by TSVM.

Therefore, minimization must be performed with respect to $\mathbf{w}$, b, $\mathbf{x}_j^*$ and y_j^* for $j = 1 \cdots N$, in contrast to standard SVM where minimization must be performed with respect to $\mathbf{w}$ and b only. To be able to handle non-separable data, slack variables ζ_i are introduced as in standard SVM classifiers. Algorithms for solving this optimization problem are described in [99, 100]. The TSVM used in our study, were implemented using $\text{SVM}^{\text{Light}}$ [101].

4.3.3.2 Transductive SVM results

TSVM were applied to the four datasets presented in section 4.3.2.3, namely $S1$, $S2$, $S3$ and $S4$. Experimental results are shown in Table 4.4. The performance is presented as the percentage of correctly classified test examples. The first 100 unlabeled examples of each room in $S2$, $S3$ and $S4$ sets were used for TSVM training to adjust the model, the remaining examples were used for testing. For SVM classifiers, we use the model trained on set $S1$ to test the test data in sets $S2$,

$S3$ and $S4$. Only linear one-vs-all multi-class scheme was used because this method gave the best performance in section 4.3.2.2.

Table 4.4 – Comparison of SVM and TSVM

Test Set	**Training Set**	**SVM**	**TSVM**
$S1$	$S1$	94.2%	–
$S2$	$S1$	60.4%	78.4%
$S3$	$S1$	39.7%	58.8%
$S4$	$S1$	32.3%	49.6%

As can be seen in Table 4.4, when building the classifier with set $S1$ and testing it on sets $S2$, $S3$ and $S4$ taken in different time periods, the performance varies dramatically, from about 94% for "fresh" data ($S1$ set), down to as low as 32% ($S4$ set). However, by using only 100 new unlabeled examples of each room with the TSVM, a substantial amount of the lost performance can be recovered.

The TSVM approach is interesting because it presents a way of recovering some of the performance loss due to RSS drift, at the cost only of obtaining some recent unlabeled RSS measurements. In practice, such data might be obtained from scans performed on the handsets of users of the localization system, but without the need to manually label the data. Though the improvement obtained with the TSVM is still not sufficient, the results nevertheless suggest that any scheme that keeps the classifier model "current", by tracking the evolution of the RSS values, should be of interest to us.

4.3.4 Evaluation of the "time sampling" scheme

TSVM overcome in part the performance decrease due to RSS drift by taking some unlabeled data and re-training the model. However, this is a remedial action, which still necessitates time and labor consuming sample measurement and model training with limited success. As for the data-driven classification problems, it is not necessary the more samples for training the better performance can be achieved. If most of the fingerprint examples are identically duplicate, the performance of localization system based on such training samples will not improve. Furthermore, a model constructed based on a large number of training samples can be quite effective for the "current" test examples, but it is not tolerant for the RSS changes over time. As a result, to make the localization model robust over time, it is necessary to collect training examples in a more representative way that incorporating as much as possible of the RSS fluctuations.

4.3.4.1 The "time sampling" scheme and datasets

As discussed in section 4.3.2.3, RSS suffers from fluctuations on different time scales. To counteract the effect of these fluctuations, a "time sampling" scheme was also used in recording the datasets. On each day where measurements were made, fingerprints were recorded at different time periods from morning to evening. Such training data, over extended period of time, are thus expected to provide a better sampling of RSS fingerprint values.

Scans were recorded during random walks in all seven rooms shown of Figure 4.5 and manually labeled with the corresponding room numbers. While scanning a room, the TEMS Pocket was turned on and held in hand while walking; then, after a few minutes, the scan was stopped. Datasets were recorded on thirty-four different days between December 15, 2012 and March 01, 2013.

4.3.4.2 Results of the "time sampling" scheme

Classification results using "time sampling" are shown in Figure 4.10, where we present the percentage of correctly classified test examples as a function of time for different sizes of the training set (one day, two days and eight days for training respectively). The classifier used was a set of linear one-vs-all SVM with regularization constant $C = 0.01$. It can be seen that the larger the training data set, the better the results obtained. When the localization model is trained using a dataset in only one day, the correct classification rates afterward are around 50%. In contrast, if the localization model is trained using data recorded in the first two days, the test performance afterwards is improved dramatically to between 70% and 80%, and stays reasonably constant. An even better performance is obtained by the model trained using a dataset of 8 days, which reaches 90% accuracy a few days after the model is built and, in most cases, retains a performance in excess of 80% even more than fifty days after training. Training during longer periods does not further increase the performance.

Figure 4.10 also shows that after about fifty days, two sharp decreases in classification accuracy occurred in our experiments. These can be traced back to significant RSS shifts of some GSM channels as discussed in section 4.3.2.3, where sudden shifts of RSS of two GSM channels (carrier index 135 and 278) were observed. Such shifts are quite simple to detect, which suggests a simple scheme, such as a fixed RSS monitoring installation, which could be introduced to render performance robust against such changes. Figure 4.11 shows the results of retraining the models after removing unstable channels from the fingerprint vectors fed to the classifier. The performance

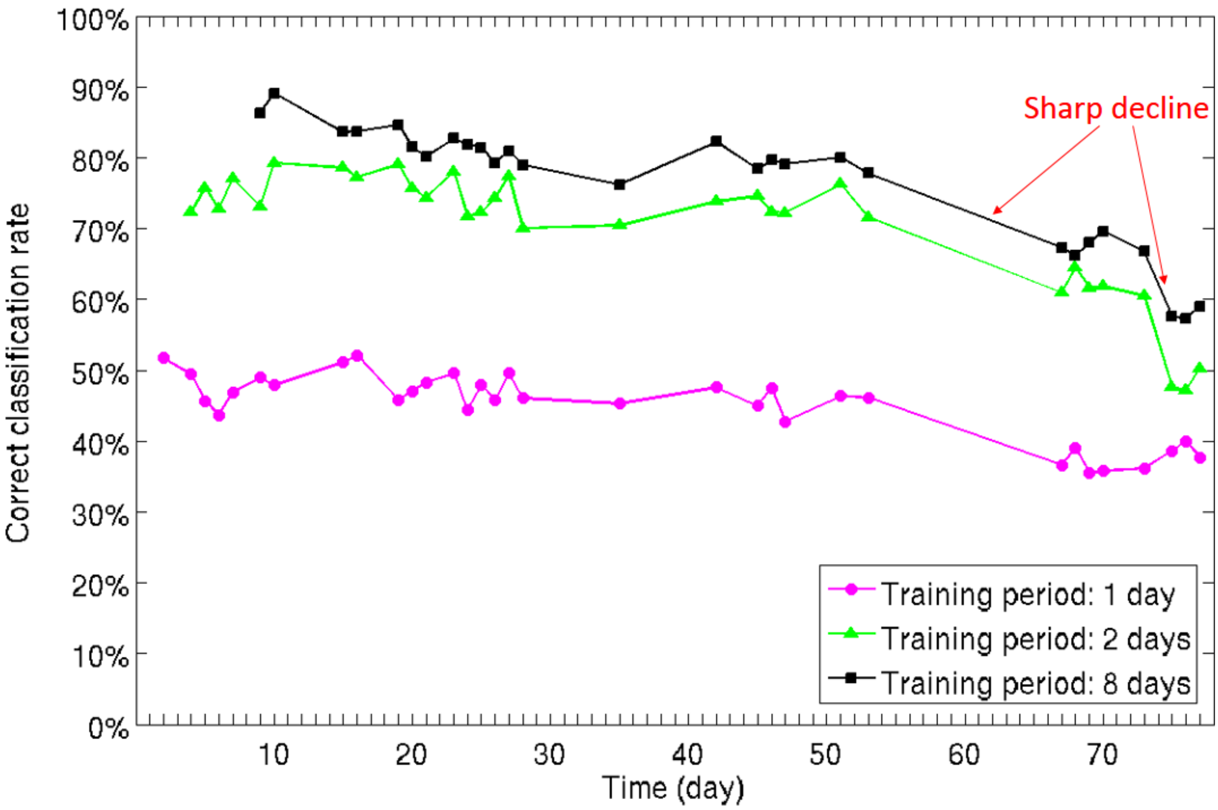

Figure 4.10 – Classification results based on models using different training period of time.

of the updated classifier is relatively stable and consistent with the more gradual performance degradation observed before the network changes occurred.

4.4 Bayesian filter post-processing

Localization accuracy achieved by the current measurement can be improved by taking previous measurements into account. Due to the fast scanning property of TEMS Pocket, about three measurements per second can be obtained. In practical scenarios, updating the location every second is acceptable, since a mobile user does not move too far away in one second. Hence, a simple approach to improve the localization accuracy is to apply a low-pass filter, either to the RSS measurements or to the raw results.

In this thesis, post-processing takes into account both the time constraints (the receiver moves with a finite velocity) and the space constraints (presence of walls and furniture, occupancy of the room, etc.). This is achieved by Bayesian filtering, which allows combining the current and previous SVM classifier outputs and taking into account space constraints [102].

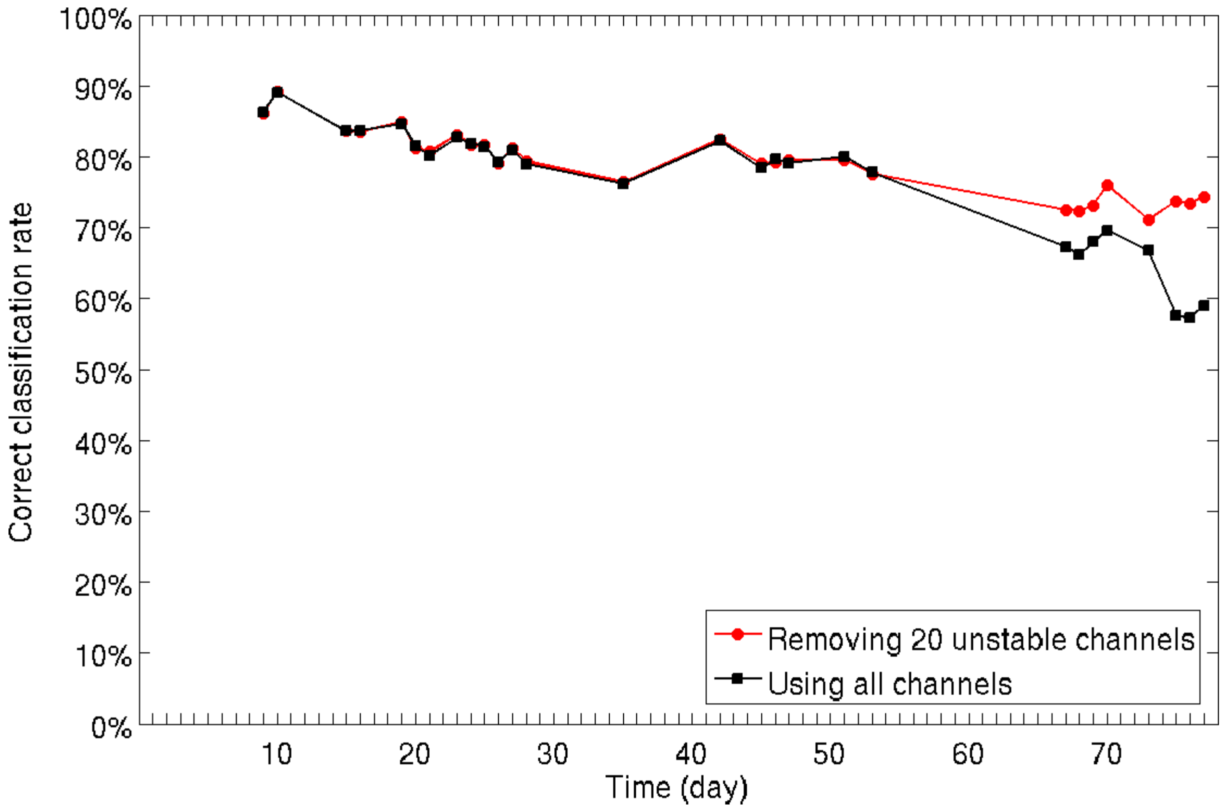

Figure 4.11 – Classification results after removing 20 unstable GSM channels.

4.4.1 Recursive Bayesian filtering

For room-level indoor localization, let the state x_t at discrete time t be the actual room number of the mobile target at time t, and the observation y_t the output of the SVM classifier at the same time. We assume that the state at time t depends only on the state at time $t-1$. From Bayes' theorem [103], the probability of the target being in room x_t given the past and present outputs of the SVM classifier is:

$$P(x_t|y_t, y_{t-1}) = \frac{P(y_t|y_{t-1}, x_t)P(y_{t-1}|x_t)P(x_t)}{P(y_t, y_{t-1})} \tag{4.11}$$

Since the classifier at time t does not take into account its previous output, we can write:

$$P(y_t|y_{t-1}, x_t) = P(y_t|x_t) \tag{4.12}$$

Applying Bayes' theorem to x_t and y_t, we have:

$$P(x_t|y_{t-1}) = \frac{P(y_{t-1}|x_t)P(x_t)}{P(y_{t-1})} \tag{4.13}$$

Therefore, relation (4.11) can be rewritten as

$$\begin{aligned} P(x_t|y_t, y_{t-1}) &= \frac{P(y_t|x_t)P(x_t|y_{t-1})P(y_{t-1})}{P(y_t, y_{t-1})} \\ &= \frac{P(y_t|x_t)P(x_t|y_{t-1})}{P(y_t|y_{t-1})} \end{aligned} \tag{4.14}$$

where $P(y_t|x_t)$ is the likelihood probability of receiving the label y_t from the classifier, when the target is in room x_t, and $P(x_t|y_{t-1})$ is the probability of the target being in location x_t given the label assigned by the SVM classifier at time $t-1$. For our room-level indoor localization, we have a finite number of rooms, i.e. finite number of states for filtering. Therefore, we can write:

$$P(x_t|y_{t-1}) = \sum_{x_{t-1}=1}^{N} P(x_t|x_{t-1})P(x_{t-1}|y_{t-1}) \tag{4.15}$$

where N is the number of states, and $P(x_t|x_{t-1})$ is the state transition probability from x_{t-1} to x_t, which is constrained by the prior information of room layout, target velocity, maximum room occupancy, etc, as described in the next subsection.

Finally we obtain:

$$P(x_t|y_t, y_{t-1}) = \frac{P(y_t|x_t) \sum_{x_{t-1}=1}^{N} P(x_t|x_{t-1})P(x_{t-1}|y_{t-1})}{P(y_t|y_{t-1})} \tag{4.16}$$

It is assumed that the initial probabilities $\{P(x_0|y_0) = P(x_0), x_0 = 1, \cdots, N\}$ of the state are known or taken equal to $1/N$. Then, in principle, the posterior probabilities$\{P(x_t|y_t, y_{t-1}), x_t = 1, \cdots, N\}$ are obtained, recursively, in two stages: prediction and update, as described in (4-15) and (4-16) respectively. The final estimation of location is taken to be that of the state with the largest posterior probability:

$$\hat{x}_t = \underset{x_t}{\operatorname{argmax}}\, P(x_t|y_t, y_{t-1}) \tag{4.17}$$

4.4.2 Prior information

In this work, the aim is to obtain the most probable location of the device. For the "laboratory site", the indoor environment is modeled as nodes and paths as shown in Figure 4.12. Rooms are the nodes numbered from 1 to 7, and the corridor is split into three sections and modeled as three additional nodes numbered from 8 to 10. The edges between nodes denote feasible paths between rooms. It is desired that the Bayesian filter provides a trajectory that uses feasible paths, and is consistent with the usual velocity of the target.

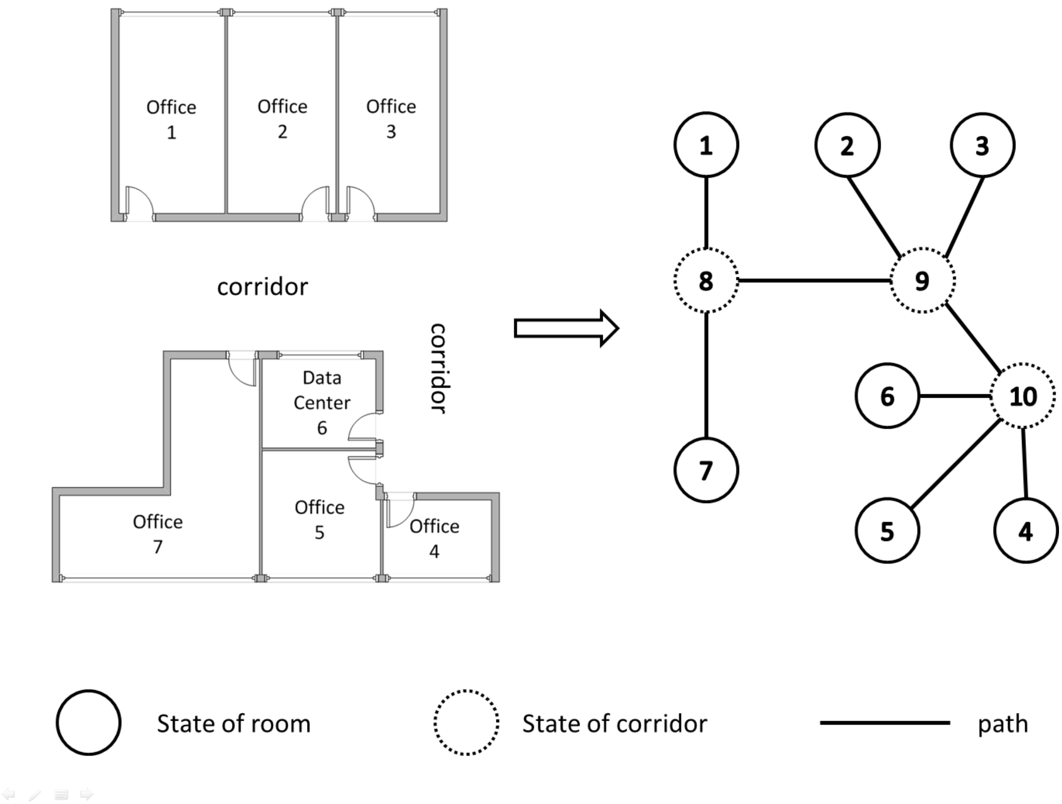

Figure 4.12 – Node and path model abstracted from the experimental site

Therefore, the state transition probability $P(x_t|x_{t-1})$ in relation (4.15) is defined in this thesis as:

$$P(x_t|x_{t-1}) = \begin{cases} P_0, & if \text{ pathlength}(x_t, x_{t-1}) = 0 \\ P_1, & if \text{ pathlength}(x_t, x_{t-1}) = 1 \\ 0, & if \text{ pathlength}(x_t, x_{t-1}) > 1 \end{cases} \tag{4.18}$$

where pathlength(i, j) is the length of the path from room i to room j. In this work, the lengths of all the paths that directly link two rooms are assigned the value 1.

4.4.3 Observation model

The observations in our case are the decisions of the SVM classification described above (section 4.3.1.2). The likelihood $P(y_t|x_t)$ in relation (4.16) can be estimated, given the available data, from the SVM confusion matrix, such as Table 4.3. In a confusion matrix, let C_{ij} be the number of examples that are assigned to class i while the target is actually in room j. Then

$$P(y_t = i|x_t = j) \approx \frac{C_{ij}}{\sum\limits_{l=1}^{N} C_{il}} \tag{4.19}$$

4.4.4 Evaluation of Bayesian filtering post-processing

4.4.4.1 Datasets for Bayesian filtering

The datasets for Bayesian filtering were taken while a user, holding the TEMS mobile phone, walked between the seven rooms, continuously recording the RSS of the moving traces. The actual traces followed were recorded using the mobile phone camera. Nine such tracking datasets were recorded in our experiments. Datasets were recorded on nine different days between December 24, 2012 and February 03, 2013. A dataset for building the confusion matrix of ten states were recorded in April 15 and 17, 2013. We note that Bayesian filtering must unfortunately be applied offline, as the TEMS Pocket does not allow us to access RSS fingerprints in real time.

4.4.4.2 Results of Bayesian filtering

Bayesian filtering results are shown in Table 4.5, where the raw results of SVM classification are compared with the results obtained after Bayesian filtering. The classification model used here was trained on datasets obtained within the first two days of the "time sampling" experiments (section 4.3.4.2), i.e. the triangle line in Figure 4.10. The results presented only consider test examples actually recorded within rooms. In the actual traces, some fingerprints were in fact acquired in the corridor, and thus were not taken into account, since the SVM only classifies the 7 rooms. The results obtained from SVM classification without Bayesian filtering are similar to those presented on Figure 4.10 in the same conditions (training period of two days). It is clear that Bayesian filtering provides a substantial improvement over raw classification results, even though the classifier is optimally trained using a large dataset. In addition, the results are stable over time.

Table 4.5 – Comparison of SVM Classification and Bayesian Filtering

Test Dataset	**Classification accuracy before Bayesian filtering**	**Classification accuracy after Bayesian filtering**
Dec 24, 2012	74.3%	98.8%
Dec 29, 2012	70.6%	99.1%
Dec 30, 2012	72.4%	99.4%
Jan 02, 2013	77.1%	99.6%
Jan 03, 2013	75.9%	98.9%
Jan 04, 2013	70.0%	98.4%
Jan 06, 2013	83.2%	99.7%
Jan 07, 2013	68.3%	97.1%
Feb 03, 2013	77.7%	99.5%

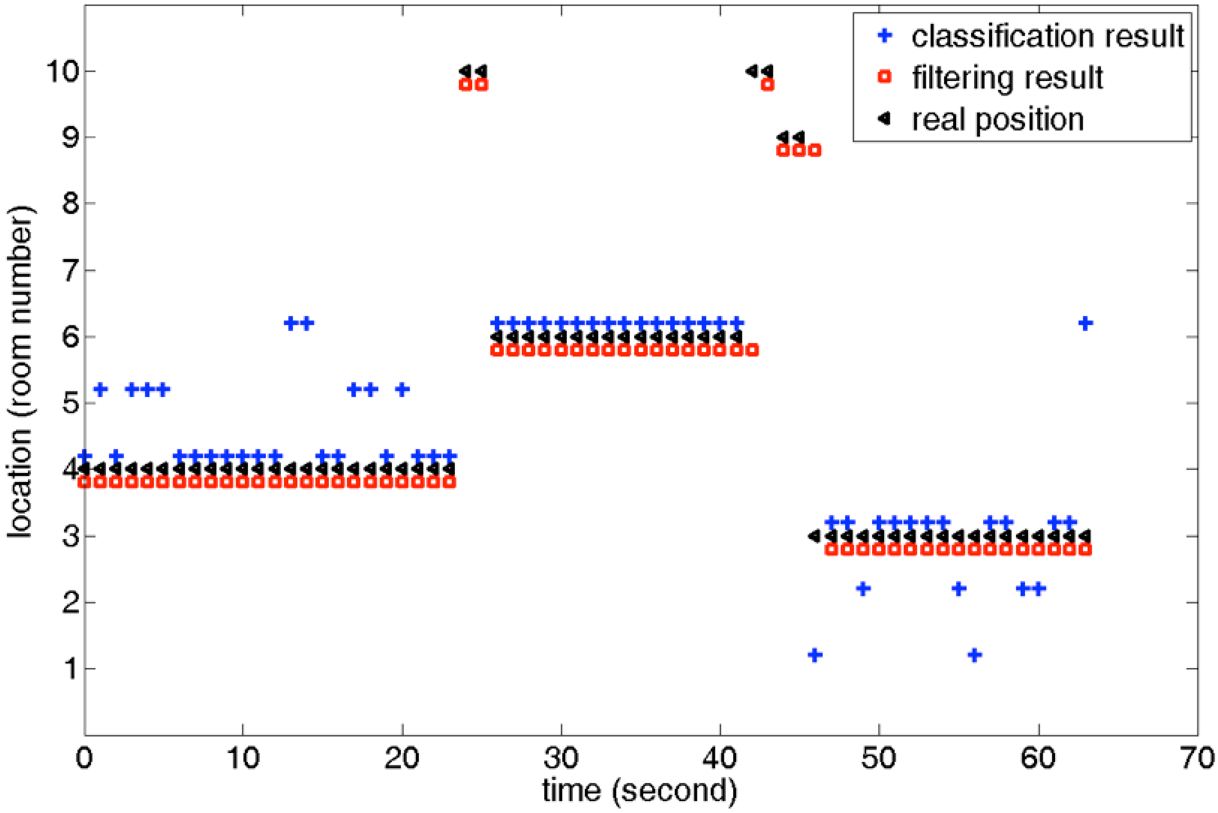

Figure 4.13 – Target tracking results of trace December 30

Figure 4.13 presents the results on one test trace (December 30), showing the real position, SVM classification results and Bayesian filtering results. Locations 1 to 7 correspond to rooms 1 to 7, while location 8 to 10 are the sections of the corridor illustrated in Figure 4.12. The Bayesian filtering method correctly tracked the moving target, except for a few mistakes in the corridor.

4.5 Summary

In this chapter, indoor localization using RSS fingerprints from the GSM network is investigated, including an analysis of the relationship between signal strength and location, the proposed room-level indoor localization, the degradation of localization performance over time and its solutions, and the Bayesian filtering post-processing.

In a study of ambient RSS distribution in an indoor environment using SVM regression, no smooth functional relationship could be discovered between GSM RSS and position for the indoor environment tested, implying that interpolation-based techniques that use a certain number of reference points are not likely to be successful. The use of ambient GSM RSS-based classifiers trained with data collected throughout the areas of rooms, however, presents a viable alternative. The SVM classification has been tested on a dataset acquired in a laboratory building under realistic conditions, and experimental results show that the percentage of correct room labeling can be up to 94% if the model is used when no significant RSS drift sets in.

A performance degradation over time is observed in experiments across several months. In order to cope with this degradation caused by RSS drift over time, transductive inference was introduced to update the SVM classifiers with new unlabeled data. When tested on data sets collected over nine months, this approach proved capable of restoring a significant part of the lost performance. A more time and labor saving solution is studied, using a proposed “time sampling” scheme to collect RSS fingerprint examples in a more representative way. Experimental results indicate that the “time sampling” data collection scheme leads to a more robust localization, with performances relatively stable over a couple of months.

Bayesian filtering is investigated for localization post-processing, which combines the SVM classification outputs with the characteristics of user movements and the indoor layout constraints. The indoor layout is modeled as nodes and paths, providing accessible tracks that a target can move in, and this model is consistent with the usual velocity of the target. Experimental results show that the Bayesian filter substantially improved the raw classification results.

In addition to the experiments in a laboratory building, the proposed room-level indoor localization approach and Bayesian filtering post-processing were also tested in a completely different environment, the results of which will be presented in chapter 6.

Chapter 5

Combination of GSM fingerprinting and mobile sensors

5.1 Introduction

With the popularity of smart devices such as mobile phones and tablets, more and more mobile sensors are now built into mobile devices. The multiple mobile sensors have the advantages of rapid response rate, light weight and low power consumption. Such mobile sensors as accelerometer and gyroscope provide additional location sources, which are potentially viable for improving indoor localization. Sensor dead-reckoning can be useful for indoor localization by estimating the displacement of a pedestrian accurately over a short distance; however, it is not a usable standalone solution, since it needs a known starting point to integrate the displacement. Sensor drift, noise and disturbances can influence the accuracy of sensor dead-reckoning, and mobile sensors provide information about the mobile device itself, which can differ from those of the user. In this chapter, the thesis investigates the combination of the GSM classification technique with mobile sensor dead-reckoning, acquiring the merits of both techniques and forming a bridge between discrete, room-level localization and continuous coordinate-level localization.

The mobile sensor readings are first introduced, as they are critical to indoor location estimation. The characteristics of three location related mobile sensors, accelerometer, gyroscope and magnetic field sensor, are examined. Then, the fundamentals of sensor dead-reckoning, step detection, stride length and orientation estimation respectively are studied. Steps are detected by monitoring the peaks and troughs of the acceleration amplitude, plus extra time and amplitude thresholds that prevent step misdetections. A stride length model adaptation technique is proposed to automatically estimate the best parameters for different users and environments. Both the gyroscope and the magnetic field sensor are used for accurate and reliable orientation estimations, using a complementary filter. In addition, device positions related to the user in practical scenarios, e.g., in a hand or a pocket, are investigated and a solution is provided to handle arbitrary position changes of the mobile device.

Particle filters have become a powerful tool in location estimation and target tracking systems: they allow combining localization data from a variety of sources – for example, beacon data, embedded smartphone sensors, and building layout constrains. Particle filter data fusion is investigated in section 5.3. It uses room-level positioning results from GSM fingerprinting to correct for accumulated inertial dead-reckoning errors, while also referring to a building map to exclude inaccessible regions and forbid unreasonable movements such as crossing a wall. With this approach, the localization system produces accurate coordinate locations rather than room labels.

5.2 Mobile sensor dead-reckoning

As introduced in section 2.2.4, sensor dead-reckoning is the process of estimating the unknown current position based on the last estimated position by adding the displacement computed from the heading direction and the speed information over the elapsed time. For mobile devices, dead-reckoning mainly consists of step detection, stride length determination and orientation estimation, which are based on the mobile sensor readings of the accelerometer, gyroscope and magnetic field sensor.

5.2.1 Mobile sensor readings

There are multiple MEMS sensors embedded in mobile devices collecting different kinds of data. Accelerometer, gyroscope and magnetic field sensor are the most common sensors integrated in most smart devices. Mobile sensor readings are tested in this section to get the characteristics of different sensors. The tests are based on a Google Nexus 7 tablet with Android open source operating system [104]. Data acquisition software is programmed using the Java programming language. Sampling rate is 50 Hz. The coordinates of the Google Nexus 7 tablet are defined in Figure 5.1.

Figure 5.1 – Coordinate definition of the Google Nexus 7 tablet

5.2.1.1 Accelerometer

The accelerometer measures the acceleration of a mobile device along three axes. When the mobile device is put in the pocket or held in hand, user movements or gestures are reflected in the acceleration measurements. If the mobile device is placed on a stationary object, the accelerometer measures the acceleration of gravity. A sample of accelerometer readings was taken when the tablet was held in hand walking a small distance. The accelerations along the three axes are shown in Figure 5.2.

It is seen in Figure 5.2 that accelerations fluctuate while walking, exhibiting an approximately periodic rhythm. Since the acceleration of gravity is decomposed into different coordinate axes, the mean accelerations on the different axes are at different levels. As expected, the fluctuations on the Z axis are much larger than on the other axes, which is a result of user walking.

5.2.1.2 Gyroscope

The gyroscope measures angular velocity around three axes. An example of the gyroscope sensor readings was recorded while the tablet was held in hand walking and turning, as shown in Figure 5.3.

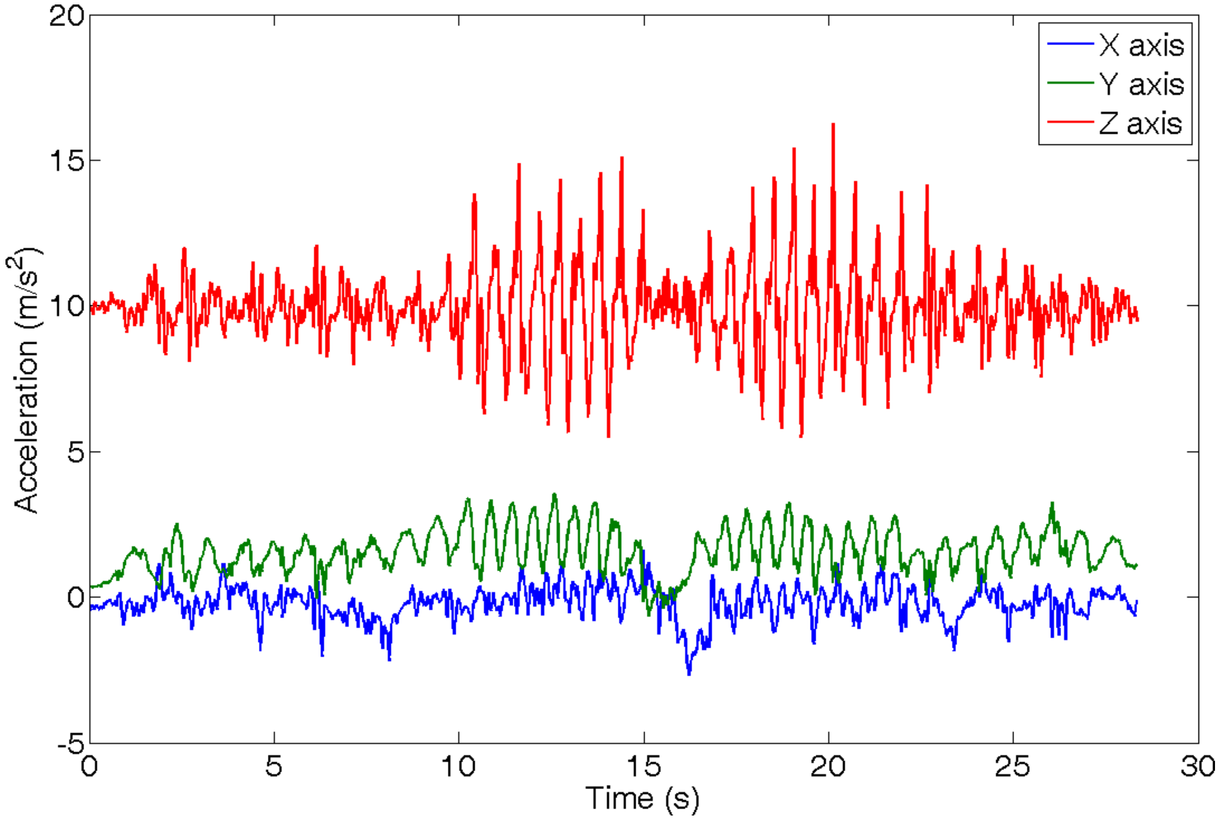

Figure 5.2 – The accelerometer readings

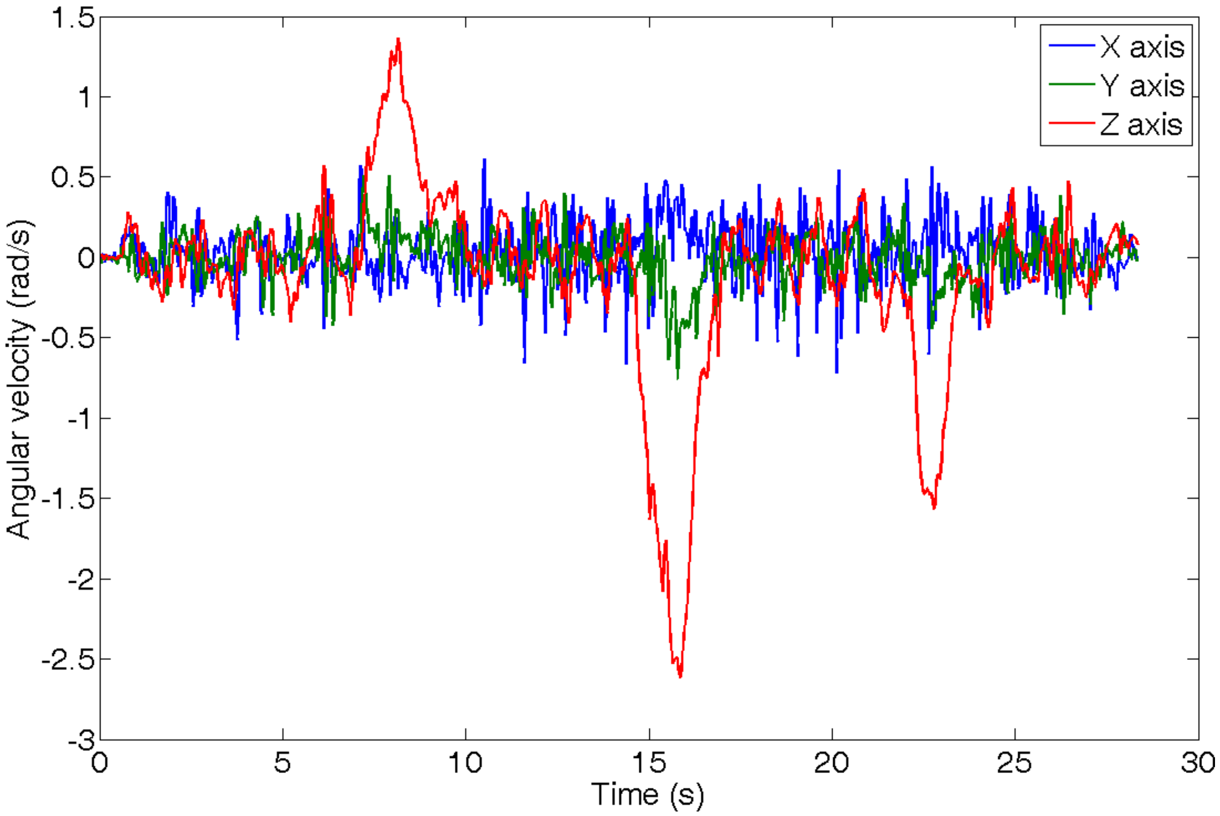

Figure 5.3 – The gyroscope readings

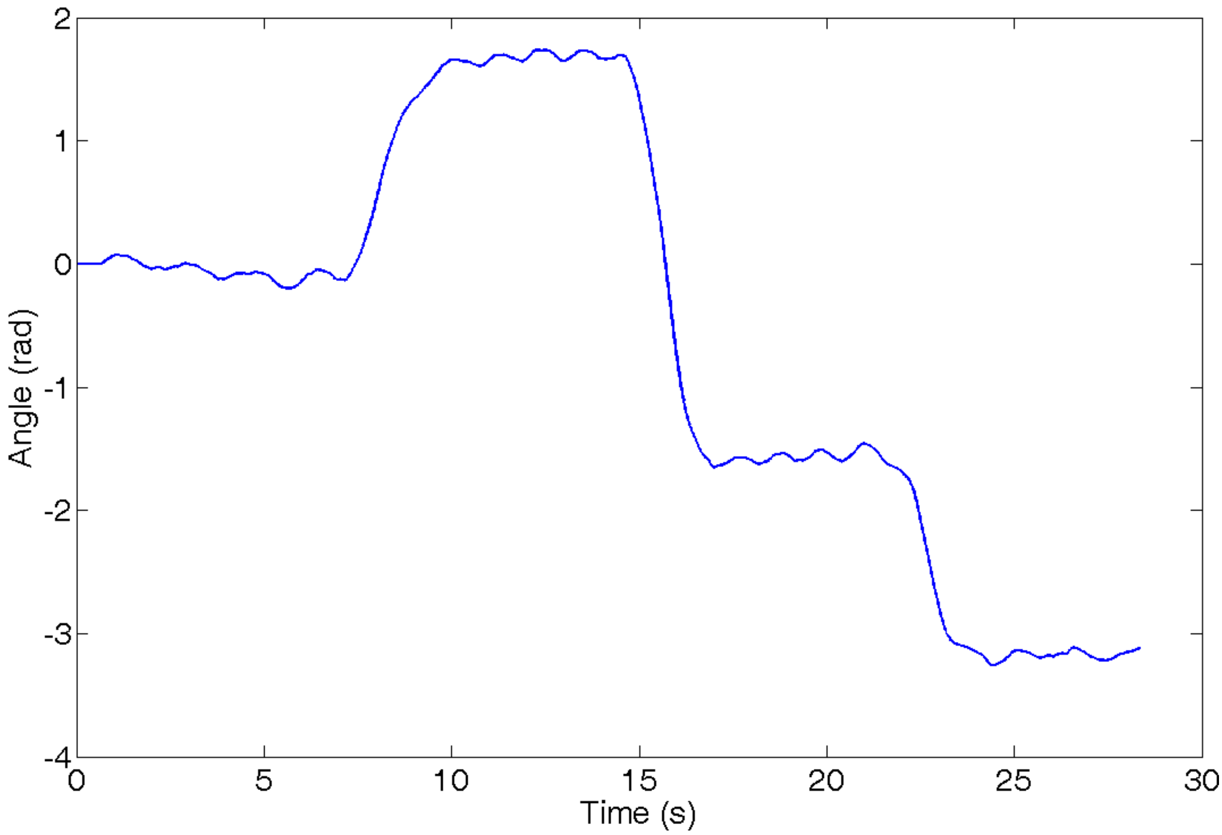

Figure 5.4 – Turning angle obtained from the gyroscope

Since the tablet is held with Z axis facing up, the turning movements are mainly reflected on the Z axis, with the angular rate rising and falling sharply when turning. Relative turning angle can be obtained based on the gyroscope sensor readings by integrating angular velocity over time as shown in Figure 5.4.

5.2.1.3 Magnetic field sensor

The magnetic field sensor measures the direction and strength of the magnetic field along the three axes of the mobile device. An example of the three axes magnetic field sensor readings recorded simultaneously with the gyroscope readings is shown in Figure 5.5

For indoor localization these measurements are converted into a direction, known as the azimuth angle. The advantage of the magnetic field sensor measurement is that it can provide absolute orientation of the mobile device. However, the measurements of the magnetic field sensor have quite a low precision and experience a lot of disturbances in indoor environments. The absolute orientation from the magnetic field sensor and the relative orientation from the gyroscope can be used together to result in a better orientation measurement.

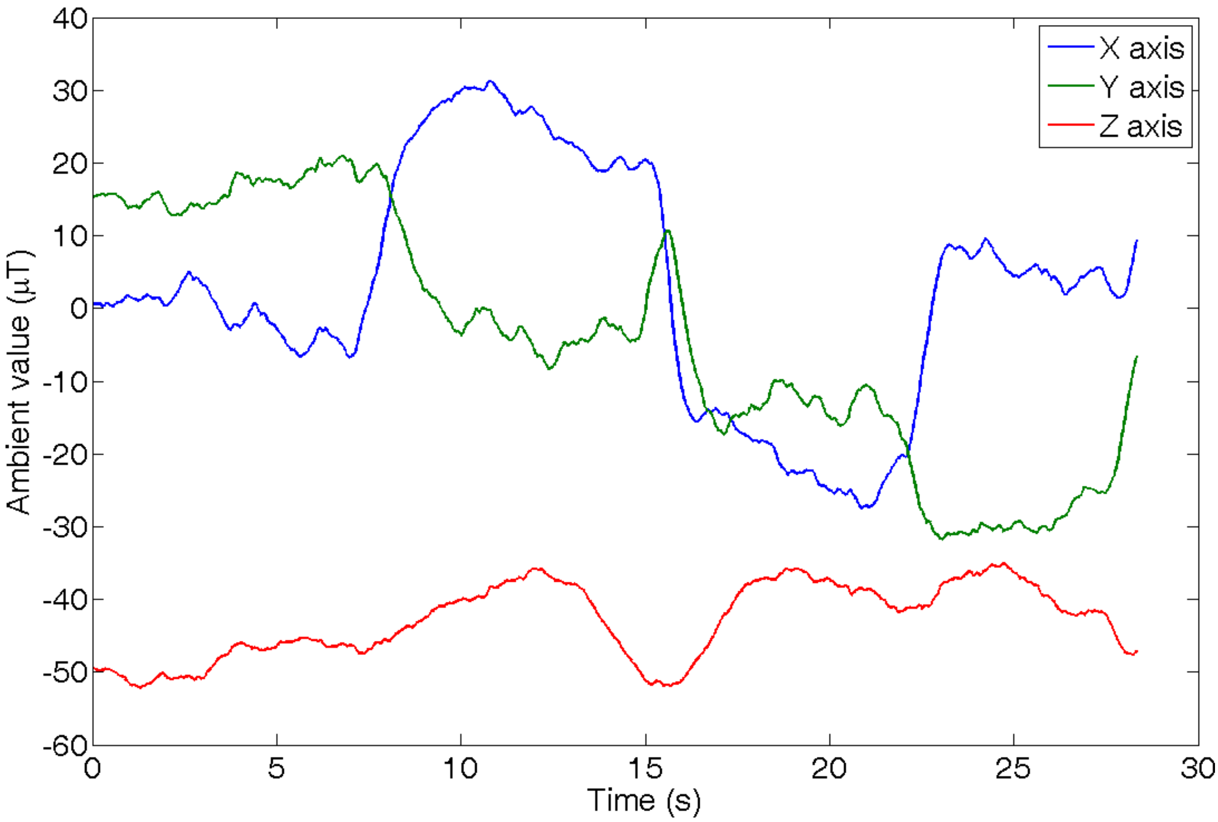

Figure 5.5 – The magnetic field sensor readings

5.2.2 Step detection

Step detection is a basic but key part of sensor dead-reckoning, which is commonly based on accelerometer information. Though a variety of step detection algorithms exist in the literature, the peak and trough search approach is reliable and widely used. While walking, position of the mobile device fluctuates with the rhythm of the walking pace, and the accelerometer periodically outputs such fluctuations as up and down acceleration values. If the acceleration value goes from a peak to a trough or vice versa, it is assumed the mobile user has taken one step. The peak and trough seeking algorithm implemented for step detection consists of the following four steps:

1. Initialize the step detector: Set $a_{\max} = a_{\min} = g$, where $a_{\max}$ is the current maximum acceleration magnitude, $a_{\min}$ is the current minimum acceleration magnitude and g is the acceleration value due to gravity.

2. Compute the magnitude of the acceleration a_i, for current sample i from the measurements using:

$$a_i = \sqrt{a_i^{x2} + a_i^{y2} + a_i^{z2}} \tag{5.1}$$

3. Peak and trough search: Compare the current magnitude of the acceleration with previous

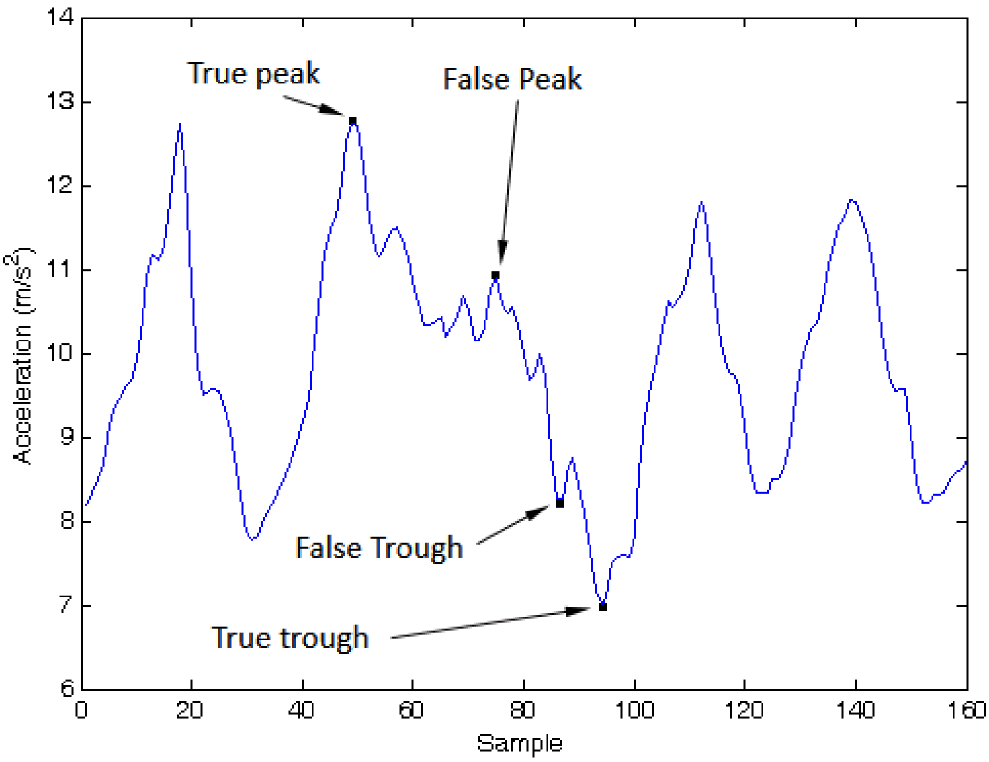

Figure 5.6 – Step determination using acceleration amplitude

maximum and minimum values to get the peak and trough values

$$\begin{cases} if\ a_i > a_{\max}, a_{\max} = a_i \\ if\ a_i > a_{\max}, a_{\max} = a_i \\ else,\ peak\ or\ trough\ found \end{cases} \tag{5.2}$$

4. Step determination: If the current acceleration magnitude is either a new maximum value or a new minimum value, the previous sample is a peak value or a trough value. However, not all the detected peaks and troughs correspond to meaningful step boundaries. As shown in Figure 5.6, due to the noisy measurements, there are "false peaks and troughs". Two thresholds, Δa and Δt, are used to filter out spurious step detections caused by acceleration fluctuations that are either too small in magnitude or too short in time duration. If a distinct step is detected, the algorithm goes back to step 1) and start a new loop of step detection, otherwise the algorithm goes back to step 2) to receive new samples of sensor readings.

5.2.3 Adaptive stride length model

A stride length value is required in order to estimate the displacement associated with a step. However, stride length varies significantly for different persons and walking styles. The literature

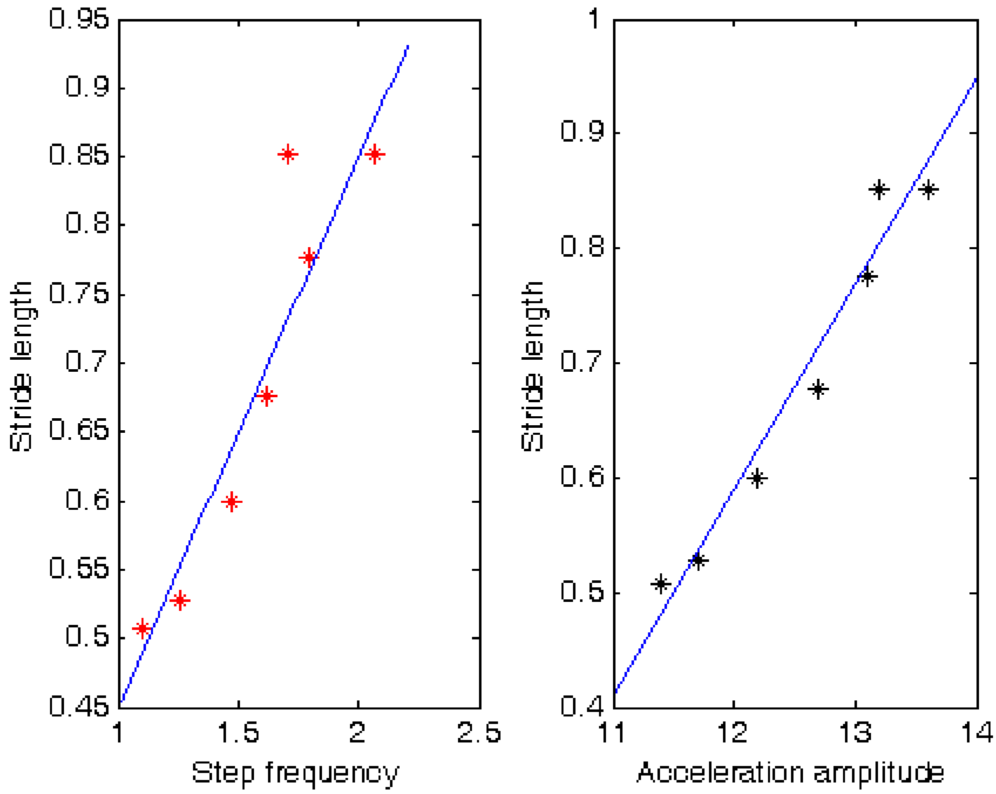

Figure 5.7 – Stride length with step frequency and acceleration amplitude

contains a variety of models indicating that the stride length is related to the stride frequency and the "bounce" of the hip, which we shall refer to as the "frequency model" and "bounce model" [105, 106], respectively.

To verify these, we performed an experiment in which subjects walked a specified path several times at different walking speeds. Step numbers and durations were recorded, while the length of the path was known in advance. The results are shown in Figure 5.7. As seen in the figure, the stride length has a linear relationship with both the step frequency and the acceleration amplitude, indicating that the models are reasonable. Most dead-reckoning solutions using existing models must choose the parameters or estimate them by training on different users and environments.

The "frequency model" requires an estimate of the step frequency over a previous period of time, which introduces a delay if no step is detected. By contrast, the accuracy of "bounce model" is easily influenced by environmental differences, such as going up and down stairs. As there is no stride length model that fits all subjects and environments, we propose to use a particle filter (section 5.3) to adaptively select the best parameters from a range of parameters. The "bounce model" is used in our experiments and we define:

$$\varphi = p(a_{max} - a_{min}) + q \tag{5.3}$$

where φ is the stride length of the current step, p and q are the two parameters that will be estimated in the particle filter.

5.2.4 Orientation estimation

The orientation of a mobile user in our system was estimated based on the accelerometer, gyroscope and magnetic field sensor. Both magnetic field sensor and gyroscope can provide orientation information, but neither gives accurate and reliable moving orientation. The turn rate from a gyroscope can be integrated into an angle increment and the orientation can be obtained by adding it to a known initial azimuth angle; however, integration over long time can introduce an unacceptable cumulative error. Orientation from a magnetic field sensor has no cumulative error, but the magnetic field sensor measurement has slow response rate and poor accuracy, especially in indoor environments where field disturbances always exist. For these reasons, a complementary filter was applied to combine these two orientation sources.

The principle of the complementary orientation filter is shown in Figure 5.8. Suppose the real orientation of the mobile phone at time t is ψ_t. The orientation obtained from the magnetic field sensor ψ_t^{mag} and gyroscope ψ_t^{gyr} containing high and low frequency noises can be denoted as $\psi_t + \sigma_t^{hf}$ and $\psi_t + \sigma_t^{lf}$ respectively. On one hand, a low pass filter is applied to the orientation obtained from the magnetic field sensor, which filters the high frequency noises and has the Laplace transfer function as:

$$\hat{\Psi}^{mag}(s) = \frac{1}{1+Ts}\left(\Psi(s) + \Sigma^{hf}(s)\right) \approx \frac{1}{1+Ts}\Psi(s) \tag{5.4}$$

where $\Psi^{mag}(s)$, $\Psi(s)$ and $\Sigma^{hf}(s)$ are the Laplace transforms of ψ_t^{mag}, ψ_t and σ_t^{hf}. On the other hand, a high pass filter is applied to the orientation obtained from the gyroscope, which filters the low frequency noises and has the transfer function as:

$$\hat{\Psi}^{gyr}(s) = \frac{Ts}{1+Ts}\left(\Psi(s) + \Sigma^{lf}(s)\right) \approx \frac{Ts}{1+Ts}\Psi(s) \tag{5.5}$$

where $\Psi^{gyr}(s)$ and $\Sigma^{lf}(s)$ are the Laplace transforms of ψ_t^{gyr} and σ_t^{lf}.

The final orientation estimation takes to be the combination of the outputs of the low pass filter and high pass filter. The transfer function reads:

$$\hat{\Psi}(s) = \hat{\Psi}^{mag}(s) + \hat{\Psi}^{gyr}(s) \approx \frac{1+Ts}{1+Ts}\Psi(s) = \Psi(s) \tag{5.6}$$

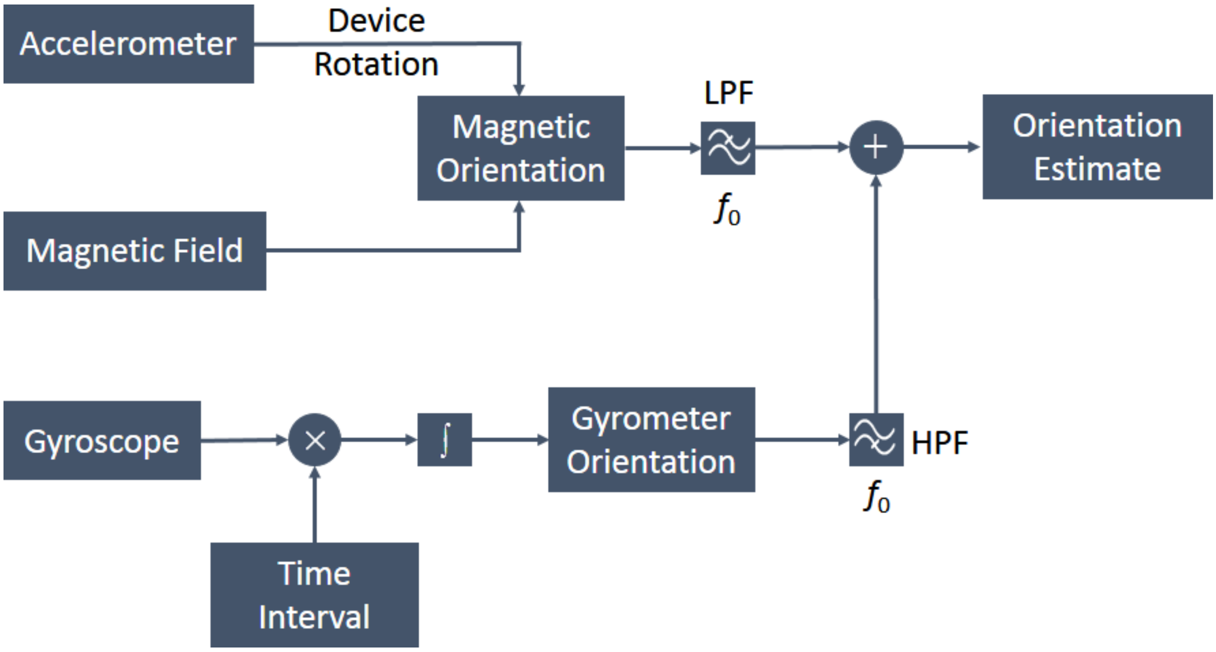

Figure 5.8 – Complementary filter for orientation estimate

Such a complementary filter recovers the real orientation, which has a fast response time and a low drift. The accelerometer here is used to determine the gravity direction, since the 3D position of mobile phone is unknown.

As sensor readings are all discrete time series, a simple implementation of low pass filter, with output y_t and input x_t at time t, has the form:

$$y_t = \alpha y_{t-1} + (1 - \alpha)\, x_t \tag{5.7}$$

where the output y_t is the orientation output, and α is a parameter determined by the desired cut-off frequency. Since the low pass filter is applied to magnetic field sensor readings, the input x_t here is the orientation given by the magnetic field sensor ψ_t^{mag}.

On the other hand, a simple implementation of discrete-time high pass filter with the same cut-off frequency has the form:

$$z_t = \alpha z_{t-1} + \alpha\,(u_t - u_{t-1}) \tag{5.8}$$

where the output z_t is the orientation output, and since the low pass filter is applied to gyroscope readings, the input u_t here is the orientation obtained by integrating gyroscope readings, i.e. $(u_t - u_{t-1}) = \psi_t^{gyr} \Delta t$, where ψ_t^{gyr} are the gyroscope readings.

The final orientation θ_t can be obtained by putting (5.7) and (5.8) together, now we have the form of complementary orientation filter:

$$\theta_t = \alpha \left(\theta_{t-1} + \psi_t^{gyr} \Delta t\right) + (1 - \alpha)\, \psi_t^{mag} \tag{5.9}$$

The orientation complementary filter in our experiments is based on Google Android sensor-related APIs [107].

While walking, a mobile device can be held in the hand or pocket in a variety of different orientations, which is very challenging for accurate orientation estimation, an issue largely ignored in most previous studies. Unlike foot-mounted or head-mounted inertial measurement units affixed to the body, the orientation of a mobile device is not always consistent with the user's orientation, depending on the relative motion of mobile device and user. Here, a "switching" scheme is introduced to handle arbitrary position changes of mobile devices, considering the following three situations:

- When the mobile device is held with the screen upwards, typically meaning the user is checking content, the orientation of the mobile device and the user are assumed to be consistent. In this case, the orientation of the user is estimated using the complementary filter as introduced above. The orientations obtained in such conditions can be used as reference orientations to calibrate the system.
- When the orientation of gravity changes with respect to the mobile device, as shown in Figure 5.9, the mobile device is assumed to be changing its orientation. In this situation, the orientation estimate stops and the particle filter draws random orientations for each particle to estimate the location.
- When the mobile device is not held with screen upward and the orientation of gravity is not changing axis, the mobile device is assumed to be held stationary or placed in a pocket. In this situation, the complementary filter stops and the orientation is estimated only using the gyroscope:

$$\theta_t = \theta_{t-1} + \psi_t^{gyr} \Delta t \tag{5.10}$$

5.3 Particle filter data fusion

We aim to obtain the best position estimate of a mobile user at each time step by combining both the GSM fingerprinting result and the sensor dead-reckoning result. The idea behind this is to take the advantage of sensor dead-reckoning that accurately estimates coordinate locations

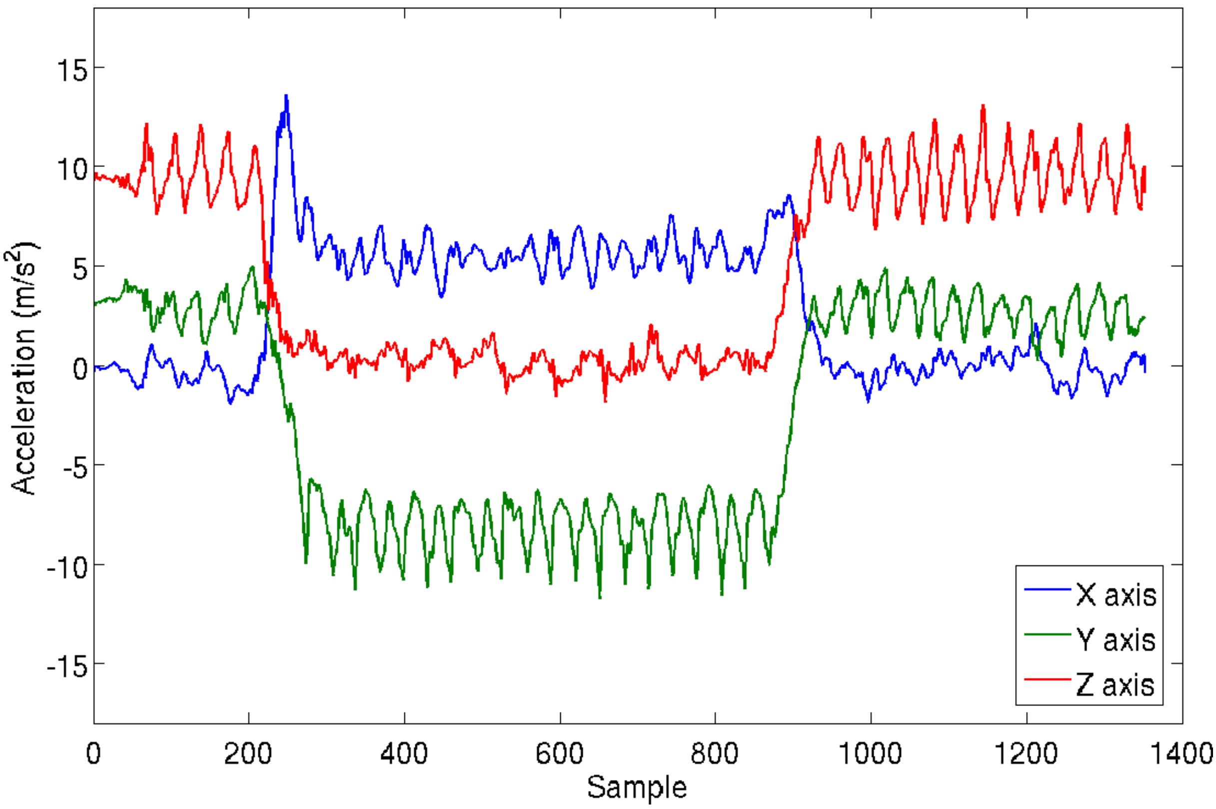

Figure 5.9 – Acceleration changes reflect mobile device position changes

of a mobile user, and in the meantime, use rough room-level SVM classification results and the room layout information to correct the possible mistakes made by long time integrating of sensor readings. The state space filtering approach is used in order to combine the information from different sources and sequentially estimate the variables of interest. Since the posterior distribution is non-Gaussian, the particle filter is thought to be more appropriate and robust than extended or unscented Kalman filters.

5.3.1 System model

Let $s_t = [x_t, y_t, p_t, q_t,]^T$ be the state of the system, at time t, where x_t and y_t are the position coordinates of the mobile user, and p_t and q_t are the parameters of stride length model explained in section 5.2.3. The state transition model can be characterized in terms of a state transition density $p(s_t|s_{t-1})$. The state transition density $p(s_t|s_{t-1})$ is determined by, in our system, both multiple sensor information and map layout information. When a step is detected, based on multiple sensor dead-reckoning, we have:

$$\begin{cases} x_t = x_{t-1} + \varphi_{t-1} cos(\theta_{t-1}) + w^x_{t-1} \\ y_t = y_{t-1} + \varphi_{t-1} sin(\theta_{t-1}) + w^y_{t-1} \\ p_t = p_{t-1} + w^p_{t-1} \\ q_t = q_{t-1} + w^q_{t-1} \end{cases} \tag{5.11}$$

where φ_{t-1} is the stride length (equation (5.3)), θ_{t-1} is the orientation estimation, and w^x_{t-1}, w^y_{t-1}, w^p_{t-1} and w^q_{t-1} model noise and disturbances.

Not all the state transitions based on sensor dead-reckoning are feasible, for example, the state transition may suggest that the mobile user passed through a wall, which is usually due to an erroneous orientation estimate. Map layout information is used to remove these transitions, as explained in the following particle filter procedures.

The observation at time step t in our case is the fingerprint classifier output h_t, i.e. the room number. The observation probability $P(h_t|s_t)$ describes the probability, given the state s_t, that room number h_t is obtained from GSM fingerprinting result. As described in section 4.4.3, such probability can be estimated based on the confusion matrix. Since the state s_t here is continuous coordinate positions, rather than discrete room labels, equation (4.19) can be modified as:

$$P(h_t = i|\text{room}(s_t = j)) \approx \frac{c_{ij}}{\sum_{l=1}^{M} c_{il}} \tag{5.12}$$

where room(s_t) is the room number associated to location (x_t, y_t) and M is the number of rooms.

5.3.2 Particle filter recursion

The particle filter is a technique that uses the Monte Carlo method to implement recursive Bayesian filtering. In section 4.4.1, the discrete form of Bayesian filtering is applied, since the states are discrete variables. However, for the filtering problem discussed here, the states are continuous and infinite, and as a result, the task is to obtain the distribution of state s_t given the observations h_t, which is the *a-posteriori* density of the state $p(s_t|h_t)$. For a system with state transition density $p(s_t|s_{t-1})$ and observation density $p(h_t|s_t)$, the Bayesian filter recursively computing the current posterior density $p(s_t|h_t)$ based on the posterior density of the previous state $p(s_{t-1}|h_{t-1})$ and the most recent observation h_t, in two steps: 1) prediction:

$$p(s_t|h_{t-1}) = \int p(s_t|s_{t-1})p(s_{t-1}|h_{t-1})ds_{t-1} \tag{5.13}$$

2) update:

$$p(s_t|h_t) = \frac{p(h_t|s_t)}{p(h_t|h_{t-1})} p(s_t|h_{t-1}) \tag{5.14}$$

where $p(h_t|h_{t-1})$ is the normalizing constant:

$$p(h_t|h_{t-1}) = \int p(h_t|s_t) \cdot p(s_t|h_{t-1}) ds_t \tag{5.15}$$

Particle filters use a finite number of random samples (called particles) with associated weights that provide a discrete approximation of the posterior density [108]. If the number of particles is very large, the discrete approximation approaches the true posterior density with arbitrary accuracy. The particle filter uses a set of particles taken from the previous time step $\{pt^1_{t-1}, pt^2_{t-1}, \cdots, pt^n_{t-1} \sim p(s_{t-1}|h_{t-1})\}$ and the most recent observation h_t to produce a set of particles approximately following the distribution of $p(s_t|h_t)$. The particle filter algorithm used in our system is implemented in the following four steps:

1. Initialize the particles: Since sensor dead-reckoning requires a starting position for integration, N particles are sampled, based on the output of the SVM classifiers, all with the same weight $1/N$. The coordinates (x, y) of the particles are distributed uniformly in each room, while the number of particles in each room depends on the observation distribution $p(h_0|s_0)$. The stride length model parameters p_0 and q_0 are drawn from a uniform distribution over a suitable range.

2. Make predictions based on the system model: When a step is detected, each particle is moved using sensor dead-reckoning results. Map information is used in this step to remove impossible movements. As shown in Figure 5.10, if a particle made a movement that crosses a wall or enters an inaccessible region, it is removed, which, in filtering, is realized by setting the weight of the particle to 0.

3. Update the weights based on observation model: When SVM classifier result is received, the likelihood $p(h_t|s_t)$ is applied to each particle to update the weight.

4. Resample particles based on their weights: Through previous steps, the number of particles reduces and the weights of particles diminishes and the weights of the particles change considerably. To better represent the posterior density $p(s_t|h_t)$, particles are resampled to the same number N with probabilities equal to their weights.

The final location estimate is taken to be the centroid of all particles.

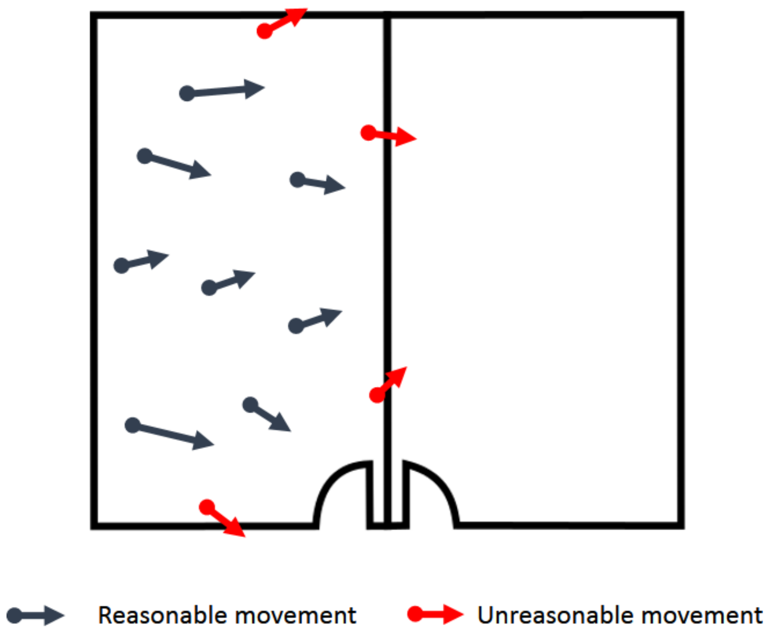

Figure 5.10 – Elimination of particles based on map layout

5.4 Evaluation

5.4.1 Data acquisition and datasets

The experiments were done in the same site as introduced in chapter 4. The rooms are numbered from one to seven, while the corridor is divided into three sections numbered from eight to ten, as shown in Figure 5.11. Map layout information of doors, walls and fixed-position obstacles and their orientations is stored in a map database for later use. Two types of data were recorded: GSM fingerprints and multiple sensor readings. GSM RSS fingerprints were collected using the GSM trace mobile TEMS Pocket, while the multiple sensor readings were obtained by the Google Nexus 7 tablet.

TEMS Pocket and Nexus 7 tablet were bundled together and held in hand, recording both GSM fingerprints and multiple sensor readings. Although two different devices were used in our experiments for recording both GSM fingerprints and sensor readings, it must be pointed out that a new generation of TEMS Pocket products allow to record all the data in the same device.

Training data was recorded first for building the SVM classifier, and test data were recorded separately as explained above. The training data was taken in the 10 possible locations with TEMS Pocket and manually labeled with the corresponding room numbers. The test trajectory started from the south-west corner of room 7, going through the corridor 8 and 9 into room 3 and finally stopped at the door of room 6, as shown in Figure 5.11.

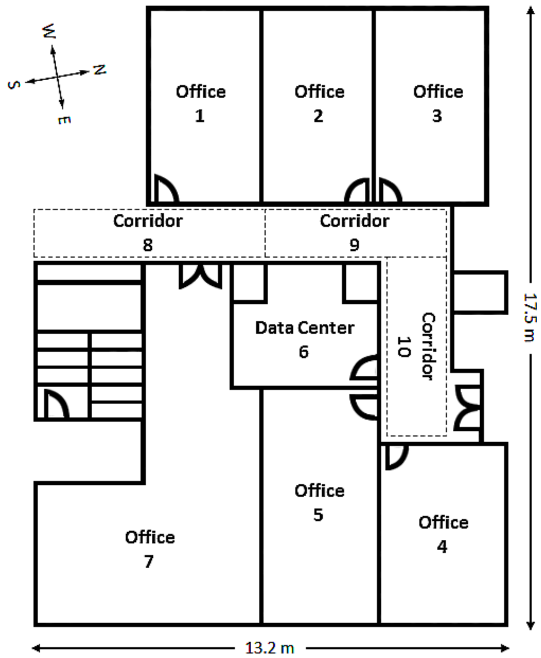

Figure 5.11 – Experimental site

5.4.2 Results

Raw GSM fingerprinting results are shown in Figure 5.12, where the X axis gives the sample number along the trajectory and the Y axis the SVM classifier outputs. As seen in the figure, the SVM classifier gives the correct room numbers for most of the test examples, but there are still misclassifications especially in adjacent rooms. The percentage of overall correct classification is 70%. (This result was obtained with a small training set and is not considered to be optimized).

Figure 5.13 shows the sensor dead-reckoning results and the results of a particle filter that combines sensor dead-reckoning and map layout constraints. The dashed line in the figure shows the actual trajectory provided for comparison. It can be seen that multiple sensor dead-reckoning, even given a correct starting position, makes many mistakes due to the sensor drift and inaccurate stride length. In a more realistic case, of course, the starting position is unknown. The magenta dot line in Figure 5.13 shows the particle filter results, where only map layout constraints are applied, and the initial locations of particles distribute evenly in room 7. It can be seen in the figure, after a few mistakes at the beginning of the trace, the particle filter quickly outputs the correct location and moving direction of the target. This is due to the map layout constraints, which eliminates all the particles with impossible movements. However, the particle filter makes some mistakes between corridor 8 and room 1, which is the limits of only using map layout constraints. When there are more than one accessible paths, due to inaccurate step detection, stride length or orientation estimation, particles may move to a incorrect path, and thus the

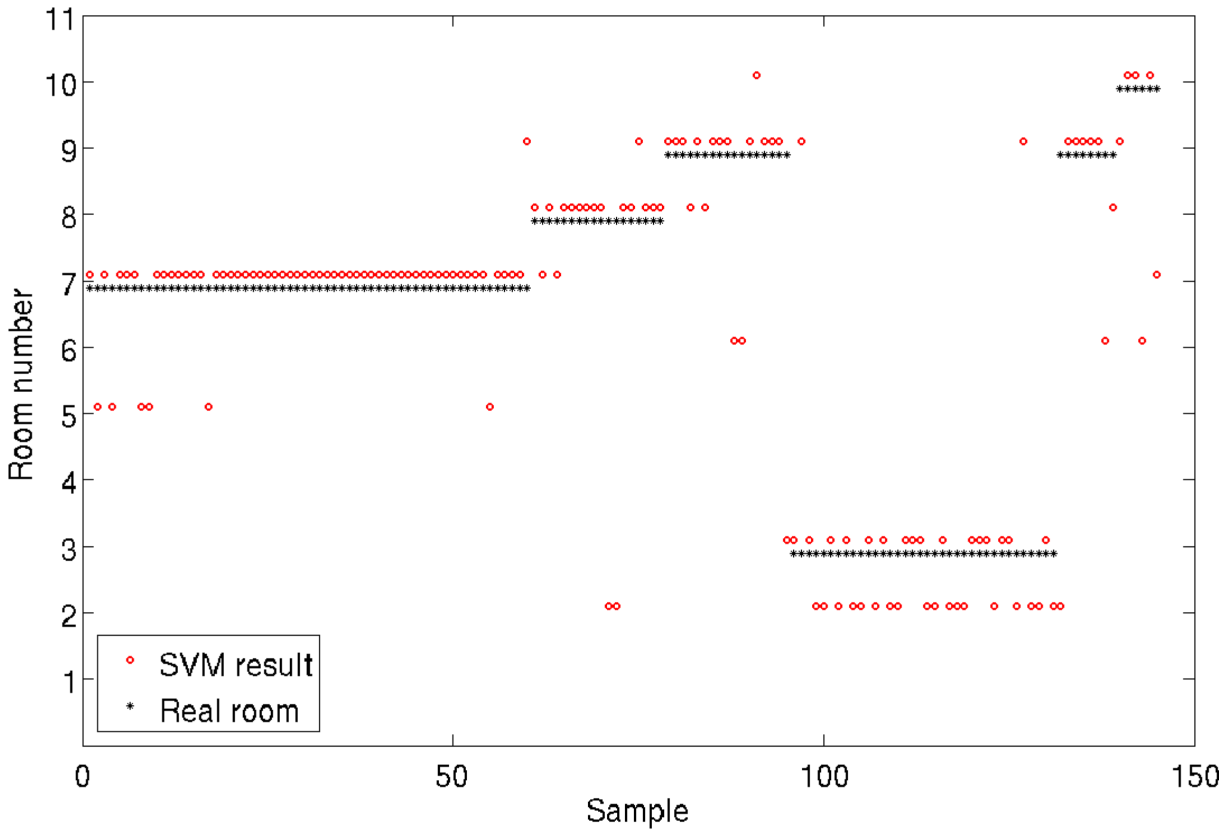

Figure 5.12 – GSM fingerprinting results

final location estimations can be inaccurate. Another case is shown in Figure 5.14, where all particles are trapped in a small region based on map layout constraints. (As this thesis was being completed, a similar study appeared in [88] with promising results, albeit necessitating specialized torso-mounted hardware.)

In Figure 5.15, GSM fingerprinting, sensor dead-reckoning and map layout restrictions are combined. In this case, only a few mistakes are made at the beginning, due to the unknown starting position, since the SVM classifier only outputs room-level location, not a precise position. The advantage of a system combining an absolute but noisy measure, GSM, with precise but local dead-reckoning, and map constraints, is clearly demonstrated.

5.5 Summary

Hybrid schemes are promising for indoor localization, which take advantage of different types of location sources that are available. In this chapter, a hybrid approach for indoor localization is presented using a particle filter to combine GSM fingerprinting room-level classification, sensor dead-reckoning, and map layout information.

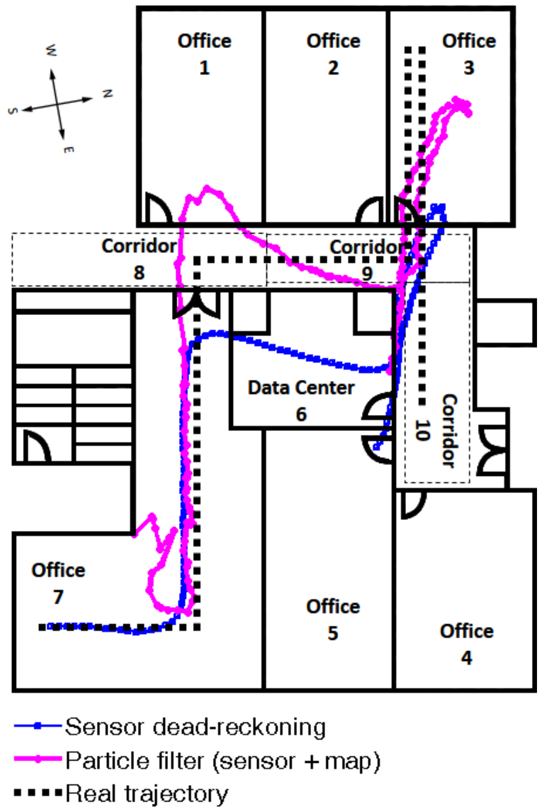

Figure 5.13 – Results of sensor dead-reckoning and a particle filter that only combines sensor dead-reckoning and map layout constraints (case 1)

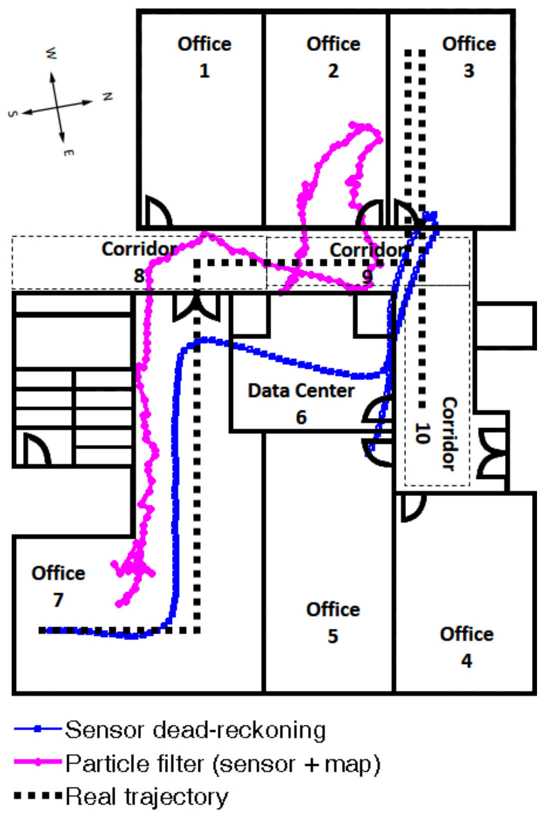

Figure 5.14 – Results of sensor dead-reckoning and a particle filter that only combines sensor dead-reckoning and map layout constraints (case 2)

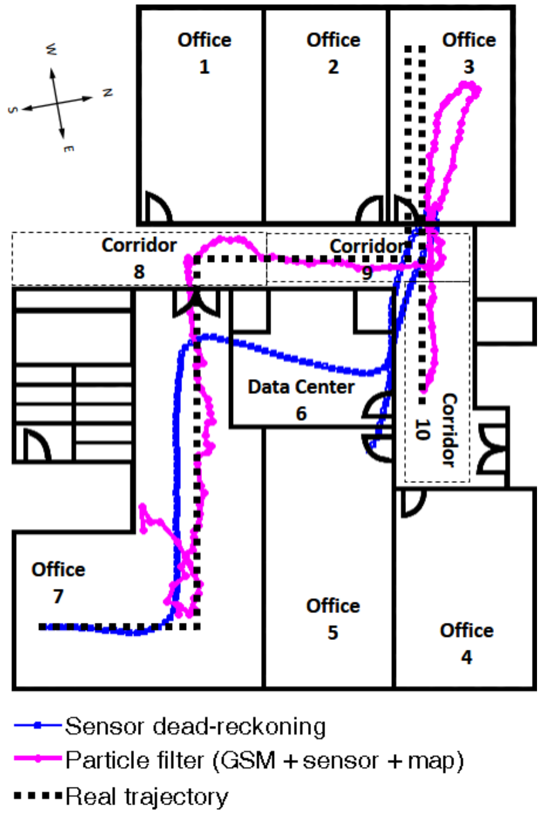

Figure 5.15 – Sensor dead-reckoning and particle filter results that combine GSM fingerprinting, sensor dead-reckoning and map layout restrictions

In sensor dead-reckoning, the stride length model based on acceleration amplitude is made adaptive, allowing for different subjects and environments. The complementary filter for orientation estimation takes the advantage of the gyroscope's high accuracy and magnetic field sensor's robustness. Moreover, mobile orientation with respect to user orientation is automatically detected by accelerometer and gyroscope, which estimate orientation by picking the correct orientation coordinate.

The proposed particle filter uses a number of particles to represent the distribution of the current location. The movement of particles is derived from the sensor dead-reckoning, while unreasonable movements such as traversing a wall are eliminated based on the map layout constraints. The location is updated integrating the GSM fingerprinting results when available.

This hybrid approach, which uses GSM fingerprints and multiple sensors that are easily obtainable due to the growing popularity of smart phones, is potentially ready for a practical implementation. Experimental results show that this approach can determine a mobile user's trajectory in coordinate locations with good accuracy.

The core elements of this thesis on GSM fingerprinting for indoor localization have been covered now. The overall conclusions and perspectives will be outlined in the final chapter.

However, we wish to introduce some complementary experiments also carried out in the context of the thesis. This will be the subject of chapter 6.

Chapter 6

Complementary Experiments

6.1 Introduction

In addition to the main body of work that is presented in the previous chapters, a number of complementary experiments were also carried out.

Firstly, the SVM RSS fingerprint classification technique was also tested in outdoor environments, in order to see whether the approach was viable there. The results indicate that the strength of the RSS fingerprinting approach lies in its application in complex indoor environments. The approach was also evaluated in a railway and subway transfer station, where it was quite successful, demonstrating that it can provide accurate and reliable indoor localization in practical, dynamic underground environments.

In the thesis, indoor localization is done by classifying RSS vectors from a large number of GSM carriers. In another experiment, carrier selection techniques were studied to remove GSM carriers that are less relevant for distinguishing different locations. It was found that carrier selection helps in simplifying the system, but does not improve performance. Performance however could be improved using post-processing schemes.

Finally, indoor localization based on WiFi was also studied, since WiFi is increasingly ubiquitous, from outdoor public environments to indoor private spaces. Here, indoor localization is investigated based on the RSS of WiFi, which can be obtained easily using standard mobile devices.

6.2 Work related to the SVM classification

6.2.1 Experiments in other sites

6.2.1.1 The outdoor space

The good performance of indoor localization using RSS fingerprints is based on the assumption that, due to the complexity of indoor environments, shadowing and multipath effects render RSS fingerprint distinctive even for fingerprints taken at relatively nearby points. It follows that in outdoor space, where variations of RSS are mainly attributed to the path loss, accurate localization might be difficult to achieve. Zimmermann et al. [48] employed sparse GSM fingerprints, containing RSS from the current serving cell and six neighbor cells, to do outdoor localization, resulting in an accuracy of 80 meters within 67% of the time in the urban scenario. In [90], the accuracy of GSM fingerprinting in outdoor environments was reported as 75 meters, compared to 2 to 5 meters they obtained in indoor environments. To study the phenomenon using our method, an outdoor experiment was conducted.

Data was acquired in the outdoor space of the campus where the "laboratory site" mentioned earlier in the thesis is located. Seven location cells were defined in which to record the RSS, as shown in Figure 6.1. Each location cell is a square with side length of around 4 meters, which is roughly equivalent to a room-level classification. On November 21 and 22, 2013, twenty one datasets were recorded; the distribution of datasets in time and place is shown in Table 6.1, where an "×" represents that data is recorded in the given time and location, containing about 600 GSM fingerprint measurements. As the outdoor space is a public parking area, in some time periods, parked cars prevented certain measurements, leading to some irregularities in the datasets.

Table 6.1 – Datasets of the outdoor experiment

Time	**Location**						
	1	**2**	**3**	**4**	**5**	**6**	**7**
Nov. 21, AM	×	×	×	×	×	×	
Nov. 21, PM	×	×	×	×	×	×	×
Nov. 22, AM	×		×			×	×
Nov. 22, PM	×		×			×	×

Experimental results are shown in Table 6.2, where the percentage of correctly classified test examples is presented. The SVM classifiers are trained with the same settings as in the indoor room-level classification. It is seen in the table that the performance in the outdoor space are much worse compared to the indoor experiments. SVM classification within the selected three

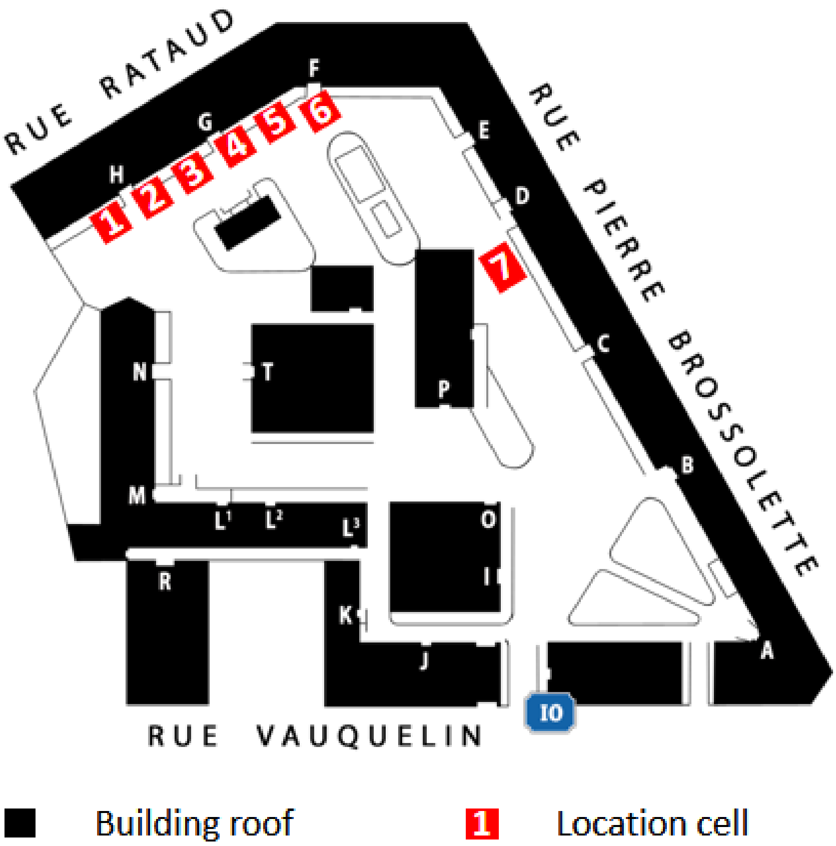

Figure 6.1 – The outdoor experimental site

locations (1, 3 and 6) gives an acceptable performance. However, only 56% of the test examples can be correctly classified if distinguishing the four locations of 1, 3, 6 and 7. This performance drops to only 34.8% if classification is done within the six locations (1, 2, 3, 4, 5 and 6). The outdoor experiment suggests that the GSM fingerprinting technique has advantages for indoor environments with complex shadowing profiles, while for outdoor environments, which lack such structure, much lower accuracy is obtained.

Table 6.2 – Outdoor experimental results

Training Set	Test Set	Locations	Result
Nov. 21, AM	Nov. 21, PM	1, 2, 3, 4, 5, 6	34.8 %
Nov. 21 AM Nov. 21 PM	Nov. 22 AM Nov. 22 PM	1, 3, 6	88.1 %
Nov. 21 PM	Nov. 22 PM	1, 3, 6, 7	56.0 %

6.2.1.2 The underground space

The proposed localization technique was validated in an underground environment, the "Gare de Lyon" railway and subway transfer station located in southeast Paris. This experiment was

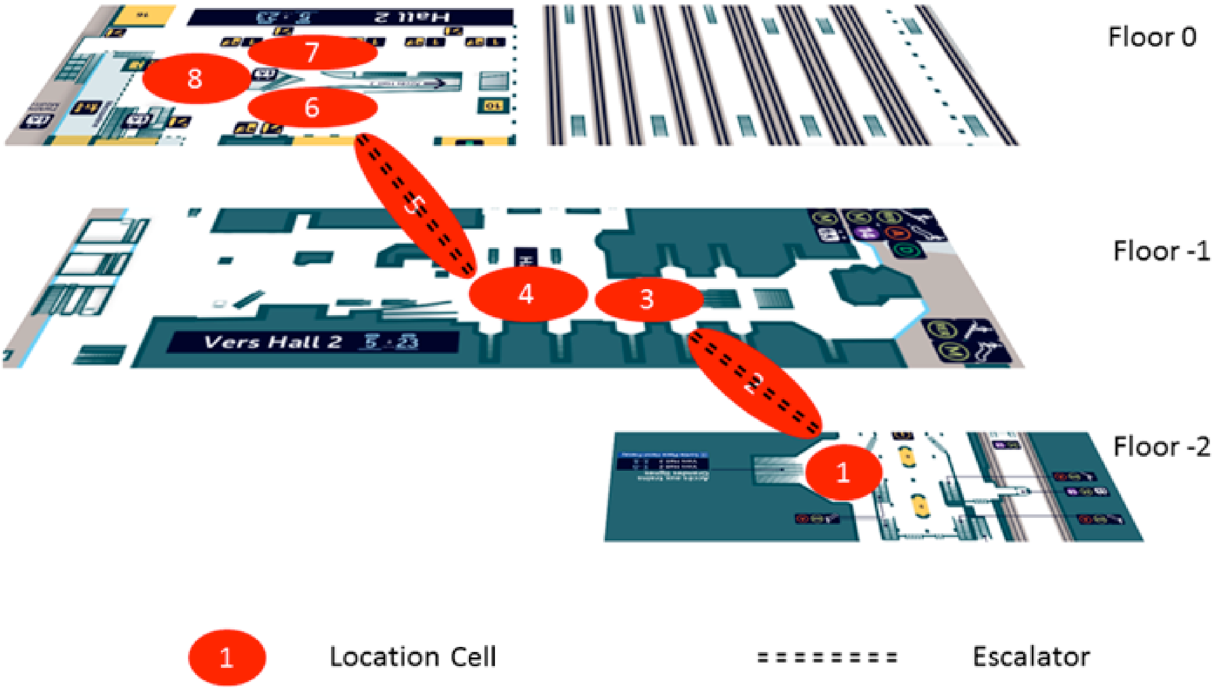

Figure 6.2 – The underground experimental site and the location cell definition

performed as a demonstration in a response to a call for proposals by the *Société Nationale des Chemins de Fer* (SNCF, the French national railway company), and was carried out under the supervision of the SNCF. The station consists of three floors, with waiting areas and transit corridors, as shown in Figure 6.2. Experiments here were carried out in an area extending from the waiting area on the ground floor to the entrance of the subway station, on the second underground floor, and back again. For recording fingerprints, location zones were defined in the area as shown in Figure 6.2. To make these zones more meaningful, they were based on conventionally defined areas such as halls, entrances, escalators, etc.

The experiment was a practical demonstration, where data was collected as a normal traveler carrying the TEMS Pocket mobile phone during passenger traffic hours. Two training datasets were recorded during a random walk inside the station on May 24 and June 17, 2013, respectively, and labeled manually to build the classification model. The classifiers used were a set of linear one-vs-all SVM with regularization constant $C = 0.01$. Bayesian filtering was also applied to the data, in a offline pass, as we are unable to process GSM RSS fingerprints in real time with the TEMS Pocket.

Our localization/tracking demonstration was conducted on June 19, 2013. The mobile phone was handheld while walking from the waiting hall of the railway station to the subway entrance, and back. The location sequence of the trace is 8-7-5-4-3-2-1-2-3-4-5-6, as shown in Figure 6.2.

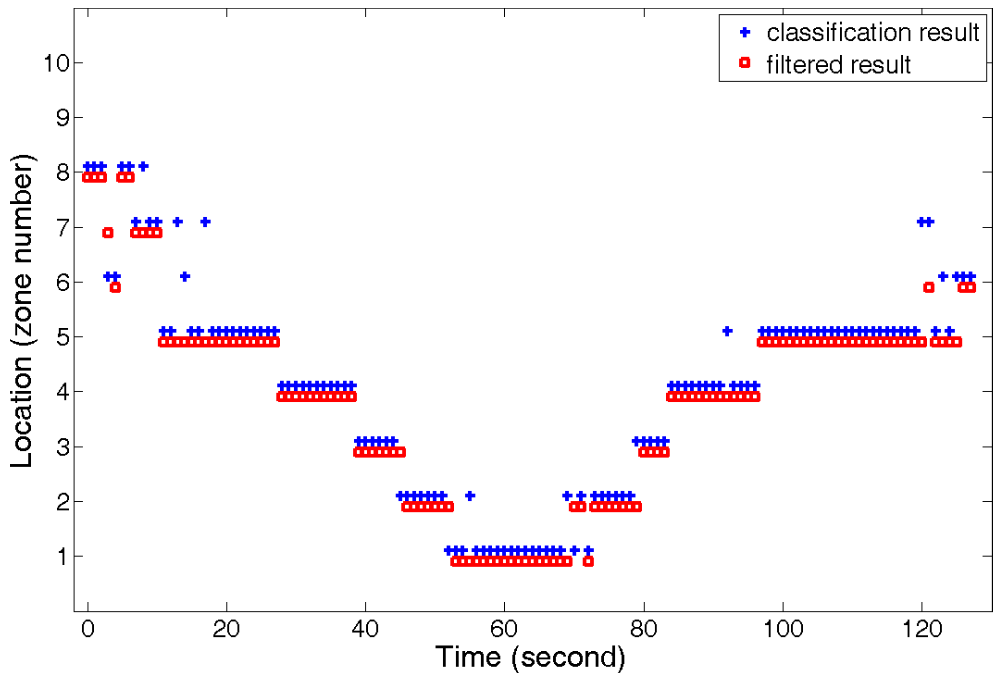

Figure 6.3 – Experimental results of underground demo trace

The results are shown in Figure 6.3, where the SVM classification result and the Bayesian filtering result can be compared. It is seen that our localization method correctly obtained the location in the test with only a few confusions between adjacent location units. The Bayesian filter corrected most of the mistakes made by the classifier.

6.2.2 Carrier selection

Carrier selection is the process of selecting a subset of relevant carriers for use in model construction. Since a GSM fingerprint contains RSS from a large number of carriers and the GSM fingerprint examples are relatively limited, a carrier selection technique can be tried to exclude redundant or less relevant carriers. One might also expect to reduce the training time and avoid overfitting by applying carrier selection. In this work, two carrier selection schemes were evaluated: Gram-Schmidt feature selection, and recursive feature elimination (RFE).

6.2.2.1 Gram-Schmidt feature selection

The Gram-Schmidt feature selection uses the Gram-Schmidt orthogonalization procedure for ranking the variables of a model that is linear with respect to its parameters.

Consider a dataset with M candidate features containing N measurements with known labels. The dataset has the form of an (N, M) matrix, where the ith column $\mathbf{x}^i = [x_1^i, x_2^i, \cdots, x_N^i]$ is the vector of sample values of feature i. The labels can be denoted by an N-vector y. Let the

(N, M) matrix fingerprint dataset be denoted as X. The linear model can then be written as $\mathbf{y} = \mathbf{X}\theta$, where θ is the vector of the parameters of the model. To rank the carriers, the first step is to find the most relevant carrier, i.e. the feature vector that best matches the labels. The problem amounts to finding the smallest angle between the feature vectors and the label vector in the N-dimensional space of observations. The angle computation can be done using the following equation

$$\cos^2\left(\mathbf{x}^i, \mathbf{y}\right) = \frac{\left(\mathbf{x}^i \cdot \mathbf{y}\right)^2}{||\mathbf{x}^i||^2 ||\mathbf{y}||^2}, \ i \in \{1, 2, \cdots, M\} \tag{6.1}$$

After the first carrier is selected, all remaining feature vectors and the label vector are projected onto the null subspace (dimension $M-1$) of the selected carrier to discard the part of the variation that has been explained by the first selected vector. In that subspace, the projected input vector that best explains the projected output is selected with the same technique as described above, and the $M - 2$ remaining feature vectors are projected onto the null subspace of the first two ranked vectors. The procedure terminates when all M input feature vectors are ranked, or when a termination criterion is met.

6.2.2.2 SVM Recursive feature elimination

The SVM recursive feature elimination approach ranks the relevant GSM carriers based on the weights of SVM classification model. As introduced in section 4.3.1.1, a linear SVM classification model defines the separating surface as

$$f(\mathbf{x}) = \sum_{i=1}^{n} \alpha_i y_i (\mathbf{x}_i \cdot \mathbf{x}) + \alpha_0 \tag{6.2}$$

where α_i is the weight of carrier i. If the weight of a carrier is very small, the contribution of this carrier to the overall function value is small. It follows that removing such a carrier does not cause much impact to the separating function.

To rank the carriers using the SVM recursive feature elimination technique, the classifier is trained recursively to pick out the carrier with the smallest weight and put it in a “ranking array” at each time. As a result, for M GSM carriers, in all $M - 1$ sessions of SVM training need to be performed to rank the carriers. Though this is quite time consuming, all the work is done offline and does not influence the real-time online localization.

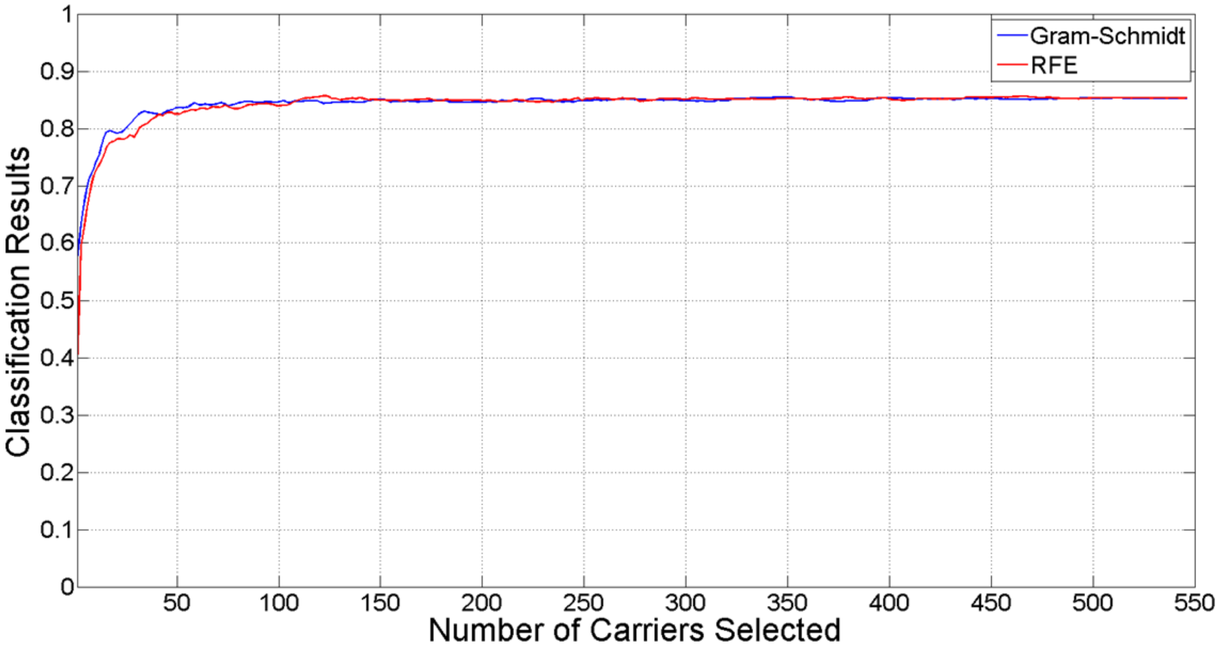

Figure 6.4 – Performance comparison of Gram-Schmidt and SVM RFE

6.2.2.3 Comparison of carrier selection approaches

The two carrier selection approaches, Gram-Schmidt and RFE, are performed and tested on a dataset. Here the training is done using a relatively small number of fingerprint examples, which does not achieve as good performance as that shown in section 4.3.2.2, but the aim here is to compare the two carrier selection techniques. Figure 6.4 shows the performance with different number of carriers selected by the two approaches. As is seen in the figure, neither of the carrier selection approaches improves the performance by selecting a subset of high rank carriers. The performance of the two approaches is similar in general, and increases with the number of carriers. The results indicates with only 50 carriers the performance is reaching steady and close to the top value obtained using the full carrier, which means there are a lot of redundant and irrelevant carriers providing no more information than the selected features. Removing these carriers will reduce the complexity of SVM classifiers, but could potentially decrease the robustness of the localization system. Since the computation load in the online localization stage is not high, we keep all the carriers in the localization system.

6.2.3 Post-processing

Post-processing involves the procedures that are applied to the raw results of SVM classifiers. In section 4.4, a Bayesian filtering post-processing was investigated, while some more techniques are studied here.

6.2.3.1 Low pass filter

The first post-processing technique uses the principle of the low pass filter, which considers several successive SVM outputs to make one decision. Suppose the overall correct classification rate of a binary classifier is P, the probability of giving the correct class number. If N outputs are taken into account, the probability of obtaining a correct location will be

$$\sum_{i=\left[\frac{N+1}{2}\right]}^{N} C_N^i P^i \left(1-P\right)^{N-i} \tag{6.3}$$

where $[*]$ is the smallest integer greater than $*$, and N is the window size which is the number of fingerprint measurements used for post-processing.

Figure 6.5 is a simulated result showing the impact of increasing the window size used for post-processing, where the correct classification rate of a single fingerprint is set to 80%. It is seen in the figure that the larger the window size, the better the performance. Such a post-processing is a simple and effective approach to improve the performance. Nonetheless, the latency problem should be taken into consideration if the window size is very large. Since the localization accuracy is room level, in practice a window containing measurements over one to three seconds, is acceptable, representing three to nine fingerprints used for post-processing.

Figure 6.6 is a simulated result showing when the window size is set to three fingerprint measurements, the relationship between the post-processing result and the raw SVM result. It is seen in the figure that if the correct classification rate is below 50%, such a post-processing technique does not improve the performance but actually decreases it. This is consistent with the experimental results on real fingerprint measurements as shown in Table 6.3. This table compares the post-processing results with the raw SVM results using datasets as described in section 4.3.2.3. It is seen in the table that for the test dataset $S1$ and $S2$, the raw results are 94.2% and 60.4% respectively. After post-processing, which combines every three raw results into one, test results for dataset $S1$ and $S2$ increase to 99.7% and 71.6% respectively. However, for the test dataset $S3$ and $S4$, the raw results are so low that the post-processing process does not improve but decrease the performance.

6.2.3.2 Probability based rejection

Another post-processing technique involves using the reject option of classification. The rejection here is based on the probabilistic output of SVM classification. A binary SVM classifier

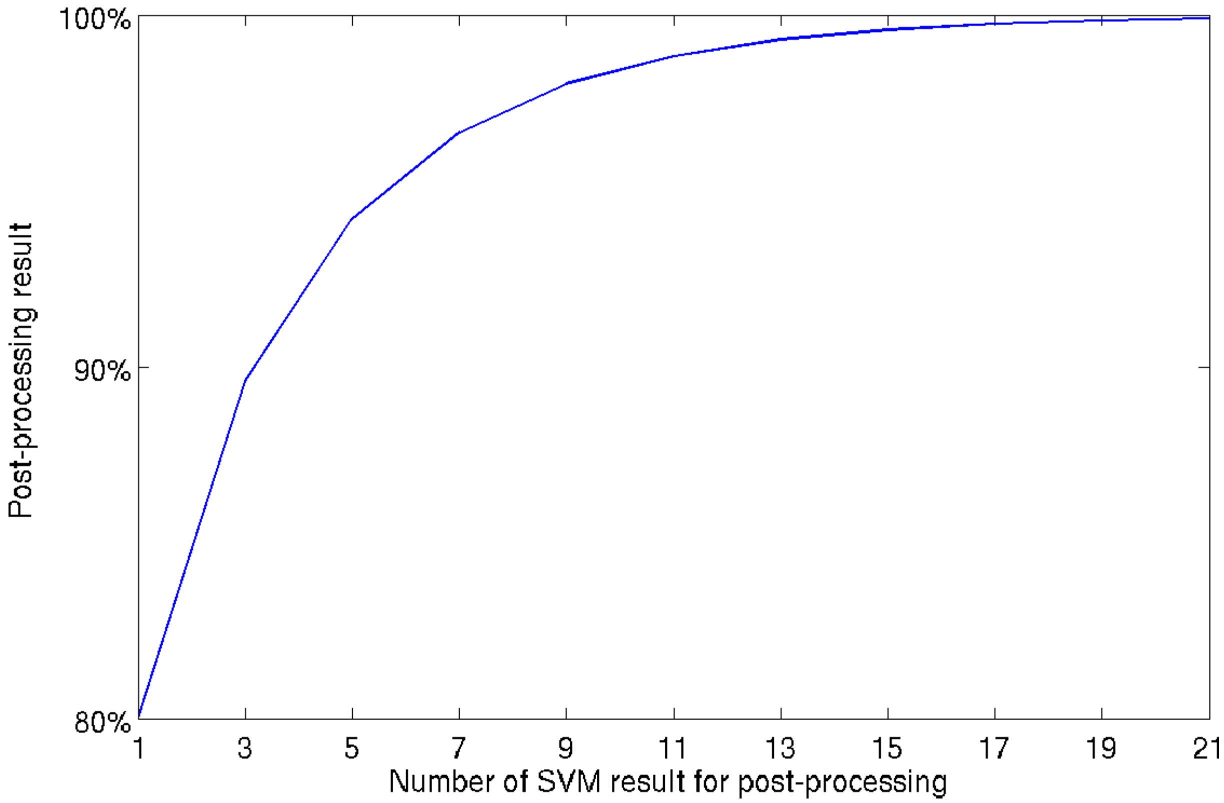

Figure 6.5 – Post-processing results with different sizes of window

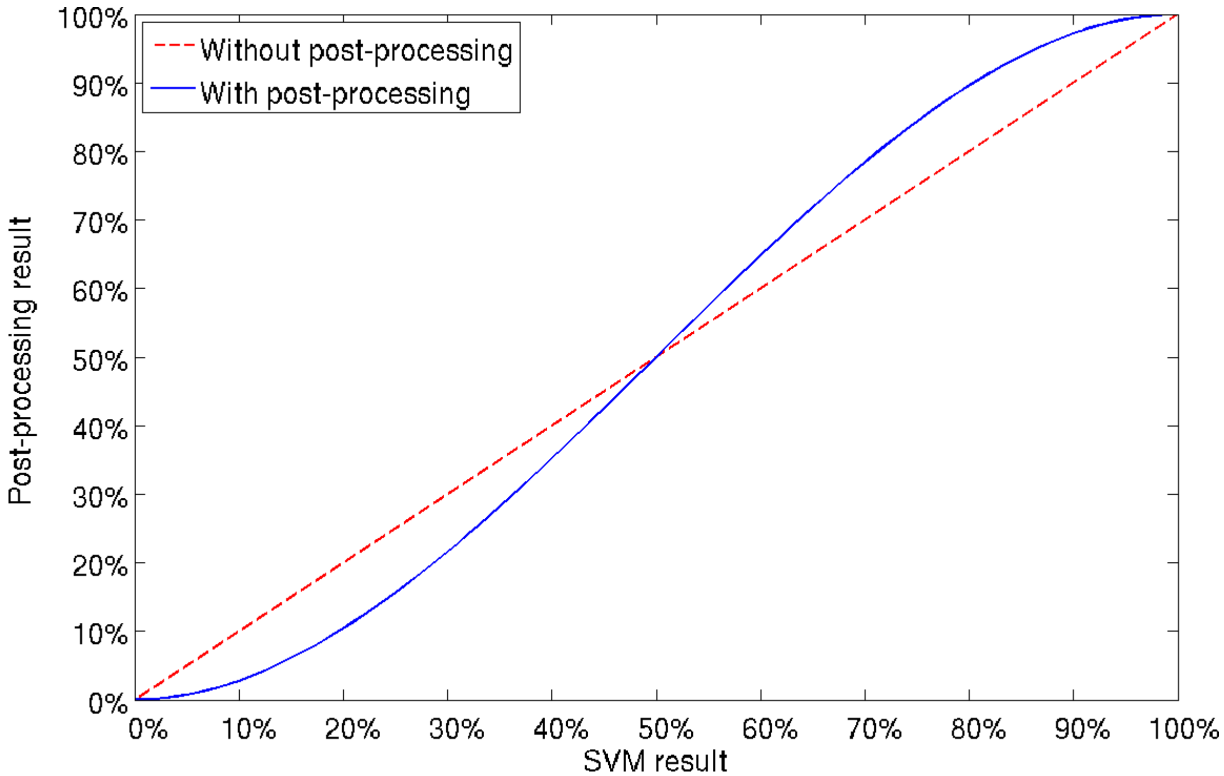

Figure 6.6 – Post-processing results (blue curve) as a function of raw SVM result

Table 6.3 – Post-processing results for different test datasets

Test Set	Training Set	SVM	Post-processing
$S1$	$S1$	94.2%	99.7%
$S2$	$S1$	60.4%	71.6%
$S3$	$S1$	39.7%	33.4%
$S4$	$S1$	32.3%	30.1%

separates a test example into either of the two classes with the output $+1$ or -1. However, in some settings it is favorable to obtain an estimation of the probability of a test example $\mathbf{x}$ belonging to either of the two classes, i.e. the probability $P(y=+1|\mathbf{x})$ or $P(y=-1|\mathbf{x})$.

There are several approaches to estimate posterior probabilities from SVM results, and in this thesis the method of Platt is applied [109]. In this method, the posterior probability is approximated by a sigmoid function

$$P(y=+1|x) \approx P_{A,B}(f) = \frac{1}{1+\exp(Af+B)} \tag{6.4}$$

where f is the output of the SVM classifier. The parameters A and B are obtained by minimizing the negative log likelihood of the training data:

$$\begin{aligned} &\text{minimize } -\sum_{i=1}^{l}\left(t_i log(p_i) + (1-t_i) log(1-p_i)\right) \\ &\text{subject to } p_i = P_{A,B}(f_i) \text{ and } t_i = \begin{cases} \frac{N_+ + 1}{N_+ + 2}, & \text{if } y_i = +1 \\ \frac{1}{N_- + 2}, & \text{if } y_i = -1 \end{cases},\ i \in \{1, 2, \cdots, l\} \end{aligned}$$

where N_+ and N_- are the numbers of positive and negative examples.

In the post-processing stage, two rejection thresholds are set for the binary SVM classifiers:

- **Threshold 1:** If the function values of all the classifiers are smaller than this threshold, this example is not to be classified into any of the classes with a high degree of belief. However, the multiclass decision rule has to pick out a class among them, which is unreliable and as a result rejected.
- **Threshold 2:** If more than one SVM classifier outputs very high values, the decision is also suspicious. Therefore, if the difference of the two largest values is below this threshold, the example is rejected.

Experimental results of this post-processing approach are shown in Figure 6.7. In a test where the correct classification rate of SVM classification is 80%, if the rejection rate is set to 10%, the performance improves to 83%. Applying this post-processing procedure considerably improves

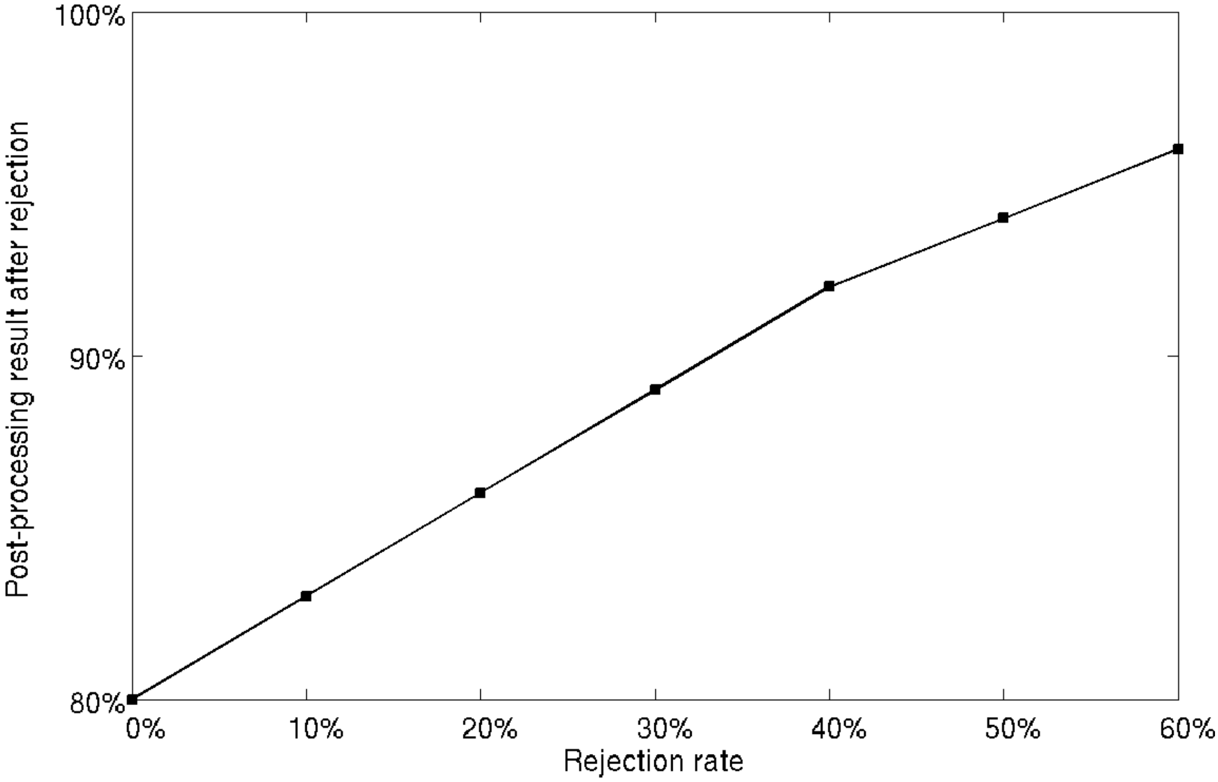

Figure 6.7 – Post-processing result after rejection as a function of rejection rate

the performance to 96% by rejecting nearly half of the test examples. The main disadvantage of this approach is still the possible latency problem caused by rejecting consecutive test samples.

6.3 WiFi indoor localization

WiFi is at present the most widely used wireless local area network technology. WiFi hotspots are extensively deployed in home, shop, office and public spaces, and WiFi is a standard feature on nearly all the mobile devices. As a consequence, WiFi has been widely explored as a means for localization in both indoor and outdoor environments.

For outdoor localization, WiFi is complementary to GPS localization, when the GPS signal is too weak or blocked in the urban canyons. Since the accuracy requirement in outdoor space is not very high, a proximity technique is often used, which simply assigns to the mobile user the location of WiFi access point with the highest received power. Alternatively, a centroid or weighted centroid of several WiFi access points is used to get a more accurate location estimate. For indoor environments, proximity approaches are not appropriate in most cases, and although WiFi is nearly ubiquitous, it has been deployed not for localization services, but for data transmission. As a consequence, localization techniques using WiFi have been developed, but the performance

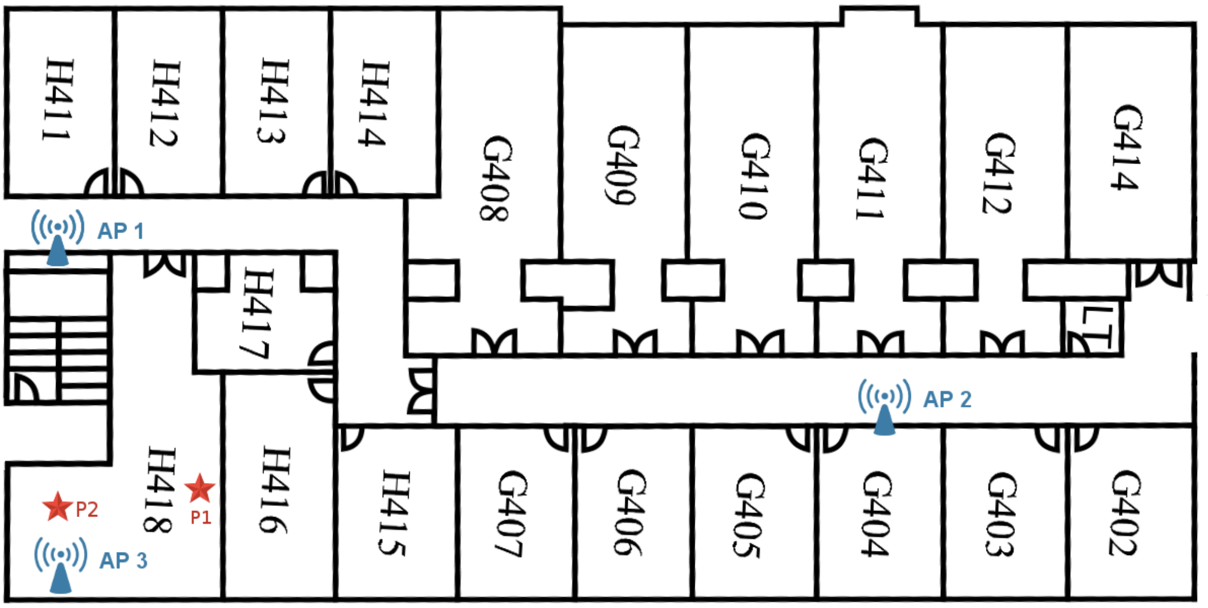

Figure 6.8 – WiFi access point and data acquisition positions

is currently far from satisfactory.

In this section, indoor localization based on RSS from an existing WiFi network is studied. The experimental setups are first introduced, followed by an analysis of the RSS characteristics of WiFi. Two indoor localization approaches, using fingerprinting and triangulation techniques, respectively, are presented and discussed at the end of the section.

6.3.1 Experimental setups

The WiFi indoor localization experiments were done in the same laboratory building as the laboratory site introduced in section 4.3.2.1. Inside the building are three WiFi AP which are part of the campus wireless local area network and have known positions. In addition, there are also many WiFi AP in other buildings outside the laboratory. The positions of these WiFi AP are unknown, but the signals are available inside the laboratory building. Figure 6.8 shows the experimental site and the locations of the known-position WiFi AP, labeled from one to three.

Data was recorded using a HTC ChaCha smartphone with an Android open source operating system. The data acquisition program was developed using Java programming language and Android SDK, and the main interface of the program is shown in Figure 6.9. The program can scan RSS and MAC address from all the available WiFi AP at a rate of ten RSS and MAC pairs per second.

Figure 6.9 – WiFi data acquisition program interfaces

6.3.2 RSS characteristics

Since indoor localization is based on the RSS of WiFi, the characteristics of WiFi signals are first examined with RSS measurements, obtaining the time-varying and location-correlation properties. To achieve an accurate and reliable indoor localization, the RSS is expected to be distinctive in different locations but robust over time.

Figure 6.10 shows RSS from AP2 in two different positions (P1 and P2 in Figure 6.8) over ten minutes. The distances from the AP to the two positions are 20 meters and 25 meters respectively. In the first position, RSS were recorded when the data acquisition smartphone was put on a desk, while in the second position, the smartphone was held in hand. It is seen in the figure, WiFi RSS is not stable in either of the positions, and especially when the smartphone was held in hand, the RSS have severe fluctuations. The standard deviations of the RSS in the two positions are 1.5 dBm and 4.6 dBm respectively. Meanwhile, the RSS do not show much distinction between the two different positions in the figure, indeed the RSS values from two AP overlap in some instances. This indicates that RSS from an individual WiFi channel is not reliable for distinguishing different locations.

The comparison between RSS from WiFi and GSM are presented in Figure 6.11, where it can be seen that WiFi RSS have much larger variation.

6.3.3 Fingerprinting

Most of the existing WiFi localization techniques are fingerprint based, using a two stage process as introduced in section 2.2.3. The localization accuracy using WiFi RSS fingerprinting is reported to achieve a few meters in some 90% of the time (4 meters in 95% of the time [56], 3.3 meters in 98% of the time [57], and 2 meters in 90% of the time [58]).

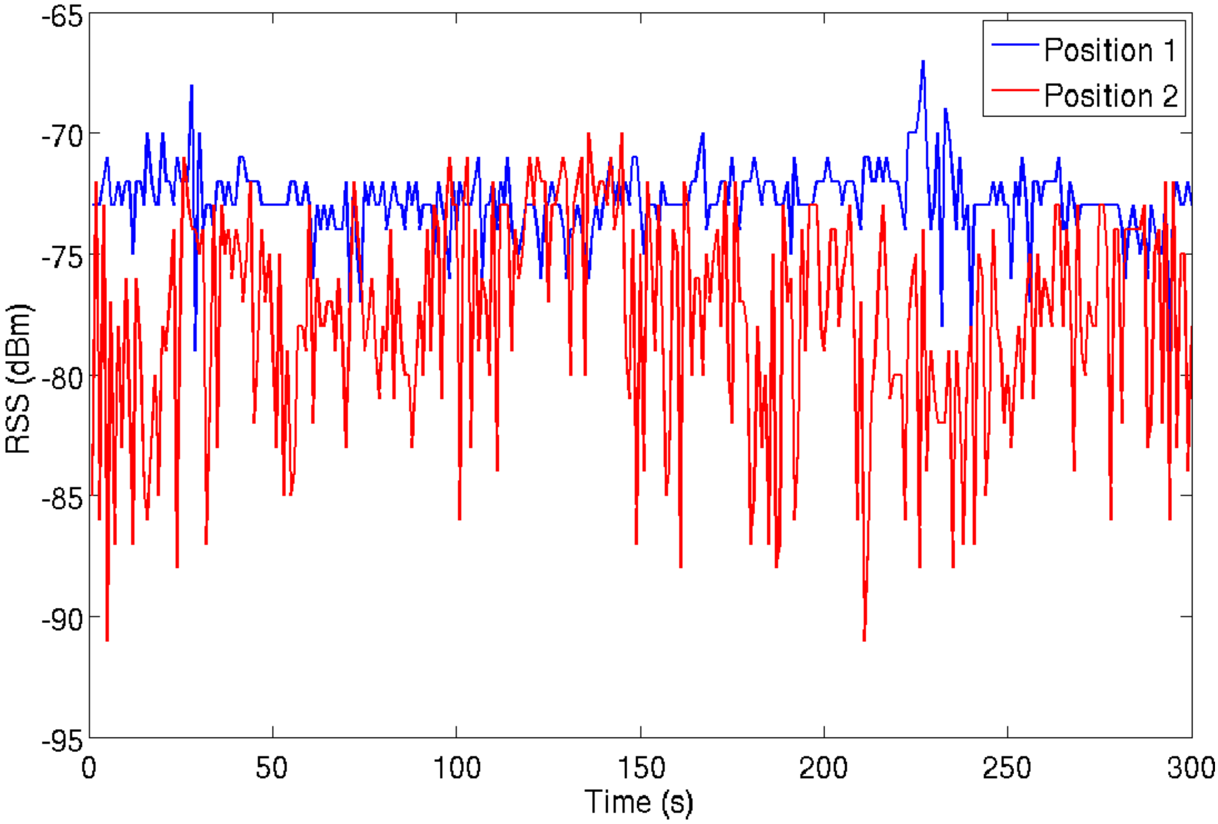

Figure 6.10 – WiFi RSS with different distances to the access point

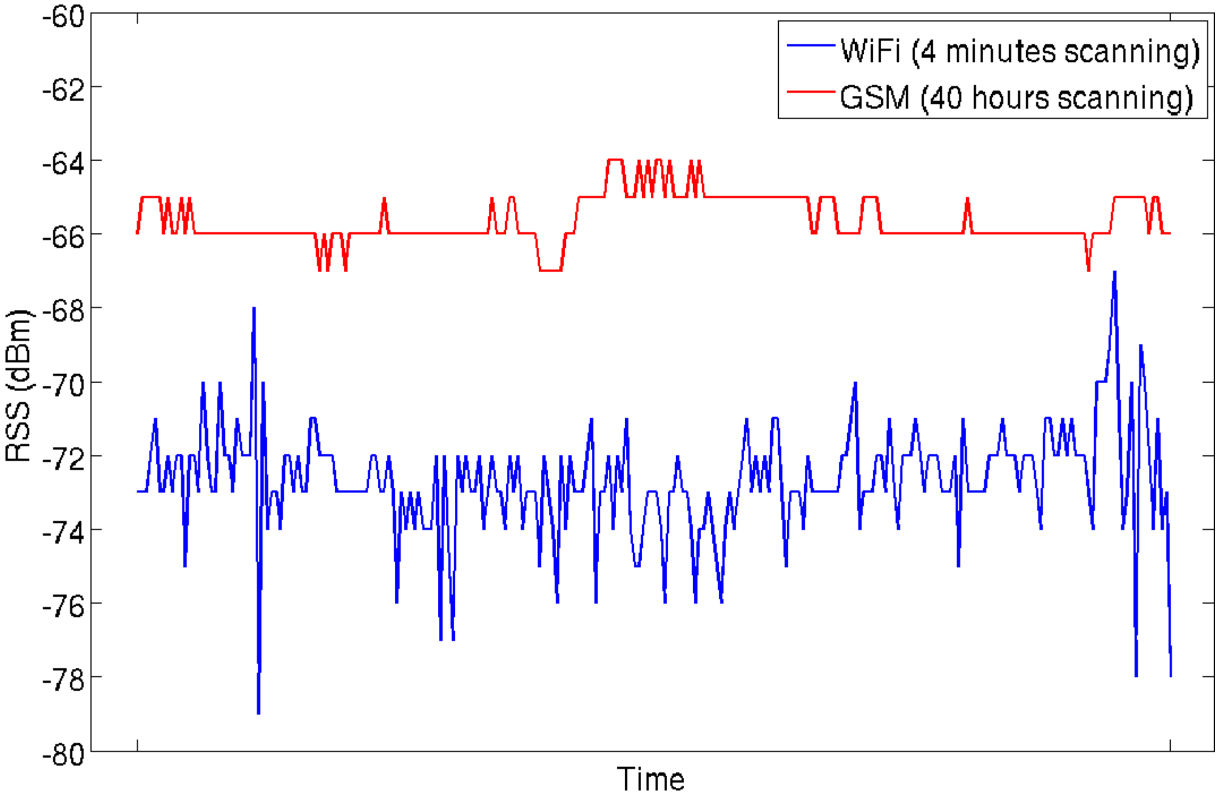

Figure 6.11 – RSS comparison between WiFi and GSM

In this thesis, location fingerprinting is also tested using RSS from WiFi networks. The experiment was done in the same seven rooms as for the GSM indoor localization discussed in section 4.3.2.1. In the experiment, ambient WiFi signals are used without knowing the positions of the AP. The training dataset and test dataset were taken separately in all the seven rooms, each of which contains 300 fingerprint examples containing RSS from 10 AP. The localization model is constructed using the SVM classifier and one-vs-all decision rule.

The overall correct classification rate obtained is 82%, i.e. in 82% of the time, the correct room number can be obtained with a single WiFi fingerprint sample. This result is not bad considering the localization accuracy is achieved based on the WiFi signals that are not specially deployed. Except the three AP with known positions, signals from the rest AP appear intermittently. The experiment also tested including additional WiFi beacons, where two wireless USB adapters were set into AP mode and put inside room H418 and room H414. The correct classification rate then improved to 91%. It is reasonable to assume that the presence of further WiFi AP would provide even better spatial discrimination.

The fingerprinting based approach is simple, does not require special hardware and can rely on the existing WiFi infrastructures. However, in many scenarios the number of available WiFi signals is not sufficient to provide an acceptable localization accuracy, which in turn would require the deployment of additional WiFi AP. In addition, WiFi RSS is reported to be time varying [110], which leads to the localization performance decrease over time.

6.3.4 Triangulation

Another approach for indoor localization using WiFi RSS is triangulation, the technical fundamentals of which were introduced in section 2.2.2.4. In WiFi triangulation, location is estimated by computing the intersection point of circles with centers at the AP and radius equal to the estimated distances to the mobile target. The key to improve the triangulation performance is to obtain accurate distance estimates between mobile target and the WiFi AP. Hence, the emphasis here is put not on location estimation algorithms, but on estimating distance from WiFi RSS.

As Figure 6.10 presented above, though they fluctuate significantly, the RSS of AP2 recorded in position P2 are generally lower than those in position P1, due to the position P2 is 5 meters further from the AP than position P1. However, estimating distance from RSS via an attenuation model is a challenge. Figure 6.12 shows the RSS recorded from AP1 in the same two positions

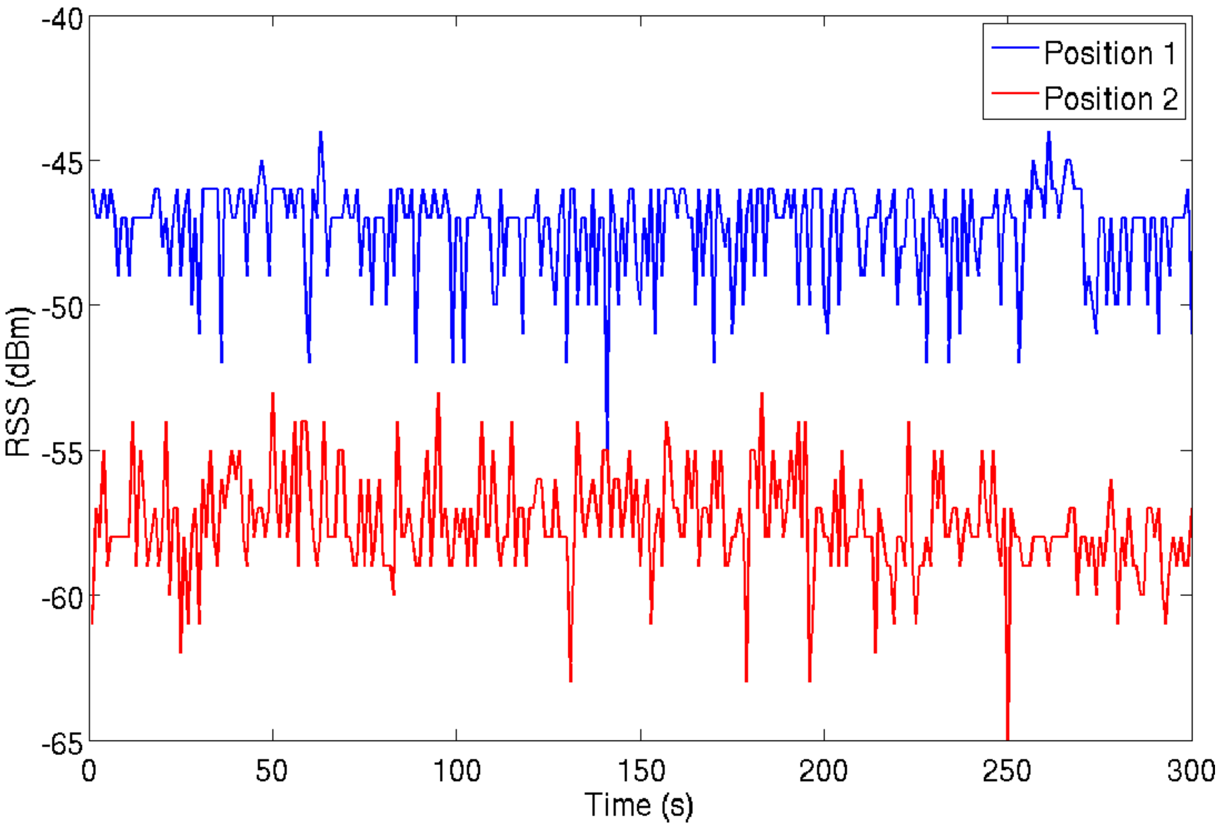

Figure 6.12 – Wall attenuation effect of WiFi RSS

as before. The distances from AP1 to position P1 and position P2 are almost equal, but RSS in location P2 are much lower than RSS in location P1. This may be attributed to the multiple walls between AP1 and position P2.

To obtain knowledge about the wall attenuation effect, RSS are first examined at different distances without wall attenuation in the LOS signal propagation path. Measurements were acquired by the mobile phone held in hand, walking away from the access point. During the whole measuring process, the access point is visible. Figure 6.13 shows the RSS measurements with different distances to the access point, where the relationship between distance and RSS is clear. A distance-RSS function model was obtained using the least square polynomial approximation. In the figure, the red star points are the distance predictions from the RSS measurements.

The distance predictions from RSS indicates that without wall attenuation effect a smooth functional relationship between distance and RSS can be obtained, i.e., weaker RSS correspond to greater distances. In the general case including NLOS, walls need to be taken into account for estimating the distances from an access point. In the thesis, a piecewise functional model was built based on the number of walls between the access point and receiver, using a machine learning method. Figure 6.14 shows the samples and models obtained for the three access points

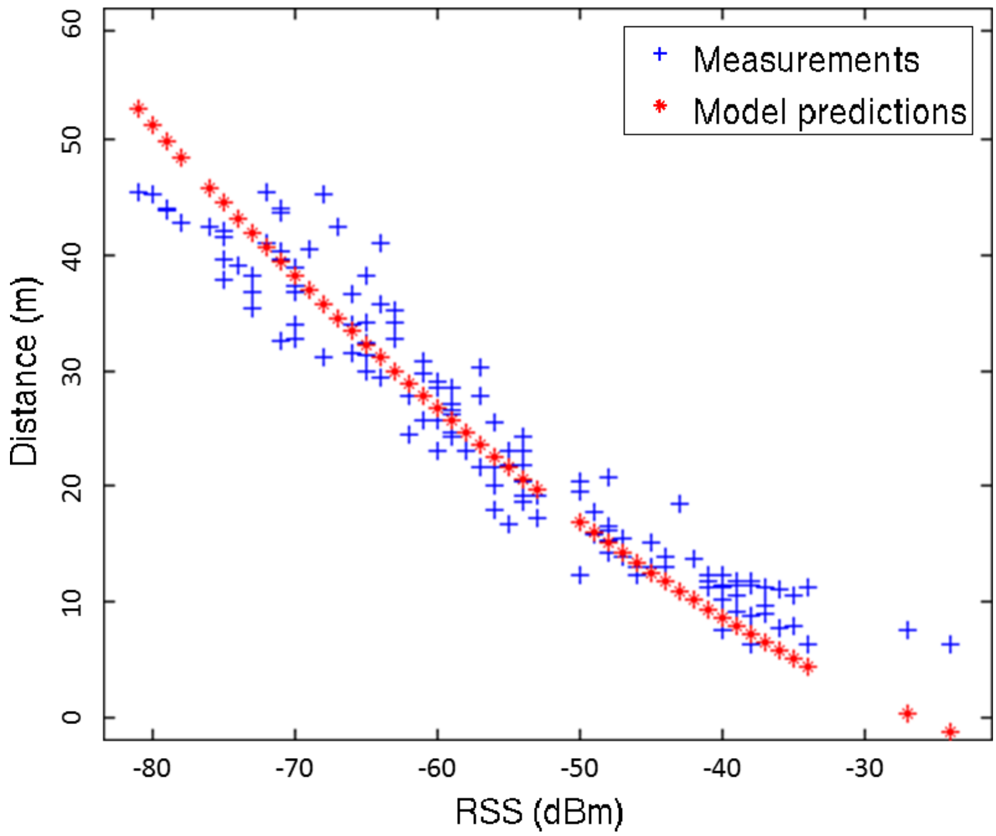

Figure 6.13 – Relationship between distance and RSS in LOS propagation path

and different numbers of walls. It is seen in the figure, for different numbers of walls, that the relationships between distance and RSS are quite different, and using multiple models based on the number of walls between WiFi AP and receivers accordingly can output more reliable distance estimation from RSS. However, even when separated by an equal number of walls, the RSS at a given distance still has a wide distribution. It follows that RSS, used in this way, is not a reliable distance indicator, which can be used for simple but not very accurate indoor localization. Nevertheless, if there are more WiFi access points to provide redundant distance estimations, the performance could certainly be improved.

6.4 Summary

This chapter encompasses the fragmented work that is done during the thesis, including the work related to the SVM classification and indoor localization based on WiFi networks.

The indoor localization approach proposed in this thesis is tested in outdoor and underground spaces. Experimental results demonstrate that such an approach can be accurate and reliable in indoor and underground environments, while in outdoor spaces it is not ideal.

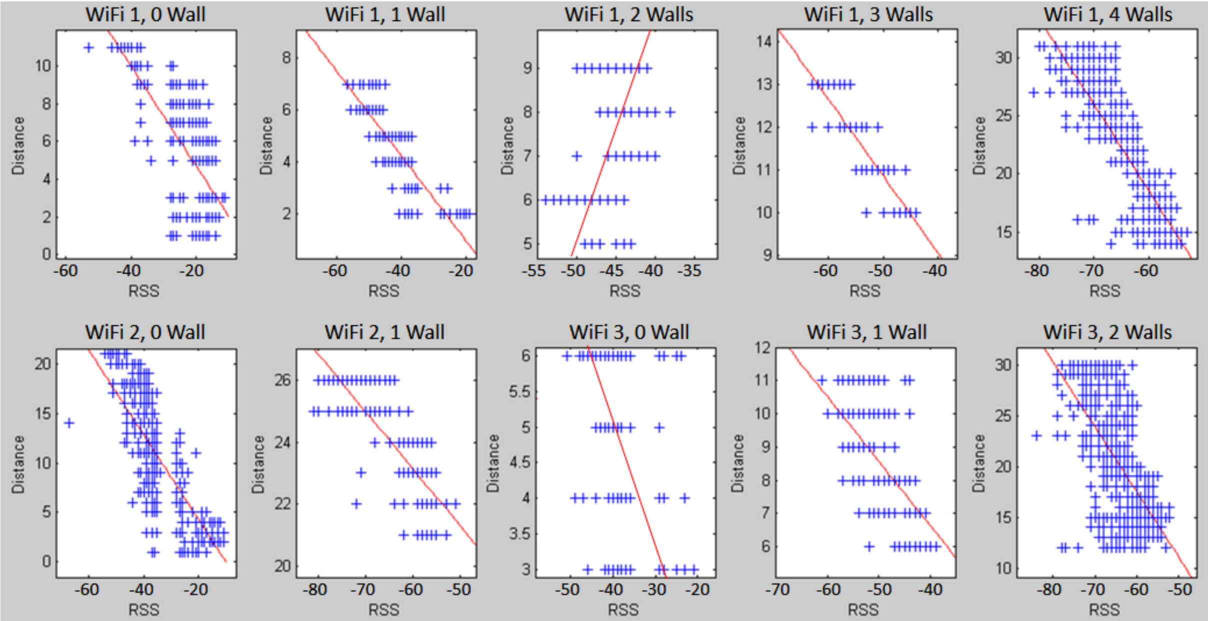

Figure 6.14 – The piecewise model construction between distance and RSS

Different carrier selection methods are evaluated, but none was shown to improve the performance. Two post-processing approaches are also tried to improve the performance of indoor localization, with interesting results.

As another widely available wireless signal, WiFi indoor localization is studied. The RSS characteristics of WiFi are examined, and fingerprinting and triangulation techniques based on WiFi RSS are evaluated. It is demonstrated that WiFi RSS is not stable over distance and it can provide a simple, but not very accurate indoor localization.

Chapter 7

Conclusions and perspectives

7.1 Conclusions

The inability of GPS receivers to function adequately in indoor environments has launched an ongoing search for new techniques of indoor localization that can provide seamless and ubiquitous service for mobile users. Indeed, accurately and reliably locating mobile users and objects in indoor environments is an attractive and challenging goal that holds promise for many location based services and applications.

A wide variety of solutions have been proposed in the literature, the great majority involving measuring physical quantities associated to radio networks of various kinds, independently, or in combination with inertial sensors in hybrid schemes. Most, however, require the deployment and maintenance of a specific radio network infrastructure, which is costly and time consuming.

The common logic has tended to say that cellular radiotelephony networks would be somehow less useful for indoor localization, perhaps due to discouraging results obtained in some early studies. This thesis was undertaken to capitalize on more recent work exploiting RSS measurements from the GSM standard in order to investigate the possibility of creating a genuinely useful, accurate, and reliable indoor localization system based on radiotelephony signals. Indeed the ability to measuring RSS rapidly is a primordial task in any mobile cellular device, and consequently the focus of this work has been on exploring the possibility of installing such an indoor localization system on a standard mobile device, such as a smartphone or tablet.

Although raw RSS values are noisy, methods to prevent performance decreases engendered by these fluctuations have been demonstrated, as well as a technique to improve accuracy and enhance reliability by combining RSS with information from inertial and other types of sensors common in mobile devices today, as well as map layout information of the site under study.

The characteristics of GSM signals were first examined, outlining the location-dependent and time varying properties of GSM RSS. In general, RSS are quite stable in certain locations but with fluctuations in different time scales. RSS from a single GSM carrier, either a beacon channel or a non-beacon channel, does not reveal much location distinction. However, a whole set of RSS from a number of GSM channels, known as a GSM fingerprint, indicates location-dependent attribute that the fingerprint distance is quite related to the geometric distance between different locations.

In complex indoor environments, a valid GSM signal propagation model is difficult to obtain, as RSS is the effect of superimposition of signals from multiple paths with rapidly varying phases. In the initial effort to seek a functional relationship between RSS fingerprint and coordinate position using regression techniques, no such relationship could be discovered, implying that location interpolation schemes based on RSS measurements at a small number of points are probably not useful.

From there, the study embarked on associating high dimensionality cellular telephone network RSS fingerprints to distinct spatial regions. The indoor localization problem, in this work, was considered as a classification problem, where spatial regions are discriminated by classifying the RSS fingerprints taken from these regions. Based on the building structure, the room is defined as the minimum location unit and data was collected using a standard cellular handset while randomly moving in each room at normal walking speed, with fingerprint scanning performed at a large number of points over the entire room rather than at only a few representative points.

A localization model, consisting of a group of binary SVM classifiers and a multiclass decision rule, is constructed offline based on the fingerprint examples, which will be used to determine the room number of an online collected test example. When tested under realistic conditions in seven rooms of an office building, experimental results demonstrated that out of a total of 17500 test fingerprints, the correct room number was obtained 94% of the time, with only some minor difficulties in distinguishing adjacent rooms.

A formidable challenge for the two-stage (offline training and online testing) fingerprinting techniques is the severe, performance-degrading fluctuations to which radiotelephony RSS values are susceptible. Since frequently rebuilding the localization model is time and labor consuming, the thesis attempted to apply semi-supervised learning to update the localization model with unlabeled fingerprints. Tested on data sets collected over 6 months, this approach, though capable to restore a significant part of the lost performance, is still a trade-off between performance decrease and cost of total retraining.

A better solution was discovered by examining the time-varying characteristic of GSM RSS, which fluctuate on different time scales. As a result, when fingerprint examples were taken in a more general way that spread examples over a long time rather than concentrating in a short time period, the performance of the indoor room-level localization system remained stable over a period of months.

Obtained localization accuracy can be improved by taking into account a priori information and other location sources. Considering room-level indoor localization, the physical indoor space can be abstracted into a topological structure, in which a target moves from one room to another room via feasible paths with finite velocity. Bayesian filtering was applied to employ the information about indoor environment and mobile's trajectory, which, in tests on datasets recorded in different scenarios, was able to correct most of the localization errors made by the room classifier.

In parallel we remarked that mobile sensors such as accelerometer, gyroscope and magnetic field are increasingly popular for smart phones, which provide additional location sources such as detecting steps, determining moving orientations, etc. Mobile sensor dead-reckoning alone, of course, is not a reliable indoor localization approach, as it necessitates a known starting position and accumulates errors from the sensor measurements over time. The thesis investigated combining room-level classification results with sensor dead-reckoning using a particle filter, which estimates the mobile location based on the sensor dead-reckoning, while obtaining the starting position and correcting localization errors based on GSM room classification results coupled with map constraints. Results showed that without additional deployment of beacons, reliable and accurate indoor localization can indeed be achieved. This is the principle new result of this thesis, that is, to demonstrate that the so-called "common logic" about cellphone signals is incorrect: radiotelephony RSS measurements are indeed a rich and promising source of indoor location-dependent information, which can be coupled with onboard sensors found in mobile devices in ways similar to those used in the more frequently seen WiFi or Bluetooth based indoor localization solutions.

In addition to the main work presented, a study on room-level GSM classification also includes evaluations of the proposed techniques in outdoor and underground environments, carrier selection schemes, and post-processing of support vector classification. As another widely available wireless signal, indoor localization based on WiFi RSS is studied, showing that RSS fingerprinting is still an effective approach, although it is difficult to model signal propagation in complex indoor environments, even if taking account of walls could improve distance estimation from the RSS.

7.2 Perspectives

The study has offered a promising approach to simple but practical indoor localization solution. However, it also encountered certain limitations, as well as brought to light a number of new ideas, both of which could be addressed in future work.

- Firstly, RSS from all GSM channels, as the indoor localization basis in the thesis, were obtained using specialized network investigation engineering devices (e.g., TEMS Pocket). The fact is that from a hardware standpoint, these are actually standard mobile phones with just a software modification, hence, any mobile cellular device thus modified should have the capability to obtain fast RSS scans in exactly the same way. This means that if cellphone manufactures can be convinced that GSM-based indoor localization is viable, it should be relatively inexpensive to create new products since they can be based upon existing ones with modified software. This also opens the door to being able to access RSS values in real time, in order to combine them with sensor information and map constraints, which, today, with TEMS products, is not possible. To date, unfortunately, cellphone manufacturers have yet to show a particular interest in opening up cellphone firmware to such developments. In such a case, an alternative could be to develop a system on chip, independent of the onboard cellphone processor, to scan RSS fingerprints, which could be embedded in mobile phones much in the same way the WiFi or Bluetooth modules are today. Either approach would provide the final impetus to extend the results obtained in the present study to a genuinely practical solution for indoor localization.
- Secondly, the RSS based approach benefits from the very large number of GSM carriers, and it has been shown that performance continues to increase as more are added to the fingerprint. Thus, incorporating RSS from other available signals, for instance combining several cellphone networks (including LTE), or cellphone plus WiFi/Bluetooth, FM radio, etc., could improve the localization performance even further.
- Thirdly, as in multipath indoor environments RSS fluctuate considerably, it could be interesting to attempt to improve robustness by including the channel impulse response into the fingerprints, in order to characterizing the multipath environment and use it as an additional variable related to position.
- Finally, although the presented study used a hybrid scheme that combines GSM

fingerprinting and mobile sensor dead-reckoning, hybrid schemes making use of mobile sensors could be explored even further, as the number and variety of sensors incorporated into mobile devices today is constantly growing as these devices become more intelligent and location aware.

Appendix A

Publications

Fast, Handset-Based GSM Fingerprints for Indoor Localization

Ye Tian, Bruce Denby
SIGMA Laboratory and
Université Pierre et Marie Curie
Paris, France
ye.tian@etu.upmc.fr,
denby@ieee.org

Iness Ahriz
LAETITIA/CEDRIC Laboratory
Conservatoire National des Arts et Métiers
Paris, France
iness.ahriz@cnam.fr

Pierre Roussel, Gérard Dreyfus
SIGMA Laboratory
ESPCI ParisTech
Paris, France
pierre.roussel@espci.fr,
gerard.dreyfus@espci.fr

***Abstract*—Accurately localizing users in indoor environments remains an important and challenging task. The article presents new results on room-level indoor localization, using cellular Received Signal Strength fingerprints collected with a standard cellular handset programmed to perform fast scans of the 900 and 1800 Megahertz GSM bands as a user explores an indoor environment at a normal walking pace. Support Vector Machines are used to deal with the high dimensionality of the fingerprints. The study demonstrates that an appropriately programmed standard cellular handset can provide a simple, inexpensive solution for accurate room-level indoor localization.**

Keywords-localization; indoor; fingerprint; machine learning; support vector machine

I. Introduction

The inability of GPS receivers to function adequately in 'urban canyon' and indoor environments has prompted a search for new techniques of indoor localization that can provide seamless and ubiquitous service for mobile users. Accurately and reliably locating persons and objects in indoor environments is a challenging, but attractive, goal that holds promise for a variety of location-based services and applications [1]. For many such services, room-level precision, in which the localization system discriminates between rooms rather than estimating coordinates *per se*, is an adequate goal; this is the approach that will be adopted here.

A variety of indoor localization techniques have been proposed. Methods based on Received Signal Strength (RSS), in Wi-Fi and Bluetooth networks, for example, or using infrared or acoustic signals, appear promising [2-7]. A drawback of these approaches, however, is that they necessitate the deployment and maintenance of an infrastructure, which can be time consuming and costly.

In addition to such short-range signals, indoor localization based on fingerprints from wide-area radiotelephone networks, such as GSM and CDMA, have also been proposed [8-13]. The full coverage, near-ubiquity and relative stability of GSM networks may provide an attractive alternative for indoor localization.

Recent results have suggested that accurate and efficient indoor localization can be achieved using RSS information acquired from very large numbers of GSM channels [10-13]. Those studies, however, did not represent a genuinely practical solution since the RSS scanning devices operated without user intervention only at a small number of representative points within each room. In this work, we present a more realistic solution, in which a user can be localized at room level regardless of his exact position in a room. This is achieved using a handheld acquisition device – actually a standard cellphone with a software modification – that can obtain an RSS fingerprint of the entire 900 and 1800 MHz GSM bands in only about 300 milliseconds. This enables the collection of large amounts of data on a reasonable timescale, at points throughout the interiors of the rooms, rather than at only a few representative points, while moving at a normal walking pace.

Our results show that GSM fingerprints acquired in this way can be used to differentiate rooms of about 10 square meters size in some 94% of cases, indicating that the method may indeed be used as part of a simple, practical, inexpensive indoor localization system. The data collection procedure employed is described in section II, and the room classification algorithms in section III. Results are presented in section IV, while conclusions and future perspectives appear in the final section.

II. Data Collection and Datasets

The data used in the experiments was obtained by scanning the entire GSM band in 7 rooms of a 4th floor laboratory building (steel frame, concrete and plaster walls) in central Paris, France. The data acquisition device used was the GSM trace mobile "TEMS Pocket", which is in fact a standard Sony Ericsson W995 mobile phone to which network investigation software has been added by the manufacturer [14]. In April of 2012, on a Saturday afternoon from 2pm to 6pm, 5500 scans (representing about one half hour of recording per room) were recorded in each of the 7 unoccupied rooms and manually labeled with the corresponding room numbers, as illustrated in Figure 1. Each scan contains the RSS of all 548 carriers in the GSM900 and GSM1800 bands, with values ranging from -117 to -38dBm. All scans were made via "random walks" in the 7 rooms with the TEMS Pocket handheld by the user. The exact positions of the individual scans within a room were not recorded; indeed all points in a given room are treated as belonging to that room, consistent with the room-level indoor localization approach adopted here.

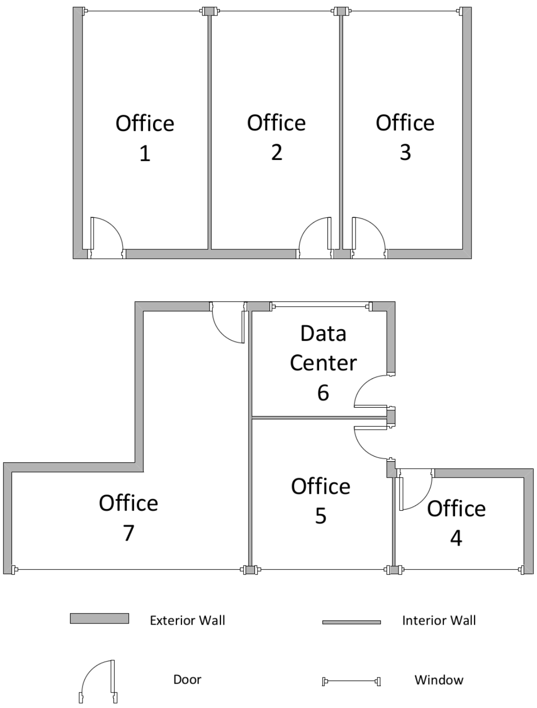

Figure 1. Layout of the laboratory where the data set was recorded

III. Classification Algorithms

The room-level indoor localization problem is considered as a multi-class classification problem, where each room is a class. As is usual in data-driven classification problems, the algorithm works in a two-stage process. The first stage is off-line training, in which the equations of the discriminant functions are determined using training data with known labels. The second stage is on-line testing, in which, given a fingerprint that is not present in the training dataset, the classifier must provide the label of the room where it was measured, using the previously defined separating surfaces. Only the first off-line stage may require heavy computations, the second stage merely needs to compute the values of the discriminant functions. As a starting point for multi-class classification, a pairwise (also termed 'two-class or 'binary') classifier is introduced first.

A. *Pairwise Classifier*

Since the number of variables is very large and the size of the training set is relatively limited, Support Vector Machine (SVM) classifiers were deemed appropriate because of their built-in regularization mechanism [15].

Consider a set of M examples of items belonging to either of two classes A and B, each example being described by a p-dimensional vector $\mathbf{x}_i$. Further assume that the examples are linearly separable, i.e. that there are, in descriptor space, linear surfaces of equation $f(\mathbf{x}) = 0$ that separate all examples without error: $f(\mathbf{x}_i) > 0$ for all examples i belonging to class A and $f(\mathbf{x}_i) < 0$ otherwise. It can be proved that $f(\mathbf{x})$ can be written under the form

$$f(\mathbf{x}) = \sum_{i=1}^{M} \alpha_i y_i (\mathbf{x}_i \cdot \mathbf{x}) + \alpha_0 \qquad (1)$$

where the α_i (i = 0..M) are parameters whose values are estimated from the examples, $y_i = +1$ if example i belongs to class A and $y_i = -1$ otherwise.

A linear SVM is a linear classifier such that the minimum distance between the separation surface $f(\mathbf{x}) = 0$ and the examples that are closest to it (called *support vectors*) is maximum, thereby guaranteeing the best generalization given the available data. The values of the parameters α_i of such a classifier are obtained by solving a quadratic optimization problem under linear inequality constraints. The support vectors are the only examples whose α_i are nonzero.

If the examples are not linearly separable, one resorts to nonlinear SVMs, whereby the separation surface is of the form

$$f(\mathbf{x}) = \sum_{i=1}^{M} \alpha_i y_i K(\mathbf{x}_i \cdot \mathbf{x}) + \alpha_0 \qquad (2)$$

where $K(\mathbf{x}, \boldsymbol{y})$ is a *kernel* function that must be such that the (M, M) matrix of general term $K(\mathbf{x}_i, \mathbf{x}_j)$ is positive semi-definite. As for linear SVMs, the α_i are obtained by solving a quadratic optimization problem under constraints. If the constraints can be satisfied only if a large proportion of examples are support vectors, i.e. if the classifier has a large number of nonzero parameters, the constraint that all examples are classified without error and lie outside the margin can be relaxed; that "soft-margin" approach reduces the complexity of the classifier by performing a tradeoff between accuracy of classification of the training examples and ability to generalize; the price to pay is the introduction of a "regularization" constant whose value must be chosen appropriately.

There exists a repertoire of valid kernel functions, among which the RBF kernel

$$K(\mathbf{x}, \mathbf{y}) = \exp\left(-\frac{\left\|\mathbf{x}-\mathbf{y}\right\|^2}{2\sigma^2}\right) \qquad (3)$$

with appropriate width σ, is used in the present study. The values of σ and the regularization constant are chosen by cross-validation

To summarize, a GSM environment described by the fingerprint $\mathbf{x}$ is assigned to room A or room B according to the sign of $f(\mathbf{x})$, defined by (1) or (2) depending for linear or nonlinear SVM classification respectively. $\mathbf{x}_i$ is the fingerprint dataset entry i, i.e. row i of RSS, GSM900 or GSM1800 depending on the fingerprint used by the classifier.

The SVMs used in our study, both with linear and RBF kernels, were implemented using the Spider toolbox [16].

In order to obtain a "baseline" result, nearest neighbor (1-NN) and *k*-nearest neighbor (*k*-NN) classifiers using the Euclidean distance in RSS-space were also implemented. The hyper parameter *k* was determined by the same cross-validation procedure as for the hyper parameters of SVMs.

B. Decision Rules for Multiclass Discrimination

When the discrimination problem involves more than two classes, it is necessary, for pairwise classifiers such as SVM, to define a method that allows combining multiple pairwise classifiers into a single multiclass classifier. This can be done in two ways: one-vs-one and one-vs-all.

1) One-vs-one

This approach decomposes the multiclass problem into the set of all possible one-vs-one problems. Thus, for an *n*-class problem, $n(n-1)/2$ classifiers must be designed. Figure 2 illustrates the architecture associated with this method.

The decision rule in this case is based on a vote. First, the outputs of all classifiers are calculated. Now let C_{ij} be the output of the classifier specializing in separating class *i* from class *j*. If C_{ij} is 1, the tally for class *i* is increased by 1; if it is -1, the class tally of class *j* is increased by 1. Finally, the class assigned to the example is that having the highest vote tally.

A disadvantage of the one-vs-one technique is of course the increase in the number of classifiers required as compared to one-vs-all discussed below. In our case of seven classes, 21 classifiers are required, which still remains manageable.

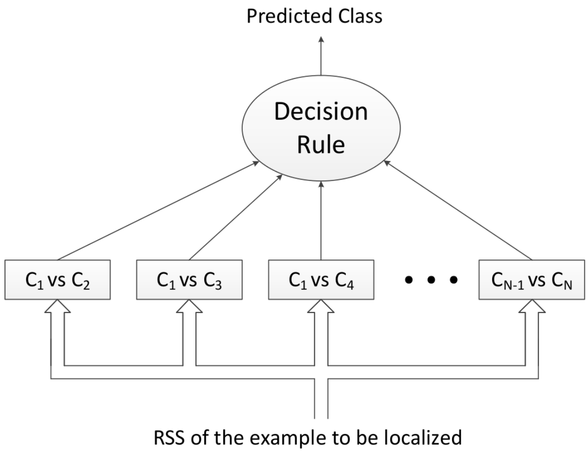

Figure 2. One-vs-one classification

2) One-vs-all

The one-vs-all approach consists of dividing the *n*-class problem into an ensemble of *n* pairwise classification problems, each of which is specialized in separating one class from all others. Figure 3 illustrates the procedure. In the first stage, each of the *n* classifiers is trained separately, and in the second stage, the following decision rule is applied : the outputs of all *n* classifiers are first calculated and, following the conventional procedure, the predicted class is taken to be that of the classifier with the largest magnitude of *f*(**x**) (relation (1) or (2)) [17]. The one-vs-all technique is advantageous from a computational standpoint, in that it only requires a number of classifiers equal to the number of classes, in our case, 7.

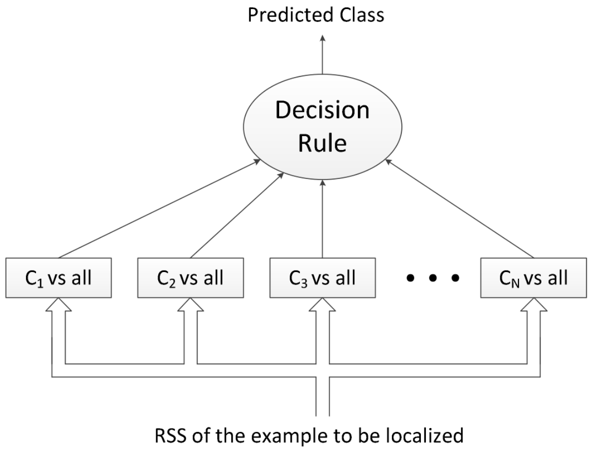

Figure 3. One-vs-all classification

IV. RESULTS

The performance of each classifier is presented as the percentage of correctly classified test examples. In our dataset, in each room, the first 3000 examples are used off-line for training the classifiers (quadratic optimization under constraints) and finding the appropriate values of the hyper parameters by cross-validation. The final 2500 of the 5500 scans make up the test set. Testing involves the computation of the sign of *f*(**x**) from relations (1) or (2), which is very fast.

Experimental results are shown in Table I. The soft margin parameter *C* and RBF kernel parameter σ are selected through cross-validation, giving $C = 10^{-4}$ in linear one-vs-one and linear one-vs-all classifiers, $C = 10^{-4}$ and $\sigma = 100$ in RBF one-vs-one and one-vs-all classifiers. Results for 1-NN and *k*-NN classifiers are also given for comparison, where the parameter *k* was optimized by cross validation.

TABLE I. PERCENTAGE OF CORRECT CLASSIFICATION ON TEST SET

Classifier	**Fingerprint Type**		
	GSM900	***GSM1800***	***Both Bands***
1-NN	56.2%	54.4%	62.7%
k-NN	62.4%(*k*=77)	61.2%(*k*=21)	67.9%(*k*=14)
Linear 1-vs-1	86.3%	83.2%	93.9%
Linear 1-vs-rest	87.1%	85.0%	94.2%
RBF 1-vs-1	85.5%	84.6%	93.0%
RBF 1-vs-rest	87.2%	85.7%	94.1%

As can be seen in the table, the SVM room classifiers give correct results about 94% of the time with no significant difference between linear and nonlinear kernels. As expected, results from nearest-neighbor classifiers are significantly poorer. We also note that the GSM900 (174 carriers) and GSM1800 (374 carriers) bands are complementary in that better localization accuracy is obtained when both bands are present in the fingerprint. In Figure 4 we also show how the accuracy improves with fingerprint size, for the linear one-vs-all algorithm, by increasing the number of carriers in steps of 50, according to the ordered sequence numbers of the GSM carriers.

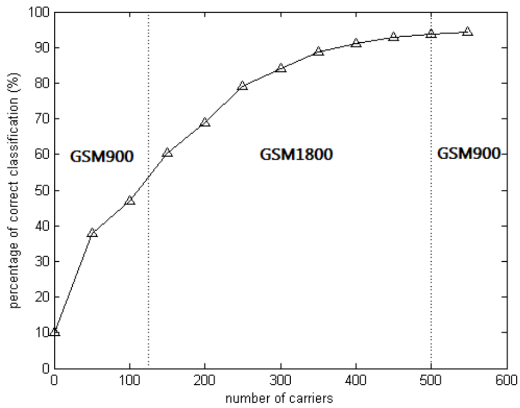

Figure 4. Classification results as a function of fingerprint size

In figure 5 we examine the effect of increasing the number of training examples for each of the 7 rooms, again using the linear one-vs-one algorithm. The figure plots the percentage of correct room classifications as a function of the training set size. We see that a rather substantial reduction in training set size gives only a very moderate degradation in performance. For example, 93% of the test examples were correctly classified using only 1000 training examples. This is a very interesting result as far as acquisition time is concerned, as the TEMS Pocket requires less than 10 minutes to record 1000 training examples.

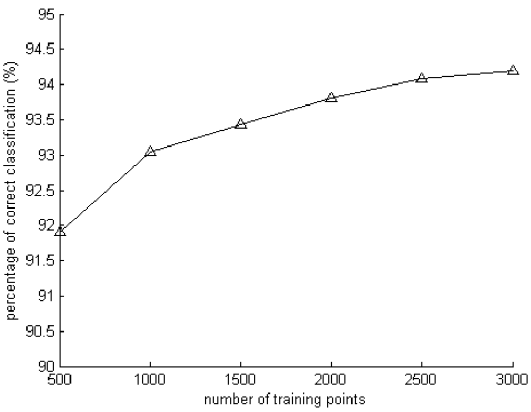

Figure 5. Classification results as a function of training set size

Table II presents the confusion matrix for the case of the linear one-vs-one algorithm, showing how the mis-classified examples are distributed. It can be seen that most confusions occur between adjacent rooms, as could be expected. Rooms located on opposite sides of the corridor are easily discriminated.

TABLE II. CONFUSION MATRIX FOR 7 ROOMS CLASSIFICATION

Predicted Class	True Class						
	1	*2*	*3*	*4*	*5*	*6*	*7*
1	91.1%	4.7%	4.2%	0%	0%	0%	0%
2	3.9%	94.9%	1.2%	0%	0%	0%	0%
3	2.6%	1.7%	95.7%	0%	0%	0%	0%
4	0%	0%	0%	96%	1.1%	0%	2.9%
5	0%	0%	0%	0.8%	97.1%	0.5%	1.6%
6	0%	0%	0%	0%	0%	99.9%	0.1%
7	0%	0.6%	0%	4.1%	4.3%	3%	88%

V. CONCLUSIONS AND PERSPECTIVES

We have presented an approach for indoor localization based on the use of RSS with very large numbers of GSM carriers, which has been tested on a dataset acquired in a laboratory building under realistic conditions. Data was collected in such a way as to explore the entire surface area of a room, using a standard cellular handset as the acquisition device. Experimental results demonstrate that out of a total of 17500 (2500*7) test fingerprints, the correct room label was obtained 94% of the time, thus indicating that the method can indeed serve as the basis for a simple, inexpensive indoor localization system.

Future tests will involve studying how performance evolves over longer periods of time, as well as experimenting with different methods for combining the scans from the two GSM bands used, and investigating whether W-CDMA network data or other types of variables can also be incorporated into our scans. Also, the experiments reported here were performed during a weekend, so that the presence of people in the environment will need to be investigated. We note that only one TEMS pocket device was used in these tests; in the future, will want to perform tests with several terminals, to verify device independence of our results. Finally we intend to try integrating *a priori* information and notions of physical trajectories into our location estimation algorithms, via particle or other types of filters. Such an approach will allow considering the entire indoor environment, not only rooms.

ACKNOWLEDGMENT

The authors wish to acknowledge the support of the China Scholarship Council.

REFERENCES

[1] A. Küpper, Location-Based Services: Fundamentals and Operation, John Wiley & Sons, New York, NY, USA, 2005.

[2] AM. Ladd, KE. Bekris, A. Rudys, LE. Kavraki, DS. Wallach, “On the feasibility of using wireless ethernet for indoor localization,” IEEE

Trans on Robotics and Automation. vol. 20, no. 3, pp.555-559, June 2004.

[3] Q. Yang, S. Jialin Pan, V. Wenchen Zheng, "Estimating location using Wi-Fi," IEEE Intelligent Systems, vol. 23, no. 1, pp.8-13, January/February 2008.

[4] S-H. Fang, T-N. Lin, P-C. Lin, "Location fingerprinting in a decorrelated space," IEEE Trans on Knowledge Data Engineering. vol. 20, no. 5, pp.685-691, May 2008.

[5] S-H. Fang, T-N. Lin, "Indoor location system based on discriminant-adaptive neural network in IEEE 802.11 environments," IEEE Trans on Neural Network, vol. 19, no. 11, pp.1973-1978, Nov 2008.

[6] S-H. Hong, B-K. Kim, D-S Eom, "Localization algorithm in wireless sensor networks with network mobility," IEEE Trans on Consumer Eectronic. vol. 55, no. 4, pp.1921-1928, Nov 2009.

[7] S-P. Kuo, Y-C. Tseng, "A scrambling method for fingerprint positioning based on temporal diversity and spatial dependency,". IEEE Trans Knowledge Data Eng. vol. 20, no. 5, pp.678-684, May 2008

[8] V. Otsason, A. Varshavsky, A. LaMarca, E. de Lara, "Accurate GSM indoor localization," in Proceedings of the 7th International Conference on Ubiquitous Computing, pp.141-158, Tokyo, Japan, September 2005.

[9] W. ur Rehman, E. de Lara, S. Saroiu, "CILoS, a CDMA indoor localization system," in Proceedings of the 10th International Conference on Ubiquitous Computing, pp.21-24, Seoul, South Korea, September 2008.

[10] B. Denby, Y. Oussar, I. Ahriz, G. Dreyfus, "High-performance indoor localization with full-band GSM fingerprints," in Proceedings IEEE International Conference on Communications, Workshop on Synergies in Communication and Localization, pp. 1-5, Dresden, Germany, June 2009

[11] I. Ahriz, Y. Oussar, B. Denby, G. Dreyfus, "Carrier relevance study for indoor localization using GSM," in Proceedings of the 7th Workshop on Positioning, Navigation and Communication, pp.11-12, Dresden, Germany, March 2010.

[12] I. Ahriz, Y. Oussar, B. Denby, G. Dreyfus, "Full-band GSM fingerprints for indoor localization using a machine learning approach," International Journal of Navigation and Observation. vol. 2010

[13] Y. Oussar, I. Ahriz, B. Denby, G. Dreyfus, "Indoor localization based on cellular telephony RSSI fingerprints containing very large numbers of carriers," EURASIP Journal on Wireless Communications and Networking, vol. 2011, no. 1, pp.1-14.

[14] Test Mobile System. [Online]: www.ascom.com/tems

[15] N. Cristianini, J. Shawe-Taylor. Support Vector Machines and Other Kernel-Based Learning Methods, Cambridge University Press, 2000

[16] The Spider. [Online]: http://people.kyb.tuebingen.mpg.de/spider/

[17] Y. Lee, Y. Lin, and G. Wahba, "Multicategory support vector machines: theory and application to the classification of microarray data and satellite radiance data," Journal of the American Statistical Association, vol. 99, no. 465, pp. 67–81, 2004.

Practical Indoor Localization using Ambient RF

Ye Tian, Bruce Denby (SM'99)
SIGMA Laboratory and
Université Pierre et Marie Curie
Paris, France
ye.tian@etu.upmc.fr,
denby@ieee.org

Iness Ahriz
LAETITIA/CEDRIC Laboratory
Conservatoire National des Arts et Métiers
Paris, France
iness.ahriz@cnam.fr

Pierre Roussel,
Rémi Dubois (M'09),
Gérard Dreyfus (F'12)
SIGMA Lab, ESPCI ParisTech
Paris, France
firstname.lastname@espci.fr,

Abstract—**The article presents a simple, practical approach for indoor localization using Received Signal Strength fingerprints from the GSM network, including an analysis of the relationship between signal strength and location, and the evolution of localization performance over time. Support Vector Machine regression applied to very high dimensional fingerprints does not reveal any smooth functional relationship between fingerprints and position. Classification using Support Vector Machines however provides very good results on discriminating different rooms in an indoor environment, albeit with performance that degrades over time. Transductive inference, introduced as a means of updating models to overcome degradation over time, provides hints that accurate indoor localization can be achieved by applying classification methods to cellular Received Signal Strength fingerprints, performance robustness being maintained via model updating and refining.**

Keywords—localization; indoor; fingerprint; transductive support vector machine

I. Introduction

Indoor localization systems are an important extension to Location Based Services (LBSs), for assisted living scenarios, tracking of Alzheimer's patients, and in more general situations [1]. As GPS receivers are unable to function in indoor environments, a variety of indoor localization strategies have been proposed to try to tackle this challenging task [2-11]. Methods based on the measurement of Received Signal Strength (RSS) in RF networks such as Wi-Fi and Bluetooth networks, for example, have proven to be effective [2-6]. However, time and labor intensive deployment and maintenance of these networks is a drawback that reduces the impact of these techniques.

Aside from these specially deployed networks, indoor localization based on ambient radiotelephone networks, such as GSM and CDMA, has also been studied [8-10]. In the past few years, methods based on the use of RSS fingerprints acquired from large numbers of GSM channels have appeared promising [10, and references therein]. Recent results also suggest that an appropriately programmed standard cellular mobile phone can provide a simple, inexpensive solution for accurate room-level indoor localization [11].

The studies proposed in [10-11], however, were preliminary for two reasons. First, they did not attempt to explore the spatial distribution of measured RSS values, or to discover a functional relationship between RSS and position in indoor environments. Secondly, no prescription was made for correcting for RSS drifts over time, which is a well-known challenge in RSS based systems, particularly for long-range signals [12]. Indeed, due to shadowing, multipath and environmental effects such as building geometry, network traffic, presence of people, and atmospheric conditions, RSS is expected to be nonlinear with distance, non-Gaussian, and time varying [2], which can lead to performance degradation over time.

In this article, after an initial description of the data collection procedures used (section II), we turn our attention to seeking a functional relationship between GSM RSS and position, using Support Vector Machine (SVM) regression. The results, in fact, presented in section III, show that no such relationship exists for the indoor environments tested, indicating that interpolation/extrapolation schemes based on RSS measurements at a small number of points will not be viable for localization. .

On the other hand, because of the local nature of shadowing and multipath effects, RSS fingerprints acquired over entire rooms can potentially be useful for room-level classification, as proposed in [11]. The scheme is presented in section IV, using data collected during "random walks" that explore an entire area. This section also presents long term tests showing that the performance of our RSS based indoor localization method degrades over time. We introduce transductive inference, which uses new, incoming unlabeled data to update SVM classifiers as a means of reducing performance degradation caused by RSS drift. The use of small amounts of new labeled data as a model update scheme is also explored here. Overall conclusions and some perspectives appear in section V.

II. Measurement Sites and Datasets

Two types of datasets were collected, for regression and classification experiments, respectively, both recorded on the 4th floor of a laboratory building (steel frame, concrete and plaster walls) in central Paris, France (Fig. 1). The first set, which we shall call the regression set, was collected in a single room (office 7) using so-called machine-to-machine, or M2M, GSM/GPRS modules [13], which can be driven using standard and manufacturer-specific AT modem commands. We used eight identical modules, with nominally identical specifications and technical parameters. During data collection, the M2M

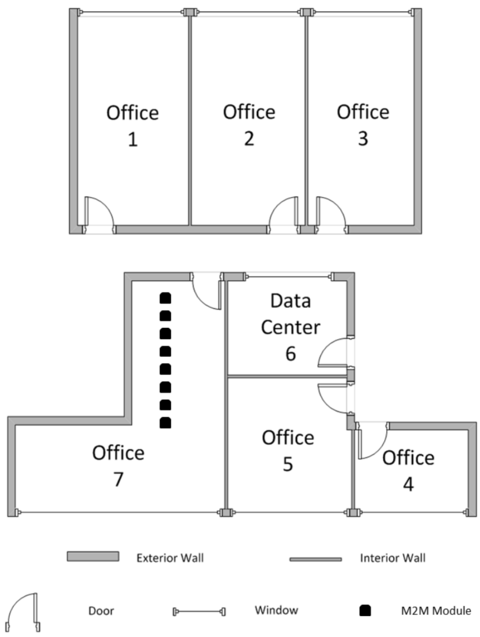

Figure 1. Layout of the laboratory where the datasets were recorded

modules were placed at fixed positions, in a line, spaced at an interval of 0.6m, as illustrated in Fig. 1. A total of 600 GSM scans for each module were recorded over five working days. Each scan contains the RSS of all 548 carriers in the GSM900 and GSM1800 bands, and consists of RSS values ranging in value from -108dBm to -40dBm. All the scans were labeled manually with location from 0m to 4.2m indicating where the scan was made.

The second dataset, which will be used for SVM classification, was collected in seven rooms of the laboratory as described in [11]. The data acquisition device in this case is a Sony-Ericsson mobile phone with embedded scanning software, which is able to obtain a scan of the entire GSM900 and GSM 1800 bands in about 300 milliseconds. Scans were recorded in each of the seven rooms and manually labeled with the corresponding room numbers during "random walks". Six datasets were recorded during weekends over a period of nine months in the same setting, hereafter called *S1*, *S2*, *S3*, *S4*, *S5* and *S6* in chronological order as shown in Table I.

TABLE I. CLASSIFICATION DATASETS

Name of Dataset	Recording Time	Number of Examples
S1	April 14	5000
S2	May 06	2000
S3	June 09	1000
S4	September 09	1000
S5	November 25	1000
S6	December 15	2000

III. POSITION FROM RSS

It was shown in [10] that the classification of RSS vectors recorded at fixed points works quite well. The objective here is to see if a regression method allows to measure locations at intermediate positions between the fixed points by finding a functional relationship between location and RSS in this indoor environment.

A. SVM Regression Algorithms

Since the number of variables is very large (548 carriers) and the size of the training set is relatively limited, SVM regression was deemed appropriate because of its built-in regularization mechanism [16].

Consider a given dataset of n RSS scans $\{(\mathbf{x}_1, y_1), (\mathbf{x}_2, y_2), \cdots, (\mathbf{x}_n, y_n)\}$, where $\mathbf{x}_i$ is the fingerprint vector at location i and y_i is the coordinate of the location (assuming that 1-D localization is performed as described above). There exists a variety of Support Vector Regression (SVR) techniques, serving different purposes. $\varepsilon - SVR$, which was used in our experiments, aims to find a parameterized function $f(\mathbf{x}, \Theta)$ such that prediction errors $\left\| y_i - f(\mathbf{x}_i, \Theta) \right\|$ do not exceed a given value ε for all elements of the training set, and, at the same time, is as regular as possible, i.e. does not oscillate unnecessarily [14]. Assume that we are looking for a linear relationship between the RSS fingerprint and the location. The function has the form:

$$f(\mathbf{x}, \Theta) = \mathbf{w} \cdot \mathbf{x} + b \tag{1}$$

where $\Theta = \begin{bmatrix} \mathbf{w} & b \end{bmatrix}^T$. The parameters are sought as solutions to the constrained optimization problem:

$$\begin{aligned} &\text{minimize} \quad \frac{1}{2}\left\|\mathbf{w}^2\right\| \\ &\text{subject to} \quad \left\| y_i - (\mathbf{w} \cdot \mathbf{x}_i - b) \right\| \le \varepsilon \end{aligned} \tag{2}$$

The optimal solution, if it exists, can be shown to be of the form

$$f(\mathbf{x}) = \sum_{i=1}^{n} \alpha_i y_i (\mathbf{x}_i \cdot \mathbf{x}) + \alpha_0 \tag{3}$$

where α_0 and all the α_i are solutions of a constrained quadratic optimization problem.

If such a solution does not exist, slack variables ζ_i and ζ_i^* can be introduced to relax the constraints, allowing some examples of the training set to be predicted with an error larger than ε. The problem becomes:

$$\begin{aligned} &\text{minimize} \quad \frac{1}{2}\left\|\mathbf{w}^2\right\| + C\sum_{i=1}^{n}(\zeta_i + \zeta_i^*) \\ &\text{subject to} \quad \begin{cases} y_i - \mathbf{w} \cdot \mathbf{x}_i - b \le \varepsilon + \zeta_i \\ \mathbf{w} \cdot \mathbf{x}_i + b - y_i \le \varepsilon + \zeta_i^* \quad \forall i \\ \zeta_i,\ \zeta_i^* \ge 0 \end{cases} \end{aligned} \tag{4}$$

where C is a hyperparameter called "regularization constant".

If we want to look for a non-linear relationship between the RSS fingerprint and the location, non-linear regression can be realized by first performing a nonlinear transformation of the variables that defines a more suitable feature space, in which linear regression is performed. The final solution is in the form

$$f(\mathbf{x}) = \sum_{i=1}^{n} \alpha_i y_i K(\mathbf{x}_i, \mathbf{x}) + \alpha_0 \quad (5)$$

where $K(.,\ .)$ is called the *kernel* function. In our experiments, linear and nonlinear regression (using Gaussian and Polynomial kernels) were performed, using the Spider toolbox [15].

B. Results

The results of SVRs are estimated through the mean squared localization error $\frac{1}{8}\sum_{k=1}^{8}\sqrt{\frac{1}{600}\sum_{i=1}^{600}\left[y_k - f\left(\mathbf{x}_{ik}, \boldsymbol{\theta}^{-k}\right)\right]^2}$,

TABLE II. REGRESSION RESULTS

Regression Method	Mean Square Localization Error
Linear LS-Regression	2.3m
Linear SVM Regression	1.8m
Polynomial SVM Regression (d = 5)	1.3m
Gaussian SVM Regression	2.4m

where y_k is the position of measuring device k, $\mathbf{x}_{ik}$ is the RSS vector measured during scan i taken at location k, and $\boldsymbol{\theta}^{-k}$ is the parameter vector found by training from the data pertaining to all locations except location k.

The results for linear and non-linear regressions are shown in Table II. The soft margin parameter C, polynomial degree d and Gaussian kernel parameter σ were selected through cross-validation. Results from linear least squares regression (LS-Regression) are also given for comparison.

As shown in the table, the mean positioning error of all the regression methods is so large as to be unexploitable. The regression error is approximately equal to the average distance between the 8 locations, meaning that no linear or non-linear relationship between RSS and the position in a small indoor environment is evident. This appears to rule out using full-band RSS GSM vectors obtained in this way to interpolate between fixed positions in an indoor localization method.

IV. ROOM LEVEL CLASSIFICATION AND RSS DRIFT

An alternative scheme, first introduced in [11], is to perform room-level classification based on RSS measurements made during "random walks". In this case, we use classifiers to perform room-level indoor localization, where each room is a class. Data-driven classification problems are often solved in two stages: off-line training; and on-line testing. In the off-line training stage, discriminant functions are determined using training data and known labels, while in the on-line testing stage, a new test fingerprint is presented to the classifier and given a label based on the discriminant functions.

The RSS-based room level SVM classifiers in [10] gave good results when training and test data were obtained over the same one-month period. Here, we explore the time dependence of the "random walk" approach, proposing transductive inference to continuously adjust a discriminant function with newly collected unlabeled data, in order obtain an updated classifier.

A. SVM Pairwise Classifier

SVM classifiers were used in our experiments, since they are deemed appropriate to deal with the high dimensional RSS fingerprints for the same reasons as described above for SVRs.

Consider a set of n examples of items belonging either to class A or class B, each example being described by a p-dimensional vector $\mathbf{x}_i$. Further assume that the examples are linearly separable, i.e. that there exists a hyperplane of equation $f(\mathbf{x}) = 0$ that separate all examples without error: $f(\mathbf{x}_i) > 0$ for all examples i belonging to class A and $f(\mathbf{x}_i) < 0$ otherwise. It can be proved that $f(\mathbf{x})$ can be written under the form

$$f(\mathbf{x}) = \sum_{i=1}^{n} \alpha_i y_i (\mathbf{x}_i \cdot \mathbf{x}) + \alpha_0 \quad (6)$$

where the α_i ($i = 0 \cdots n$) are parameters whose values are estimated from the examples; $y_i = +1$ if example i belongs to class A and $y_i = -1$ otherwise.

If the examples are not linearly separable, a "soft-margin" approach can be used to reduce the complexity of the classifier by introducing slack variables ζ_i and performing a tradeoff between accuracy of classification of the training examples and ability to generalize; the price to pay is the introduction of a "regularization" constant C whose value must be chosen appropriately.

B. Decision Rule for Multiclass Discrimination

The room-level localization problem is a multiclass discrimination problem, which necessitates a decision rule to combine the results of multiple pairwise classifiers. The one-vs-all multiclass classifiers were used in this paper.

The one-vs-all approach consists of constructing one SVM classifier per class, which is trained to distinguish the examples of one class from the examples of all the remaining classes. In the first stage, each of the n classifiers is trained separately, and in the second stage, the following decision rule is applied: the outputs of all n classifiers are first calculated and, following the conventional procedure, the predicted class is taken to be that of the classifier with the largest magnitude of $f(\mathbf{x})$ (relation (6)).

C. Transductive SVM Classifier

Transductive SVMs take unlabeled test examples into account and adjust the separating surface to separate both training examples and test examples with maximum margin. For a linearly separable data case, this leads to the following optimization problem [17]:

$$\begin{aligned} &\text{minimize} \quad \frac{1}{2}\left\|\mathbf{w}^2\right\| \\ &\text{subject to} \quad \begin{cases} y_i\left(\mathbf{w}\cdot\mathbf{x}_i + b\right) \geq 1 \\ y_j^*\left(\mathbf{w}\cdot\mathbf{x}_j^* + b\right) \geq 1 \end{cases} \quad \forall i, j \end{aligned} \quad (7)$$

where x_j^* is the unlabeled data and y_j^* is the label corresponding to x_j^* given by TSVMs. Therefore, minimization must be performed with respect to $\mathbf{w}$, b, $\mathbf{x}_j^*$ and y_j^*, $j = 1 \ldots N$, by contrast to standard SVMs where minimization must be performed with respect to **w** and b only. To be able to handle non-separable data, slack variables ζ_i are introduced as in standard SVM classifiers. Algorithms for solving this optimization problem are described in [17, 18].

The transductive SVMs used in our study, were implemented using SVM^{light} [19].

D. Results, and Comparison to "Re-Training"

Experimental results are presented as the percentage of correctly classified test examples. Table III presents the confusion matrix of testing set *S2* with SVM classifier trained on set *S1*, showing the detailed test results. It is shown in the table that compared with the confusion matrix shown in [11], rooms located on the opposite sides of the corridor are still easily discriminated over time. Most of the confusions occur in the same side of the corridor, i.e. adjacent rooms. For example, 41.8% of the test examples in room 2 were assigned to room 1, while 42.1% were assigned to room 3. The performance in some rooms, room 3 and room 6 for example, however, did not decrease seriously over time.

TABLE III. CONFUSION MATRIX OF TEST SET S2

True Class	Predicted Class						
	1	*2*	*3*	*4*	*5*	*6*	*7*
1	68.1%	0.9%	27.1%	0%	0.2%	3.4%	0.3%
2	41.8%	14.6%	42.1%	0.5%	0.1%	0.8%	0.1%
3	13.2%	3.7%	81.8%	0.5%	0.2%	0.5%	0.1%
4	1.9%	0%	2.6%	65.5%	23.8%	3.6%	2.6%
5	3.4%	0%	0.1%	11.0%	78.2%	0.2%	7.1%
6	1.1%	0%	12.8%	0.2%	0.5%	83.9%	1.4%
7	1.1%	0%	0.9%	4.5%	47.4%	0.1%	45.9%

In Table IV we compare the results of SVM and TSVM classifiers on datasets *S1* to *S6*. For SVM classifiers, we use the model trained on set *S1* to classify the data of sets *S2*, *S3, S4, S5* and *S6*. The result of testing set *S1* was published in [11] and reproduced here for comparison. For TSVM training, the first 100 examples of each room in *S2*, *S3, S4, S5* and *S6* sets were used as unlabeled examples to adjust the model, the remaining examples were used for testing. As can be seen in the table, when building the classifier with set *S1* and testing it on sets *S2*, *S3, S4, S5* and *S6* taken in different time periods, the performance varies dramatically, from about 94% for "fresh" data (*S1* set), down to as low as 27% (*S6* set). However, by using only 100 new unlabeled examples of each room with the TSVM, a substantial amount of the lost performance can be recovered, with accuracies up to 78.4%.

TABLE IV. COMPARISON OF SVM AND TSVM

Test Set	Training Set	SVM	TSVM
S1	*S1*	94.2%	—
S2	*S1*	60.4%	78.4%
S3	*S1*	39.7%	58.8%
S4	*S1*	32.3%	49.6%
S5	*S1*	34.4%	55.3%
S6	*S1*	26.7%	46.1%

The TSVM approach is interesting because it presents a way of recovering some of the performance loss due to RSS drift, at the cost only of obtaining some recent *unlabeled* RSS measurements. In practice, such data might be obtained from scans performed on the handsets of users of the localization system, but without the need to manually label the data. Though the improvement obtained with the TSVM is still not sufficient, the results nevertheless suggest that any scheme that keeps the classifier model "current", by tracking the evolution of the RSS values, should be of interest to us.

This hypothesis is supported by Table V, which presents the results of training a new classifier "from scratch" based on a small number (100 in our experiments) of new *labeled* scans of each room. In this scenario, "hand" labeling of the update data is necessary, but could perhaps be performed by specially designated employees, or by volunteers in exchange for some "reward" (i.e., *crowdsourcing*). The table shows that even if the current model is too outdated to give good performance, e.g. on sets *S3*, *S4*, *S5* and *S6*, it can be trained using only a small amount of labeled data and give substantially improved performance.

TABLE V. RESULTS OF RE-TRAINING THE MODEL

Dataset	S3	S4	S5	S6
Result	83.3%	77.4%	88.1%	80.8%

V. CONCLUSIONS AND PERSPECTIVES

In a study of ambient RSS distribution in an indoor environment using SVM regression, no smooth functional relationship could be discovered between GSM RSS and position for the indoor environment tested, implying that interpolation-based techniques are not likely to be successful. The use of ambient GSM RSS-based classifiers trained with data collected throughout the areas of rooms, however, presents a viable alternative, and experimental results show that the percentage of correct room labeling can be up to 94% if the model is used before significant RSS drift sets in. The performance degradation over time is mainly caused by confusions between adjacent rooms. In order to cope with performance degradation caused by RSS drift over time, transductive inference was introduced to update the SVM classifiers with new unlabeled data. When tested on data sets collected over nine months, this approach proved capable of restoring a significant part of the lost performance. The use of small amounts of current labeled data to create "current" room classifiers also appears to be a promising approach, even if performance still needs to be improved. In future work, we will continue to strive for a continuously updatable, high-performance indoor room classifier. We also intend to investigate the use of W-CDMA network data in our measurements.

ACKNOWLEDGMENT

The authors wish to acknowledge the support of the China Scholarship Council.

REFERENCES

[1] A. Küpper, Location-Based Services: Fundamentals and Operation, John Wiley & Sons, New York, NY, USA, 2005.

[2] A.M. Ladd, K.E. Bekris, A. Rudys, L.E. Kavraki, D.S. Wallach, "On the feasibility of using wireless ethernet for indoor localization," IEEE Trans on Robotics and Automation. vol. 20, no. 3, pp.555-559, June 2004.

[3] Y. Zhou, C.L. Law, Y.L. Guan, and F.P.S. Chin, "Indoor elliptical localization based on asynchronous UWB range measurement", IEEE Trans. on Instrumentation and Measurement, vol 6, issue 1, pp.248-257, January 2011.

[4] Q. Yang, S. Jialin Pan, V. Wenchen Zheng, "Estimating location using Wi-Fi," IEEE Intelligent Systems, vol. 23, no. 1, pp.8-13, January/February 2008.

[5] S-H. Fang, T-N. Lin, P-C. Lin, "Location fingerprinting in a decorrelated space," IEEE Trans on Knowledge Data Engineering. vol. 20, no. 5, pp.685-691, May 2008.

[6] S-H. Fang, T-N. Lin, "Indoor location system based on discriminant-adaptive neural network in IEEE 802.11 environments," IEEE Trans on Neural Network, vol. 19, no. 11, pp.1973-1978, Nov 2008.

[7] S-H. Hong, B-K. Kim, D-S. Eom, "Localization algorithm in wireless sensor networks with network mobility," IEEE Trans on Consumer Eectronic. vol. 55, no. 4, pp.1921-1928, Nov 2009.

[8] V. Otsason, A. Varshavsky, A. LaMarca, E. de Lara, "Accurate GSM indoor localization," in Proceedings of the 7th International Conference on Ubiquitous Computing, pp.141-158, Tokyo, Japan, September 2005.

[9] W. ur Rehman, E. de Lara, S. Saroiu, "CILoS, a CDMA indoor localization system," in Proceedings of the 10th International Conference on Ubiquitous Computing, pp.21-24, Seoul, South Korea, September 2008.

[10] Y. Oussar, I. Ahriz, B. Denby, G. Dreyfus, "Indoor localization based on cellular telephony RSSI fingerprints containing very large numbers of carriers", EURASIP J. Wireless Comm. and Network. 2011, 2011:81.

[11] Y. Tian, B. Denby, I. Ahriz, P. Roussel, G. Dreyfus. "Fast, handset-based GSM fingerprints for indoor localization," In Proceedings of the The 9th International Symposium on Wireless Communication Systems, pp. 641-645, Paris, France, August, 2012.

[12] V.W. Zheng, E.W. Xiang, Q. Yang, and D. Shen. "Transferring localization models over time," In Proceedings of the 23rd National Conference on Artificial Intelligence, vol. 3, pp. 1421-1426.

[13] Telit GM862-GPS module, [Online]: http://www.telit.com/en/products/gsm-gprs.php

[14] A.J. Smola, and B. Schölkopf, "A tutorial on support vector regression," 1998.

[15] The Spider, [Online]: http://people.kyb.tuebingen.mpg.de/spider/

[16] N. Cristianini, J. Shawe-Taylor. Support Vector Machines and Other Kernel-Based Learning Methods, Cambridge University Press, 2000

[17] T. Joachims, "Transductive inference for text classification using support vector machines," International conference on Machine Learning , pp. 200-209, Bled, Slovenia, June 1999.

[18] Y. Chen, G. Wang, and S. Dong, "Learning with progressive transductive support vector machines," IEEE International Conference on Data Mining , Maebashi City, Japan, December 2002.

[19] SVMlight Support Vector Machine, [Online]: http://svmlight. joachims .org.

Hybrid Indoor Localization using GSM Fingerprints, Embedded Sensors and a Particle Filter

Ye Tian, Bruce Denby
Université Pierre et Marie Curie
and SIGMA Laboratory, ESPCI
Paris, France
ye.tian@etu.upmc.fr,
denby@ieee.org

Iness Ahriz
LAETITIA/CEDRIC Laboratory
Conservatoire National des Arts et Métiers
Paris, France
iness.ahriz@cnam.fr

Pierre Roussel, Gérard Dreyfus
SIGMA Laboratory, ESPCI
ParisTech
Paris, France
pierre.roussel@espci.fr,
gerard.dreyfus@espci.fr

***Abstract*—The article presents an indoor localization scheme for mobile devices based on GSM Received Signal Strength fingerprints combined with embedded sensor information and an area site map. Displacements of a mobile user are first estimated using a sensor dead-reckoning approach that adapts stride length to different users and environments, and a dynamically switched orientation estimation scheme responding to orientation changes of the mobile device. Positions derived from GSM fingerprints, along with constraints imposed by a site map, are then integrated using a particle filter in order to prevent the accumulation of dead-reckoning errors over time. The study demonstrates that a standard handset with cellular network access and embedded inertial sensors can provide a good solution for indoor localization.**

Keywords—indoor localization; fingerprinting; support vector machine; sensor dead-reckoning; particle filter

I. INTRODUCTION

Global Navigation Satellite Systems (GNSS), such as GPS and GLONASS, furnish navigation, tracking, and monitoring services in outdoor environments [1]; however, due to propagation effects, they are unable to operate effectively in indoor environments. This situation has led to intense activity in developing indoor localization techniques that provide seamless and ubiquitous services for mobile users [2].

Beacon-based approaches proposed over the past decade include such technologies as infrared [3], Bluetooth [4], Radio-Frequency Identification (RFID) [5], Wireless Local Area Networks (WLAN) [6], Ultra-wideband (UWB) [7], acoustic signals, etc. The need to deploy and maintain an underlying infrastructure unfortunately renders these methods somewhat less desirable. Indoor localization based on fingerprints from ambient radiotelephone networks, such as GSM and CDMA, has also been proposed [8][9]. Indoor localization based on classification of RSS fingerprints of very large number of GSM channels has been reported in [10][11][12], albeit providing a simple room label rather than a physical coordinate.

Beacon-free solutions relying only on sensors such as accelerometers, gyrometers, magnetometers, and barometer, can track users by continuously estimating their displacement from a known starting point. Many such studies, ([13] [14] [15] [16] [17] [18]), invoke dedicated Inertial Measurement Units (IMU) mounted at waist, leg or head, or Micro-Electro-Mechanical Systems (MEMS) embedded in smartphones, with few taking into account the orientation of the phone in practical scenarios, e.g., in a hand or a pocket. Furthermore, due to the drift and low precision of MEMS sensors, integration of sensor readings can result in an unacceptable accumulation of error.

The particle filter has become a powerful tool in location estimation and target tracking systems, that allows to combine localization data from a variety of sources – for example, beacon data, embedded smartphone sensors, and building layout constraints. In this paper, we present a particle filter based indoor localization system that uses room-level positioning results from GSM fingerprinting to correct for accumulated inertial dead-reckoning errors, while also accessing a building map to exclude inaccessible regions and forbid unreasonable movements such as traversing a wall. The approach, which outputs coordinates rather than room labels, also incorporates a novel, adaptive stride-length step detection algorithm that can handle arbitrary position changes of the mobile device. This system is to the best of our knowledge the first to use a particle filter to combine GSM fingerprints with inertial sensors and a site map, and to incorporate an adaptive stride/orientation model.

The article is organized as follows. The GSM fingerprinting algorithm is presented in section II, the sensor dead-reckoning algorithm in section III, and the particle filter data fusion in section IV. An evaluation of results is presented in section V, while conclusions and future perspectives appear in the final section.

II. GSM FINGERPRINTING ALGORITHM

GSM is the most widely available cellular telephony standard in the world, with 800 mobile operators deployed in over 220 countries, and is expected to remain in service for many years to come [19]. Here, we benefit from this ubiquitous GSM coverage to carry out indoor localization without the necessity of deploying and maintaining a dedicated infrastructure. RSS values from all 548 carriers in both 900 MHz and 1800 MHz GSM bands are used to create fingerprints to be used for localization.

Room-level indoor localization is considered as a multi-class classification problem, which is usually carried out in two phases:

- An offline training phase, also known as the site survey. In this phase, GSM RSS fingerprints are

978-1-4799-5863-4/14/$31.00 ©2014 IEEE

recorded in each of the rooms and labeled with the corresponding room number. A discriminative model is then built using the training fingerprints and known labels, so as to best separate the training examples into their correct classes (i.e., the correct rooms).

- An online localization phase, in which new fingerprints are given to the localization system and a room number is output based on the previously defined model.

Only the offline training phase entails a heavy computational load, whereas during localization, the system needs simply evaluate a small number of discriminant functions. The Support Vector Machine (SVM) classifiers used in our work are deemed appropriate for dealing with very large numbers of variables and training examples due to their built-in regularization mechanism [20]. Before introducing the multi-class SVM classifier used in our work, we first present a pairwise (2-class) SVM classifier.

A. Pairwise SVM Classifier

Consider a set of M examples of items belonging either to class A or class B, each example being described by a p-dimensional vector $\mathbf{x}_i$. Further assume that the examples are linearly separable, i.e. that there exists a hyperplane of equation $f(\mathbf{x}) = 0$ that separate all examples without error: $f(\mathbf{x}_i) > 0$ for all examples i belonging to class A and $f(\mathbf{x}_i) < 0$ otherwise. It can be proven that $f(\mathbf{x})$ can be written under the form

$$f(\mathbf{x}) = \sum_{i=1}^{M} \alpha_i y_i (\mathbf{x}_i \cdot \mathbf{x}) + \alpha_0 \quad (1)$$

where the α_i ($i = 0 \ldots M$) are parameters whose values are estimated from the examples; $y_i = +1$ if example i belongs to class A and $y_i = -1$ otherwise.

If the examples are not linearly separable, a “soft-margin” approach can be used to reduce the complexity of the classifier by introducing slack variables ζ_i and performing a tradeoff between accuracy of classification of the training examples and ability to generalize; the price to pay is the introduction of a “regularization” constant C whose value must be chosen appropriately. To summarize, a GSM environment described by the fingerprint $\mathbf{x}$ is assigned to room A or room B according to the sign of $f(\mathbf{x})$, defined by (1).

B. Decision Rule for Multiclass Classification

When the discrimination problem involves more than two classes, it is necessary, for pairwise classifiers such as SVM, to define a method that allows combining multiple pairwise classifiers into a single multiclass classifier. We applied one-vs-all multiclass classifiers in this paper.

The one-vs-all approach consists of dividing the n-class problem into an ensemble of n pairwise classification problems, each of which consists in separating one class from all others. In the first stage, each classifier is trained separately, and in the second stage, the following decision rule is applied : the outputs of all n classifiers are first calculated and, following the conventional procedure, the predicted class is taken to be that of the classifier with the largest magnitude of $f(x)$ (relation (1)). The one-vs-all technique is advantageous from a computational standpoint, in that it only requires a number of classifiers equal to the number of classes.

The SVM used in our study, were implemented using LIBSVM toolbox[21].

III. Sensor Dead-Reckoning Algorithm

Sensor dead-reckoning aims to estimate the displacement from a previous location, usually consisting of a step detection module, a stride length model, and an orientation estimator. The reliable and widely-used “peak/trough” technique was chosen for step detection [22]. Stride length determination and orientation estimate, however, are critical to estimating user displacement. In order to render our system user-independent and robust against orientation changes, a novel stride length adaptation approach and orientation estimate “switching” scheme were introduced, as described below.

A. Adaptive Stride Length Model

It is necessary to use a value for stride length in order to estimate the displacement due to a step. However, stride length varies significantly for different persons and walking styles. The literature contains a variety of models indicating that stride length is related to stride frequency and the “bounce” of the hip, which we shall refer to as the “frequency model” and “bounce model”, respectively [23][24].

To verify these, we performed an experiment in which subjects walked a specified path several times at different walking speeds and stride frequencies. Step numbers and durations were recorded, while the length of the path was known in advance. The results are shown in Fig. 1. As seen in the figure, stride length has a linear relationship with both step frequency and acceleration amplitude, indicating that the models are reasonable. Most dead-reckoning solutions using existing models must fix the coefficients or obtain them from training on different users and environments.

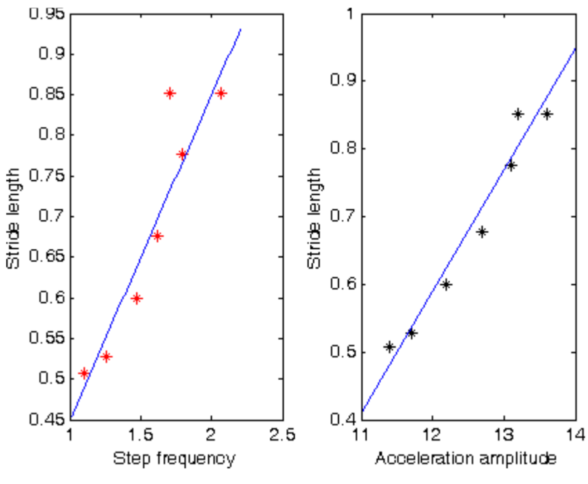

Fig. 1. Stride length with step frequency and acceleration amplitude, cooresponding to “frequency model” and “bounce model”

The “frequency model” necessitates an estimate of step frequency over a previous period of time, which can introduce delay if there is no step detected. In contrast, the accuracy of "bounce model" is easily influenced by environmental differences, such as going up and down stairs. As there is no stride length model that fits all subjects and environments, we propose to use a particle filter to adaptively select the best coefficients from a range of coefficients. The "bounce model" is used in our experiments and we define:

$$\varphi = p\left(a_{\max} - a_{\min}\right) + q \tag{2}$$

where φ is the stride length, and p and q are the two coefficients that will be automatically adjusted by the particle filter.

B. Orientation Estimate

The orientation of the mobile user in our system was estimated based on accelerometer, gyrometer and magnetometer. Both magnetometer and gyrometer can provide orientation information, but neither gives accurate and reliable moving orientation. Turn rate from a gyrometer can be integrated into an angle increment and the orientation obtained with a known initial azimuth angle; however, integration over a long period can introduce an unacceptable cumulative error. Orientation from a magnetometer is time independent, however the magnetometer has slow response rate and poor accuracy, especially in indoor environments where field disturbances always exist. For these reasons, a complementary filter was applied to combine these two orientation sources [25].

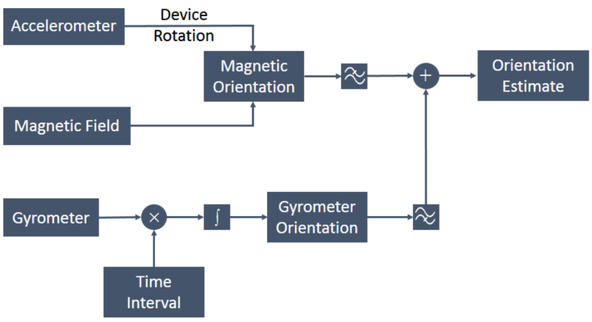

Fig. 2. Complementary filter for orientation estimate

The principle of the complementary orientation filter is shown in Fig. 2. A low pass filter is applied to the orientation obtained from the gyrometer, while a high pass filter is applied to that from the magnetometer and accelerometer. These high and low frequency orientation components are added at the input of the orientation estimate, which has a fast response time and minimizes drift over long periods. The orientation complementary filter in our experiments is based on Google Android sensor-related APIs [26].

While walking, a mobile device can be held in the hand or pocket in a variety of different orientations, which is very challenging for accurate orientation estimation, a point largely ignored in most previous studies. Unlike foot-mounted or head-mounted IMUs affixed to the body, the orientation of a mobile device is not always consistent with the user's orientation, depending on the relative motion of mobile device and user. In this article, a "switching" scheme is introduced to handle arbitrary position changes of mobile devices, considering the following three situations:

- When the principal component of gravity changes with respect to the mobile device, the mobile device is assumed to be changing its orientation (Fig. 3). In this situation, the orientation estimate stops and the particle filter draws random orientations for each particle to estimate the location.
- When the mobile device is held with the screen upwards, typically meaning the user is checking content, the orientation of the mobile device and the mobile user are assumed to be consistent. In this case, the orientation of the mobile user is estimated using the complementary filter as introduced above.
- When the mobile device is not held with screen upward and the principal component of gravity is not changing, the mobile device is assumed to be held stationary or placed in a pocket. In this situation, the complementary filter stops and the orientation is estimated only using the gyrometer: a rotation that is orthogonal with the direction of gravity indicates the orientation of the mobile device and user changes.

$$\omega = R^T G \tag{3}$$

where $R = [R_x, R_y, R_z]^T$ is the turn rate readings from gyrometer, and $G = [G_x, G_y, G_z]^T$ is the gravity vector obtained from the acceleration data by filtering.

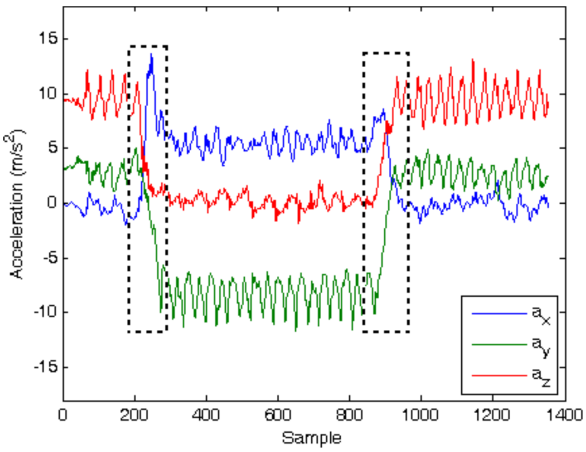

Fig. 3. Acceleration changes reflect mobile device position changes

IV. Particle Filter Data Fusion

We aim to obtain the best position estimate of a mobile user at each current time step by combining both the GSM fingerprinting result and the sensor dead-reckoning result. The state space filtering approach is used for sequentially estimating the variables of interest. Since the posterior distribution is non-Gaussian, the particle filter is thought to be more appropriate and robust compared with extended or unscented Kalman filters [27].

A. System Model

In our system, at time step *t* the state of the system is $s_t = [x_t, y_t, p_t, q_t]^T$, where x_t and y_t are the position coordinates of the mobile user, and p_t and q_t are the coefficients of the stride length model explained in section III-*A*. The observation at time step *t* in our case is the fingerprint classifier output h_t, i.e. the room number. The state transition model can be characterized in terms of a state transition density $p(s_t \mid s_{t-1})$.

In our system, the state transition density $p(s_t \mid s_{t-1})$ is determined by both multiple sensor information and map layout information. As for state $s_t = [x_t, y_t, p_t, q_t]^T$, when a step is detected, based on multiple sensor dead-reckoning we have:

$$\begin{aligned} x_t &= x_{t-1} + \varphi_{t-1} \cdot \cos(\theta_{t-1}) + w_{t-1}^x \\ y_t &= y_{t-1} + \varphi_{t-1} \cdot \sin(\theta_{t-1}) + w_{t-1}^y \\ p_t &= p_{t-1} + w_{t-1}^p \\ q_t &= q_{t-1} + w_{t-1}^q \end{aligned} \tag{4}$$

where φ_{t-1} is the stride length (relation (2)), θ_{t-1} is the orientation estimation, and w_{t-1}^x, w_{t-1}^y, w_{t-1}^p and w_{t-1}^q represent system noise.

Not all the state transitions based on sensor dead-reckoning are reasonable; for example, the state transition may suggest that the mobile user passed through a wall, usually due to a false orientation estimate. Map layout information can be used to eliminate this kind of state transitions, as explained in the description of the second step of the particle filter, in subsection IV-*C*.

The observation density $p(h_t \mid s_t)$ represents the likelihood, given the state s_t, that room number h_t is obtained from the GSM fingerprinting result. Given the available data, the required probability can be estimated from the SVM confusion matrix, whose element C_{ij} is the number of examples that are assigned to class *i* while the target is actually in room *j*. Then

$$P\left(h_t = i \middle| room(s_t) = j\right) \approx \frac{C_{ij}}{\sum_{k=1}^{7} C_{ik}} \tag{5}$$

where $room(s_t)$ is the number of the room to which the components x_t and y_t of state s_t belong.

B. Bayesian Filter

The task here is to obtain the belief of the state s_k given the observations, which is the *a posteriori* density of the system state $p(s_t \mid h_t)$. A general approach to estimating the state over time from observations is the Bayesian filter. For a system with a state transition density $p(s_t \mid s_{t-1})$ and observation density $p(h_t \mid s_t)$, the Bayesian filter recursively computes posterior density of the state at time *t* $p(s_t \mid h_t)$ based on posterior density of the previous state $p(s_{t-1} \mid h_{t-1})$ and the most recent observation h_t, in two steps, prediction and update:

$$p(s_t \mid h_{t-1}) = \int p(s_t \mid s_{t-1}) \cdot p(s_{t-1} \mid h_{t-1}) ds_{t-1} \tag{6}$$

$$p(s_t \mid h_t) = \frac{p(h_t \mid s_t)}{p(h_t \mid h_{t-1})} p(s_t \mid h_{t-1}) \tag{7}$$

where $p(h_t \mid h_{t-1})$ is the normalizing constant

$$p(h_t \mid h_{t-1}) = \int p(h_t \mid s_t) \cdot p(s_t \mid h_{t-1}) ds_t .$$

C. Particle Filter

The particle filter is a technique for implementing a recursive Bayesian filter by Monte Carlo sampling, which uses a finite number of random samples (called particles) with associated weights that provide a discrete approximation of the posterior density [28]. If the number of particles is very large, the discrete approximation approaches the true posterior density with arbitrary accuracy. The particle filter uses a set of particles taken from the previous time step ($pt_{t-1}^1, pt_{t-1}^2, \ldots pt_{t-1}^n \sim p(s_{t-1} \mid h_{t-1})$) and the most recent observation h_t to produce a set of particles approximately following the distribution of $p(s_t \mid h_t)$. The particle filter algorithm used in our system is realized in the following four steps:

- Initialize the particles: Since sensor dead-reckoning requires a starting position for integration, we sample *N* particles based on the output of the SVM classifier, which have the same weight that is equal to $1/N$. The coordinates (*x*, *y*) of the particles are distributed uniformly in each room, while the number of particles in each room depends on the observation distribution $p(h_0 \mid s_0)$. The stride model coefficients p_0 and q_0 are drawn uniformly over a suitable range.
- Make predictions based on the system model: When a step is detected, each particle makes a movement using sensor dead-reckoning. Map information is used in this step to remove unreasonable movements. As shown in Fig. 4, if a particle makes a movement that crosses a wall or enters an inaccessible region, it is removed, which, in filtering, is realized by setting the weight of the particle to 0.
- Update the weights based on the observation model: When the SVM classifier result is received, the likelihood $p(h_t \mid s_t)$ is applied to each particle to update the weight.
- Resample particles based on the weights: Through the previous steps, the number of particles diminishes and the weights of the particles change considerably. To better represent the posterior density $p(s_t \mid h_t)$, particles are resampled to the same number *N* with probabilities equal to their weights.

The final location estimate is taken to be the centroid of all particles.

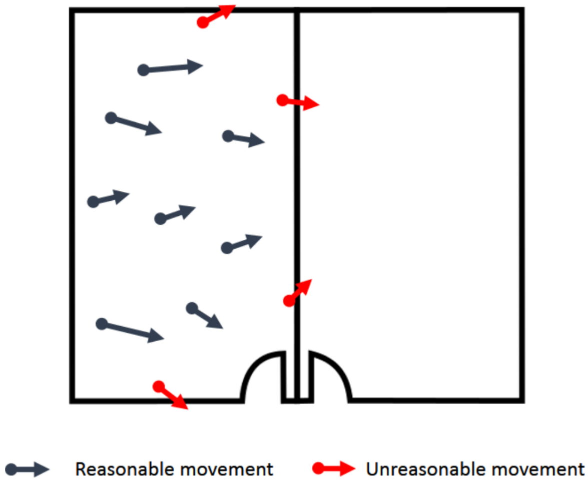

Fig. 4. Elimination of particles moving unreasonably

V. Evaluation

A. Testbed

The experimental site tested is located on the fourth floor of a laboratory building (steel frame with concrete and plaster walls) in central Paris, France (Fig. 6). The rooms are numbered from one to seven, while the corridor is divided into three sections numbered from eight to ten. Map layout information of doors, walls and fixed-position obstacles and their orientations is stored in a map database for later use.

The rooms used in our experiment are relatively small. It might be necessary to divide larger rooms into smaller pieces to get good performance, as was done, for example, for the corridor in our tests.

B. Data Acquisition Devices

In our experiments, two types of data were recorded, for GSM fingerprinting, and multiple sensor dead-reckoning, respectively. GSM RSS fingerprints were collected using the GSM trace mobile "TEMS Pocket", a standard Sony Ericsson W995 mobile phone to which network investigation software has been added by the manufacturer [29]. Using the TEMS investigation software package, this device is able to obtain a scan of the entire GSM900 and GSM 1800 bands in about 300 milliseconds. The multiple sensor readings were obtained using a commercial Google Nexus 7 tablet, containing an accelerometer, gyrometer, and magnetometer. Android open source operating system is embedded in order to program the recording of the sensor readings.

Although in our experiments, two different devices were used for recording GSM fingerprints and sensor readings respectively, there exists a newer smartphone-based generation of "TEMS Pocket" that can record all the necessary data on the same device. In addition, all GSM mobile phones are required by the GSM standard to be able to scan all channels of the GSM bands, so that our approach is potentially applicable to any commercial device supporting GSM.

C. Datasets

Training data and test data were recorded separately, for building the SVM classifier and testing the localization system, respectively. The training data was taken with the TEMS Pocket and manually labeled with the corresponding room numbers. In the testing phase, a TEMS Pocket and a Nexus 7 tablet were bundled together and held in the hand, recording GSM fingerprints and multiple sensor readings simultaneously. The TEMS Pocket and a Nexus 7 tablet were held either facing the user or swinging along with the arm. The trajectory began at the south-west corner of room 7, continuing through the corridor, 8 and 9, into room 3, and finally stopping at the door of room 6, as shown in Fig. 6.

D. Results

Raw GSM fingerprinting results are shown in Fig. 5, where the x axis gives the sample number along the trajectory and the y axis the SVM classifier outputs. As seen in the figure, the SVM classifier gives the correct room numbers for most of the test examples, but there are still misclassifications especially in adjacent rooms. The percentage of overall correct classification is 70%. (This result was obtained in a short time with a very small training set and is not considered to be optimized [11]).

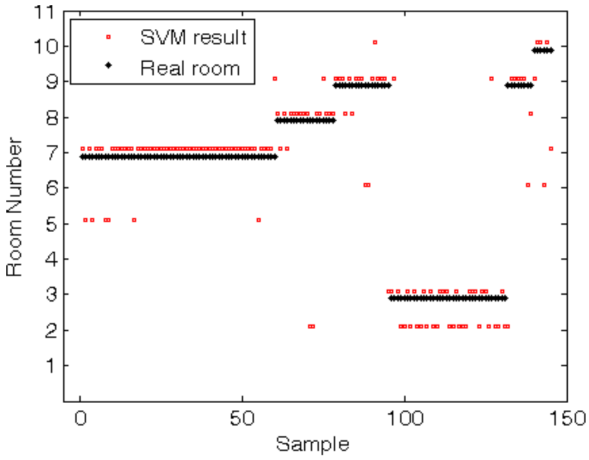

Fig. 5. GSM fingerprinting results

Fig. 6 shows the dead-reckoning results and particle filter results, where the actual trajectory is provided for comparison. It can be seen that multiple sensor dead-reckoning, even given a correct starting position, makes many mistakes. In a more realistic case, of course, the starting position is unknown. Furthermore, the obtained trajectory penetrates walls, which is not reasonable. The dashed line in Fig. 6 shows the particle filter results, in which the initial location is provided by the SVM classifier and the following location estimates evolve based on the particle filter. The localization errors are seen to be corrected by combining GSM fingerprinting, sensor dead-reckoning and map layout restrictions. Only a few mistakes occurred at the beginning of the trace, due to the unknown starting position, since the SVM classifier only outputs room-level location, not a precise position.

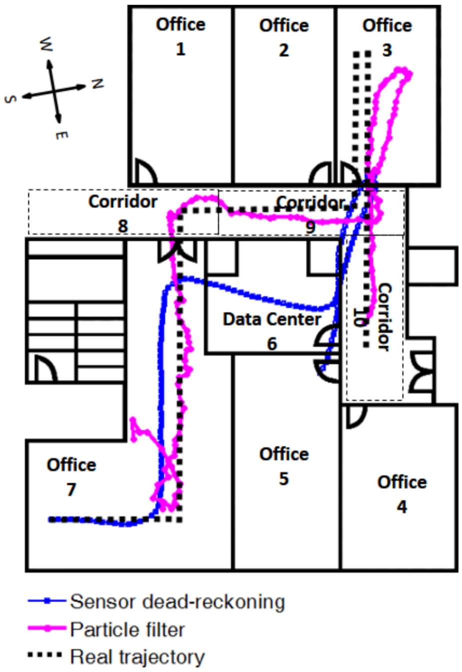

Fig. 6. Testbed and sensor dead-reckoning and particle filter results

VI. Conclusions and Future Perspectives

We have presented a hybrid approach for indoor localization using a particle filter to combine GSM fingerprinting results, sensor dead-reckoning and map layout information, which has been tested on a test trajectory acquired in a laboratory building under realistic conditions. Experimental results show that this approach can determine a mobile user's trajectory with good accuracy. The approach, which uses GSM fingerprints and multiple sensors that are easily obtainable due to the growing popularity of smartphones, is potentially ready for a practical implementation. It should be easily adaptable to upcoming 900 MHz 3G or similar new services.

References

[1] B. Hofmann-Wellenhof, H. Lichtenegger, and E. Wasle, *GNSS - Global Navigation Satellite Systems: GPS, GLONASS, Galileo, and more*. Springer, 2007.

[2] A. Küpper, *Location-Based Services: Fundamentals and Operation*, John Wiley & Sons, 2005.

[3] E. Aitenbichler and M. Muhlhauser, "An IR local positioning system for smart items and devices," *23rd Int. Conf. Distrib. Comput. Syst. Work. 2003. Proceedings.*, pp. 334 – 339, 2003.

[4] J. Hallberg, M. Nilsson, and K. Synnes, "Bluetooth Positioning," *10th Int. Conf. Telecommun. 2003 ICT 2003*, vol. 2, pp. 954–958, 2003.

[5] L. M. Ni, Y. Liu, Y. C. Lau, and A. P. Patil, "LANDMARC: Indoor Location Sensing Using Active RFID," *Wirel. Networks*, vol. 10, no. 6, pp. 701–710, Nov. 2004.

[6] H. W. H. Wang, H. Lenz, A. Szabo, J. Bamberger, and U. D. Hanebeck, "WLAN-Based Pedestrian Tracking Using Particle Filters and Low-Cost MEMS Sensors," *2007 4th Work. Positioning, Navig. Commun.*, 2007.

[7] S. Gezici and H. V. Poor, "Position Estimation via Ultra-Wide-Band Signals," *Proc. IEEE*, vol. 97, no. 2, 2009.

[8] A. Varshavsky, E. de Lara, J. Hightower, A. LaMarca, and V. Otsason, "GSM indoor localization," *Pervasive Mob. Comput.*, vol. 3, pp. 698–720, 2007.

[9] W. ur Rehman, E. De Lara, and S. Saroiu, "CILoS : A CDMA Indoor Localization System," *Proc. 10th Int. Conf. Ubiquitous Comput. - UbiComp '08*, 2008.

[10] B. Denby, Y. Oussar, I. Ahriz, and G. Dreyfus, "High-Performance Indoor Localization with Full-Band GSM Fingerprints," *2009 IEEE Int. Conf. Commun. Work.*, pp. 1 – 5, 2009.

[11] Y. Tian, B. Denby, I. Ahriz, P. Roussel, and G. Dreyfus, "Fast, handset-based GSM fingerprints for indoor localization," *2012 Int. Symp. Wirel. Commun. Syst.*, pp. 641–645, 2012.

[12] Y. Tian, B. Denby, I. Ahriz, P. Roussel, R. Dubois, and G. Dreyfus, "Practical indoor localization using ambient RF," in *2013 IEEE International Instrumentation and Measurement Technology Conference (I2MTC)*, 2013, pp. 1125–1129.

[13] B. Krach and P. Robertson, "Integration of foot-mounted inertial sensors into a Bayesian location estimation framework," *2008 5th Work. Positioning, Navig. Commun.*, 2008.

[14] S. Beauregard, "A Helmet-Mounted Pedestrian Dead Reckoning System," *Appl. Wearable Comput., 2006 3rd Int. Forum*, pp. 1–11, 2006.

[15] E. Foxlin, "Pedestrian tracking with shoe-mounted inertial sensors," *IEEE Comput. Graph. Appl.*, vol. 25, pp. 38 – 46, 2005.

[16] A. Serra, D. Carboni, and V. Marotto, "Indoor pedestrian navigation system using a modern smartphone," in *Proceedings of the 12th international conference on Human computer interaction with mobile devices and services*, 2010, pp. 397–398.

[17] O. Woodman and R. Harle, "Pedestrian localisation for indoor environments," *Proc. 10th Int. Conf. Ubiquitous Comput. - UbiComp '08*, pp. 114–123, 2008.

[18] F. Li, C. Zhao, G. Ding, J. Gong, C. Liu, and F. Zhao, "A reliable and accurate indoor localization method using phone inertial sensors," *Proc. 2012 ACM Conf. Ubiquitous Comput. - UbiComp '12*, p. 421, 2012.

[19] GSM Association, "GSM Roaming and Coverage Maps." [Online]. Available: http://maps.mobileworldlive.com/.

[20] A. Mammone, M. Turchi, and N. Cristianini, "Support Vector Machines," *Challenge*, vol. 1, pp. 1–8, 2009.

[21] C. Chang and C. Lin, "LIBSVM: a library for support vector machines," *ACM Trans. Intell. Syst. Technol.*, vol. 2, no. 3, pp. 1–39, 2011.

[22] R. W. Levei and T. Judd, "Dead reckoning navigational system using accelerometer to measure foot impacts," *United States Patent* 1996.

[23] H. Weinberg, "Using the ADXL202 in pedometer and personal navigation applications," *Analog Devices AN-602 Appl. note*, pp. 1–8, 2002.

[24] W. Zijlstra, "Assessment of spatio-temporal parameters during unconstrained walking.," *Eur. J. Appl. Physiol.*, vol. 92, no. 1–2, pp. 39–44, Jun. 2004.

[25] J. Calusdian, X. Yun, and E. Bachmann, "Adaptive-gain complementary filter of inertial and magnetic data for orientation estimation," in *2011 IEEE International Conference on Robotics and Automation*, 2011, pp. 1916–1922.

[26] "Android Sensor APIs." [Online]. Available: https://developer.android.com/reference/android/hardware/Sensor.html.

[27] K.-C. Lee, A. Oka, E. Pollakis, and L. Lampe, "A comparison between Unscented Kalman Filtering and particle filtering for RSSI-based tracking," *2010 7th Work. Positioning, Navig. Commun.*, pp. 157–163, Mar. 2010.

[28] M. S. Arulampalam, S. Maskell, N. Gordon, and T. Clapp, "A tutorial on particle filters for online nonlinear/non-Gaussian Bayesian tracking," *IEEE Trans. Signal Process.*, vol. 50, no. 2, pp. 174–188, 2002.

[29] ASCOM, "Test Mobile System." [Online]. Available: http://www.ascom.com/nt/en/index-nt/.

References

[1] J. Schiller and A. Voisard. *Location-based services*. Morgan Kaufmann Publishers, San Francisco, CA, May 2004.

[2] NENA. 911 statistics. `https://www.nena.org/?page=911Statistics`, November 2014.

[3] FCC. 911 wireless services. `https://www.fcc.gov/guides/wireless-911-services`.

[4] EENA. Position paper on the use of the GNSS to determine caller location in the context of 112 emergency calls. `http://www.eena.org/uploads/gallery/files/pdf/2014_05_EENA_Position_Paper_on_GNSS_full.pdf`, May 2014.

[5] Berg Insight. Mobile location based services. `http://www.berginsight.com/ReportPDF/ProductSheet/bi-lbs7-ps.pdf`, 2014.

[6] Strategy Analytics. `http://www.strategyanalytics.com`.

[7] B. Hofmann-Wellenhof, H. Lichtenegger, and J. Collins. *Global positioning system: Theory and practice*. Springer, Wien, Austria, 2001.

[8] A. Varshavsky, E. de Lara, J. Hightower, A. LaMarca, and V. Otsason. GSM indoor localization. *Pervasive and Mobile Computing*, 3(6):698–720, December 2007.

[9] Y. Oussar, I. Ahriz, B. Denby, and G. Dreyfus. Indoor localization based on cellular telephony RSSI fingerprints containing very large numbers of carriers. *EURASIP Journal on Wireless Communications and Networking*, 2011(1):81, August 2011.

[10] P. Brida, J. Duha, and M. Krasnovsky. On the accuracy of weighted proximity based localization in wireless sensor networks. volume 245, pages 423–432. Springer, 2007.

[11] S.S. Chawathe. Beacon placement for indoor localization using Bluetooth. In *Proceedings of the 11th International IEEE Conference on Intelligent Transportation Systems*, pages 980–985, Beijing, China, October 2008.

[12] S.S. Chawathe. Low-latency indoor localization using Bluetooth beacons. In *Proceedings of the 12th International IEEE Conference on Intelligent Transportation Systems*, pages 1–7, St. Louis, MO, USA, October 2009.

[13] Apple. iOS: understanding iBeacon. `http://support.apple.com/kb/ht6048`.

[14] A. Montaser and O. Moselhi. RFID indoor location identification for construction projects. *Automation in Construction*, 39:167–179, April 2014.

[15] B. Ozdenizci, O. Kerem, V. Coskun, and M.N. Aydin. Development of an Indoor navigation system using NFC technology. In *Proceedings of the 4th International Conference on Information and Computing*, pages 11–14, Phuket Island, Thailand, April 2011.

[16] J.J. Caffery. *Wireless location in CDMA cellular radio systems*. Kluwer Academic Publishers, Norwell, MA, USA, 1999.

[17] W. Kim, J.G. Lee, and G.I. Jee. The interior-point method for an optimal treatment of bias in trilateration location. *IEEE Transactions on Vehicular Technology*, 55(4):1291–1301, July 2006.

[18] N. Alsindi, B. Alavi, and K. Pahlavan. Spatial characteristics of UWB TOA-based ranging in indoor multipath environments. In *Proceedings of the 18th IEEE International Symposium on Personal, Indoor and Mobile Radio Communications*, pages 1–6, Athens, Greece, September 2007.

[19] N.A. Alsindi, B. Alavi, and K. Pahlavan. Measurement and modeling of ultrawideband TOA-based ranging in indoor multipath environments. *IEEE Transactions on Vehicular Technology*, 58(3):1046–1058, May 2009.

[20] D. Dardari, A. Conti, U. Ferner, A. Giorgetti, and M.Z. Win. Ranging with ultrawide bandwidth signals in multipath environments. *Proceedings of the IEEE*, 97(2):404–426, February 2009.

[21] Z. Irahhauten, G. Bellusci, G.J.M. Janssen, H. Nikookar, and C. Tiberius. Investigation of UWB ranging in dense indoor multipath environments. In *Proceedings of the 10th IEEE Singapore International Conference on Communication systems*, pages 1–5, Singapore, October 2006.

[22] J.Y. Lee and R.A. Scholtz. Ranging in a dense multipath environment using an UWB radio link. *IEEE Journal on Selected Areas in Communications*, 20(9):1677–1683, December 2002.

[23] J. Barnes, C. Rizos, J. Wang, D. Small, G. Voigt, and N. Gambale. High precision indoor and outdoor positioning using LocataNet. *Journal of Global Positioning Systems*, 2(2):73–82, 2003.

[24] N. Jardak and N. Samama. Indoor positioning based on GPS-repeaters: Performance enhancement using an open code loop architecture. *IEEE Transactions on Aerospace and Electronic Systems*, 45(1):347–359, January 2009.

[25] M. Rabinowitz and J.J. Spilker. A new positioning system using television synchronization signals. *IEEE Transactions on Broadcasting*, 51(1):51–61, March 2005.

[26] D. Moore, J. Leonard, D. Rus, and S. Teller. Robust distributed network localization with noisy range measurements. In *Proceedings of the 2nd International Conference on Embedded Networked Sensor Systems*, pages 50–61, Baltimore, MD, USA, November 2004.

[27] R. Ye and H. Liu. UWB TDOA localization system: Receiver configuration analysis. In *Proceedings of 2010 International Symposium on Signals, Systems and Electronics*, volume 1, pages 1–4, Nanjing, China, September 2010.

[28] A. Prorok, P. Tome, and A. Martinoli. Accommodation of NLOS for ultra-wideband TDOA localization in single- and multi-robot systems. In *Proceedings of 2011 International Conference on Indoor Positioning and Indoor Navigation*, pages 1–9, Guimaraes, Portugal, September 2011.

[29] J. Borkowski, J. Niemela, and J. Lempiainen. Enhanced performance of Cell ID+RTT by implementing forced soft handover algorithm. In *Proceedings of the 60th IEEE Vehicular Technology Conference*, volume 5, pages 3545 – 3549, Los Angeles, CA, USA, September 2004.

[30] J. Medbo, I. Siomina, A. Kangas, and J. Furuskog. Propagation channel impact on LTE positioning accuracy: A study based on real measurements of observed time difference of arrival. In *Proceedings of the 20th International Symposium on Personal, Indoor and Mobile Radio Communications*, pages 2213–2217, Tokyo, Japan, September 2009.

[31] S. Fischer. Observed Time Difference Of Arrival (OTDOA) positioning in 3GPP LTE. Technical report, July 2014.

[32] M. Crepaldi, M.R. Casu, M. Graziano, and M. Zamboni. UWB receiver design and two-way-ranging simulation using VHDL-AMS. *Ph.D. Research in Microelectronics and Electronics*, pages 465–468, June 2006.

[33] P. Tarrio, A.M. Bernardos, J.A. Besada, and J.R. Casar. A new positioning technique for RSS-Based localization based on a weighted least squares estimator. In *Proceedings of 2008 IEEE International Symposium on Wireless Communication Systems*, pages 633–637, Reykjavik, Iceland, October 2008.

[34] J. Yang and Y. Chen. Indoor localization using improved RSS-based lateration methods. In *Proceedings of 2009 IEEE Global Telecommunications Conference*, pages 1–6, Honolulu, HI, USA, November 2009.

[35] K. Chintalapudi, A.P. Iyer, and V.N. Padmanabhan. Indoor localization without the pain. In *Proceedings of the 16th Annual International Conference on Mobile Computing and Networking*, pages 173–184, Chicago, IL, USA, September 2010. ACM.

[36] F. Subhan, H. Hasbullah, A. Rozyyev, and S.T. Bakhsh. Indoor positioning in Bluetooth networks using fingerprinting and lateration approach. In *Proceedings of 2011 International Conference on Information Science and Applications*, pages 1–9, Jeju Island, Korea, April 2011.

[37] C.H. Ko. RFID 3D location sensing algorithms. *Automation in Construction*, 19(5):588–595, August 2010.

[38] A. E. Waadt, S. Wang, C. Kocks, A. Burnic, D. Xu, G. H. Bruck, and P. Jung. Positioning in multiband OFDM UWB utilizing received signal strength. In *Proceedings of the 7th Workshop on Positioning, Navigation and Communication*, pages 308–312, Dresden, Germany, March 2010.

[39] S.Y. Seidel and T.S. Rappaport. 914 MHz path loss prediction models for indoor wireless communications in multifloored buildings. *IEEE Transactions on Antennas and Propagation*, 40(2):207–217, 1992.

[40] NOKIA. High accuracy indoor positioning. `http://www.nomadicsolutions.biz/prod.php?lg=uk&id=51`.

[41] J. Zhou, H. Zhang, and L. Mo. Two-dimension localization of passive RFID tags using AOA estimation. In *Proceedings of 2011 IEEE Instrumentation and Measurement Technology Conference*, pages 1–5, Binjiang, China, May 2011.

[42] F. Van Diggelen. Indoor GPS theory & implementation. *IEEE Position Location and Navigation Symposium*, pages 240–247, 2002.

[43] L.D. Vittorini and B. Robinson. Optimizing indoor GPS performance. *GPS World*, 14(11):40–48, November 2003.

[44] F. Dovis, R. Lesca, D. Margaria, G. Boiero, and G. Ghinamo. An assisted high-sensitivity acquisition technique for GPS indoor positioning. In *Proceedings of 2008*

IEEE Position Location and Navigation Symposium, pages 1350–1361, Monterey, CA, USA, May 2008.

[45] S. Schön and O. Bielenberg. On the capability of high sensitivity GPS for precise indoor positioning. In *Proceedings of the 5th Workshop on Positioning, Navigation and Communication*, pages 121–127, Hannover, Germany, March 2008.

[46] P.A. Zandbergen and S.J. Barbeau. Positional accuracy of assisted GPS data from high-sensitivity GPS-enabled mobile phones. *Journal of Navigation*, 64(3):381–399, July 2011.

[47] N. Samama. *Global positioning: Technologies and performance.* Wiley Survival Guides in Engineering and Science. Wiley, New York, NY, USA, March 2008.

[48] D. Zimmermann, J. Baumann, M. Layh, F. Landstorfer, R. Hoppe, and G. Wolfle. Database correlation for positioning of mobile terminals in cellular networks using wave propagation models. In *Proceedings of the 60th IEEE Vehicular Technology Conference*, volume 7, pages 4682–4686, Los Angeles, CA, USA, September 2004.

[49] W. ur Rehman, E. de Lara, and S. Saroiu. CILoS: A CDMA indoor localization system. In *Proceedings of the 10th International Conference on Ubiquitous Computing*, pages 104–113, Seoul, Korea, September 2008.

[50] C. Gentner, E. Munoz, M. Khider, E. Staudinger, S. Sand, and A. Dammann. Particle filter based positioning with 3GPP-LTE in indoor environments. In *Proceedings of 2012 IEEE/ION Position Location and Navigation Symposium*, pages 301–308, Myrtle Beach, SC, USA, April 2012.

[51] R. Di Taranto, S. Muppirisetty, R. Raulefs, D. Slock, T. Svensson, and H. Wymeersch. Location-aware communications for 5G networks: How location information can improve scalability, latency, and robustness of 5G. *IEEE Signal Processing Magazine*, 31(6):102–112, November 2014.

[52] V. Moghtadaiee, A.G. Dempster, and S. Lim. Indoor localization using FM radio signals: A fingerprinting approach. In *Proceedings of 2011 International Conference on Indoor Positioning and Indoor Navigation*, pages 1–7, Guimaraes, Portugal, September 2011.

[53] A. Popleteev, V. Osmani, and O. Mayora. Investigation of indoor localization with ambient FM radio stations. In *Proceedings of 2012 IEEE International Conference on Pervasive Computing and Communications*, pages 171–179, Lugano, Switzerland, March 2012.

[54] Y. Chen, D. Lymberopoulos, J. Liu, and B. Priyantha. Indoor localization using FM signals. *IEEE Transactions on Mobile Computing*, 12(8):1502–1517, May 2013.

[55] P. Bahl and V.N. Padmanabhan. RADAR: An in-building RF-based user location and tracking system. In *Proceedings of the 19th Annual Joint Conference of the IEEE Computer and Communications Societies*, volume 2, pages 775–784, Tel Aviv, Israel, March 2000.

[56] C.L. Wu, L.C. Fu, and F.L. Lian. WLAN location determination in e-home via support vector classification. In *Proceedings of 2004 IEEE International Conference on Networking, Sensing and Control*, volume 2, pages 1026–1031, Taipei, Taiwan, March 2004.

[57] S. Saha, K. Chaudhuri, D. Sanghi, and P. Bhagwat. Location determination of a mobile device using IEEE 802.11b access point signals. *IEEE Wireless Communications and Networking Conference*, 3:1987–1992, March 2003.

[58] Z. Xiang, S. Song, J. Chen, H. Wang, J. Huang, and X. Gao. A wireless LAN-based indoor positioning technology. *IBM Journal of Research and Development*, 48(5.6):617–626, September 2004.

[59] Y. Ji, S. Biaz, S. Pandey, and P. Agrawal. ARIADNE: A dynamic indoor signal map construction and localization system. In *Proceedings of the 4th International Conference on Mobile Systems, Applications and Services*, pages 151–164, Uppsala, Sweden, June 2006.

[60] L. Reyero and G.Y. Delisle. Always best located, a pervasive positioning system. In *Proceedings of the 2nd International Symposium on Wireless Pervasive Computing*, San Juan, Puerto Rico, February 2007.

[61] C. Wu, Z. Yang, Y. Liu, and W. Xi. WILL: Wireless indoor localization without site survey. *IEEE Transactions on Parallel and Distributed Systems*, 24(4):839–848, April 2013.

[62] A. Rai, K.K. Chintalapudi, V.N. Padmanabhan, and R. Sen. Zee: Zero-effort crowdsourcing for indoor localization. In *Proceedings of the 18th Annual International Conference on Mobile Computing and Networking*, pages 293–304, Istanbul, Turkey, August 2012.

[63] E. Mok and G. Retscher. Location determination using WiFi fingerprinting versus WiFi trilateration. *Journal of Location Based Services*, 1(2):145–159, June 2007.

[64] E. Ferro and F. Potorti. Bluetooth and Wi-Fi wireless protocols: A survey and a comparison. *IEEE Wireless Communications*, 12(1):12–26, February 2005.

[65] M. Altini, D. Brunelli, E. Farella, and L. Benini. Bluetooth indoor localization with multiple neural networks. In *Proceedings of the 5th International Symposium on Wireless Pervasive Computing*, pages 295–300, Modena, Italy, May 2010.

[66] A.N. Raghavan, H. Ananthapadmanaban, M.S. Sivamurugan, and B. Ravindran. Accurate mobile robot localization in indoor environments using bluetooth. In *Proceedings of 2010 IEEE International Conference on Robotics and Automation*, pages 4391–4396, Anchorage, AK, USA, May 2010.

[67] R. Heydon. *Bluetooth low energy: The developer's handbook*. Pearson Education, Upper Saddle River, NJ, USA, November 2012.

[68] TI. CC2541 SensorTag development kit. `http://www.ti.com/tool/cc2541dk-sensor`.

[69] K. Sohraby, D. Minoli, and T. Znati. *Wireless sensor networks: Technology, protocols, and applications*. John Wiley & Sons, New York, NY, USA, April 2007.

[70] G. Mao and B. Fidan. *Localization algorithms and strategies for wireless sensor networks*. IGI Publishing, Hershey, PA, USA, May 2009.

[71] C. Alippi and G. Vanini. A RSSI-based and calibrated centralized localization technique for wireless sensor networks. In *Proceedings of the 4th Annual IEEE International Conference on Pervasive Computing and Communications Workshops*, pages 301–305, Pisa, Italy, March 2006.

[72] T. He, C. Huang, B.M. Blum, J.A. Stankovic, and T. Abdelzaher. Range-free localization schemes for large scale sensor networks. In *Proceedings of the 9th Annual International Conference on Mobile Computing and Networking*, pages 81–95, San Diego, CA, USA, September 2003.

[73] A.A. Kannan, G. Mao, and B. Vucetic. Simulated annealing based wireless sensor network localization. In *Proceedings of the 63rd IEEE Vehicular Technology Conference*, volume 2, pages 1022–1026, Melbourne, Vic., Australia, May 2006.

[74] M. Gholami, E. Ström, H. Wymeersch, and S. Gezici. Upper bounds on position error of a single location estimate in wireless sensor networks. *EURASIP Journal on Advances in Signal Processing*, 2014(1):4, January 2014.

[75] V. Savic, H. Wymeersch, and S. Zazo. Belief consensus algorithms for fast distributed target tracking in wireless sensor networks. *Signal Processing*, 95:149–160, February 2014.

[76] A. Pal. Localization algorithms in wireless sensor networks: Current approaches and future challenges. *Network Protocols and Algorithms*, 2(1):45–73, March 2010.

[77] J. Zhou and J. Shi. RFID localization algorithms and applications – a review. *Journal of Intelligent Manufacturing*, 20(6):695–707, August 2008.

[78] M. Bouet and A.L. dos Santos. RFID tags: Positioning principles and localization techniquesc. In *Proceedings of the 1st IFIP Wireless Days Conference*, pages 1–5, Dubai, United Arab Emirates, November 2008.

[79] L.M. Ni, Y. Liu, Y.C. Lau, and A.P. Patil. LANDMARC: Indoor location sensing using active RFID. In *Proceedings of the 1st IEEE International Conference on Pervasive Computing and Communications*, pages 407–415, Fort Worth, TX, USA, March 2003.

[80] S. Gezici, Z. Tian, G.B. Giannakis, H. Kobayashi, A.F. Molisch, H.V. Poor, and Z. Sahinoglu. Localization via ultra-wideband radios: A look at positioning aspects for future sensor networks. *IEEE Signal Processing Magazine*, 22(4):70–84, July 2005.

[81] M. Bocquet, C. Loyez, and A. Benlarbi-Delaï. Millimeter wave up-converted UWB based positioning system. In *Proceedings of the Joint Conference on Smart Objects and Ambient Intelligence: Innovative Context-aware Services: Usages and Technologies*, pages 293–296, Grenoble, France, October 2005.

[82] Y. Kilic, H. Wymeersch, A. Meijerink, M.J. Bentum, and W.G. Scanlon. An experimental study of UWB device-free person detection and ranging. In *Proceedings of 2013 IEEE International Conference on Ultra-Wideband*, pages 43–48, Sydney, NSW, Australia, September 2013.

[83] R.W. Levi and T. Judd. Dead reckoning navigational system using accelerometer to measure foot impacts. *US Patent 5583776*, 1996.

[84] S.Y. Cho, C.G. Park, and H.Y. Yim. Sensor fusion and error compensation algorithm for pedestrian navigation system. In *Proceedings of 2003 International Conference on Control, Automation and Systems*, pages 1001–1006, Gyeongju, Korea, October 2003.

[85] Y. Jin, H.S. Toh, W. S. Soh, and W.C. Wong. A robust dead-reckoning pedestrian tracking system with low cost sensors. In *Proceedings of 2011 IEEE International Conference on Pervasive Computing and Communications*, pages 222–230, Seattle, WA, USA, March 2011.

[86] F. Li, C. Zhao, G. Ding, J. Gong, C. Liu, and F. Zhao. A reliable and accurate indoor localization method using phone inertial sensors. In *Proceedings of 2012 ACM Conference on Ubiquitous Computing*, pages 421–430, Pittsburgh, Pennsylvania, September 2012.

[87] R. Feliz, E. Zalama, and J. Gómez. Pedestrian tracking using inertial sensors. *Journal of Physical Agents*, 3(1):35–42, January 2009.

[88] A. Perttula, H. Leppakoski, M. Kirkko-Jaakkola, P. Davidson, J. Collin, and J. Takala. Distributed indoor positioning system with inertial measurements and map matching. *IEEE Transactions on Instrumentation and Measurement*, 63(11):2682–2695, Nov 2014.

[89] H. Bao and W.C. Wong. A novel map-based dead-reckoning algorithm for indoor localization. *Journal of Sensor and Actuator Networks*, 3(1):44–63, 2014.

[90] A. Varshavsky, M.Y. Chen, E. de Lara, J. Froehlich, D. Haehnel, J. Hightower, A. LaMarca, F. Potter, T. Sohn, K. Tang, and I. Smith. Are GSM phones the solution for localization? *The 7th IEEE Workshop on Mobile Computing Systems & Applications*, pages 20–28, August 2006.

[91] H.H. Chen and M. Guizani. *Next generation wireless systems and networks.* John Wiley & Sons, New York, NY, USA, 2006.

[92] GSM Association. GSM roaming and coverage maps. `http://maps.mobileworldlive.com/`.

[93] Telit. GM862-GPS module. `http://www.telit.com/products/product-service-selector/product-service-selector/show/product/gm862-gps/`.

[94] ASCOM. TEMS Pocket. `http://www.ascom.com/nt/en/index-nt/tems-products-3/tems-pocket-5.htm`.

[95] N. Cristianini and J. Shawe-Taylor. *An introduction to support vector machines and other kernel-based learning methods.* Cambridge University Press, Cambridge, United Kingdom, March 2000.

[96] A.J. Smola and B. Schölkopf. A tutorial on support vector regression. *Statistics and Computing*, 14(3):199–222, August 2004.

[97] The Spider SVM toolbox. `http://people.kyb.tuebingen.mpg.de/spider/`.

[98] M. Brunato and R. Battiti. Statistical learning theory for location fingerprinting in wireless LANs. *Computer Networks*, 47(6):825–845, April 2005.

[99] T. Joachims. Transductive inference for text classification using support vector machines. In *Proceedings of the 16th International Conference on Machine Learning*, volume 99, pages 200–209, 1999.

[100] Y. Chen, G. Wang, and S. Dong. Learning with progressive transductive support vector machine. In *Proceedings of 2002 IEEE International Conference on Data Mining*, pages 67–74, Maebashi City, Japan, December 2002.

[101] T. Joachims. Advances in kernel methods. chapter Making large-scale support vector machine learning practical, pages 169–184. MIT Press, Cambridge, MA, USA, 1999.

[102] Z. Chen. Bayesian filtering: From kalman filters to particle filters, and beyond. *Statistics*, 182(1):1–69, 2003.

[103] J.M. Bernardo and A.F.M. Smith. *Bayesian theory.* Wiley, New York, NY, USA, September 2000.

[104] Google. Nexus 7 tablet. `www.google.fr/nexus/7/`.

[105] H. Weinberg. Using the ADXL202 in pedometer and personal navigation applications. *Analog Devices*, pages 1–8, 2002.

[106] W. Zijlstra. Assessment of spatio-temporal parameters during unconstrained walking. *European Journal of Applied Physiology*, 92(1-2):39–44, February 2004.

[107] Google. Android sensor APIs. `https://developer.android.com/reference/android/hardware/Sensor.html`.

[108] F. Gustafsson, F. Gunnarsson, N. Bergman, U. Forssell, J. Jansson, R. Karlsson, and P.J. Nordlund. Particle filters for positioning, navigation, and tracking. *IEEE Transactions on Signal Processing*, 50(2):425–437, February 2002.

[109] J.C. Platt. Probabilistic outputs for support vector machines and comparisons to regularized likelihood methods. *Advances in Large Margin Classifiers*, pages 61–74, March 1999.

[110] V.W. Zheng, E.W. Xiang, Q. Yang, and D. Shen. Transferring localization models over time. In *Proceedings of the 23rd AAAI Conference on Artificial Intelligence*, pages 1421–1426, Chicago, IL, USA, July 2008.